Nancy-Université
Université Henri Poincaré

AVERTISSEMENT

Ce document est le fruit d'un long travail approuvé par le jury de soutenance et mis à disposition de l'ensemble de la communauté universitaire élargie.

Il est soumis à la propriété intellectuelle de l'auteur. Ceci implique une obligation de citation et de référencement lors de l'utilisation de ce document.

D'autre part, toute contrefaçon, plagiat, reproduction illicite encourt une poursuite pénale.

➢ Contact SCD Nancy 1 : theses.sciences@scd.uhp-nancy.fr

LIENS

Code de la Propriété Intellectuelle. articles L 122. 4
Code de la Propriété Intellectuelle. articles L 335.2- L 335.10
http://www.cfcopies.com/V2/leg/leg_droi.php
http://www.culture.gouv.fr/culture/infos-pratiques/droits/protection.htm

U.F.R. FACULTE DES SCIENCES & TECHNIQUES
Secteur Physique, Géologie, Chimie, Mécanique
Ecole Doctorale Lorraine de Chimie et Physique Moléculaires, SESAMES
Département de Formation Doctoral : Chimie et Physico-Chemie moléculaires

Thèse

Présentée pour l'obtention du titre de

Docteur de l'Université Henri Poincaré, Nancy-université

Spécialité : Chimie et Electrochimie Analytiques

Par **Zhijie Wang**

Nouvelles stratégies de co-immobilisation de déshydrogénases, du cofactor NAD^+, et de médiateurs redox, au sein de films sol-gel en vue d'applications en bioélectrocatalyse

Soutenance publique prévue le 4 Octobre 2011 devant le jury composé de :

Rapporteurs :	
Dr. Thibaud Coradin	Directeur de Recherche, CNRS, Collège de France, Paris
Dr. Fethi Bedioui	Directeur de Recherche, CNRS, Chimie ParisTech-Université Paris Descartes
Examinateurs :	
Prof. Jean-Luc Blin	Professeur, Université Henri Poincaré, Nancy
Prof. Alexander Kuhn	Professeur, Université de Bordeaux 1
Dr. Alain Walcarius	Directeur de Recherche, CNRS, Nancy
Dr. Mathieu Etienne	Chargé de Recherche, CNRS, Nancy

Laboratoire de Chimie Physique et Microbiologie pour l'Environnement (LCPME)
Unité mixte de recherche -URM 7564,
405, rue de Vandoeuvre, F-54600 Villers-lès-Nancy (France)

Table of Contents

Abbreviations **1**

Preface **3**

Chapter I. Introduction **7**

1. ERUDESP project 11

2. Immobilization of enzymes on electrode surfaces 13

2.1 Sol-gel process 14

2.2 Optimization of the sol-gel process for bioencapsulation 17

2.3 Electrochemically-assisted generation of silica films 19

3. Dehydrogenase-based electrochemical reactor: the need for immobilization and cofactor regeneration 21

3.1 Enzymes and cofactor 21

3.2 Cofactor immobilization 22

3.3 Electrochemical cofactor regeneration 24

4. Immobilization of charge transfer catalyst on electrode surface 29

4.1 Carbon paste electrode 30

4.2 Surface activation 30

4.3 Precipitation 31

4.4 Monolayers 31

4.5Electropolymerization 32

5. Dehydrogenase, cofactor and mediator co-immobilization 32

6. Objective beyond the state-of-the-art 34

References 36

Chapter II. Experimental part **49**

1. Materials 51

1.1 Sol-gel reagents 51

1.2 Enzymes 52

1.3 Cofactors 52

1.4 Mediators 53

1.5 Polymer additives 58

1.6 The other chemicals and solutions 59

2. Electrodes 59

3. Preparation of sol-gel for bioencapsulation 60

4. Preparation of electrodes 62

4.1 Preparation of electrodes for chapter III 62

4.2 Preparation of electrodes for chapter IV 63

4.3 Preparation of electrodes for chapter V 64

4.4 Preparation of electrodes for chapter VI 65

5. Methods of analysis 67

5.1 Electrochemical measurements 67

5.2 UV-VIS Spectroscopy (UV) 69

5.3 Attenuated Total Reflectance–Fourier Transform Infrared Spectroscopy (ATR-FTIR Spectroscopy) 70

5.4 Scanning electron microscopy (SEM) 71

5.5 Scanning electrochemical microscopy (SECM) 72

References 73

Chapter III. Feasibility of dehydrogenase encapsulation in sol-gel matrix 77

1. Introduction 79

2. Critical effect of polyelectrolytes on the electrochemical response of dehydrogenases entrapped in sol-gel thin films 81

2.1 Preliminary observations 81

2.2 Interest of additives for DSDH encapsulation onto electrode surfaces 84

2.3 Factors affecting the electrode response 88

3. Electrochemically-assisted deposition of sol-gel bio-composite with co-immobilized dehydrogenase and diaphorase 92

3.1 Feasibility of the electrochemically-assisted deposition 92

3.2 Optimization of the electrode response 95

3.3 Relationship between the reactivity, the permeability and the film stability 96

3.4 Comparison of the enzyme activity into the film and in solution 100

3.5 Co-immobilization of DSDH and diaphorase 102

3.6 Extension to the particular case of macroporous electrodes 104

4. Conclusion 107

References 109

Chapter IV. Co-immobilization of dehydrogenase and cofactor in sol-gel Matrix 113

1. Introduction 115

2. Co-immobilization of dehydrogenase and cofactor in sol-gel matrix by drop-Coating 117

2.1 “Simple” physical entrapment of the cofactor in the sol-gel film 117

2.2 Effect of carbon nanotubes on the electrode stability 120
2.3 Encapsulation of NAD-Dextran 121
2.4 Covalent attachment to the silica matrix with Glycidoxypropylsilane 122
3. Co-immobilization dehydrogenase and cofactor in electrodeposited sol-gel thin film 130
3.1 The feasibility on GCE 130
3.2 The feasibility on flat gold electrode 131
3.3 Extension to the macroporous gold electrode 132
4. Conclusion 133
References 135

Chapter V. Mediator immobilization in sol-gel matrix and co-immobilization with dehydrogenase and cofactor 139
1. Introduction 141
2. Fc-PEI as co-immobilized mediator 143
2.1 Co-immobilization in drop-coated sol-gel film 143
2.2 Co-immobilization in electrogenerated sol-gel films 144
3. Fc-silane as co-immobilized mediator 148
3.1 Co-immobilization in drop-coated sol-gel film 149
3.2 Co-immobilization in electrogenerated sol-gel film 151
4. Os-polymer as co-immobilized mediator 154
4.1 Co-immobilization in drop-coated sol-gel film 154
4.2 Co-immobilization in electrogenerated sol-gel film 157
5. Conclusion 159
References 161

Chapter VI. Mediator immobilization on carbon nanotubes and co-immobilization with dehydrogenase and cofactor 165

1. Introduction 167

2. Deposition sol-gel film at macrowaved MWCNTs 169

2.1 Electrocatalytic oxidation of NADH at GCE/MWCNTs-μW 169

2.2 Importance of bilayers (drop-coated sol-gel film) 170

2.3 Electrodeposition of sol-gel thin films at GCE/MWCNTs-μW 172

3. Deposition of sol-gel film at MWCNTs modified by poly (methylene green) (GCE/MWCNTs-PMG) 175

3.1 Electrocatalytic oxidation of NADH at GCE/MWCNTs-PMG 175

3.2 Drop-coating of sol-gel film at GCE/MWCNTs-PMG 176

3.3 Electrodeposition of sol-gel thin film at GCE/MWCNTs-PMG 180

4. Deposition of sol-gel film at MWCNT wrapped by Osmium(III) polymer (GCE/MWCNTs-Os) 183

4.1 Carbon nanotubes as Osmium immobilization support 183

4.2 Drop-coating of sol-gel film at GCE/MWCNTs-Os 185

4.3 Electrodepostion of sol-gel film at GCE/MWCNTs-Os 186

5. The interest of SWCNTs for $[Cp^*Rh(bpy)Cl]^+$ immobilization: towards a device operating in reduction 189

5.1 $[Cp^*Rh(bpy)]^{2+}$ as suitable mediator for NADH regneration 189

5.2 Substituent effects and mediator immobilization attempts 190

5.3 Interest of carbon nanotubes as immobilization support 192

6. Conclusion 194

References 195

Conclusion and outlook ---------- **201**

Appendix ---------- **209**

Abbreviations

Materials:

DSDH: D-sorbitol dehydrogenase

GatDH: Galactitol dehydrogenase

DI: Diaphorase

NAD^+: β-Nicotinamide adenine dinucleotide

NAD^+-dextran: β-Nicotinamide adenine dinucleotide-dextran

PEI-NAD^+: Poly (ethylenimine)-NAD^+

NAD-GPS: NAD^+-Glycidoxypropylsilane

Fc-NAD: Ferrocene-boronic acid-NAD^+

NADH: β-Nicotinamide adenine dinucleotide (reduced dipotassium salt)

TEOS: Tetraethoxysilane

TMOS: Tetramethoxysilane

APTES: Aminopropyltriethoxysilane

GPS: 3-Glycidoxypropyl-trimethoxysilane

PDDA: Poly(dimethyldiallylammonium chloride)

PAA: Poly (allylamine)

PEI: Poly (ethylenimine)

FDM: Ferrocenedimethanol

FM: Ferrocenemethanol

MG: Methylene green

MB: Meldola's blue

Nb: Nile blue

NF: Nafion, perfluorinated ion-exchange resin

PMG: Poly (methylene green)

PEI-Fc: Ployethylenimine-ferrocene

Fc-silane: Ferrocene functionalized organoalkoxysilane

MWCNTs: Multiwalled carbon nanotubes

SWCNTs: Single-walled carbon nanotubes

Tris: Tris(hydroxymethyl) amino-methane

PBS: Phosphate buffer solution

Electrodes:

CE: Counter electrode

WE: working electrode

GCE: Glassy carbon electrodes

MGE: Macroporous gold electrodes

Techniques

CV: Cyclic voltammetry

UV: UV-vis spectrophotometry

IR: infrared spectrophotometry

GPES: General Purpose Electrochemical System

SECM: Scanning electrochemical microscopy

SEM: Scanning electron microscopy

Preface

Considerable interests have been drawn in the development of electrochemical reactors for the manufacture of fine chemicals with dehydrogenases as a process with almost zero waste emission. The system requires that all active compounds like cofactor, mediator and dehydrogenase can be functionally immobilized on the working electrode surface in such a way that dehydrogenases are durably immobilized and active, their cofactor is durably immobilized close to the enzyme, and the mediator can reduce the overpotential without leaching. However, it is still a challenge to construct this kind of functional layer with long term stability. This is the goal of the present thesis prepared in the frame of an European program (ERUDESP, enantioselective……).

Stable immobilization of active enzyme on electrodes is a prerequisite for bio-electrochemical applications. Sol-gel-derived silica-based materials have proven to provide a rather suitable environment for biomolecules entrapment, ensuring conformation changes similar to their water solution and even enhanced stability. The quite recent development of the electrochemically-assisted deposition of sol-gel silica thin films opens new opportunities for enzyme encapsulation into sol-gel thin film onto electrode surfaces [1]. In this method, a sufficiently negative potential was applied to the electrode surface to generate hydroxyl ions, which play the role of the catalyst for the polycondensation [2]. In comparison with the traditional sol-gel methods which involve deposition by evaporation (dip-, spin-, spray-coating) and can only be applied to basically flate surfaces, the combination of electrochemistry with the sol-gel process makes possible the well controlled modification of complex electrode surfaces, for example, macroporous gold electrodes. This approach is promising for the electrochemical biocatalysis application. Although there have been a long history of studying and using sol-gel material to encapsulate enzymes, little has been reported regarding the encapsulation of enzyme in sol-gel silica films in the course of their electrodeposition, especially for dehydrogenase encapsulation.

The realization of cofactor regeneration with both the dehydrogenase and its cofactor immobilized is the biggest challenge in construction of the functional layer. One obstacle for this approach is that the water soluble cofactor is a relatively small molecule, so it is likely to diffuse away from the electrode surface into solution, thus limiting the long-time durability of the

modified electrode. Another obstacle is that high overpotential at electrode surfaces leading to undesired side reactions producing enzymatically-inactive dimers and isomers of cofactors. As far as biocatalysis with electrochemical regeneration of cofactor is concerned, the effectiveness of electron transfer is a key parameter affecting the performance of the process so that the resort to charge transfer mediators has often been proposed to improve the turnover of the overall reaction. However, further difficulties may arise with many mediators due to their poor stability or due to electrode modification procedures.

Taking into account the above problems that are likely to exist in the construction of such functional films, this research developed a series of sol-gel immobilization matrixes to improve the perfomance and long-term stability of the biocomposite films. The details are summarized as follows:

In Chapter I, the first part is devoted to a brief introduction to the ERUDESP project and to a definition of the subject. Then, we describe the main immobilization methods of enzyme, cofactor and mediator reported sofar in the literature.

In the experimental section (Chapter II), we describe the physico-chemical properties of the studied compounds, various sol-gel preparation methods, electrode modifications and the experimental techniques used in this work.

In Chapter III, we show the feasibility of dehydrogenase encapsulation in sol-gel matrices by both drop-coating and electrodeposition. DSDH was found to be very sensitive to the silica gel environment, first, the influence of polyelectrolyte additives on the sol-gel encapsulation of dehydrogenases has been evaluated by drop-coating. Then, we report that the electrochemically-assisted deposition of silica thin films can be a good strategy for DSDH immobilization as well as DSDH and diaphorase co-immobilization in an active form (Diaphorase is an useful enzyme to catalyze cofactor regeneration in a smooth way).

In Chapter IV, one has compared various strategies for cofactor immobilization in sol-gel matrices, i.e. the simple encapsulation of the native cofactor, the encapsulation via attachment to a

high molecular weight compound (NAD-Dextran), the adsorption on carbon nanotubes introduced in the sol-gel matrix and finally the use of glycidoxypropylsilane (GPS) as additive.

In Chapter V, the immobilization of mediators (ferrocene species and osmium polymer) in the sol-gel matrix is first studied. The influence of GPS as additives for the mediator immobilization is also presented. Then, the feasibility of co-immobilization base on sol-gel film is evaluated by one step drop-coating and electrodeposition.

In Chapter VI, different strategies for mediator immobilization on CNTs are developed. Here, the co-immobilization strategies base on CNTs/sol-gel matrix are used to develop a reagent free device because of the problems encountered with mediator immobilization through one step electrodepostion in chapter V. The first layer of CNTs functionalized with mediator is covered with an additional drop-coated or electrodeposited sol-gel layer containing the dehydrogenase (and eventually diaphorase) and the cofactor covalently bond to GPS.

[1] Shacham, R.; Avnir, D.; Mandler, D., *Adv. Mater.* **1999,** *11*, 384

[2] Walcarius, A.; Mandler, D.; Cox, J. A.; Collinson, M. M.; Lev, O., *J. Mater. Chem.* **2005,** *15*, 3663.

Chapitre I. Introduction

Ce chapitre introductif présente tout d'abord le projet ERUDESP dans le cadre duquel s'est déroulé ce travail de thèse. L'objectif de cette étude était la co-immobilisation au sein d'une couche mince sol-gel d'une déshydrogénase, du cofacteur enzymatique NAD^+ et du médiateur électrochimique permettant de catalyser la régénération électrochimique de ce cofacteur. Cette couche mince devant ensuite être déposée sur la surface interne d'une électrode d'or macroporeuse et être intégrée dans le réacteur pour application en électrosynthèse enzymatique (ces derniers travaux étant menés dans le projet ERUDESP, mais hors du cadre de cette thèse).

L'état de l'art sur les différents aspects de ce projet est ensuite donné (chap. I). Les méthodes couramment utilisée pour obtenir l'immobilisation d'une protéine sous une forme active à la surface d'une électrode sont présentés. Le procédé sol-gel et son application en bioencapsulation sont décrits. Enfin la génération de couche minces sol-gel par assistance électrochimique est présentée ainsi que son utilisation pour l'immobilisation de protéines.

Nous discutons ensuite des difficultés et des besoins concernant l'immobilisation du cofacteur enzymatique NAD^+ et de sa régénération électrochimique à l'aide de médiateurs électrochimiques dans le cadre particuliers de l'électrosynthèse enzymatique. Les méthodes conventionnelles pour la régénération du cofacteur sont alors présentées. Finalement, une revue des travaux existant sur la co-immobilisation de déshydrogénases, du cofacteur enzymatique et de médiateurs est donnée.

La présentation de cette étude expérimentale a été organisée en différents chapitres décrivant les étapes successives de cette recherche. L'encapsulation de déshydrogénase au sein de la matrice sol-gel a tout d'abord été décrite, par les méthodes de drop-coating et d'électrogénération. Bien que l'encapsulation de protéines, voire de déshydrogénase au sein de couches minces sol-gel ait été décrite, il est vite apparu que la matrice de silice perturbait fortement l'activité enzymatique de la protéine. L'addition de charges positive au sein du matériau sol-gel, par introduction de polyélectrolyte chargés positivement dans le sol, a alors permis l'encapsulation de déshydrogénases sous leur forme active. Le matériau sol-gel peut alors être déposé sur l'électrode sous forme de couche mince par évaporation ou par électrogénération (chap. III). La co-immobilisation de la déshydrogénase avec une diaphorase a également été étudiée. La diaphorase catalyse alors l'oxydation de NADH en présence d'un médiateur électrochimique en solution, par exemple le ferrocenedimethanol.

La déshydrogénase catalyse les réactions d'oxydation ou de réduction du substrat enzymatique en présence du cofacteur NAD^+/NADH. Contrairement à d'autres cofacteurs enzymatiques qui sont liés à la protéine (par exemple FAD), NAD^+ est libre de diffusé en solution. Il y a alors un grand intérêt à immobiliser cette molécule pour limiter le coût du procédé (en diminuant la quantité de molécules utilisées). Différentes stratégies d'immobilisation ont été comparés dans le chapitre IV, la simple encapsulation dans le sol-gel, l'adsorption sur des nanotubes de carbone immobilisés, l'encapsulation du NAD^+ chimiquement lié à la macromolécule dextran pour limiter sa diffusion et enfin la condensation avec le groupement epoxy du glycidoxypropylsilane (GPS). Ce dernier système a ensuite été utilisé pour élaborer une couche mince sol-gel dans laquelle sont co-immobilisées la déshydrogénase (et éventuellement la diaphorase), le cofacteur enzymatique NAD^+ et le médiateur électrochimique. Plusieurs stratégies ont été mises en œuvre, en incorporant le médiateur dans la matrice sol-gel (Chap. V) ou en utilisant des nanotubes de carbone fonctionnalisés (Chap. VI). Une attention particulière a été donnée à la préparation de la couche mince sol-gel par électrogénération. Nous verrons ainsi que si de nombreux systèmes peuvent fonctionner lorsqu'ils sont préparés par évaporation, il est beaucoup plus difficile d'atteindre la co-immobilisation de tous les éléments autorisant leur communication lorsque le matériau est généré électrochimiquement. Bien que la plupart des travaux aient été menés pour obtenir un système bioélectrocatalytique fonctionnant en oxydation, nous avons également étudié l'immobilisation sur nanotubes de carbone d'un médiateur électrochimique à base de rhodium permettant de catalyser la réduction de NAD^+.

Chapter I. Introduction

In the chapter, we start by the introduction of the ERUDESP project and the definition of the PhD subject. We then discuss the immobilization of enzymes on electrode surfaces. We recall some of the conventional enzyme immobilization methods, in particular, we introduce the sol-gel materials for enzyme encapsulation and electrochemically-assisted generation of silica films for bioencapsulation. After that, we also discuss the need for cofactor immobilization and regeneration as well as the immobilization of charge transfer catalyst on electrode surfaces. We explain the necessity and difficulties of cofactor immobilization and regeneration, and introduce the conventional methods to modify the electrode and to regenerate the cofactor. At last, we describe the functional films for co-immobilization of dehydrogenase, cofactor and mediator, and review the work of the literature dealing with such reagentless system.

1. ERUDESP project

The project full title is “Development of Electrochemical Reactors Using Dehydrogenases for Enantiopure Synthon Preparations” (ERUDESP website: http://www.erudesp.eu). The main objective of the project is the development of electrochemical reactors for the manufacture of fine chemicals with dehydrogenases as a process with almost zero waste. The production of enantiopure compounds with high enantiomeric excess (EE) can be achieved by using dehydrogenases as biocatalysts, because they express high enantioselectivity in ketone reduction combined with broad substrate spectra by some of these enzymes. As these dehydrogenases typically require co-substrate regeneration by aid of a second enzymatic reaction, we are looking for alternative solutions for cofactor regeneration to avoid the contamination of the reaction fluid by other proteins and chemical compounds. In this project we will use an electrochemical approach for the regeneration of cofactors.

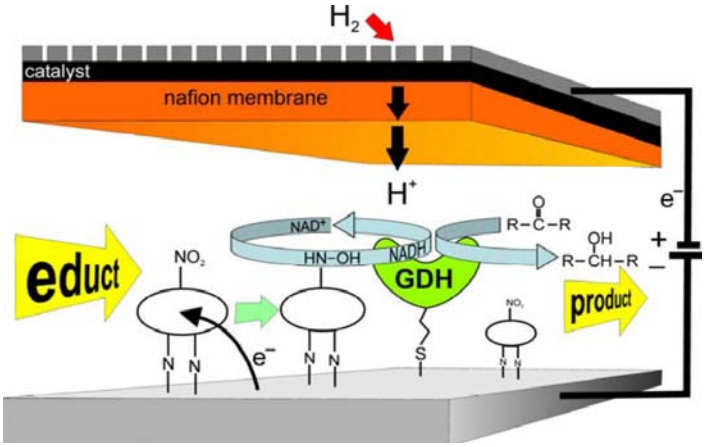

Figure I-1. *Model of an electrochemical reactor for enantiopure synthon preparation. Since all active compounds (mediator, cofactor, dehydrogenase) are immobilized only the educt and the product are components of the reaction buffer. The gas diffusion counter electrode provides clean protons and improves the long-term stability.*

Figure I-1 shows the scheme of an electrochemical reactor for enantiopure synthon preparation. Two main electrochemical reactions occur in the electrochemical reactor. Hydrogen gas is oxidized into a mixture of hydrogen ions and electrons on the anode side of the cell, then, hydrogen ions diffusion through a nafion membrane to the cathode side of the cell. If all active compounds like the mediator, the cofactor and the dehydrogenase can be functionally immobilized on the working electrode surface (on the cathode of the cell), educt in the input flow will be reduced into the product in the output flow avoiding any contaminations. The interesting thing is that the same electrochemical reactor can also be used

for oxidation reaction. In this case, all active compounds will be immobilized on the anode side of the cell. Oxygen continuously passes over the cathode, which react with the electrons and protons (coming from the oxidation reaction at the anode side of the cell) to form water. As counter electrode a gas diffusion electrode will be employed; it delivers clean protons (no liquid anolyte!) to the catholyte and simultaneously reduces the cell voltage by about 1 V; hence undesired side reactions/degradation processes will be suppressed and thus the long-term stability of the whole electroenzymatic system will be improved.

There are six participants in this project. **Participant 1** (*Saarland University, Germany*) includes two groups: Physical Chemistry and Applied Microbiology. The Physical Chemistry group designed of electrochemical multicell with 16 individual cells and electrochemical reactor with a macroporous working electrode and a proton conducting membranes/gas diffusion counterelectrode. The Applied Microbiology group provided several dehydrogenases with enhanced stability and activity in the environment of the developed electrode surfaces. **Participant 2** (*Ecole Nationale Supérieure de Chimie et de Physique de Bordeaux, Molecular Sciences, France*) developed macroporous metal electrodes with high surface area support to immobilize mediators and enzymes in functional internal surface layers using a sol-gel matrix prepared and optimized by partner 3. **Participant 3** (*CNRS, Laboratory of Physical Chemistry and Microbiology for the Environment, France*) developed electrode surface layers for functional immobilization of enzymes, cofactors and mediators. **Participant 4** (*University of Copenhagen*, *Denmark*) included two groups: Biophysical Chemistry Group and Dept. of Chemistry, Bioinformatics. The biophysical group crystallized the dehydrogenases produced by partner 1b and determined their three-dimensional atomic structures by crystallographic methods. The bioinformatics group used computer modeling to provide a molecular level description of how the enzyme activities and stabilities can be enhanced. **Participant 5 (***Middle East Technical University, Turkey)* This group developed mediators for electron transfer to the cofactor NAD^+ in the described systems. **Participant 6** (IEP GmbH Wiesbaden IEP, Germany) supported the project from an industrial point of view.

In this project, we are **Participant 3**, my PhD research was focused on designing functional layers based on silica sol-gel thin films to co-immobilize enzyme, cofactor and electron mediator to get the active systems and such modifications of electrode surfaces should be adaptable to the macroporous electrodes. Initially, the reduction of prochiral ketones to enantiopure hydroxylated products was the most desirable reaction. However, a major obstacle was encountered with the loss of reduction mediator activity upon immobilization on

electrode surface. The analyses of the actual market by the industrial partner demonstrated that the production of rare sugars was also interesting. Therefore, the oxidation of sugar alcohols to rare sugars with electrochemical cofactor oxidation has also come into focus of the project.

2. Immobilization of enzymes on electrode surfaces

The development of a simple and effective strategy for immobilizing enzymes on or into an electrode is a crucial step in the design and fabrication of electrochemical biosensors, bioreactors or biofuel cells. Ideally, this immobilization should be totally irreversible and stable with time, without deactivation of the biomolecule, while managing excellent accessibility to this biomolecule and ensuring a certain conformational mobility [1]. Adsorption [2, 3], covalent grafting [4, 5], and entrapment [6, 7] are conventional immobilization methods. Adsorption is a rather soft and the simplest immobilization method, but the disadvantage of the method is the low mechanical strength of the assembly. Desorption phenomena are regularly observed when environmental conditions (pH, ionic strength) change. Covalent grafting is a chemical immobilization technique consisting of creating a covalent bond between the sensitive element and the support. This technique permits the orientation of the grafted molecules and thus optimization of the recognition probability. However, deactivation and the irreversible immobilization of the enzyme components restrict the performance of these types of enzyme immobilization. Entrapment of the receptor in a host matrix can be done by simply mixing the various components and depositing the mixture onto a suitable support. This method is the most widespread. A large diversity of materials is thus used: inorganic materials, natural or synthetic organic polymers. However, steric stresses and interactions with the matrix may denature the species. Also diffusional limitations may occur when the receptor is not sufficiently accessible. Some other immobilized schemes and advanced materials that can improve the analytical capacities of sensor devices are highly desired.

The last decade has seen a revolution in the area of sol-gel-derived biomaterials since the demonstration that these materials can be used to encapsulate biological species such as enzymes, antibodies and other proteins in a functional state [8]. Upon encapsulation, the biomolecules retain their spectroscopic properties and biological activity [9, 10]. Silica Sol-gel could offer some advantages such as improved mechanical strength and chemical stability.

It does not swell in aqueous or organic solvents, preventing leaching of entrapped biomolecules. Silica sol-gel materials are particularly interesting, because they can be synthesized with a large variety of organic functionalities, such as hydrophobic or hydrophilic ones [11, 12, 13]. They can be used to retain metallic complexes (e.g., mediators) by covalently grafting, electrostatic pH dependent interaction or simply as adsorption by the intermediate of weak physical bonds [11]. The trapped biomolecules reside in an interconnected mesoporous network and become part of the entire material [13], and they usually exhibit better activity and longer life times than free enzymes. During encapsulation, they remain trapped within a silica cage tailored to their size, and it provides a chemical surrounding that favours the activity (***Figure I-2***)). Sol-gel immobilization is characterized by physical entrapment without chemical modification. This approach also permits the biomolecules to be isolated and stabilized against aggressive chemical and thermal environments [10, 13]. While the relatively large biomolecules are immobilized within the silica network, small ions or molecules can be easily transported into the interior of the matrix, which has been largely exploited in the field of biosensors [9, 14, 15].



Figure I-2. *The enzymes entrapped in sol-gel matrices [8].*

2.1 Sol-gel process [16]

A sol is a stable dispersion of colloidal particles or polymers in a liquid. Colloids are solid particles with diameters of 1-100 nm. A gel is an interconnected, rigid network with pores of submicrometer dimensions and polymeric chains whose average length is greater than a micrometer. A silica gel may be obtained by formation of an interconnected 3-D network by the simultaneous hydrolysis and polycondensation of a precursor. When the pore liquid is removed as a gas phase from the interconnected solid gel network under hypercritical conditions, the network does not collapse and a low density aerogel is produced. The sol-gel process generally involves the use of alkoxide precursors, which undergo hydrolysis, condensation, aging and drying to give gels or xerogel.

2.1.1 Hydrolysis

The preparation of a silica glass begins with an appropriate alkoxide, such as $Si(OR)_4$, where R is mainly CH_3, C_2H_5, or C_3H_7, which is mixed with water and a mutual solvent to form a solution. Hydrolysis leads to the formation of silanol groups (SiOH). It has been well established that the presence of H_3O^+ in the solution increases the rate of the hydrolysis reaction.

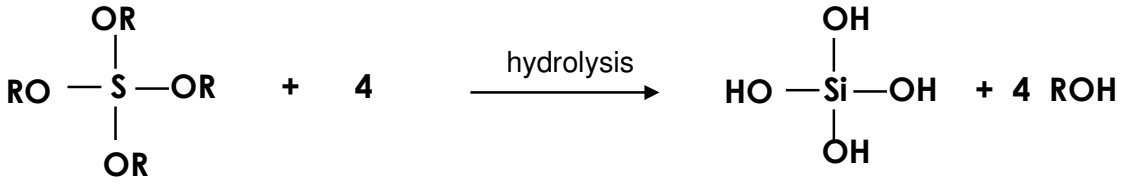

Alkoxysilane

2.1.2 Condensation

In a condensation reaction, two partially hydrolyzed molecules can link together through forming siloxane bonds (Si-O-Si). This type of reaction can continue to build larger and larger silicon-containing molecules (linkage of additional Si-OH) and eventually results in a SiO_2 network. The H_2O (or alcohol) expelled from the reaction remains in the pores of the network. When sufficient interconnected Si-O-Si bonds are formed in a region, they respond cooperatively as colloidal (submicrometer) particles or a sol.

The gel morphology is influenced by temperature, the concentrations of each species (attention focuses on R ratio, R = $[H_2O]/[Si(OR)_4]$), and especially acidity:

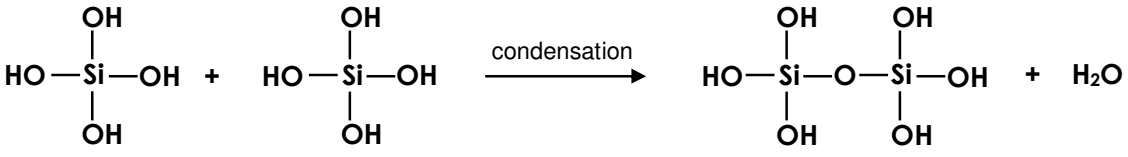

- Acid catalysis generally produces weakly-crosslinked gels which easily compact under drying conditions, yielding low-porosity microporous (smaller than 2 nm) xerogel structures (***Figure I-3a***).

- Conditions of neutral to basic pH result in relatively mesoporous xerogels after drying, as rigid clusters a few nanometers across pack to form mesopores. The clusters themselves may be microporous (***Figure I-3b***).
- Under some conditions, base-catalyzed and two-step acid-base catalyzed gels (initial polymerization under acidic conditions and further gelation under basic conditions [17, 18]) exhibit hierarchical structure and complex network topology (***Figure I-3c***).

2.1.3 Aging

Gel aging is an extension of the gelation step in which the gel network is reinforced through further polymerization, possibly at different temperature and solvent conditions. During aging, polycondensation continues along with localized solution and reprecipitation of the gel network, which increases the thickness of interparticle necks and decreases the porosity. The strength of the gel thereby increases with aging. An aged gel must develop sufficient strength to resist cracking during drying.

2.1.4 Drying

The gel drying process consists in removal of water from the interconnected pore network, with simultaneous collapse of the gel structure, under conditions of constant temperature, pressure, and humidity. Large capillary stresses can develop during drying when the pores are small（＜20 nm). These stresses will cause the gels to crack catastrophically unless the drying process is controlled by decreasing the liquid surface energy by addition of surfactants or elimination of very small pores, by hypercritical evaporation, which avoids the solid-liquid interface, or by obtaining monodisperse pore sizes by controlling the rates of hydrolysis and condensation.

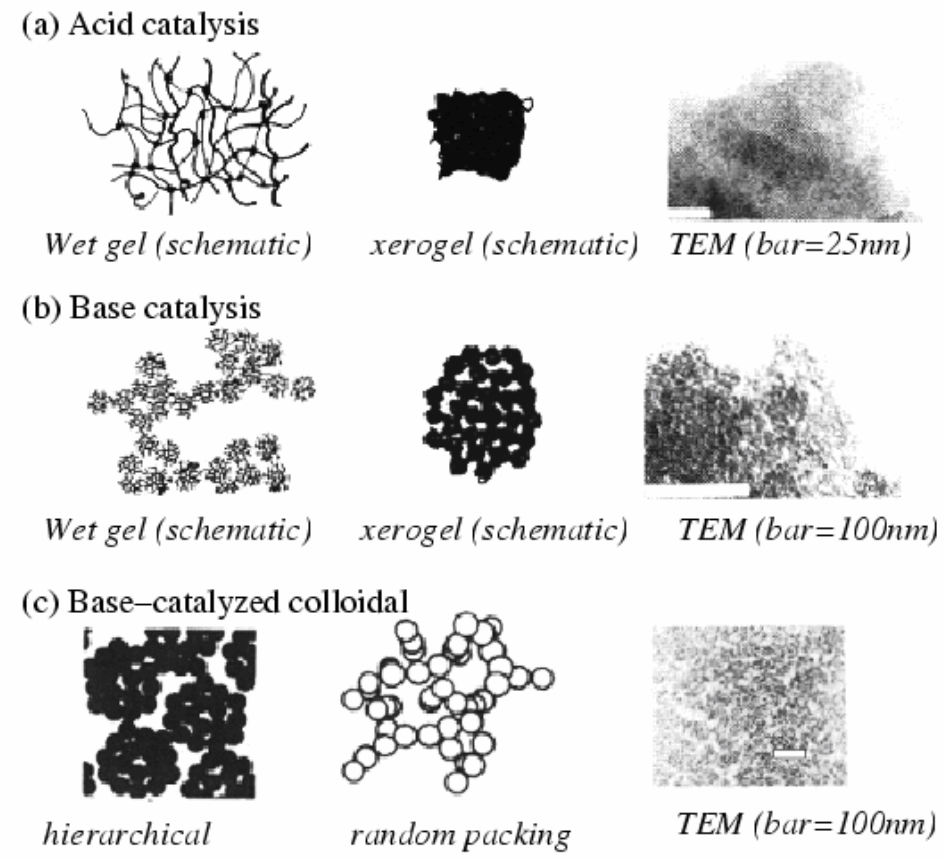

Figure I-3. *Schematic wet and dry gel morphologies and representative transmission electron micrographs. (Adapted from Brinker and Scherer, Sol Gel Science, chapter 9, figures 2a-2c. [19].)*

2.2 Optimization of the sol-gel process for bioencapsulation

Sol-gel is known to be a suitable matrix for bioencapsulation. However, sol-gel conditions are sometimes not mild enough for biomolecules. Recent efforts have been made to optimize the process by controlling the porosity of bioencapsulates and the chemical environment of trapped species [8]. This notably involved the use of biocompatible silane precursors, sugars and amino acid N-methylglycine or polymers.

2.2.1 Biocompatible silane precursors

The release of alcohol during the hydrolysis-condensation of silicon alkoxides has been considered an obstacle, due to its potential denaturing activity on the entrapped biological moiety. Biocompatible silane precursors have to be used for avoiding enzyme denaturation due to alcohol release. TMOS, $Si(OMe)_4$, is therefore currently used instead of TEOS, $Si(OEt)_4$, as methanol is less harmful than ethanol. However some enzymes are specially

sensitive to traces of alcohol so that the usual two-step alkoxide route has to be modified. One way to overcome this drawback would be to remove the alcohol via evaporation under vacuum in order to get a fully hydrolyzed solution before adding enzymes [20]. Aqueous sol–gel processes have been developed in order to avoid any trace of alcohol, for example a sodium silicate solution [21], or a mixture of sodium silicate and Ludox suspension [22]. Another way to avoid denaturation by alcohol is to use biocompatible alcohols such as polyol-based silanes as hydrolyzable groups that can be hydrolyzed under mild pH conditions [23]. A biocompatible reagent, glycerol, is produced so that the catalytic efficiency and long-term stability of enzymes are significantly improved [24].

2.2.2 Sugar and amino acid N-methylglycine additives

Sugar and amino acid N-methylglycine additives can be used to stabilize enzymes within sol-gel matrices. Chymotrypsin and ribonuclease T1 have been trapped in the presence of sorbitol and N-methylglycine. Both osmolytes significantly increase the thermal stability and biological activity of the proteins by altering their hydration and increasing the pore size of the silica matrix [25]. D-glucolactone and D-maltolactone have also been covalently bound via a coupling reagent aminopropyltriethoxysilane (APTES) to the silica network giving nonhydrolyzable sugar moieties. Firefly Luciferase, trapped in such matrices, has been used for the ultra sensitive detection of ATP via bioluminescent reactions [26].

2.2.3 Polymer additives

The silica matrix forms around the trapped biomolecule, but some shrinkage always occurs during the condensation process and the drying of the gel. Stresses can then lead to some partial denaturation of the enzymes. Polymers have been used as additives to form hybrid organic–inorganic gels in order to reduce shrinkage via a ‘pore filling’ effect. Some polymer additives such as polyethylene glycol (PEG) or polyvinyl alcohol (PVA) have been introduce in sol-gel matrix to increase the catalytic activity of entrapped enzyme [27, 28, 29].

Electrostatic interactions may also occur between silicate sites and specific residues on the protein surface. Silica surfaces are negatively charged above the point of zero charge (pH =3) and electrostatic interactions mainly depend on the isoelectric point of the protein. Sometimes, electrostatic interactions decrease the catalytic activity of the enzyme. However, the detrimental effects of these electrostatic interactions can be reduced by complexing the enzyme with a polyelectrolyte that shields the critical charged sites [30, 31].

2.3 Electrochemically-assisted generation of silica films

2.3.1 Principle and significant

Usually, sol-gel silica films are prepared by polycondensation of silicon alkoxides (alone or in the presence of organosilanes) as induced by evaporation of a sol solution via spin-coating, dip-coating or spraying. When the sol is doped with biomolecules, the silica framework is formed around them, leading to the desired composite films containing physically encapsulated biomolecules [32]. Such "conventional" sol-gel film formation procedures are however restricted to flat surfaces, which are unsuited to porous substrates. At the end of the nineties, a novel method to prepare silica-based thin films on electrode surfaces has been proposed by Shacham et al [33], involving an elegant combination of electrochemistry with the sol-gel process. The principle (***Figure I-4)*** is based on the electrochemical manipulation of pH on the electrode surface affecting thereby the kinetics associated to the sol-gel process. The electrode is immersed in a stable silica sol (mild acidic medium: pH 3-4) where a negative potential is applied to increase the pH locally at the electrode/solution interface, inducing therefore polycondensation of the silica precursors only on the electrode surface which makes the process applicable to deposit thin films on non-planar surfaces [34].

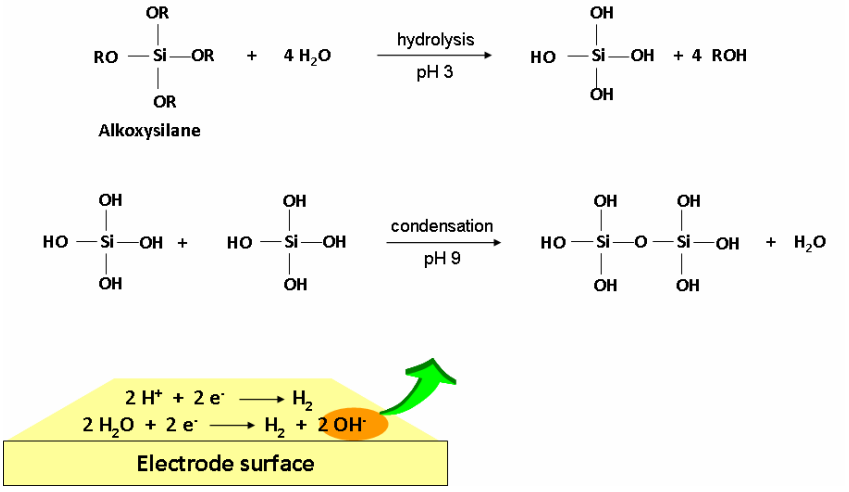

Figure I-4. *The principle of electrochemically-assisted generation of silica film on the electrode surface.*

The electrochemically-assisted generation of sol-gel thin films have been applied to produce porous silica deposits [35, 36], zirconia or titania thin films [37, 38], as well as

protective layers against corrosion [39]. The versatility of this novel process was also exploited to produce functionalized silica coatings [40] or molecularly imprinted silica films [41], which can be used for electrochemical sensing purposes [41]. It is noteworthy beyond these considerations that such electrochemically-assisted deposition can be advantageously combined with the surfactant templating process to generate highly ordered mesoporous silica films with unique mesopore orientation normal to the underlying support [42, 43] and this was also exploited to prepare vertically aligned silica mesochannels bearing organo-functional groups [44, 45].

2.3.2 Application in bioencapsulation

The developed electrochemically-assisted generation of sol gel thin films is interesting for biomolecules immobilization. ***Figure I-5*** shows the process of protein enscapsulated in thin sol-gel film through electrodeposition. In the presence of a biomolecule in the starting sol, this electrodeposition process leads to its encapsulation within the thin film, after washing and drying, a thin sol-gel film containing biomolecule modified electrode is obtained. The possible application was shown recently by some research groups [46, 47, 48]. Nadzhafova, et al. point out that electrogeneration of silica gel (SG) films on glassy carbon electrodes (GCEs) can be applied to immobilize biomolecules – hemoglobin (Hb) or glucose oxidase (GOD) or both of them in mixture [46]. After encapsulation, Hb was found to keep its peroxidase properties and GOD its enzymatic activity, and the biomolecules are very close to the electrode surface as direct electrochemistry has been pointed out. At the same time, Xia, et al. also present a strategy for the one-step immobilization of GOD in a 3D porous silica matrix using an electrochemically promoted sol gel process and bubble template [47], and the formed silica structure was proven to reduce mass transport resistance greatly because the porous structure existed. Tian, et al. report the development of microelectrode biosensors based on a Ruthenium Purple (RP)-coated gold electrode [48]. A desired gel layer is formed on the RP modified electrode using controllable sol-gel deposition technique to fabricate ATP and hypoxanthine amperometric biosensors. The formation of the gel film is not affected by the inner RP layer and the bioactivity of enzymes entrapped in gel film is well retained.

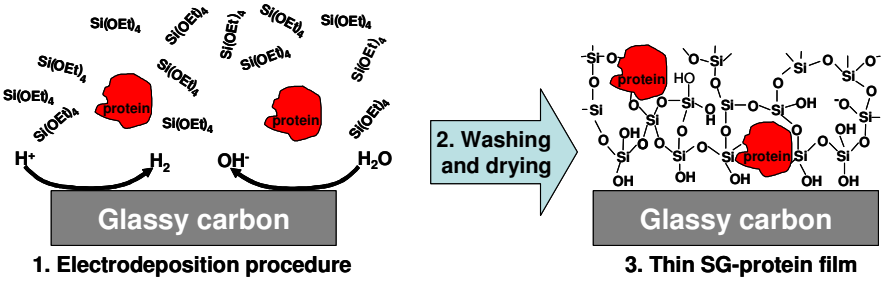

Figure I-5.*The process of protein enscapsulated in thin sol-gel film through electrodeposition.*

Despite these different examples, the application of electrochemically-assisted generation of sol gel thin films in bioencapsulation has been little exploited. To date, and to our knowledge, no attempt has been made to use this synthetic approach to entrap dehydrogenase in sol-gel silica films in the course of their electrodeposition, moreover, such modifications has not been applied to non-planar supports to functionalize the internal surfaces of macroporous (pore size, 0.5 - 1 μm) gold electrodes.

3. Dehydrogenase-based electrochemical reactor: the need for immobilization and cofactor regeneration

3.1 Enzymes and cofactor

Electroenzymatic reaction can provide a promising process to synthesize chiral compounds. Furthermore, in most cases no side reactions occur and therefore downstream processing can be simplified. It is reported that there are more than 250 NAD-dependent dehydrogenases and 150 NADP dependent dehydrogenases which can catalyze the oxidation/reduction of a variety of substrates. The advantage of dehydrogenase enzymes over the oxidases is that they are oxygen-independent, more abundant, and more substrate specific. [49].

The dehydrogenase needs a small molecule, called a cofactor, in order to be active [50]. The cofactor acts an acceptor or donor of small groups or atoms or electrons and provides the driving force for the oxidation or reduction of the substrate. The reactions are:

Oxidation reaction: $SH_2 + NAD(P)^+ \xrightarrow{\text{dehydrogenase}} S + NAD(P)H + H^+$

Reduction reaction: $S + NAD(P)H + H^+ \xrightarrow{\text{dehydrogenase}} SH_2 + NAD(P)^+$

Where SH_2 represents the reduced substrate and S the oxidized substrate, $NAD(P)^+$ and NAD(P)H represents respectively the oxidized and the reduced form of β-Nicotinamide adenine dinucleotide (***Figure I-6***).

However, the applications of dehydrogenase in electrosynthesis and biosensor are not yet a success story. This can be attributed to some restrictions in the use of dehydrogenases. The primary limitation is that, in contrast to oxidases, which have redox cofactors tightly bound within their molecules, the NAD(P) cofactor is not bound to dehydrogenase molecules. Therefore, unlike the case of oxidase-based biosensors, dehydrogenase-based systems cannot be readily incorporated into reagentless devices. The latter systems require that both a dehydrogenase and its cofactor are immobilized in such a way that a cofactor has an easy access to the enzyme. Another limitation in using dehydrogenases is the fact that their cofactors are recycled only at high potentials at most electrodes, which leads to interferences from redox active species and usually yield enzymatically inactive NAD-dimers [49].

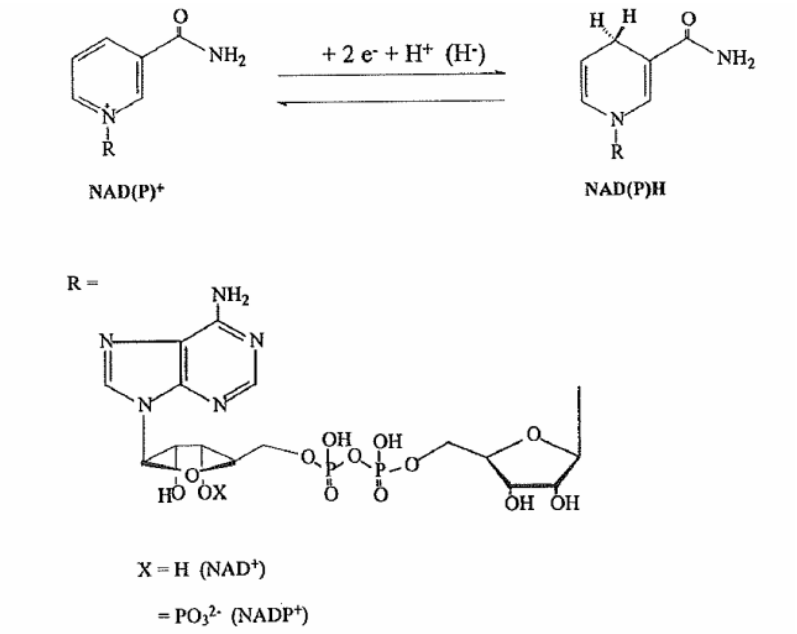

Figure I-6. *The structures of cofactors $NAD(P)^+$ and NAD(P)H.*

3.2 Cofactor immobilization

3.2.1 Physical entrapment

The easiest solution to immobilize the cofactor is to bulk-modify carbon paste like materials and this approach is quickly adopted for the majority of studies involving NAD-

dependent dehydrogenase electrode. In this case the cofactor is mixed with carbon power and a binder (typically paraffin oil) before being packed into a cavity to form the electrode [51]. Noguer et al. designed amperometric acetaldehyde biosensor based on sol-gel immobilization of aldehyde dehydrogenase (AlDH) and NAD^+ on screen-printed electrodes [52]. However, the simple encapsulation displays a major drawback, as it leads to rapid leaching of the cofactor in the solution during the electrochemical operation.

3.2.2 Covalent bonding

One possibility to improve the stability of the immobilization is the chemical attachment of the cofactor to a macromolecule that can be encapsulated or immobilized on the electrode without leaching. Mobility of the cofactor is vital for its efficient interaction with enzymes. The spacer is usually linked to the adenine moieties of the $NAD(P)^+$ molecule, and should provide some flexibility for the bioactive part of the cofactors, allowing them to be associated with the enzyme molecules. One approach of cofactor immobilization involves the covalent coupling of the $NAD(P)^+$ derivatives to some water-soluble polymers, dextran [53, 54, 55], poly(ethylenimine) (PEI) [56], poly(ethyleneglycol) (PEG) [57] or chitosan [49]. For example, a reagentless ethanol biosensor was developed by incorporating alcohol dehydrogenase, NADH-oxidase and NAD^+-dextran in a poly(vinylalcohol) (PVA) matrix on an electrode surface [54]. Zheng et al [56] explored a reagentless biosensor by using a ferrecene-labled high meolecular weight cofactor derivative (PEI-Fc-NAD^+). Mak et al [57] presents an amperometric formate biosensor using FDH and SHL coimmobilized with PEG-NAD^+ (MW=20 000) in a photopolymerized PVA matrix in front of a Clark- electrode. Zhang et al [49] developed an electrochemical biosensor through the co-immobilization of glucose dehydrogenase (GDH) and its cofactor NAD^+ on the scaffolds of a biopolymer chitosan, in this method, the dehydrogenase and the cofactor are covalently attached to the polymeric chains on the surface of the electrode. This electrode displays a good operational stability during continuous 25-h long experiments.

Of related interest is the immobilization of the cofactor on particles. Liu et al. reported that the cofactor NAD^+ covalently attached to silica nanoparticles could be successfully coordinated with particle-immobilized enzymes and enabled multistep biotransformations [58]. In this method, NAD^+ was immobilized onto the silica particles by forming covalent bonds through the epoxide group on the surface of Glycidoxypropyl trimethoxysilane (GPS)

functionalized silica nanoparticles. One limitation of covalent coupling comes from the rather complex modification, which results in a substantial decrease of cofactor efficiency. However, the reaction between epoxide group and the adenine moieties of the cofactor is rather simple, which allows good activity of cofactor to be detected with high stability. In the present work, we will consider GPS for direct attachment of NAD^+ in sol-gel thin film.

3.2.3 π-π stacking

The soft immobilization of NAD^+ on carbon nanotubes by π-π-stacking is also a promising avenue to avoid decrease of their efficiency. Zhou et al [59] describes a facile approach to the preparation of integrated dehydrogenase-based electrochemical biosensors through noncovalent attachment of NAD^+ onto carbon nanotubes with the interaction between the adenine subunit in NAD^+ molecules and multiwalled carbon nanotubes (MWCNTs). Compared with the existing methods for surface confinement of NAD^+ cofactor, this method is simple and is thus envisaged to be useful for general development of integrated dehydrogenase-based bioelectrochemical devices. To date, however, this method was not estimated with the use of additional electron transfer mediator.

3.3 Electrochemical cofactor regeneration

The electrochemistry of $NAD(P)^+$/NAD(P)H is highly irreversible, and the oxidation of NADH or the reduction of NAD^+ at bare electrode only occurs at high overpotential. Several efficient methods have been developed for cofactor regeneration. Syntheses where the cofactor $NAD(P)^+$ / NAD(P)H has to be regenerated to its oxidized/reduced state can be carried out with direct, indirect and enzyme-coupled electrochemical cofactor regeneration [60] (***Figure I-7***). Direct regeneration means that the species to be regenerated itself reacts at the electrode (***Figure I-7A***). Indirect regeneration means that another substance (a so-called mediator, ***Figure I-8***) acts as an electron shuttle between the electrode and the cofactor used (***Figure I-7B***). If a second enzyme is used as the electron shuttle the process is called enzyme-coupled electrochemical cofactor regeneration (***Figure I-7C***). Direct regeneration is not normally used in practice, so we only focus on indirect regeneration and enzyme-coupled electrochemical cofactor regeneration.

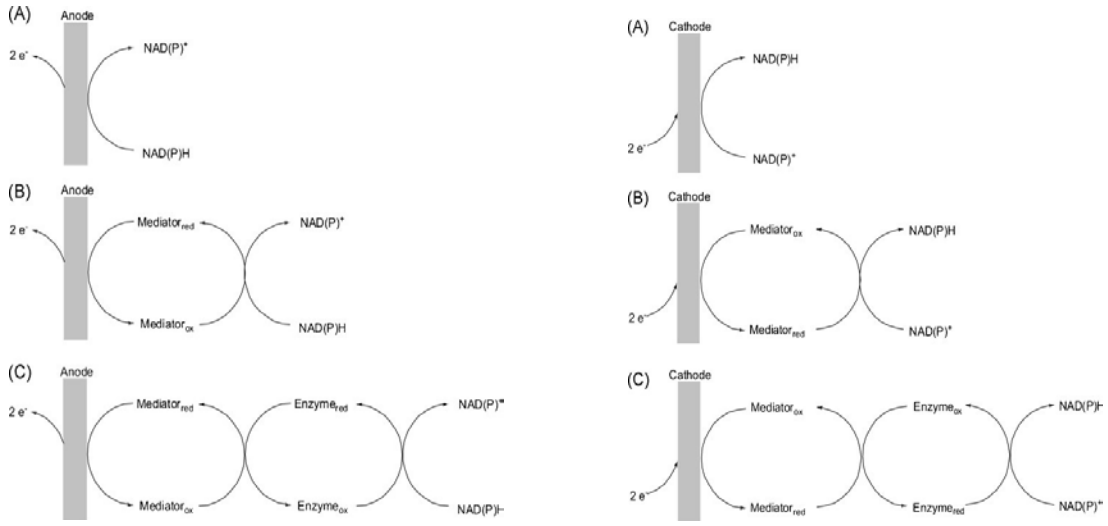

NAD(P)$^+$-dependent oxidation reactions NAD(P)H-dependent reduction reactions

Figure I-7. *NAD(P)$^+$/NAD(P)H-dependent reactions: (A) direct electrochemical regeneration, (B) indirect electrochemical regeneration, (C) enzyme-coupled electrochemical regeneration [60].*

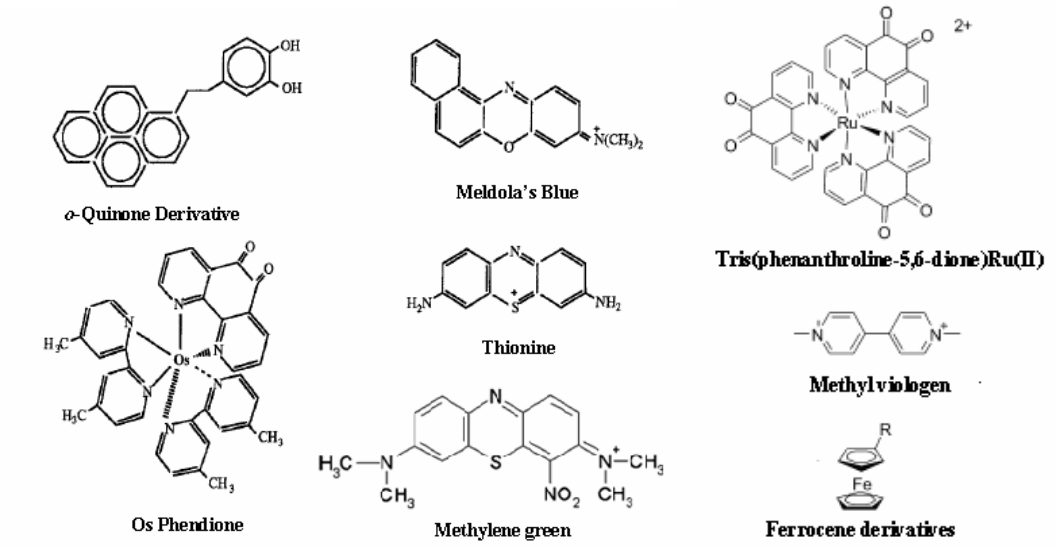

Figure I-8. *Structures of some typical mediators.*

3.3.1 Indirect electrochemical regeneration

Indirect electrochemical regeneration is widely used to overcome the problems of the high overpotential and the formation of inactive NAD-dimers. A mediator meeting the following criteria has to be applied [61]:

(1) The mediator must be stable.

(2) The electrochemical activation of the mediator must be possible at suitable potentials.

(3) The mediator must not transfer the electrons to the substrate.

(4) Only enzymatically active cofactor must be formed.

3.3.1.1 $NAD(P)^+$-dependent oxidation reactions

For the efficient electrochemical oxidation of NAD(P)H, mediated electrocatalysis is necessary, and a wide range of mediators has been studied. Organic compounds that undergo two-electron reduction-oxidation processes and also function as proton acceptors-donors upon their redox transformations have been found to be ideal for the mediation of NAD(P)H oxidation. Some redox mediators such as quinones [62,63,64], diamines [65, 66] and phenazine and phenoxazine dyes [67, 68, 69] have been used to recycle the NADH back to the enzymatically active NAD^+. The activity of these mediators toward the NADH oxidation has been explained in terms of a hydride transfer mechanism in which the mediator accepts the hydride and has the ability to delocalize the electrons. The oxidation of NADH has also been investigated using ferrocene derivatives [70], transition-metal complexes [71], conductive polymers [72, 73], nitrofluorenone derivatives [74, 75], dichloroindophenol [76], and tetracyanoquinodimethane-tetrathiafulvalene [77]. Some compounds demonstrate very high rates for the mediated oxidation of NAD(P)H in aqueous solutions. However, such mediator-based electrodes have displayed intrinsic difficulties, which were related to the limited stability of mediators and their leaching from the electrodes.

Another approach to the facilitated oxidation of NADH included the use of electrodes based on different forms of carbon, e.g., carbon nanotubes (CNTs) [78, 79, 80] and pyrolytic graphite [81]. Such materials significantly decreased the NADH overpotential, which was ascribed to the edge-plane sites/defects present in the pyrolytic graphite and suspected in CNTs [82]. Recently, one interesting paper demonstrates that further decrease in the NADH overpotential can be achieved at CNTs that were activated by microwaving CNTs in concentrated nitric acid [83], as indicated by a shift in the anodic peak potential of NADH (E_{NADH}) from 0.4 V to 0.0 V.

3.3.1.2 NAD(P)H-dependent reduction reactions

Contrary to the wide range of mediators available for NADH oxidation, the number of mediators for the regeneration of reduced cofactors is relatively small. The mediator for the

regeneration of reduced cofactors must indeed operate at potentials less cathodic than -0.9 V (otherwise direct electrochemical reduction of $NAD(P)^+$ will lead to dimmer formation) and more cathodic than the standard potential of the cofactor redox couple (i.e., -0.59V vs. SCE for NAD^+/NADH [84]) to make the reduction reaction thermodynamically feasible. The systems to date fulfilling these requirments are (2, 2'-bipyridyl)rhodium complexes, Rh(bpy)). The electrocatalytic process includes the regioselective transfer of two electrons and a proton to $NAD(P)^+$.

In these systems, hydrido-rhodium species are assumed to be the active catalytic moiety. Tris(bipyridine)rhodium (III) [85], (pentamethylcyclopentadienyl-2, 2'-bipyridine-chloro) rhodium (III) [86, 87], and chlorotris[diphenyl(m-sulfonatophenyl)phosphine] rhodium (I) [88] have been used as homogeneous mediation of electrons to $NAD(P)^+$. The catalytic efficiency of a series of Rh-complexes has been studied [89] and it was shown that the catalyst activity decreases in the presence of electron-withdrawing substituents in the 2, 2'-bipyridine ligand and increases by electron-donating substituents. Substituents in the 6-position of the ligand slow the catalytic reaction because of steric effects. Structure-activity relationships were found in the mechanism of the regioselective reduction of NAD^+ by Rh-complexes [90].

3.3.2 Enzyme-coupled electrochemical regeneration

When considering electrosynthesis applications, it is essential to perform a very smooth regeneration of the cofactor, especially if the cofactor is successfully immobilized with the protein(s), to prevent non-controlled oxidation of the expensive NADH (or reduction of NAD^+). The regeneration of NAD(P)H with the participation of mediator-contacted enzymes ensures that the regeneration of cofactor proceeds selectively, and only enzymatically active cofactor is produced.

3.3.2.1 $NAD(P)^+$-dependent oxidation reactions

It is possible to combine indirect regeneration of $NAD(P)^+$ with an enzymatic regeneration step. For example, diaphorase has been applied to oxidize NADH using a variety of quinone compounds [91], ferrocene derivatives [92, 93], or osmium redox polymers [94, 95] as mediators between the enzyme and electrode. Ferrocene/diaphorase is commonly employed for NAD^+ regeneration. Kashivagi et al. report the study on the characteristics of poly(acrylic acid) coated electrode coimmobilizing Fc and diaphorase and the application of the electrode to macro-electrocatalytic oxidation of NADH [92]. To continue the studies, this group has

carried out further immobilization of ADH into poly(acrylic acid) layer of the above modified electrode and achieved a smooth electrocatalytic oxidation of alcohol [93]. Osmium/diaphorase is also an efficient system for NAD^+ regeneration. Nikitina et al. report on the development of a bi-enzyme biosensor using diaphorase and formaldehyde dehydrogenase (FDH) as bio-recognition elements. The sensor architecture comprises a first layer containing diaphorase cross-linked with an osmium complex-modified redox polymer. On its top, a second layer was formed by additional cross-linking of FDH with poly(ethylene glycol)(400)diglycidyl ether [94]. Antiochia et al. develop an amperometric biosensor for glucose monitoring. Glucose dehydrogenase(GDH) and diaphorase (DI) were co-immobilized with NAD^+ into a carbon nanotube paste (CNTP) electrode modified with an osmium functionalized polymer [95].

NADH oxidase is also immobilized on the electrode surface for NAD^+ regeneration. Its stability and its range of useful pH are better than those of diaphorase. A series of dehydrogenase biosensors without cofactor addition have been developed by Marty's group, which depended on the immobilized NADH oxidase to regenerate NAD^+ [53, 54, 55]. The biosensors were developed through the combination of alcohol dehydrogenase, NADH oxidase and NAD-dextran with addition of a mediator hexacyanoferrate (III). The detection was based on the oxidation of the mediator hexacyanoferrate (III) by applying a potential difference of 100 mV between two platinum electrodes in the presence of an excess of hexacyanoferrate (III), corresponding to 250 mV versus SCE [53, 55]. Contrary to diaphorase, NADH oxidase also accepts oxygen as an electron acceptor. A reagentless sensor without addition of cofactor and mediator can thus be designed since oxygen is always present in the working medium [54]. NADH oxidase catalyses the reaction of NADH oxidation in the presence of oxygen to generate hydrogen peroxide. Hydrogen peroxide can be detected by applying a potential difference of 550 mV between two platinum electrodes, equivalent to ca. 600 mV versus SCE.

3.3.2.2 NAD(P)H-dependent reduction reactions

As it is very difficult to find an electrochemical redox catalyst that fulfils all requirements for regenerating NAD(P)H effectively, the interest of this second enzyme is to extend the choice of mediators that are likely to regenerate NAD(P)H. Many enzymes have been used in this context to provide the bioelectrocatalytic reduction of $NAD(P)^+$. ferredoxin-$NADP^+$ reductase (FNR) [96], lipoamide dehydrogenase (LipDH) [97], diaphorase [98, 99], alcohol

dehydrogenase [100], and hydrogenase [101, 102]. A variety of low potential electron-transfer mediators have been used to activate the reductive enzymes, for instance viologen derivatives [97, 98, 99], flavins [101], quinones [96], or the redox protein ferredoxin [103]. Some redox enzymes can directly communicate with electrode supports and thus stimulate the regeneration of the NAD(P)H cofactor. For example, hydrogenases (from *Rhodococcus opacus* and *Atcaligenes eutrophus H16*) have been successfully applied for the bioelectrocatalytic regeneration of NADH without the application of a redox-mediator [104]. However, the electrocatalytic rates of these systems are generally too slow to produce observable catalytic current on the cyclic voltammetric time scale. Among the electron-transfer mediators, viologen is often used in combination with enzyme for NADH regeneration. The viologen together with LipDH has been tested in a continuous process. Bergel et al. applied this regeneration system in their Dialysis-Membrane Electrochemistry Reactor (D-MER) together with an alcohol dehydrogenase for the synthesis of cyclohexanol from cyclohexanone [97]. Kashiwagi, et al present a poly(acrylic acid) coated graphite felt electrode immobilizing all the components of viologen, diaphorase, NAD^+, and alcohol dehydrogenase for the enzymatic reaction. NADH was regenerated with viologen together with diaphorase [98]. The regeneration system viologen/diaphorase is also used incombination with NAD^+ and D-lactate dehydrogenase, The optimal concentration of diaphorase, viologen and NAD^+ in the mediated electrocatalytic reduction of NAD^+ were studied by applying cyclic voltammetry [99].

Among the enzymes for cofactor regeneration, diaphorase is the most interesting one. The same diaphorase can be used for both NADH oxidation and NAD^+ reduction. The co-immobilization in active forms of both dehydrogenase and diaphorase would allow the reactor to perform alternatively oxidation or reduction reaction with simply changing the mediator system and the applied potential. For this reason the preparation of such active bio-composite layers would be of great value for electrosynthesis application.

4. Immobilization of charge transfer catalyst on electrode surface

For a technologyically useful configuration, the mediator must be immobilized on the electrode surface. A successful system should show good stability of the immobilized mediator, regenerate NAD^+ faster than it can be consumed by the enzyme, to appropriately

shift the dehydrogenase equilibrium towards the product side so that high current densities can be obtained. A wide variety of ways to immobilize mediator species at the electrode surfaces have been described in the literature. They are briefly summarized hereafter.

4.1 Carbon paste electrode

The carbon paste (CP) electrodes provide a straightforward way to immobilize the mediators. In several cases mediators have been directly incorporated in CP electrodes [105, 106, 107] to produce NADH and dehydrogenase substrate electrodes. Weiss et al. present a base-stable electron mediator, 3,4-dihydroxybenzaldehyde (3,4-DHB), modified electrode with the mediator mixed directly into the carbon paste [107]. The kinetics of the catalytic oxidation of NADH is studied at these modified carbon paste electrodes. However, the voltammograms were unstable and change upon continued scanning. The key element for such configurations is that the mediator has to have a higher affinity for the hydrophobic carbon paste phase than for the aqueous analytical matrix. This has not always been achieved, and mediator leaching could be the limiting stability factor in this case. To solve the problem, Yao, et al synthesized an oil-soluble mediator, 7-dimethylamine-2-methyl-3-b-naphtamido-phenothiazinium chloride (3-NTB) and apply the mediator to the CP/dehydrogenase electrode [108]. In the case of the 3-NTB modified electrode, 3-NTB was not soluble in an aqueous solution, so that the magnitude of the current response did not change for 2 weeks. Thus, the usage of an oil-soluble mediator can improve the long term stability of the CP electrode.

4.2 Surface activation

Surface activation approaches have also been reported in the last few years. As mentioned earlier, these electrodes cause electrocatalytic oxidation at lower potentials but not necessarily at those mediators. For example, electrochemical anodization [109, 110], microwave plasma [83], vacuum heat treatments [111] are used to improve the heterogenenous electron transfer rate of selected redox couples at various forms of carbon electrode. Remarkable stability and retention of the electrocatalytic activity were observed when carbon fibers were electro-activated, and this carbon fiber was used for NADH detection and discrimination from interferents with fast scan voltammetry [109, 110]. In a recent publication, CNTs were activated by microwaving in concentrated nitric acid, the shift in E_{NADH} was due to the redox mediation of NADH oxidation by traces of quinone species that were formed on the surface of treated CNTs [83].

4.3 Precipitation

One simple method included "precipitation" on electrode surfaces of various transition metal hexacyanoferrate [112]. Among the transition metal hexacyanoferrates, cobalt hexacyanoferrate is considered as attractive material to modify the electrode surfaces for NADH oxidation due to its excellent reversible redox behavior [113, 114]. The simple electrochemical deposition process can lead to the formation of the metal hexacyanoferrate on the electrode surface. In general, this type of modified electrodes, showed low detection limits, well behaved electrochemistry, fast response times, and high sensitivities to NADH, while being amenable to careful mechanistic studies and valid conclusions for mediator design for NADH electrochemical oxidation. However, their stability was generally low.

4.4 Monolayers

Various ways to immobilize mediator monolayers are available. Self assembled monolayers could be formed if the mediator contains groups that absorb strongly, such as thiol groups on gold [115,116]. Another way to form monolayers is to covalently attach the mediator to the electrode surface [117, 118]. To do this the electrode surface is first fuctionalized by generation of groups that will permit the subsequent covalent attachment of the mediators, for example, the surface of electrode could be functionalized by a strongly absorbed species, such as thiol compound on gold, which has an amino or carboxylic group at the other end. In this case, the sulfur strongly absorbs onto the gold surface, giving an electrode functionalized with NH_2 or COOH groups. The mediator species themselves can then be covalently attached to the electrode by forming a chemical bond to the NH_2 or COOH groups. Recently, one interesting application of the monolayer is developed. For the first time the inner surface of highly organized macroporous electrodes was modified with monlayer catalyst [119] and also a model bioelectrocatalytical system containg a redox mediator, a cofactor, and dehydrogenase [120, 121]. Such monolayer could provide a means to control the distribution and orientation of immobilized species, however, the concentration of mediator groups at the electrode surface is limited by steric packing constraints.

4.5 Electropolymerization

Conducting polymers are a natural choice for preparing arrays of voltammetric sensors because they have a rich electrochemical behavior and their electrochemical properties can be modulated by introducing chemical modifications in the sensitive materials [122]. Electropolymerization is a good approach to prepare polymer modified electrodes (PMEs) as adjusting electrochemical parameters can control film thickness, permeation and charge transport characteristics. PMEs have many advantages in the detection of analytes because of its selectivity, sensitivity and homogeneity in electrochemical deposition, strong adherence to electrode surface and chemical stability of the film [123]. Various dyes like Meldola blue [124], phenothiazine [125], thionine [126], and methylene green [127] have been immobilized on electrode by polymerization for detection of NADH at low potential. These films typically have a 10^{-6}-10^{-8} mol/cm^2 surface coverage and they present more important swelling problems in aqueous solutions than the previously mentioned adsorbed monolayers. These problems are reflected in longer response time, higher detection limit, and lower, in general, sensitivity for NADH detection.

5. Dehydrogenase, cofactor and mediator coimmobilization

Dehydrogenases have attracted considerable attention because they are of increasing interest for electroenzymatic synthesis, biosensor and bio-fuel-cells or biobattery. The main technological barrier in the fabrication these reagent free devices is the development of functional film allowing the stable immobilization of all component of the electrochemical detection like cofactor, mediator and dehydrogenase at the surface of the transducer. Ideally, the immobilization should be done in such a way (***Figure I-9***) that dehydrogenases are durably immobilized and active, the cofactor is durably immobilized close to the enzyme, and mediator can reduce the overpotential without leaching. Moreover, in this system, it is essential that the produced NADH (or NAD^+) is instantaneously consumed by the mediator (or another enzyme on the electrode surface for cofactor regeneration), otherwise the equilibrium will be reached and the further production of NADH (or NAD^+) will cease. The reduced (or oxidised) mediator in turn must also be rapidly reoxidised (or reduced) to recreate its active form. In essence, this means that all three reaction steps (enzymatic, mediated and electrochemical) need to occur very close in space for a successful approach. To achieve the

co-immobilization, a suitable matrix should be found, which should have good balance between the permeability of the substrate or products and the retention of the enzyme, cofactor and mediator. Consequently, and predictably, the development of this kind of functional film has been rather slow, only few examples in the application of biosensor are available. Typically, such biosensors have been designed using redox mediators to recycle enzyme cofactors and immobilizing the dehydrogenases and their cofactors by entrapping them in carbon pastes, membranes, composite materials, macroporous electrodes, and assembled layers. ***Table I-1*** shows the comparison of amperometric reagentless biosensors based on dehydrogenase/cofactor system. We can observe from the table, some of them show low sensitivity, some of them have the problem of the stability. So it is still a challenge to construct this kind of functional layer.

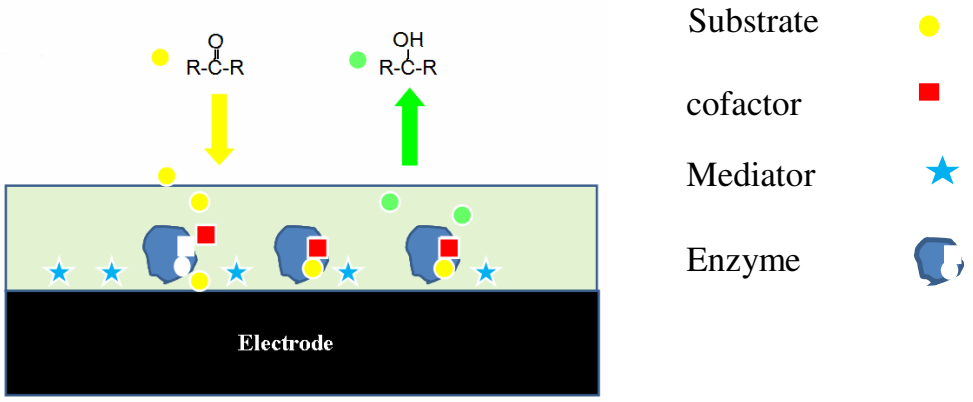

Figure I-9 *A scheme of functional film.*

Up to now, sol-gel chemistry was not considered for durable cofactor immobilization, which is however mandatory for the elaboration of reagentless devices. The focus of the thesis is on the comparison of different strategies in order to get the stable immobilization of a bi-enzymatic system (a dehydrogenase and a diaphorase), the cofactor NAD^+/NADH and an electron mediator in a sol-gel matrix deposited as a thin film on an electrode surface. This layer can be applied in electro-enzymatic synthesis, but the finding of this work can also be applied in reagent free amperometric sensors and bio-fuel-cells or biobattery.

Table I-1. *Comparison of Amperometric Reagentless Biosensors Based on Dehydrogenase /Cofactor System*

Sensor assembly[a]	Sensitivity (mA M^{-1} cm^{-2})	Stability[b]	Linear range (mM)	Ref
GC/CNT/GDI/CHIT/Nafion (GDH)	1.8	(24 h, 100%)/ (1.5 months, 64%)	0.02-2.0	49
GC/ TFC/Ca^{2+}/PL(GDH)	0.67	?	?	128
GC/ MB/Nafion(GDH)	0.49	?	?	127
CP/PS-TBO(GDH)	4.0	?	0.1-5.0	129
CP/PMA(GDH)	0.014	?/(4 months, ?)	5-36	130
CP/PMA/Nafion(GDH)	0.002	?	10-330	130
CP/osphendione(GDH)	?	(8 h, 92%)/(1 month, 92%)	?	131
CP/Ru complex(GDH)	?	?/(7 days, 60%)	?	132
CP/MB(GDH)	?	(1 day, 10%)	?-20	133
Au/Ca^{2+}/Nafion(GDH)	?	(10 cycles, ?)/?	?	134
GC/NAD^{+}/MWCNT(GDH)	?	?	0.01-0.30	59
Au/PEI-Fc-NAD (ADH)	?	?	?-30	56
Pt/PVA-SbQ/NADH oxidase /NAD-dextran/ cellophane membrane (ADH)	2	(80 assays)/(6 days)	0.0003-0.1	54

[a] GC*, glassy carbon;* TFC*, trinitrofluorenonecarboxylic acid;* PL*, polylysine;* MB*, Meldola Blue;* CP*, carbon paste;* PS*, modified polystyrene;* TBO*, toluidine blue O;* PMA*, polymethacrylate;* CHIT*, chitosan;* GDI*, glutaric dialdehyde*;; PVA-SbQ*, Poly(vinylalcohol) bearing styrylpyridinium groups;* GDH*, Glucose Dehydrogenase;* ADH*, Alcohol dehydrogenase; CNT, carbon nanotubes;* PEI-Fc-NAD, *A ferrocene-labeled high molecular weight cofactor derivative;?, not reported.* [b] *Operational stability (hours, h)/long-term stability (days or months).*

6. Objective beyond the state-of-the-art

Based on the works reported in the literature, we have first investigated in detail the preparation of different kinds of sol-gel routes for dehydrogenase encapsulation. It was known that protein and enzyme encapsulation into electrogenerated sol-gel thin films was possible [46, 47, 48]. However, first attempt to use similar approach for bioencapsulation of dehydrogenase was not successful. DSDH was found to be very sensitive to the silica gel environment. The addition of a positively-charged polyelectrolyte was necessary to ensure effective operational behavior of the biomolecules, which allow the successful encapsulation of dehydrogenase inside sol-gel matrix by using both drop-coating and electrodeposition (chapter III). Dehydrogenase is dependent on free diffusing cofactor in stoichiometric amounts to shuttle the redox equivalents from the enzyme to the substrate. We have investigated different strategies allowing the stable immobilization of this cofactor in the sol-

gel matrix (chapter IV). In order to overcome the inherent difficulties of cofactor regeneration, a common approach is to confine the mediator at the electrode surface to facilitate the interfacial electron transfer reaction. Several strategies for mediator immobilization have been developed and used for the elaboration of reagentless device with co-immobilized dehydrogenase and cofactor (chapter V and chapter VI). A special attention was given to the preparation of the sol-gel layer by electrochemically-assisted deposition. While several systems operated well when the sol-gel layer was prepared by drop-coating, it was much more difficult to co-immobiliz all the elements of the biocomposite by electrochemical deposition..... Most of the studies presented in this thesis have been performed in the oxidation reaction. In addition, we also studied the immobilization of Rh(III) mediator on carbon nanotubes for the electrocatalytic reduction of NAD^+.

References

[1] Fouletier, J.; Fabry, P., Chemical and biologyical microsensors, 1st Edition. John Wiley & Sons Chichester, UK, **2010**; p 140-142.

[2] Wollenberger, U.; Bogdanovskayn, V.; Bobrin, S., Enzyme electrodes using bio-electrocatalytic reduction of hydrogen peroxide. *Anal. Lett.* **1990**, *23(10)*, 1795-1808.

[3] Topoglidis, E.; Cass, A. E. G.; Gilardi, G., Protein adsorption on nanocrystalline TiO_2 films: an immobilization strategy for bioanalytical devices. *Anal. Chem.* **1998**, *70 (23)*, 5111-5114.

[4] Sacks, V.; Eshkenazi, I. ; Neufeld, T., Immobilized parathion hydrolase: an amperometric sensor for parathion. *Anal. Chem.* **2000**, *72 (9)*, 2055-2058.

[5] Zhang, G. J.; Zhou, Y. K.; Yuan, J. W., A chemiluminescence fiber-optic biosensor for detection of DNA hybridization. *Anal. Lett.* **1999**, *32 (14)*, 2725-2736.

[6] Zhang, Z. E.; Liu, H. Y.; Deng, J. Q., A glucose biosensor based on immobilization of glucose oxidase in electropolymerized o-aminophenol film on platinized glassy carbon electrode. *Anal. Chem.* **1996**, *68 (9)*, 1632-1638.

[7] Adeloju, S. B.; Moline, A. N., Fabrication of ultra-thin poly-pyrrole-glucose oxidase film from supporting electrolyte-free monomer solution for potentiometric biosensing of glucose. *Biosens. Bioelectron.* **2001**, *16 (3)*, 133-139.

[8] Avnir, D.; Coradin, T.; Lev, O.; Livage, J., Recent bio-applications of sol-gel materials. *J. Mater. Chem.* **2006,** *16(11)*, 1013-1030.

[9] Polska, K.; Fiedurek, J.; Radzki, S., Bioencapsulation of biologically active compounds in matrixes obtained by sol-gel method and its application. *Biotecnologia* **2007**, *1*, 77-95.

[10] Besanger, T. R.; Brennan, J. D., Entrapment of membrane proteins in sol-gel derived silica. *J. Sol-Gel Sci. Technol.* **2006**, *40(2/3)*, 209-225.

[11] Pierre, A. C., Sol-gel immobilization of catalytic molecules and applications: a review. *Adv. Sci. Technol.* **2006,** 45, 2127-2136.

[12] Tripathi, V. S.; Kandimalla, V. B.; Ju, H., Preparation of ormosil and its application in the immobilizing biomolecules. *Sens. Actuators B* **2006**, *114(2)*, 1071-1082.

[13] Lan, E.H.; Dunn, B.; Zink, J. I., Nanostructured systems for biological materials. *Meth. Molec. Biol*. **2005**, *300*, 53-79.

[14] Gupta, R.; Chaudhury, N. K., Entrapment of biomolecules in sol-gel matrix for applications in biosensors: problems and future prospects. *Biosens. Bioelectron.* **2007**, *22(11)*, 2387-2399.

[15] Xu, Z.; Chen, X.; Dong, S., Electrochemical biosensors based on advanced bioimmobilization matrices. *Trends Anal. Chem.* **2006**, *25(6)*, 899-908.

[16] Hench, L. L.; West, J. K., The sol-gel process. *Chem. Rev.* **1990**, *90(1),* 33-72.

[17] Brinker, C. J., Structure of sol-gel-derived glasses. Academic Press, Inc., Boston, **1990**, In Glass Science and Technology, *volume 4A*, 169-230.

[18] Brinker, C. J.; Clark, D. E.; Ulrich, D. R., Better Ceramics Through Chemistry. Materials Research Society, North-Holland, **1984**, *volume 32 of Symposia Proceedings*, 25-32.

[19] Brinker, C. J.; Scherer, G. W., Sol-Gel Science. Acad. Press, San Diego, 1990.

[20] Ferrer, M. L.; del Monte, F.; Levy, D., A Novel and Simple Alcohol-Free Sol-Gel Route for Encapsulation of Labile Proteins. *Chem. Mater.* **2002**, *14(9)*, 3619-3621.

[21] Bhatia, R. B.; Brinker, C. J.; Gupta, A. K.; Singh, A. K., Aqueous Sol-Gel Process for Protein Encapsulation. *Chem. Mater.* **2000**, *12(8)*, 2434-2441.

[22] Nassif, N.; Roux, C.; Coradin, T.; Bouvet, O. M. M.; Livage, J., Bacteria quorum sensing in silica matrices. *J. Mater. Chem.* **2004**, *14(14)*, 2264-2268.

[23] Gill, I.; Ballesteros, A., Encapsulation of biologicals within silicate, siloxane, and hybrid sol-gel polymers: an efficient and generic approach. *J. Am. Chem. Soc.*, **1998**, *120(34)*, 8587-8598.

[24] Besanger, T. R.; Chen, Y.; Deisingh, A. K.; Hodgson, R.; Jin, W.; Mayer, S.; Brook, M. A.; Brennan, J. D. Screening of Inhibitors Using Enzymes Entrapped in Sol-Gel-Derived Materials. *Anal. Chem.* **2003**, *75(10)*, 2382-2391.

[25] Brennan, J. D.; Benjamin, D.; DiBattista, E.; Gulcev, M. D., Using Sugar and Amino Acid Additives to Stabilize Enzymes within Sol-Gel Derived Silica. *Chem. Mater.,* **2003**, *15(3)*, 737-745.

[26] Cruz-Aguado, J. A.; Chen,Y.; Zhang, Z.; Elowe, N. H.; Brook, M. A.; Brennan, J. D., Ultrasensitive ATP detection using firefly luciferase entrapped in sugar-modified sol-gel-derived silica. *J. Am. Chem. Soc.*, **2004**, *126(22)*, 6878-6879.

[27] Reetz, M. T., Entrapment of biocatalysts in hydrophobic sol-gel materials for use in organic chemistry. *Adv.mater.***1997,** *9(12)*, 943-954

[28] Keeling-Trucker, T.; Rakic, M.; Spong, C.; Brenman, J. D., Controlling the Material Properties and Biological Activity of Lipase within Sol-Gel Derived Bioglasses via Organosilane and Polymer Doping. *Chem.mater.* **2000**, *12(12)*, 3695-3704.

[29] Pierre, A.; Buisson, P., Influence of the porous texture of silica gels on the enzymatic activity of lipases in esterification reactions. *J. Mol. Catal. B.* **2001**, *11(4-6)*, 639-647.

[30] Chen, Q.; Kenausis, L.; Heller, A., Stability of Oxidases Immobilized in Silica Gels. *J. Am. Chem. Soc.* **1998**, *120(19)*, 4582-4585.

[31] Heller, J.; Heller, A., Loss of Activity or Gain in Stability of Oxidases upon Their Immobilization in Hydrated Silica: Significance of the Electrostatic Interactions of Surface Arginine Residues at the Entrances of the Reaction Channels. *J. Am. Chem. Soc.* **1998**, *120(19)*, 4586-4590.

[32] Kandimalla, V. B.; Tripathi, V. S.; Ju, H., Immobilization of biomolecules in sol-gels: biological and analytical applications. *Crit. Rev. Anal. Chem.* **2006**, *36(2)*, 73-106.

[33] Shacham, R.; Avnir, D.; Mandler, D., Electrodeposition of methylated sol-gel films on conducting surfaces. *Adv. Mater.* **1999**, *11(5)*, 384-388.

[34] Sibottier, E.; Sayen, S.; Gaboriaud, F.; Walcarius, A., Factors affecting the preparation and properties of electrodeposited silica thin films functionalized with amine or thiol groups. *Langmuir* **2006,** *22(20)*, 8366-8373.

[35] Deepa, P. N.; Kanungo, M.; Claycomb, G.; Sherwood, P. M. A.; Collinson, M. M., Electrochemically deposited sol-gel-derived silicate films as a viable alternative in thin-film design. *Anal. Chem.* **2003**, *75(20)*, 5399-5405.

[36] Collinson, M. M.; Moore, N.; Deepa, P. N.; Kanungo, M., Electrodeposition of Porous Silicate Films from Ludox Colloidal Silica. *Langmuir* **2003**, *19(18)*, 7669-7672.

[37] Shacham, R.; Mandler, D.; Avnir, D., Electrochemically induced sol-gel deposition of zirconia thin films. *Chem. Eur. J.* **2004**, *10(8)*, 1936-1943.

[38] Shacham, R.; Avnir, D.; Mandler, D., Electrodeposition of dye-doped titania thin films. J. Sol–Gel Sci. **2004**, *31(1/2/3)*, 329-334.

[39] Sheffer, M.; Groysman, A.; Mandler, D., Electrodeposition of sol-gel films on Al for corrosion protection. *Corros. Sci.* **2003**, *45(12)*, 2893-2904.

[40] Sayen, S.; Walcarius, A., Electro-assisted generation of functionalized silica films on gold. *Electrochem. Commun.* **2003**, *5(4)*, 341-348.

[41] Zhang, Z.; Nie, L.; Yao, S., Electrodeposited sol-gel-imprinted sensing film for cytidine recognition on Au-electrode surface. *Talanta* **2006**, *69(2)*, 435-442.

[42] Walcarius, A.; Sibottier, E.; Etienne, M.; Ghanbaja, J., Electrochemically assisted self-assembly of mesoporous silica thin films. *Nat. Mater* **2007**, *6(8)*, 602-608.

[43] Goux, A.; Etienne, M.; Aubert, E.; Lecomte, C.; Ghanbaja, J.; Walcarius, A., Oriented Mesoporous Silica Films Obtained by Electro-Assisted Self-Assembly (EASA). *Chem. Mater.* **2009**, *21(4)*, 731-741.

[44] Guillemin, Y.; Etienne, M.; Aubert, E.; Walcarius, A., Electrogeneration of highly methylated mesoporous silica thin films with vertically-aligned mesochannels and electrochemical monitoring of mass transport issues. *J. Mater. Chem.* **2010**, *20(32)*, 6799-6807.

[45] Etienne, M.; Goux, A.; Sibottier, E.; Walcarius, A., Oriented mesoporous organosilica films on electrode: a new class of nanomaterials for sensing. J. Nanosci. Nanotechnol. **2009**, *9(4)*, 2398-2406.

[46] Nadzhafova, O.; Etienne, M.; Walcarius, A., Direct electrochemistry of hemoglobin and glucose oxidase in electrodeposited sol-gel silica thin films on glassy carbon. *Electrochem. Commun.* **2007**, 9(5), 1189-1195.

[47] Jia, W. Z.; Wang, K.; Zhu, Z. J.; Song, H. T.; Xia, X. H., One-step immobilization of glucose oxidase in a silica matrix on a Pt electrode by an electrochemically induced sol-gel process. *Langmuir* **2007**, *23(23)*, 11896-11900.

[48] Tian, F.; Llaudet, E.; Dale, N., Ruthenium Purple-Mediated Microelectrode Biosensors Based on Sol-Gel Film. *Anal. Chem.* **2007**, *79(17)*, 6760-6766.

[49] Zhang, M.; Mullens C.; Gorski, W., Coimmobilization of dehydrogenases and their cofactors in electrochemical biosensors. *Anal. Chem.* **2007**, *79(6)*, 2446-2450.

[50] Gorton, L.; Bartlett, P. N., NAD(P)-based biosensor. Bioelectrochemistry: Fundamentals, experimental techniques and applications. John Wiley & Sons Ltd, **2008**; p158-197.

[51] Weiss, D. J.; Dorris, M.; Amanda, L.; Peterson, L., Dehydrogenase based reagentless biosensor for monitoring phenylketonuria. *Biosens. Bioelectron.* **2007**, 22 (11) 2436–2441.

[52] Noguer, Th.; Szydlowska, D.; Marty, J.-L.; Trojanowicz, M., Sol-gel immobilization of aldehyde dehydrogenase and NAD^+ on screen-printed electrodes for designing of amperometric acetaldehyde biosensor. *Polish J. Chem.* **2004**, *78(9)*, 1679-1689.

[53] Leca, B.; Marty, J.-L., Reusable ethanol sensor based on a NAD^+ -dependent dehydrogenase without coenzyme addition. *Anal. Chim. Acta*, **1997**, *340 (1-3)*, 143-148.

[54] Leca, B.; Marty, J. -L., Reagentless ethanol sensor based on a NAD-dependent dehydrogenase. *Biosens. Bioelectron.* **1997**, *12(11)*, 1083–1088.

[55] Montagnk, M.; Marty, J. -L., Bi-enzyme amperometric D-lactate sensor using macromolecular NAD^+. *Anal. Chim. Acta*, **1995,** *315(3)*, 297-302.

[56] Zheng, H.; Zhou, J.; Zhang, J.; Huang, R.; Jia, H.; Suye, S., Electrical communication between electrode and dehydrogenase by a ferrocene-labeled high molecular-weight cofactor derivative: application to a reagentless biosensor. *Microchim Acta* **2009,** 165(1-2), 109–115.

[57] Mak, K. K. W., Wollenberger, U, Scheller, F. W., Renneberg, R. An amperometric bi-enzyme sensor for determination of formate using cofactor regeneration. *Biosens. Bioelectron.* **2003**, 18(9), 1095-1100.

[58] Liu, W.; Zhang, S.; Wang, P., Nanoparticle-supported multi-enzyme biocatalysis with in situ cofactor regeneration. *J. Biotechnol.* **2009**, *139(1)*, 102-107.

[59] Zhou, H.; Zhang, Z.; Yu, P.; Su, L.; Ohsaka, T.; Mao, L., Noncovalent attachment of NAD^+ cofactor onto carbon nanotubes for preparation of integrated dehydrogenase-based electrochemical biosensors. *Langmuir* **2010**, *26(8)*, 6028–6032.

[60] Kohlmann, C.; Markle, W.; Lutz, S., Electroenzymatic synthesis. *J. Molecular Catalysis B: Enzymatic* **2008**, *51*, 57–72.

[61] Steckhan, E., Electroenzymic synthesis. *Top. Curr. Chem.* **1994**, *170 (electrochemistry V)*, 83-111.

[62] Tse, D. C.; Kuwana, T., Electrocatalysis of dihydronicotinamide adenosine diphosphate with quinones and modified quinone electrodes. *Anal. Chem.* **1978**, *50(9)*, 1315–1318.

[63] Carlson, B. W.; Miller, L. L., Mechanism of the oxidation of NADH by quinones. Energetics of one-electron and hydride routes. *J. Am. Chem. Soc.* **1985**, *107(2),* 479–485.

[64] Antiochia, R.; Gallina, A.; Lavagnini, I.; Magno, F., Kinetic and thermodynamic aspects of NAD-related enzyme-linked mediated bioelectrocatalysis. *Electroanalysis* **2002**, *14(18)*, 1256–1261.

[65] Kitani, A.; So, Y. H.; Miller, L. L., Electrochemical study of the kinetics of NADH being oxidized by diimines derived from diaminobenzenes and diaminopyrimidines. *J. Am. Chem. Soc.* **1981**, *103(25)*, 7636–7641.

[66] Kitani, A.; Miller, L. L., Fast oxidants for NADH and electrochemical discrimination between ascorbic acid and NADH. *J. Am. Chem. Soc.* **1981**, *103(12)*, 3595–3597.

[67] Wu, S.W.; Huang, H. Y.; Guo, Y. C.; Wang, C. M. ALO-Patternable Artificial Flavin: Phenazine, Phenothiazine, and Phenoxazine. *J. Phys. Chem. C* **2008**, *112(25)*, 9370–9376.

[68] Lawrence, N. S.; Wang, J., Chemical adsorption of phenothiazine dyes onto carbon nanotubes: Toward the low potential detection of NADH. Electrochem. Commun. **2006**, *8(1)*, 71–76.

[69] Zhang, M.; Gorski, W., Electrochemical sensing platform based on the carbon nanotubes/redox mediators-biopolymer system. *J. Am. Chem. Soc.* **2005**, *127(7)*, 2058-2059.

[70] Kwon, S. J.; Yang, H.; Jo, K.; Kwak, J., An electrochemical immunosensor using p-aminophenol redox cycling by NADH on a self-assembled monolayer and ferrocene-modified Au electrodes. *Analyst* **2008**, *133(11)*, 1599-1604.

[71] Wu, Q.; Maskus, M.; Pariente, F.; Tobalina, F.; Fernandez, V. M.; Lorenzo,E.; Abruna, H. D. Electrocatalytic Oxidation of NADH at Glassy Carbon Electrodes Modified with Transition Metal Complexes Containing 1,10-Phenanthroline-5,6-dione Ligands. *Anal. Chem*. **1996**, *68(18)*, 3688–3696.

[72] Manesh, K. M.; Santhosh, P.; Gopalan, A.; Lee, K. P., Electrocatalytic oxidation of NADH at gold nanoparticles loaded poly (3,4-ethylenedioxythiophene)-poly(styrene sulfonic acid) film modified electrode and integration of alcohol dehydrogenase for alcohol sensing. *Talanta* **2008**, *75(5)*, 1307–1314.

[73] Valentini, F.; Salis, A.; Curulli, A.; Palleschi, G., Chemical reversibility and stable low-potential NADH detection with nonconventional conducting polymer nanotubule modified glassy carbon electrodes. *Anal. Chem.* **2004**, 76(11), 3244–3248.

[74] Munteanu, F. D.; Mano, N.; Kuhn, A.; Gorton, L. J., NADH electrooxidation using carbon paste electrodes modified with nitro-fluorenone derivatives immobilized on zirconium phosphate. *Electroanal. Chem.* **2004**, *564(1-2)*, 167–178.

[75] Mano, N.; Kuhn, A., Electrodes modified with nitrofluorenone derivatives as a basis for new biosensors. *Biosens. Bioelectron.* **2001**, *16(9-12)*, 653–660.

[76] Forrow, N. J.; Sanghera, G. S.; Walters, S. J.; Watkin, J. L., Development of a commercial amperometric biosensor electrode for the ketone D-3-hydroxybutyrate. *Biosens. Bioelectron.* **2005**, *20(8)*, 1617–1625.

[77] Pandey, P. C.; Upadhyay, S.; Upadhyay, B. C.; Pathak, H. C., Ethanol biosensors and electrochemical oxidation of NADH. *Anal. Biochem.***1998**, *260(2)*, 195–203.

[78] Zhou, M.; Shang, L.; Li, B.; Huang, L.; Dong, S., The characteristics of highly ordered mesoporous carbons as electrode material for electrochemical sensing as compared with carbon nanotubes. *Electrochem. Commun.* **2008**, *10(6)*, 859–863.

[79] Wang, Y.; Iqbal, Z.; Mitra, S., Rapidly Functionalized, Water-Dispersed Carbon Nanotubes at High Concentration. *J. Am. Chem. Soc.* **2006**, *128(1)*, 95-99.

[80] Musameh, M.; Lawrence, N. S.; Wang, J., Electrochemical activation of carbon nanotubes. *Electrochem. Commun.* **2005**, *7(1)*, 14-18.

[81] Moore, R. R.; Banks, C. E.; Compton, R. G., Basal plane pyrolytic graphite modified electrodes: comparison of carbon nanotubes and graphite powder as electrocatalysts. *Anal. Chem.* **2004**, 76(10), 2677-2682.

[82] Banks, C. E.; Compton, R. G., Edge plane pyrolytic graphite electrodes in electroanalysis: An overview. *Anal. Sci.* **2005**, 21(11), 1263–1268.

[83] Wooten, M.; Gorski, W., Facilitation of NADH Electro-oxidation at Treated Carbon Nanotubes. *Anal. Chem.* **2010**, 82(4), 1299–1304.

[84] Karyakin, A. A.; Ivanova, Y. N.; Karyakina, E. E., Equilibrium (NAD^+/NADH) potential on poly(Neutral Red) modified electrode. *Electrochem. Commun.* **2003**, 5(8), 677-680.

[85] Wienkamp, R.; Steckhan, E., Indirect electrochemical regeneration of NADH by a bipyridinerhodium(I) complex as electron-transfer agent. *Angew. Chem. Int. Ed. Engl.* **1982**, 21, 782-783.

[86] Ruppert, R.; Herrmann, S.; Steckhan, E., Efficient indirect electrochemical in situ regeneration of NADH: electrochemically driven enzymatic reduction of pyruvate catalyzed by D-LDH. *Tetrahedron Lett.* **1987**, 28(52), 6583-6586.

[87] Koelle, U.; Ryabov, A.D., The effect of chloride on the electroreduction of NAD^+ in the presence of $[Cp^*RhIII]^{2+}$ species. *Mendeleev Commun.* **1995**, 5, 187-189.

[88] Willner, I.; Maidan, R.; Shapira, M. Thermal and photochemical regeneration of nicotinamide cofactors and a nicotinamide model compound using a water-soluble rhodium phosphine catalyst. *J. Chem. Soc., Perkin Trans. 2* **1990**, 4, 559-564.

[89] Steckhan, E.; Herrmann, S.; Ruppert, R.; Dietz, E.; Frede, M.; Spika, E., Analytical study of a series of substituted (2,2'-bipyridyl) (pentamethylcyclopentadienyl) rhodium and -iridium complexes with regard to their effectiveness as redox catalysts for the indirect electrochemical and chemical reduction of $NAD(P)^+$. *Organometallics* **1991**, 10(5), 1568-1577.

[90] Lo, H.C.; Buriez, O.; Kerr, J.B.; Fish, R.H., Bioorganometallic chemistry part 11. regioselective reduction of NAD^+ models with $[Cp^*Rh(bpy)H]^+$: structure-activity relationships and mechanistic aspects in the formation of the 1,4-NADH derivatives. *Angew. Chem. Int. Ed.* **1999**, 38(10), 1429-1432.

[91] Ogino, Y.; Takagi, K.; Kano, K.; Ikeda, T., Reactions between diaphorase and quinone compounds in bioelectrocatalytic redox reactions of NADH and NAD^+. *J. Electroanal. Chem.* **1995**, 396(1-2), 517-524.

[92] Kashivagi, Y.; Osa, T., Electrocatalytic oxidation of NADH on thin poly(acrylic acid) film coated graphite felt electrode coimmobilizing ferrocene and diaphorase. *Chem. Lett.* **1993**, 677-680.

[93] Osa, T.; Kashivagi, Y.; Yanagisawa, Y., Electroenzymatic oxidation of alcohols on a poly(acrylic acid) film coated graphite felt electrode terimmobilizing ferrocene, diaphorase and alcohol dehydrogenase. *Chem. Lett.* **1994**, 367-370.

[94] Nikitina, O.; Shleev, S.; Gayda, G.; Demkiv, O.; Gonchar, M.; Gorton, L.; Csoeregi, E.; Nistor, M., Bi-enzyme biosensor based on NAD^+- and glutathione-dependent recombinant formaldehyde dehydrogenase and diaphorase for formaldehyde assay. *Sens. Actuators B* **2007**, *125(1)*, 1-9.

[95] Antiochia, R.; Gorton, L., Development of a carbon nanotube paste electrode osmium polymer-mediated biosensor for determination of glucose in alcoholic beverages. *Biosens. Bioelectron.* **2007**, *22(11)*, 2611-2617.

[96] Kano, K.; Takagi, K.; Ogino, Y.; Ikeda, T., Quinone-mediated bioelectrochemical reduction of $NAD(P)^+$ catalyzed by flavoproteins. Chem. Lett. **1995**, 7, 589-590.

[97] Delecouls-Servat, K.; Basseguy, R.; Bergel, A., Designing membrane electrochemical reactors for oxidoreductase-catalysed synthesis. *Bioelectrochemistry* **2002**, *55(1-2)*, 93-95.

[98] Kashiwagi, Y.; Yanagisawa, Y.; Shibayama, N.; Nakahara, K.; Kurashima, F.; Anzai, J.; Osa, T., Preparative, electroenzymic reduction of ketones on an all components-immobilized graphite felt electrode. *Electrochim. Acta* **1997**, *42(13-14)*, 2267-2270.

[99] Kang, Y.; Kang, C.; Hong, J.; Yun, S., Optimization of the mediated electrocatalytic reduction of NAD^+ by cyclic voltammetry and construction of electrochemically driven enzyme bioreactor. *Biotechnol. Lett.* **2001**, *23(8)*, 599-604.

[100] Yuan, R.; Kuwabata, S.; Yoneyama, H., Fabrication of novel electrochemical reduction systems using alcohol dehydrogenase as a bifunctional electrocatalyst. *Chem. Lett.* **1996**, 2, 137-138.

[101] Cantet, J.; Bergel, A. Comtat, M., Bioelectrocatalysis of NAD^+ reduction. *Bioelectrochem. Bioenerg.* **1992**, 27(3), 475-486.

[102] Delecouls, K.; Saint-Aguet, P.; Zaborosch, C.; Bergel, A., Mechanism of the catalysis by Alcaligenes eutrophus H16 hydrogenase of direct electrochemical reduction of NAD^+. *J. Electroanal. Chem.* **1999**, 468(2), 139-149.

[103] Nishiyama, K.; Ishida, H.; Taniguchi, I., Aminosilane modified indium oxide electrodes for direct electron transfer of ferredoxin. *J. Electroanal. Chem.* **1994**, 373(1-2), 255-258.

[104] P. Gros, C. Zaborosch, H.G. Schlegel, A. Bergel, Direct electrochemistry of Rhodococcus opacus hydrogenase for the catalysis of NAD^+ reduction. *J. Electroanal. Chem.* **1996**, 405(1-2), 189-195.

[105] Dominguez, E.; Lan, H. L.; Okamoto, Y.; Hale, P. D.; Skotheim, T. A.; Gorton, L., A carbon paste electrode chemically modified with a phenothiazine polymer derivative for electrocatalytic oxidation of NADH. Preliminary study. *Biosens. Bioelectron.* **1993**, *8(3-4)*, 167-175.

[106] Koyuncu, D.; Erden, P. E.; Pekyardimci, S.; Kilic, E., A new amperometric carbon paste enzyme electrode for ethanol determination. *Anal. Lett.* **2007**, *40(10)*, 1904-1922.

[107] Weiss, D. J.; Dorris, M.; Loh, A.; Peterson, L., Dehydrogenase based reagentless biosensor for monitoring phenylketonuria. *Biosens. Bioelectron.* **2007**, *22(11)*, 2436-2441.

[108] Yao, Q.; Yabuki, S.; Mizutani, F. Preparation of a carbon paste /alcohol dehydrogenase electrode using polyethylene glycol-modified enzyme and oil-soluble mediator. *Sens. Actuators B* **2000**, *B65(1-3)*, 147-149.

[109] Kuhr, W. G.; Barrett, V. L.; Gagnon, M. R.; Hopper, P.; Pantano, P., Dehydrogenase-modified carbon-fiber microelectrodes for the measurement of neurotransmitter dynamics. 1. NADH voltammetry. *Anal. Chem.* **1993**, *65(5)*, 617-622.

[110] Nowall, W. B.; Kuhr, W. G., Electrocatalytic Surface for the Oxidation of NADH and Other Anionic Molecules of Biological Significance. *Anal. Chem.* **1995**, *67(19)*, 3583-3588.

[111] Fagan, D. T.; Hu, I. F.; Kuwana, T., Vacuum heat-treatment for activation of glassy carbon electrodes. *Anal. Chem.* **1985**, *57(14)*, 2759-63.

[112] Chen, S.; Chan, C., Preparation, characterization, and electrocatalytic properties of copper hexacyanoferrate film and bilayer film modified electrodes. *J. Electroanal. Chem.* **2003**, *543 (2)*, 161-173.

[113] Cai, C. X.; Ju, H. X.; Chen, H. Y., Cobalt hexacyanoferrate modified microband gold electrode and its electrocatalytic activity for oxidation of NADH. *J. Electroanal. Chem.***1995**, *397(1-2)*, 185-190.

[114] Chen, S.; Wu, M.; Thangamuthu, R.; Preparation, Characterization, and Electrocatalytic Properties of Cobalt Oxide and Cobalt Hexacyanoferrate Hybrid Films. *Electroanalysis* **2008**, *20(2)*, 178 – 184.

[115] Lorenzo, E.; Sanchez, L.; Pariente, F; Tirado, J.; Abrufia, H. D., Thermodynamics and kinetics of adsorption and electrocatalysis of NADH oxidation with a self-assembling quinone derivative. *Anal. Chim. Acta* **1995**, *309(1-3)*, 79-88.

[116] Raj C R; Ohsaka, T., Facilitated electrochemical oxidation of NADH and its model compound at gold electrode modified with terminally substituted electroinactive self-assembled monolayers. *Bioelectrochem.* **2001**, *53(2)*, 251-6.

[117] Liu, H.; Lu, J.; Zhang, M.; Pang, D., Electrochemical properties of Nile Blue covalently immobilized on self-assembled thiol-monolayer modified gold electrodes. *Anal. Sci.* **2002**, *18(12)*, 1339-1344.

[118] Kwon, S. J.; Yang, H.; Jo, K.; Kwak, J., An electrochemical immunosensor using p-aminophenol redox cycling by NADH on a self-assembled monolayer and ferrocene-modified Au electrodes. *Analyst* **2008**, *133(11)*, 1599-1604.

[119] Ben-Ali, S.; Cook, D. A.; Evans, S. A. G.; Thienpont, A.; Bartlett, P. N.; Kuhn, A., Electrocatalysis with monolayer modified highly organized macroporous electrodes. *Electrochem. Commun.* **2003**, *5(9)*, 747-751.

[120] Ben-Ali, S.; Cook, D. A.; Bartlett, P. N.; Kuhn, A., Bioelectrocatalysis with modified highly ordered macroporous electrodes. *J. Electroanal. Chem.* **2005**, *579(2)*, 181-187.

[121] Szamocki, R.; Velichko, A.; Holzapfel, C.; Muecklich, F.; Ravaine, S.; Garrigue, P.; Sojic, N.; Hempelmann, R.; Kuhn, A., Macroporous Ultramicroelectrodes for Improved Electroanalytical Measurements. *Anal. Chem.* **2007**, *79(2)*, 533-539.

[122] MacDiarmid, A.G. Synthetic Metals: A Novel Role for Organic Polymers (Nobel Lecture). *Angew. Chem.* **2001**, *40(14)*, 2581-2590.

[123] Kumar, S.A.; Tang, C.F.; Chen, S.M. Poly(4-amino-1-1'-azobenzene-3, 4'-disulfonic acid) coated electrode for selective detection of dopamine from its interferences. *Talanta* **2008**, *74(4)*, 860-866.

[124] Vasilescu, A.; Noguer, T.; Andreescu, S.; Calas-Blanchard, C.; Bala, C.; Marty, J. L., Strategies for developing NADH detectors based on Meldola Blue and screen-printed electrodes: a comparative study. *Talanta* **2003**, *59(4)*, 751-765.

[125] Gao, Q.; Sun, M.; Peng, P.; Qi, H.; Zhang, C.; Electro-oxidative polymerization of phenothiazine dyes into a multilayer-containing carbon nanotube on a glassy carbon electrode for the sensitive and low-potential detection of NADH. *Microchim Acta* **2010**, *168(3)*, 299–307.

[126] Gao, Q.; Cui, X.; Yang, F.; Ma, Y.; Yang, X. Preparation of poly(thionine) modified screen-printed carbon electrode and its application to determine NADH in flow injection analysis system. *Biosens. Bioelectron.* **2003**, *19(3)*, 277-282. .

[127] Dai, Z.H.; Liu, F.X.; Lu, G.F.; Bao, J. C., Electrocatalytic detection of NADH and ethanol at glassy carbon electrode modified with electropolymerized films from methylene green, *J. Solid State Electrochem.* **2008**, *12(2)*, 175-180.

[128] Mano, N.; Kuhn, A., Molecular lego for the assembly of biosensing layers. *Talanta* **2005**, *66(1)*, 21-27.

[129] Huan, Z.; Persson, B.; Gorton, L.; Sahni, S.; Skotheim, T.; Barlett, P., Redox polymers for electrocatalytic oxidation of NADH-cationic styrene and ethylenimine polymers. *Electroanalysis* **1996**, *8(6)*, 575-581

[130] Morales, A.; Cespedes, F.; Alegret, S. Graphite-methacrylate biocomposite material with renewable sensing surface for reagentless amperometric biosensors based on glucose dehydrogenase. *Materials Science & Engineering, C: Biomimetic and Supramolecular Systems* **2000**, *C7(2)*, 99-104.

[131] Schulz, M.; Leichmann, H.; Gunther, H.; Simon, H., Electromicrobial regeneration of pyridine nucleotides and other preparative redox transformations with Clostridium thermoaceticum. *Appl. Microbiol. Biotechnol.* **1995**, 42 (6), 916-922.

[132] Ivanova, E. V.; Sergeeva, V. S.; Oni, J.; Kurzawa, C.; Ryabov, A. D.; Schuhmann, W., Evaluation of redox mediators for amperometric biosensors: Ru-complex modified carbon-paste/enzyme electrodes. *Bioelectrochemistry* **2003**, *60(1-2)*, 65-71.

[133] Gorton, L.; Bremle, G.; Csoeregi, E.; Joensson-Pettersson, G.; Persson, B. Amperometric glucose sensors based on immobilized glucose-oxidizing enzymes and chemically modified electrodes. *Anal.Chim. Acta* **1991**, *249(1)*, 43-54.

[134] Ben-Ali, S.; Cook, D. A.; Bartlett, P. N.; Kuhn, A., Bioelectrocatalysis with modified highly ordered macroporous electrodes. *J. Electroanal. Chem.* **2005**, *579(2)*, 181-187.

Chapitre II. Partie expérimentale

Afin de mener à bien le travail expérimental présenté dans cette thèse, différents composés et techniques ont été utilisés pour préparer et caractériser les couches minces actives. Ce chapitre donne une description des précurseurs de silice, des enzymes, des polymères et des protocoles utilisés pour la préparation des molécules de cofacteur immobilisées et des médiateurs. Une série de méthodes utilisées pour préparés le sol pour la bioencapsulation et les différentes électrodes utilisés dans cette thèse sont également décrits. Enfin, les techniques analytiques utilisées dans cette étude sont présentées.

Chapter II. Experimental part

To conduct the work presented in this thesis, several chemicals and techniques have been used to prepare and characterize the active film. This chapter presents the description of the sol-gel precursors, enzymes, cofactors, mediators, Polymer additives and the protocols used for the cofactor and mediator synthesis. A series of methods used to prepare the starting sols and the working electrodes in this thesis are also described. At last, the analytical techniques used in the studies are described.

1. Chemicals and biomolecules

1.1. Sol-gel reagents

This work focuses on designing functional layers based on silica sol-gel thin films to co-immobilize dehydrogenase, cofactor and mediator. A series of precursor with different properties are used ***(Table II-1)***. Tetraethoxysilane and Tetramethoxysilane are the most common precursors used to prepare sol-gel film. 3-Glycidoxypropyl-trimethoxysilane has three OCH_3 groups and a glycidoxy group. The epoxy ring at the end of the glycidoxy group displays chemical activity and can react with other active groups. Aminopropyltriethoxysilane is an aminopropyl-functionalized silane precursor. The positive charges held by the protonated aminopropyl groups could provide suitable environment for bioencapsulation. sodium metasilicate, Ludox® HS-40 colloidal and Sodium silicate solution have been used for protein encapsulation in order to avoid any trace of alcohol (i.e. aqueous sol-gel route) .

Table II-1. *Information of used precursors*

Chemicals	Formula	Grade	MW ($g.mol^{-1}$)	Suppliers
Tetraethoxysilane (TEOS)	$Si(OC_2H_5)_4$	98 %	208.33	Alfa Aesar
Tetramethoxysilane (TMOS)	$Si(OCH_3)_4$	99 %	152.22	Aldrich
3-Glycidoxypropyl-trimethoxysilane (GPS)	$C_9H_{20}O_5Si$	98 %	236.34	Aldrich
Aminopropyltriethoxysilane (APTES)	$H_2N(CH_2)_3Si(OC_2H_5)_3$	99 %	221.37	Aldrich
Sodium metasilicate	Na_2SiO_3	95 %	122.06	Aldrich
Ludox® HS-40 colloidal	SiO_2	40 %	60.08	Sigma-Aldrich
Sodium silicate solution	Na_2O	10.6 %		Sigma-
	SiO_2	26.5 %		Aldrich
Sodium silicate solution (water glass)	Na_2O	8.7 %		Molekula
	SiO_2	28.4 %		

1.2 Enzymes

In the production of chiral compounds, the oxidation or reduction of prochiral substrates by dehydrogenases is the preferred reaction. Two kinds of dehydrogenase have been cloned and used in this project, D-sorbitol dehydrogenase (DSDH) and galactitol dehydrogenase (GatDH). DSDH and GatDH have been applied in both anodic and cathodic modes, using respectively D-sorbitol and fructose (for DSDH) and hexanediol and hydroxyacetone (for GatDH).

D-sorbitol dehydrogenase solution (DSDH, 10 mg/mL, 100 units/mg) and Galactitol dehydrogenase (GatDH, 10 mg/mL, 14 units/mg) have been provided by Pro. G. W. Kohring (The group of microbiology of Saarland University, Germany), which have been prepared by overproduction of the His(6) tagged protein in Escherichia coli BL21GOLD (DE3) and purification of the enzyme with Histrap columns (GE Healthcare). The activity of the protein suspension was measured as NADH production by oxidation of D-glucitol in a photometric assay at 340 nm.

Diaphorase (DI, 1020 units/mg) was obtained from Unitika, Japan.

1.3 Cofactors

1.3.1 Commercial cofactors

The Nicotinamide redox cofactors (NAD^+ and NADH) play important roles in biological electron carriers, which are based on the transfer of two electrons and one proton. β-Nicotinamide adenine dinucleotide (NAD^+, ~98 %), β-Nicotinamide adenine dinucleotide, reduced dipotassium salt (NADH, ~97 %) and β-Nicotinamide adenine dinucleotide-dextran (NAD^+-dextran, attached through C8 to soluble dextran, D-4133, with a 6 carbon spacer) were supplied by Sigma.

1.3.2 NAD- derivatives Synthesis

1.3.2.1 PEI-NAD

PEI-NAD was prepared according to the reference [1]. NAD^+ (200 mg) was dissolved in 40 mL dimethylsulfoxide containing 8 g succinic anhydride. After 24 h at room temperature, the NAD^+ components (mixture of unreacted NAD^+ and succinyl-NAD) were precipitated with 60 mL acetone. The precipitate was washed 3 times with acetone and recovered by centrifugation. After centrifugation, 20 mL buffer containing 700 mg EDC was added, and pH was adjusted to 4.7 for activating the carboxylic groups of succinyl-NAD for 1 h. After

activation, 300 mg PEI was added and reacted for another 12 h at 4 °C. The reaction mixture was dialysis against 50 mM phosphate buffer (pH 7.0) for 12 h at 4 °C.

1.3.2.2 NAD-GPS

The method involves the direct in situ functionalization of NAD^+ with a glycidopropyl-silane, GPS, precursor [2]. NAD^+ and GPS educts were typically prepared by mixing together 25 mg NAD^+ and 37.5 mg GPS in 400 µL Tris-HCl buffer solution (pH 7.5) at 4°C under shaking for 12 h.

1.4 Mediators

1.4.1 Electron mediator for oxidation of NADH

1.4.1.1 Commercial electron mediator

The use of an electron-transfer mediator can help to overcome the problems observed during the direct electrochemical oxidation of NADH. In this work, we have tested a series of mediators (***Table II-2***).

Table II-2. *Information of used electron mediator for NADH oxidation*

Chemicals	Formula	MW ($g.mol^{-1}$)	Suppliers
Methylene Green (MG)	$C_{16}H_{17}ClN_4O_2S.0.5ZnCl_2$	433.01	Sigma
Meldola's blue (MB)	$C_{18}H_{15}ClN_2O.xZnCl_2$	370.78	Acros organics
Nile blue chloride (Nb)	$C_{20}H_{20}ClN_3O$ 85%	353.85	fluka
Ferrocenedimethanol (FDM)	$C_{12}H_{14}FeO_2$ 98 %	246.09	Aldrich
Ferrocenemethanol (FM)	$C_{11}H_{12}FeO$ 97 %	216.07	Aldrich

1.4.1.2 Synthesis of non commercially-available electron mediator

① PEI-Fc

Ferrocene was tethered to poly(ethyleneimine) (PEI) based on the procedure reported in the literature [3, 4]. FcCHO (90 mg) was dissolved in 15 mL ethanol and added within 1 h to 30 mL of ethanol solution containing 400 mg PEI. The mixture was stirred for 1 h at room temperature, then $NaBH_4$ was carefully added in portions at 0 °C, and stirred continually for

another 2 h. Finally, the mixture was dried under vacuum condition and the residue was extracted with distilled water. The aqueous solution was purified by membrane dialysis against water for 12 h and dried. The polymer so obtained was referred as PEI-Fc.

② Ferrocene functionalized organoalkoxysilane: ferrocene-alkyl-silane

(provided by the group of A. Demir, METU, Ankara, Turky)

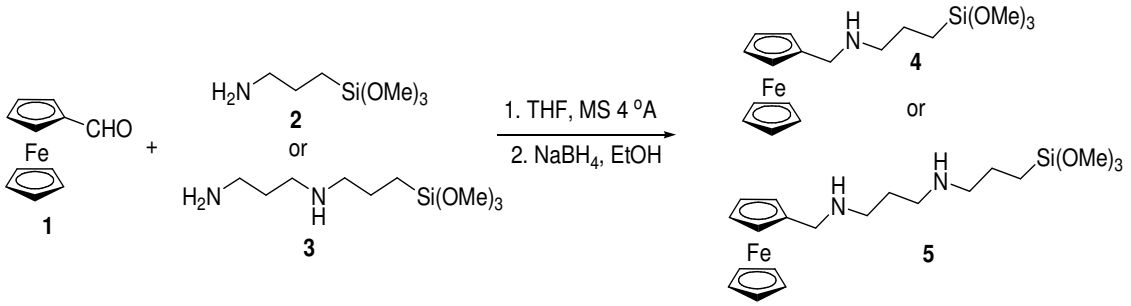

Figure II-1. *Functionalization strategies of Ferrocene-type mediators with siloxy-functions.*

Synthesis of siloxane end-group mediators was also considered for possible immobilization in sol-gel thin films. For the synthesis of ferrocene-siloxane compounds with different chain lengths (***Figure II-1***), two methoxysilane derivatives **2** and **3** was used. 1 mM of **1** (214 mg) and 1 mM of **2** or **3** were dissolved in 10 ml of dry THF in the presence of 100 mg of MS 4 ^{o}A under argon atmosphere. The mixture was stirred overnight and filtered off to remove molecular sieves. The filtrate was concentrated and dissolved in 10 ml of absolute ethanol. 2 mmole of $NaBH_4$ was added portionwise to the solution in a ice-bath. After 3 h, the ethanol was removed. The remaining mixture was dissolved in 10 ml of DCM and extracted with 10 ml of water. The aq. phase was washed with 10 ml of DCM. The combined organic phases was dried over $MgSO_4$ and concentrated to give **4** or **5**.

③ Synthesis of Os-containing redox polymers

Os-containing redox polymers were kindly provided by group of Prof. Wolfgang Schuhmann, and synthesised by Sascha Pöller (*Analytische Chemie – Elektroanalytik & Sensorik & Center for Electrochemical Sciences – CES; Ruhr-Universität Bochum, Bochum, Germany*). Molecular structures of the synthesized Os-containing redox polymers are shown in ***Figure II-2.***

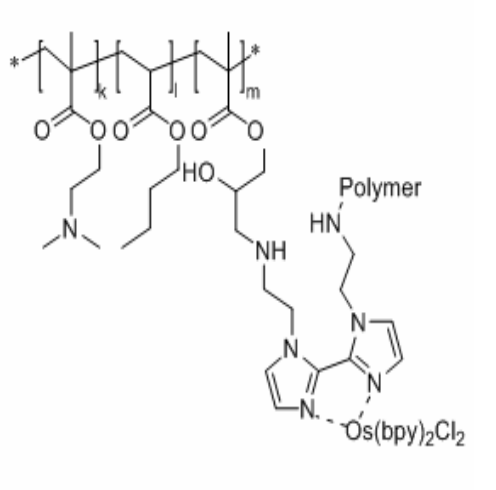

Compound1

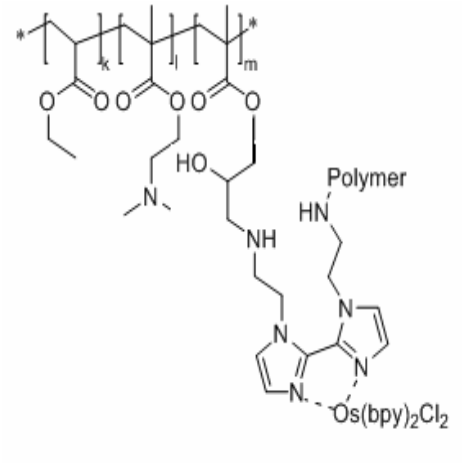

Compound 2

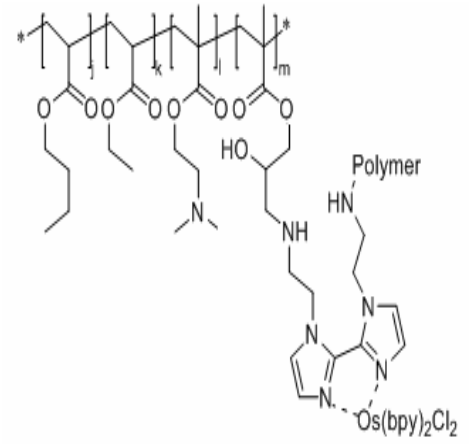

Compound 3

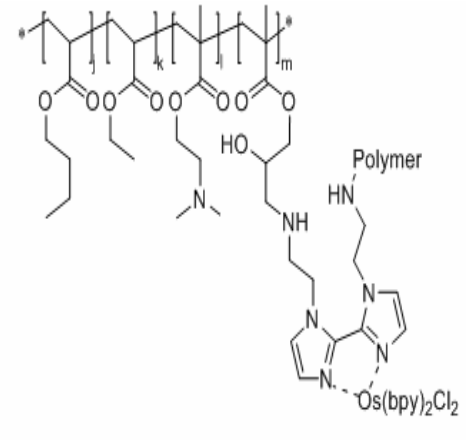

Compound

Figure II-2. Molecular structures of the synthesized Os-containing redox polymers.

④ Commercial carbon nanotubes and functionalization

The different carbon nanotubes used in this work are presented in ***Table II-3***. The functionalization has been obtained by microwaved treatment, methylene green polymerization and wrapping by the osmium polymer.

Table II-3. *Characteristic and origin of carbon nanotubes used in this thesis*

Chemicals	Diameter (nm)	Length (µm)	Purity	Suppliers
Multi-walled carbon nanotubes (MWCNTs)	5.5	5	95 %	Aldrich
Carboxylic acid functionalized Single-walled carbon nanotubes (SWCNTs-COOH)	4-5	0.5-1.5	90 %	Aldrich
Carboxylic acid functionalized Muti-walled carbon nanotubes (MWCNTs-COOH)	15±5	1-5	95 %	Nanolab
Multi-walled carbon nanotubes (MWCNTs)	15±5	1-5	95 %	Nanolab

• *Microwaved MWCNTs (MWCNTs-µW)*

Different kinds of MWCNTs were treated by microwaving based on the procedure reported in the previous article [5]. ***Table II-3*** shows their information. The MWCNTs were microwaved in a concentrated nitric acid (70%) for 10-20 min. The microwaving was performed at 50 °C, 20 psi, and 100% power using the Discover Labmate single-mode microwave oven (CEM, 300 W). After microwaving, the MWCNTs were subjected to at least three centrifugation/decanting cycles in fresh aliquots of deionized water to remove any remaining impurities. In addition, the acid-treated MWCNTs suspensions were neutralized with a sodium hydroxide solution and washed extensively with water to a neutral pH. The final rinsing was performed with ethanol. The MWCNTs were dried in an oven at 85 °C overnight and stored in closed vials at room temperature.

• *Polymerized methylene green(MG) on the MWCNTs modified GCE (GCE/MWCNTs-PMG)*

Chitosan/MWCNTs suspension was prepared by dispersing 1.0 mg MWCNTs (MWCNTs, Aldrich) in 1mL of chitosan solution (0.2 % in 0.05 M acetic acid solution). An aliquot (5 µL) of this resulting solution was deposited onto the surface of the GCE. The solution was then allowed to dry at room temperature to get MWCNTs/GC electrode. Electropolymerization of MG on MWCNTs/GC electrode was carried out using cyclic voltammograms in 0.1 M pH 7.0 PBS containing 0.5 mM MG and 0.1 M KCl in a potential range from -0.5 to 1.2V at a scan rate of 50 mV/s. After successively cycling for 10 cycles, the electrodes were rinsed with doubly distilled water thoroughly and kept at room temperature drying for further use [6, 7].

• *MWCNTs-Osmium (MWCNTs-Os)*

2 mg MWCNTs (MWCNTs-COOH, Nanolab) were dispersed in 2 mL distilled water by sonication. Then, 250µL the resulting solution and 150 µL osmium-polymer solution were mixed together. The mixture was first sonicated for 1 h and then stirred for 24 h at room temperature.

1.4.2 Electron mediators for reduction of NAD^+

1.4.2.1 Syhthesis of $[Cp^*Rh(bpy)Cl]^+$ derivatives

A series of substituted (2,2'-bipyridyl) (pentamethylcyclopentadienyl)-rhodium complexes ($[Cp^*Rh(bpy)Cl]^+$) derivatives have been synthesized by by the group of A. Demir (METU, Ankara, Turky) (***Figure II-3***) according to literature [8, 9, 10, 11, 12, 13], which could be used afterwards as precursors to immobilize such compounds onto electrode surfaces for the reduction of NAD^+. Basically, the "simple" mediators (**1-10**, ***Figure II-3***) have been prepared by reaction of the corresponding unsubstituted and suitably 4,4'-derivatized 2,2'-bipyridine derivatives with $(RhCp^*Cl_2)_2$. 2,2'-bipyridine, 4,4'-dimethoxy-2,2'-bipyridine, 4,4'-dimethyl-2,2'-bipyridine, 4,4'-diamino-2,2'-bipyridine,4,4'-di-t-butyl-2,2'-bipyridine and $(RhCp^*Cl_2)_2$ are commercially available and purchased from Aldrich. Other derivatives of 2,2'-bipyridine were synthesized from 4,4'-dimethyl-2,2'-bipyridine. The preparation of the more "sophisticated" derivatives **11** & **12**, which are likely to be used as precursor reagents for immobilization on electrode surfaces, has required more elaborated synthetic procedures.

1.4.2.2 CNTs-Rh

The non functionalized $[Cp^*Rh(bpy)Cl]^+$ complex can be efficiently immobilized on the CNT surface by π-π-stacking interaction. 5 mg $[Cp^*Rh(bpy)Cl]^+$ and 2 mg CNTs (SWCNTs-COOH, nanolab) were dispersed in 2 mL distilled water. The mixture was first sonicated for 1 h and then stirred for 24 h at room temperature.

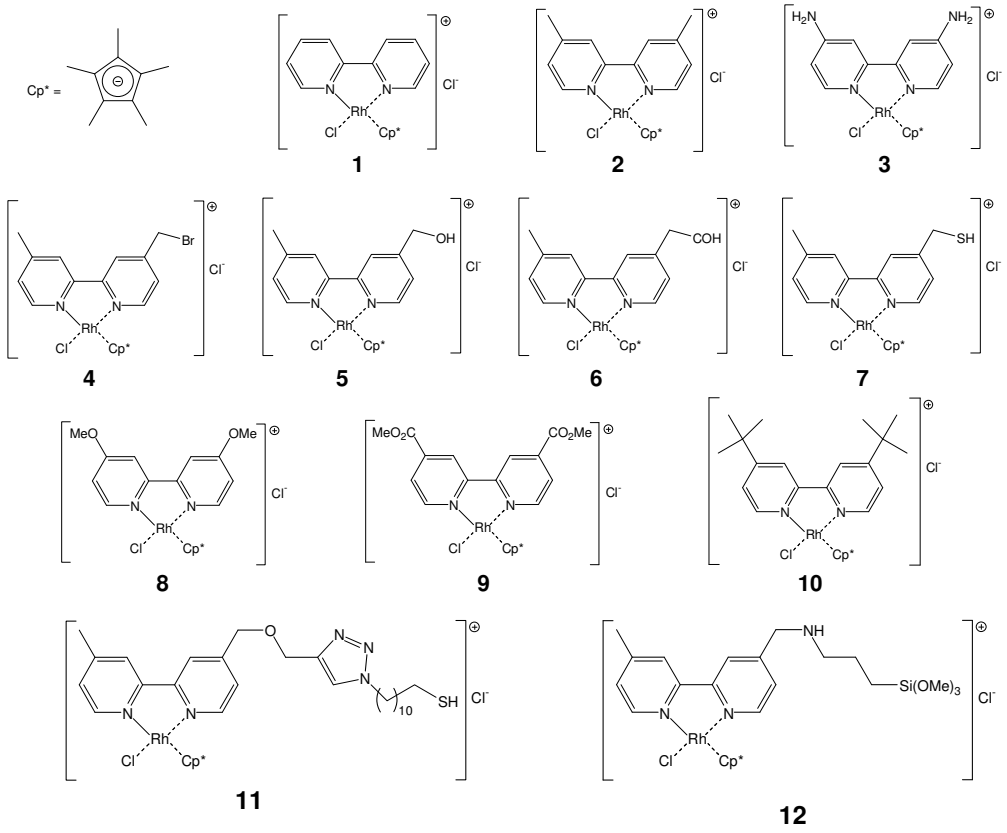

Figure II-3. *Functionalized Rh(III) mediators.*

1.5 Polymer additives

A series of polymer additives with different charges have used in this work. The effects of the introduction of these polymer additives into sol-gel for bioencapsualtion are also investigated. **Table II-4** shows the information of used polymer additives.

Table II-4. *Information of used polymer additives*

Chemicals	Short name	Concentration (wt %)	Suppliers
Poly(dimethyldiallylammonium chloride)	PDDA	20 %	Aldrich
Poly(ethyleneimine)	PEI	Water free	Aldrich
Poly(allylamine)	PAA	20 %	Aldrich
Nafion perfluorinated ion-exchange resin	NF	5 %	Aldrich.

1.6 The other chemicals and solutions

All other reagents are of analytical grade. They include K_2HPO_4 (99%, Prolabo), KH_2PO_4 (99%, Prolabo), ethanol (Merck) and HCl (36%, Prolabo). Chitosan (medium molecular weight) was supplied by Aldrich. D-Sorbitol (98%), D-fructose (99 %), ferrocene carboxyaldehyde (FcCHO), succinic anhydride, 1-ethyl-3-(3-dimethylaminopropyl) carbodiimide hydrochloride (EDC), sodium borohydride ($NaBH_4$) and tris(hydroxymethyl) amino-methane (Tris) were obtained from Sigma.

Tris-HCl (pH 9.0) buffers were prepared by adding suitable amounts of HCl to 0.1 M Tris solutions, which was used to investigate the oxidation reaction. Phosphate buffer solution (PBS, 0.1M, pH 6.5) is used to investigate the reduction reaction. All solutions were prepared with high-purity water (18 M cm^{-1}) from a Millipore milliQ water purification system.

2. Electrodes

In this work, a glassy carbon electrode (GCE, 3mm in diameter), a gold electrode (Au, 4 mm in diameter) or a macroporous gold electrode served as workiong electrode. Prior each measurement, glassy carbon electrodes (GCE) or gold electrodes were first polished on wet emery paper 4000, using Al_2O_3 powder (0.05 mm, Buehler), then rinsed thoroughly with water and ultrasonicated in water and alcohol bath to remove the embedded alumina particles.

Macroporous gold electrodes (***Figure II-4***) were provided by partner 2 (ENSCPB, Bordeaux), which were obtained by electrodeposition of gold through a silica bead colloidal crystal followed by the dissolution of the silica template. The Langmuir Blodgett technique is used to transfer successive layers of monodisperse beads on gold-coated glass substrates, previously treated by cysteamine in order to make the sample surface hydrophilic [14, 15]. The gold electrodeposition was operated at -0.66 V vs. saturated Ag/AgCl after 10 minutes dipping in the commercial gold plating bath in order to let the solution infiltrate the template. After the deposition step the samples were rinsed with distilled water and placed 10 minutes in 5% HF in order to remove the silica colloidal crystal. The pore diameter and the thickness of the porous material were controlled as described in previous work [16].

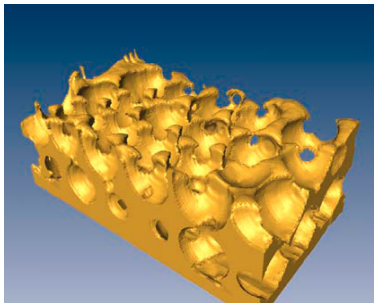

Figure II-4. *The 3-dimensional structure of macroporous gold electrode.*

3. Preparation of sol-gel for bioencapsulation

We have explored various starting sol compositions for bioencapsulation (see ***Table II-5***). The release of alcohol during the hydrolysis of **sol A** has been considered an obstacle, due to its potential denaturing activity on the entrapped protein. Methanol being less harmful than ethanol, TEOS can be replaced by TMOS (**Sol B** and **C**). Alcohol can also be removed from the sol by evaporation (**Sol D**). Aqueous sol-gel routes (**Sol E** and **F**) have been tested in order to avoid any trace of alcohol. A natural polymer (chitosan), or a polyelectrolyte (PDDA and PEI) was used as additive in **Sol G**, **H**, **I**, **J** and **K** which can be also advantageous in providing a better environment for biosencapsualtion.

Sol A and **B** have been mainly used during the first series of electrodeposition and **Sol C**, **D**, **E**, and **F** have been widely used in control experiments and tested, when possible, for spin-coating deposition, drop-coating or electrodeposition. Actually, none of them were satisfactory when used as thin biocomposite films on glassy carbon as no voltammetric signals can be detected in the presence of the enzymatic substrates, independently on the used enzyme (DSDH, GatDH), contrarily to what is observed for haemoglobin (which is found electrochemically and electrocatalytically active in all gels).

At that stage of the project, it has thus been decided to initiate studies with chitosan as an alternative encapsulation matrix, to evaluate the interest of polymeric additives and, depending on the obtained results, to exploit the conclusions to improve the response of sol-gel biocomposites. **Sol G** was developed for dehydrogenase enzymes encapsulation. All investigations performed using drop-coating or spin-coating to deposit sol-gel films have been found to lead to electrochemically detectable bioactivity. However, no detectable

electrochemical signal was observed by electrodeposition. The first experiments performed with **Sol H** and DSDH showed the feasibility of encapsulation of active enzymes in electrodeposited sol-gel thin films. However, this kind of sol-gel can not work for enzyme and cofactor co-immobilization. At this stage, **Sol I** was developed for enzyme and cofactor co-immobilization. Finally, **Sol J** and **K** are developed for co-encapsulate enzyme, cofactor and mediator.

Table II-5. *Information of different methods used to prepare the starting sols*

Materials	Procedures used to prepare the starting sols for films formation
Sol A [17]	The sol was prepared by dissolving 2.125 g TEOS, 2 mL H_2O and 2.5 mL HCl (0.01 M), which were mixed for 12 h using a magnetic stirrer, then NaOH was added in the medium to increase pH at a value of about 4 and electrodeposition was applied.
Sol B	Same system as Sol-Gel A, but using TMOS instead of TMOS
Sol C [18]	The sol was prepared by stirring 2.56 g TMOS with 0.6 mL H_2O and 0.06 mL HCl (0.62 M) for 20 min. Phosphate buffer (1.0 mL, 0.01M, pH=8.2) was added to the sol (1.0 mL) which is shaken vigorously.
Sol D [19]	The sol was prepared by stirring of 4.46 mL TEOS, 1.44 mL H_2O and 0.04 mL HCl (0.62 M) for 1 h. Then 1 mL of the resulting sol was mixed with 1 mL of deionised water, and evaporated for a weight loss of 0.62 g.
Sol E [20]	11.5 g Sodium silicate (3.25 SiO_2/Na_2O) was combined with 34 mL DI water. To this aqueous solution is added 15.4 g of strongly acidic cation-exchange resin with stirring to bring the pH of the solution to a value of 4. The resin is then filtrated. 0.3 mL of 2 M Hydrochloric acid was added to the sol to adjust the pH 2.0. A phosphate buffer (1 M, pH 7) containing enzyme was added to the sol solution in a 1:5 (volume) ratio.
Sol F [21]	0.61 g Sodium silicate was combined with 50 mL de-ionized water. To this aqueous solution was added 1.6 mL 37% HCl to decrease the pH to 0.84. 2 mL of resulting 0.1 M sodium silicate was added to 3 mL ludox (SM-30), which was shaken vigorously.
Sol G	The sol was prepared by dissolving 0.04 g TEOS, 800 µL ethanol and 1 mL HCL (0.01M), which were mixed for 2.5 h using a magnetic stirrer.
Sol H	Same system as Sol-Gel A, but diluted 3 times with water for further use.
Sol I	Same system as Sol-Gel A, but diluted 6 times with water for further use.
Sol J	The sol was prepared by dissolving 0.18g TEOS, 0.13g GPS, 0.5 mL H_2O and 0.625 mL HCl (0.01M), which were mixed for 12 h using a magnetic stirrer. Then diluted 2 times with water for further use.
Sol K	The sol was prepared by dissolving 0.18 g TEOS, 0.13 g GPS, 0.02 g Fc-silane, 0.5 mL H_2O and 0.625 mL HCl (0.01 M), which were mixed for 12 h using a magnetic stirrer. Then diluted 2 times with water for further use.

4. Preparation of electrodes

4.1 Preparation of electrodes for chapter III

4.1.1 Drop-coating

25 µL of **Sol G** was mixed with 15 µL PDDA solution (20 wt. %) and 20 µL of the enzyme solution (10 mg/mL). An aliquot (5 µL) of this resulting sol was deposited onto the surface of the GCE. The solution was then allowed to dry at 4 °C overnight. The prepared electrodes were rinsed thoroughly with water and stored in Tris-HCl buffer solution for 15 min prior to the electrochemical measurement. In attempting to optimize the film composition, the electrodes containing various amounts of TEOS and additives (PDDA, PEI, PAA, Nafion, Chitosan) were prepared by adjusting the concentrations of each component as desired and applying the same protocol as above to form the biocomposite films. Composites made of both silica and chitosan were typically prepared by mixing together 20 µL of the starting **sol G** with 20 µL of a chitosan solution (0.5 % in 0.05 M acetic acid solution), 20 µL PDDA solution and 20 µL DSDH suspension. The pure chitosan film was obtained by mixing 20 µL chitosan, 20 µL PDDA and 20 µL DSDH suspension. When PDDA was not introduced, it was replaced by the same volume of water. An aminopropyl-functionalized material was also prepared by introducing aminopropyltriethoxysilane (APTES) into the sol in addition to TEOS (1:1 molar ratio).

Some biocomposite materials were also prepared in the form of monoliths for UV-vis monitoring of the enzymatic activity. They were prepared according to a protocol from the literature [22]. **Sol 1** was prepared by mixing 125 µL of the starting **Sol C** with 125 µL of phosphate buffer (5 mM, pH 8.0) and 25 µL of the DSDH suspension. **Sol 2** was prepared as **sol 1** and 25 µL of PDDA solution was also added. The gels were allowed to age at 4°C for 6 days. Before use, the gels have been washed three times with 3 mL of 0.1M Tris-HCl (pH 9.0) to remove weakly adsorbed DSDH.

4.1.2 Electrodepostion

100 µL of DSDH (10 mg/mL) and 100µL of PDDA were added to 100µL of the above hydrolyzed **Sol H**. The mixture was put into the electrochemical cell where electrochemically-assisted deposition was performed at -1.3 V at room temperature for several tens of s. The electrodes were immediately rinsed with water, and dried overnight in a fridge at 4 °C. The prepared electrodes were rinsed thoroughly with water and stored in Tris-HCl buffer solution

for 15 min prior to the electrochemical measurements. In attempting to optimize the film composition, the electrodes containing various amounts of TEOS, PDDA and DSDH were prepared by adjusting the concentrations of each component as desired and applying the same protocol as above to form the bio-composite films.

4.2 Preparation of electrodes for chapter IV

4.2.1 Co-immobilization of DSDH and NAD^+ in sol-gel matrix prepared by drop-coating

① *Preparation of GCE/TEOS/PEI/(DSDH+DI)/NAD^+*

20 µL of **sol I** was mixed with 10 µl PEI solution (20 wt%, pH 9.0), 10 µl NAD^+ solution (90 mM), 15 µl DSDH solution (10 mg/ml) and 10 µl DI solution (5 mg/ml). The biocomposite film was then formed by drop-coating, by depositing an aliquot (5 µl) of this resulting sol onto the GCE surface and allowing the solvent to evaporate by drying overnight at 4 °C.

② *GCE/TEOS/PDDA/(DSDH+DI)/NAD^+ and GCE/TEOS/PAA/(DSDH+DI)/NAD^+* have been prepared as above by replacing the PEI solution by PDDA and PAA solutions (20 wt. % in water), respectively.

③ Electrodes doped with carbon nanotubes, *GCE/TEOS/PEI/SWCNT/(DSDH+DI)/NAD^+* and *GCE/TEOS/PEI/(DSDH+DI)/NAD-SWCNT* were obtained by suspending 1.0 mg SWCNT or NAD-SWCNT in 1.0 ml of **sol I** prior to mixing with PEI, DSDH and DI solutions and following the same drop-coating procedure afterwards. The NAD-SWCNT sample (carbon nanotubes with adsorbed/noncovalently attached NAD^+) was previously prepared according to a protocol reported in the literature [23], by mixing 2 mg SWCNT with 50 mg NAD^+ in 2 mL water under stirring for 48 h and then recovering the solid phase by filtration (0.45 µm, Millipore).

④ *GCE/TEOS/PEI/(DSDH+DI)/NAD-dextran and GCE/TEOS/PEI/(DSDH+DI)/NAD-GPS* have been also prepared as above except that the 10 µl aliquot of NAD^+ solution was replaced by respectively 10 µl of NAD-dextran solution (62.5 mg/ml in Tris-HCl buffer at pH 7.5) or 10 µl of NAD-GPS solution (typically prepared by mixing together 25 mg NAD^+ and 37.5 mg GPS in 400 µl Tris-HCl buffer solution (pH 7.5) at 4°C under shaking for 12 h.

4.2.1 Co-immobilization of DSDH and NAD^+ in electrodeposited sol-gel thin film

70 µL DSDH (10 mg/mL), 30 µL PDDA, 40 µL PEI, 40 µL DI and 50 µL NAD-GPS composite were added to 70 µL of the above hydrolyzed **Sol H**. The mixture was put into the electrochemical cell where electrochemically-assisted deposition was performed at -1.3 V at room temperature for 60 s. The electrodes were immediately rinsed with water, and dried overnight in a fridge at 4 °C. The prepared electrodes were rinsed thoroughly with water and stored in Tris-HCl buffer solution for 15 min prior to the electrochemical measurements. In attempting to optimize the film composition, the electrodes containing only PDDA or PEI were prepared by adjusting the concentrations of each component as desired and applying the same protocol as above to form the bio-composite films.

4.3 Preparation of electrodes for chapter V

4.3.1 Fc-PEI and Os-polymer as co-immobilized mediator

20 µL **Sol J** was mixed with 10 µL PEI solution (10 wt. %, pH 9.0), 15 µL the Fc-PEI or Os-polymer solution, 10µL DI (5mg/mL), 15µL DSDH and 10µL NAD-GPS. An aliquot (5 µL) of this resulting sol was deposited onto the surface of the GCE. The solution was then allowed to dry at 4 °C overnight. The prepared electrodes were rinsed thoroughly with water and stored in Tris-HCl buffer solution for 15 min prior to the electrochemical measurement. The electrodes prepared in the absence of GPS or the enzyme and cofactor were obtained by adjusting the concentrations of each component as desired and applying the same protocol as above to form the biocomposite films.

50 µL PEI, 60 µL Fc-PEI or Os-polymer solution, 40 µL DI, 60 µL DSDH and 40 µL NAD-GPS were added to 100 µL of the **Sol J**. The mixture was put into the electrochemical cell where electrochemically-assisted deposition was performed at -1.3 V at room temperature for 60 s. The electrodes were immediately rinsed with water, and dried overnight at 4°C.

4.3.2 Fc-silane as co-immobilized mediator

Drop-coated sol-gel film modified electrodes were prepared with the same protocol as above by mixing 20 µL **Sol K**, 10 µL PEI solution (10 wt. %, pH 9.0), 15 µL water, 10 µL DI (5 mg/mL), 15 µL DSDH and 10 µL NAD-GPS.

Electrodeposited so-gel film modified electrodes are prepared with the same protocol as above by mixing 50 µL PEI, 60µL water 40µL DI, 60µL DSDH, 40µL NAD-GPS and 100µL of the **Sol K**.

4.4 Preparation of electrodes for chapter VI

4.4.1 MWCNTs-µW & sol-gel matrix

GCE/MWCNTs-µW (GCE/MWCNTs) were prepared by casting 5 µL of suspension of 1.0 mg of microwaved MWCNTs (see **chapter II 1.4.1.2**) (untreated CNTs) in 1.0 mL of 0.1wt % chitosan solution on the surface of GC electrode and dried for 2 h at room temperature. The film electrodes were rinsed repeatedly with water and soaked in a pH 7.40 phosphate buffer solution while stirring to remove any loose materials. The electrodes were stored at room temperature when not in use.

① *GCE/MWCNT-µWs&TEOS/PEI/DSDH*

20 µL of **Sol I** was mixed with 20 µL PEI solution (10 wt %, pH 9.0) and 20 µL DSDH solution (10 mg/mL). An aliquot (5 µL) of this resulting sol was deposited onto the surface of the *GCE/MWCNT-µWs*. The solution was then allowed to dry at 4°C overnight.

② *GCE/MWCNT-µWs &electrodepositedTEOS/PEI/DSDH*

70 µL PEI, 80 µL DSDH and 50 µL water were added to 100 µL of the **Sol H**. The mixture was put into the electrochemical cell with *GCE/MWCNT-µWs* as working electrode where electrochemically-assisted deposition was performed at -1.3 V at room temperature for 60 s. The electrodes were immediately rinsed with water, and dried overnight at 4°C.

③*GCE/MWCNT-µWs&electrodepositedTEOS/PEI/DSDH/NAD-GPS* film modified electrode

70 µL PEI, 80 µL DSDH and 50 µL NAD-GPS were added to 100 µL of the **Sol H**. The mixture was put into the electrochemical cell with *GCE/MWCNT-µWs* as working electrode

where electrochemically-assisted deposition was performed at -1.3 V at room temperature for 60 s. The electrodes were immediately rinsed with water, and dried overnight at 4°C.

4.4.2 MWCNTs-PMG &sol-gel matrix

The preparation of *GCE/MWCNT-PMG* has been described in **chapter II 1.4.1.2**.

① *GCE/MWCNT-PMG &TEOS/PEI/DSDH* film modified electrode

20 µL of **Sol I** was mixed with 10 µL PEI solution (10 wt %, pH 9.0), 10 µL water and 20 µL DSDH solution. An aliquot (5 µL) of this resulting sol was deposited onto the surface of the *GCE/MWCNT-PMG*. The solution was then allowed to dry at 4°C overnight. The prepared electrodes were rinsed thoroughly with water and stored in Tris-HCl buffer solution for 15 min prior to the electrochemical measurement.

② *GCE/MWCNT-PMG &TEOS/PEI/DSDH/NAD-GPS* film modified electrode

20 µL of **Sol I** was mixed with 10 µL PEI solution (10 wt %, pH 9.0), 10 µL NAD (or NAD-GPS composite) solution and 20 µL DSDH solution. An aliquot (5 µL) of this resulting sol was deposited onto the surface of the *GCE/MWCNT-PMG*. The solution was then allowed to dry at 4°C overnight. The prepared electrodes were rinsed thoroughly with water and stored in Tris-HCl buffer solution for 15 min prior to the electrochemical measurement.

③ *GCE/MWCNT-PMG&electrodepositedTEOS/PEI/DSDH/NAD-GPS* film modified electrode

70 µL PEI, 80 µL DSDH and 50 µL NAD-GPS are added to 100 µL the **Sol H**. The mixture is put into the electrochemical cell with *GCE/MWCNT-PMG* as working electrode where electrochemically-assisted deposition was performed at -1.3 V at room temperature for 60 s. The electrodes are immediately rinsed with water, and dried overnight at 4°C.

4.4.3 MWCNTs-Os&sol-gel matrix

Chitosan/MWCNTs-Os solution was prepared by mixing in 1:1 volume the resulting MWCNTs-Os solution (see **chapter II 1.4.1.2**) to 0.2 % chitosan solution (0.2 % chitosan solution in 1 % acetic acid). *GCE/MWCNT-Os* was prepared by depositing 5 µL Chitosan/MWCNTs-Os solution and allowed to evaporate at the room temperature.

① *GCE/MWCNT-Os &TEOS/PEI/DSDH/NAD-GPS/DI*

20 µL of **Sol I** was mixed with 10 µL PEI solution (10 wt %, pH 9.0), 10 µL NAD-GPS solution, 10 µL DI and 15 µL DSDH solution. An aliquot (5 µL) of this resulting sol was deposited onto the surface of the *GCE/MWCNT-Os*. The solution was then allowed to dry at 4°C overnight. The prepared electrodes were rinsed thoroughly with water and stored in Tris-HCl buffer solution for 15 min prior to the electrochemical measurement.

② *GCE/MWCNT-Os &electrodepositedTEOS/PEI/DSDH/NAD-GPS/DI*

50 µL NAD-GPS, 40 µL DI (5mg/mL), 70 µL DSDH (10 mg/mL) and 60 µL PEI were added to 80 µL of the above **Sol H**. The mixture was put into the electrochemical cell with *GCE/MWCNT-Os* as working electrode where electrochemically-assisted deposition was performed at -1.3 V at room temperature for 60 s. The electrodes were immediately rinsed with water, and dried overnight at 4°C.

4.4.4 CNTs/Rh(III)&sol-gel matrix

Chitosan/CNTs/Rh solution was prepared by mixing in 1:1 volume the resulting CNTs/Rh suspension (see **chapter II 1.4.2.3**) to 0.5 % chitosan solution (0.5 % chitosan solution in 1 % acetic acid). The *CNTs-Rh* modified electrode was prepared by depositing 5 µL Chitosan/CNTs/Rh solution and allowed to evaporate at the room temperature.

5. Methods of analysis

5.1 Electrochemical measurements [24]

5.1.1 Cyclic voltammetry (CV)

Cyclic voltammetry is the most widely used technique for acquiring qualitative information about electrochemical reactions. It is often the first experiment performed in an electroanalytical study. In particular, it offers a rapid location of redox potential of the electroactive species, and convenient evaluation of the effect of various parameters on the redox process. This technique is based on varying the applied potential at a working electrode in both forward and reverse directions (at selected scan rates) while monitoring the resulting current. The corresponding plot of current versus potential is termed a cyclic voltammogram. ***Figure II-5*** shows the response of a reversible redox couple during a single potential cycle. It is assumed that only the oxidized form O is present initially. Thus, a negative-going potential scan is chosen for the first half-cycle, starting from a value where no reduction occurs. As the

applied potential approaches the characteristic E^0 for the redox process, a cathodic current begins to increase, until a peak is reached. After traversing the potential region in which the reduction process takes place, the direction of the potential sweep is reversed. During the reverse scan, R molecules (generated in the forward half cycle, and accumulated near the surface) are reoxidized back to O and an anodic peak results. The important parameters in a cyclic voltammogram are the two peak potentials (*E*pc, *E*pa) and two peak currents (*i*pc, *i*pa) of the cathodic and anodic peaks, respectively. Cyclic voltammetry can be used for the study of reaction mechanisms and adsorption processes, which can also be useful for quantitative purposes, based on measurements of the peak current.

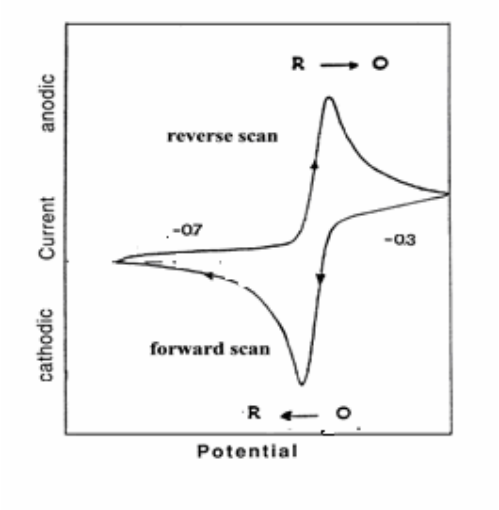

Figure II-5 *Typical cyclic voltammogram for a reversible O + ne- → R and R → O + ne- Redox process.*

5.1.2 Chronoamperometry in hydrodynamic mode

The basis of chronoamperometry techniques is the measurement of the current response to an applied potential. A stationary working electrode and stirred solution are used. The resulting current-time dependence is minitored. As mass transport under these conditions is solely by convection (steady state diffusion), the current-time curve reflects the change in the concentration gradient in the vicinity of the surface, which is directly related to concentration in solution.

In this work, all cyclic voltammetry (CV) and chrono amperometry experiments are conducted using a conventional three-electrode cell. The working electrode was a glassy carbon electrode (GCE, 3mm in diameter), a gold electrode (Au, 4 mm in diameter) or a macroporous gold electrode, a gold wire served as auxiliary electrode, and an Ag/AgCl electrode (saturate KCl internal electrolyte) was used as the reference. All electrochemical experiments have been performed at room temperature and carried out using an Autolab PGSTAT-12 potentiostat (Eco Chemie) monitored by the GPES (General Purpose Electrochemical System) software.

5.2 UV-VIS Spectroscopy (UV)

The principles of UV centre on the fact that molecules have the ability to absorb ultraviolet or visible light. This absorption corresponds to the excitation of outer electron in the molecules concerned. When a molecule absorbs energy an electron is promoted from the Highest Occupied Molecular Orbital (HOMO) to the lowest Unoccupied Molecular Orbital (LUMO).

As with any UV-Vis spectrometer, three of the main elements are a UV-light source, a monochromator and a detector. The monochromator works as a diffraction grating to dispense the beam of light into various wavelengths. The detectors role is to record the intensity of the light which has been transmitted. Before the samples are run, a reference must first be taken. This calibrates the spectra to screen out any spectral interference. In the case of liquid samples the solvent which has been used to dissolve the sample is used. However, there are certain criteria that solvent must pass before they can be deemed as suitable solvents. The main criterion is that the solvent should not absorb ultraviolet radiation in the same region as the sample being analysed. The apparatus used in this study is a UV-vis spectrophotometer Beckman Du 7500, which was used to measure NADH concentrations in solution at 340 nm.

5.3 Attenuated Total Reflectance–Fourier Transform Infrared Spectroscopy (ATR-FTIR spectroscopy)

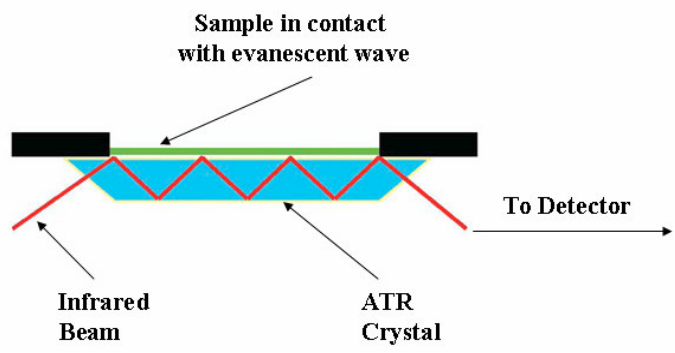

Figure II-6. *A multiple reflection ATR system.*

Infrared spectroscopy is a widely used technique that for many years has been an important tool for investigating chemical processes and structure [25]. The combination of infrared spectroscopy with the theories of reflection has made advances in surface analysis possible. Specific IR reflectance techniques may be divided into the areas of specular reflectance, diffuse reflectance, and internal reflectance. An innovative technique (ATR-FTIR spectroscopy) for monitoring the transport process of low molecular weight species was established based upon internal reflectance. This enabled the monitoring of individual species in-situ, while providing additional chemical information on any changes that may be occurring during the transport process.

Figure II-6 shows the principles of ATR-FTIR. An attenuated total reflection accessory operates by measuring the changes that occur in a totally internally reflected infrared beam when the beam comes into contact with a sample. An infrared beam is directed onto an optically dense crystal with a high refractive index at a certain angle. This internal reflectance creates an evanescent wave that extends beyond the surface of the crystal into the sample held in contact with the crystal. It can be easier to think of this evanescent wave as a bubble of infrared that sits on the surface of the crystal.This evanescent wave protrudes only a few microns (0.5 μ - 5 μ) beyond the crystal surface and into the sample. Consequently, there must be good contact between the sample and the crystal surface. In regions of the infrared spectrum where the sample absorbs energy, the evanescent wave will be attenuated or altered. The attenuated energy from each evanescent wave is passed back to the IR beam, which then

exits the opposite end of the crystal and is passed to the detector in the IR spectrometer. The system then generates an infrared spectrum.

The apparatus used in this study is a Bruker Vector 22 spectrometer equipped with a KBr beam splitter and a deuterated triglycine sulfate (DTGS) thermal detector. FTIR spectra were recorded between 4000 and 700 cm^{-1}. Recording of spectra, data storage and data processing were performed using the Bruker OPUS 3.1 software. The resolution of the single beam spectra was 4 cm^{-1}. The number of bidirectional double-sided interferogram scans was 200, which corresponds to a 2 min accumulation. All interferograms were Fourier processed using the Mertz phase correction mode and a Blackman-Harris three-term apodization function. Measurements were performed at 22 ± 1°C in an air-conditioned room. A nine-reflection diamond ATR accessory (Durasampl*IR* ™, SensIR Technologies) was used for acquiring spectra. The incidence angle was 45° and the refraction index of the crystal was 2.4. No ATR correction was performed. 80 µL of the studied solution were put on the crystal. Appropriate spectra were used to remove spectral background: an air-reference, a water-reference, or a Tris-HCl buffer solution-reference. Water vapor subtraction was performed when necessary. In the course of reaction monitoring experiments, ATR-FTIR spectra were recorded every 5 or 15 min..

5.4 Scanning electron microscopy (SEM)

The scanning electron microscope (SEM) is a type of electron microscope that images the sample surface by scanning it with a high-energy beam of electrons in a raster scan pattern. The electrons interact with the atoms that make up the sample producing signals that contain information about the sample's surface topography, composition and other properties such as electrical conductivity. Due to the very narrow electron beam, SEM micrographs have a large depth of field yielding a characteristic three-dimensional appearance useful for understanding the surface structure of a sample. A wide range of magnifications is possible, from about 10 times (about equivalent to that of a powerful hand-lens) to more than 500,000 times, about 250 times the magnification limit of the best light microscopes. Thus we are able to observe the particle morphology closely on a very fine scale.

For conventional imaging in the SEM, specimens must be electrically conductive, at least at the surface, and electrically grounded to prevent the accumulation of electrostatic charge at the surface. Nonconductive specimens are therefore usually coated with an ultrathin coating

of electrically-conducting material, commonly gold or graphite, deposited on the sample either by low vacuum sputter coating or by high vacuum evaporation.

The technique of SEM is to focus on a surface of specimen by lens using a condensed electron beam. The interaction between electrons and the material leads to the backscattered electron emission, X-rays, secondary electrons and so on. These electrons are collected by a detector, converted to a voltage and finally amplified.

In this work, The morphologies and structures of the membranes of DSDH-encapsulated electrogenerated sol-gel silica on a GCE were examined on a scanning electron microscope (SEM, Hitachi X-650, Japan).

5.5 Scanning electrochemical microscopy (SECM) [26, 27]

Scanning electrochemical microscopy (SECM) is a technique in which the current that flows through a very small electrode tip (generally an ultramicroelectrode with a tip diameter of 10 pm or less) near a conductive, semiconductive, or insulating substrate immersed in solution is used to characterize processes and structural features at the substrate as the tip is moved near the surface. The tip can be moved normal to the surface (the z direction) to probe the diffusion layer, or the tip can be scanned at constant z across the surface (the x and y directions). The tip and substrate are part of an electrochemical cell that usually also contains other (e.g., auxiliary and reference) electrodes. The device for carrying out such studies involves means of moving the tip with a resolution down to the A region, for example, by means of piezoelectric elements or stepping motors driving differential springs, and is called a scanning electrochemical microscope. The abbreviation SECM is used interchangeably for both the technique and the instrument. In SECM the current is carried by redox processes at tip and substrate and is controlled by electron transfer kinetics at the interfaces and mass transfer processes in solution, so that measurements at large spacings, e.g., the range of 1 nm to 10 pm, can be made. In addition to the electrochemical measurement, the machine can be equipped by a sheaforce detection module that helps in positioning the electrode before electrochemical measurement. Here, only the sheaforce detection was used in order to determine the film thickness on conductive surface. The apparatus has been developed in the lab on the base of the SECM instrument from Senslytics (Ruhr-Universität, Bochum, Germany).

Reference

[1] Wykes, J. R.; Dunnill, P.; Lilly, M. D., Preparation of soluble high molecular weight NAD derivative active as a cofactor. *Biochim. Biophys. Acta* **1972**, *286(2)*, 260-268.

[2] Liu, W.; Zhang, S.; Wang, P., Nanoparticle-supported multi-enzyme biocatalysis with in situ cofactor regeneration. *J. Biotechnol* **2009**, *139(1)*, 102-107.

[3] Hodak, J.; Etchenique, R.; Calvo, E. J.; Singhal, K.; Bartlett, P. N., Layer-by-Layer Self-Assembly of Glucose Oxidase with a Poly(allylamine)ferrocene Redox Mediator. *Langmuir* **1997**, *13(10)*, 2708-2716.

[4] Zheng, H.; Zhou, J.; Okezaki, Y.; Suye, S., Construction of L-lysine sensor by layer-by-layer adsorption of L-lysine 6-dehydrogenase and ferrocene-labeled high molecular weight coenzyme derivative on gold electrode. *Electroanalysis* **2008**, *20 (24)*, 2685-2691.

[5] Wooten, M.; Gorski, W., Facilitation of NADH Electro-oxidation at Treated Carbon Nanotubes. *Anal. Chem.* **2010**, 82(4), 1299–1304.

[6] Zhou, D.; Fang, H.; Chen, H.; Ju, H.; Wang, Y., The electrochemical polymerization of methylene green and its electrocatalysis for the oxidation of NADH. *Anal. Chim. Acta* **1996,** *329(1-2)*, 41–48.

[7] Dai, Z. H.; Liu, F. X.; Lu, G. F.; Bao, J. C., Electrocatalytic detection of NADH and ethanol at glassy carbon electrode modified with electropolymerized films from methylene green. *J Solid State Electrochem* **2008**, *12(2)*, 175-180.

[8] Strouse, G. F.; Schoonover, J. R.; Duesing, R.; Meyer, T. J., Long Distance, Bridge-Mediated Electron Transfer in a Ligand-Bridged ReI-ReI Complex. *Inorg. Chem.* **1995**, *34(10)*, 2725-34.

[9] Liu, H.; Zhang, K. Y.; Law, W. H.; Lo, K. K., Cyclometalated Iridium(III) Bipyridine Complexes Functionalized with an *N*-Methylamino-oxy Group as Novel Phosphorescent Labeling Reagents for Reducing Sugars. *Organometallics* **2010**, *29*, 3474–3476.

[10] Chen, D.; De, R.; Mohler, D. L., A Facile Synthesis of Thioalkyl- and Di(thioalkyl)-Substituted Bipyridines. *Synthesis* **2009**, *No. 2*, 211–216.

[11] Miyoshi, D.; Karimata, H.; Wang, Z. M.; Koumoto, K.; Suqimoto, N. Artificial G-Wire Switch with 2,2′-Bipyridine Units Responsive to Divalent Metal Ions. *J. Am. Chem. Soc.* **2007**, *129*, 5919–5925.

[12] Sommer, W. J.; Weck, M., Facile Functionalization of Gold Nanoparticles via Microwave-Assisted 1,3 Dipolar Cycloaddition. *Langmuir* **2007**, *23*, 11991–11995.

[13] Tsai, F. Y.; Wu, C. L.; Mou, C. Y.; Chao, M. C.; Linc, H. P.; Liua, S. T. Palladium bipyridyl complex anchored on nanosized MCM-41 as a highly efficient and recyclable catalysts for Heck reaction. *Tetrahedron Lett.* **2004**, *45*, 7503–7506.

[14] Reculusa, S.; Ravaine, S., Synthesis of Colloidal Crystals of Controllable Thickness through the Langmuir-Blodgett Technique. *Chem. Mater* **2003**, *15(2)*, 598-605.

[15] Reculusa, S.; Masse, P.; Ravaine, S., Three-dimensional colloidal crystals with a well-defined architecture. *J. Collois. Interface Sci.* **2004**, *279(2)*, 471-478.

[16] Szamocki, R.; Reculusa, S.; Ravaine, S.; Bartlett, P.N.; Kuhn, A.; Hempelmann, R., Tailored mesostructuring and biofunctionalization of gold for increased electroactivity. *Angew. Chem INt. Ed. Engl*. **2006**, *45(8)*, 1317-1321.

[17] Nadzhafova, O.; Etienne, M.; Walcarius, A., Direct electrochemistry of hemoglobin and glucose oxidase in electrodeposited sol-gel silica thin films on glassy carbon. *Electrochem. Commun.*, **2007**, *9(5)*, 1189-1195.

[18] A. K. Williams, J. T. Hupp, Sol-gel-encapsulated alcohol dehydrogenase as a versatile, environmentally stabilized sensor for alcohols and aldehydes. *J. Am. Chem. Soc.* **1998**, *120(18)*, 4366-4371.

[19] Salinas-Castillo, A.; Pastor, I.; Mallavia, R.; Mateo, C. R., Immobilization of a trienzymatic system in a sol-gel matrix: A new fluorescent biosensor for xanthine. *Biosensors Bioelectron*. **2008**, *24(4)*, 1059-1062.

[20] Bhatia, R. B.; Brinker, C. J.; Gupta, A. K.; Singh, A. K., Aqueous Sol-Gel Process for Protein Encapsulation. *Chem. Mater.*, 2000, *12(8)*, 2434-2441.

[21] Liu, D.M.; Chen, I.W., Encapsulation of protein molecules in transparent porous silica matrices via an aqueous colloidal sol-gel process. Acta Materialia 1999, 47(18), 4535-4544

[22] Miller, J. M.; Dunn, B.; Valentine, J. S.; Zink, J. I., Synthesis conditions for encapsulating cytochrome c and catalase in SiO_2 sol-gel materials. *J. Non-Cryst. Solids* **1996**, *202(3)*, 279-289.

[23] Zhou, H.; Zhang, Z.; Yu, P.; Su, L.; Ohsaka, T.; Mao, L., Noncovalent attachment of NAD^+ cofactor onto carbon nanotubes for preparation of integrated dehydrogenase-based electrochemical biosensors. *Langmuir* **2010**, *26(8)*, 6028–6032.

[24] Wang, J., Analytical electrochemistry, *3rd Edition.* Wiley-VCH, **2000,** P 28.

[25] Stuart, B., Infrared Spectroscopy: Fundamentals and Applications. Wiley, **2004,** P 20-21.

[26] Kwak, J.; Bard, A. J., Scanning electrochemical microscopy. Theory of the feedback mode. *Anal. Chem.* **1989**, *61(11)*, 1221-7.

[27] Bard, A. J.; Fan, F. R. F.; Kwak, J.; Lev, O., Scanning electrochemical microscopy. Introduction and principles. *Anal. Chem.* **1989**, *61(2)*, 132-8.

Chapitre III. Etude de faisabilité de l'encapsulation d'une déshydrogénase dans une matrice sol-gel

Ce chapitre montre les études qui ont été menées pour immobiliser sous une forme active la D-sorbitol déshydrogénase (DSDH) dans une couche mince sol-gel à la surface d'une électrode. Les études ont été menées sur électrodes de carbone vitreux avant d'être appliquées à la modification d'électrodes d'or macroporeuses.

Dans un premier temps, l'étude a été menée en utilisant le dépôt par évaporation à partir d'un sol à base seulement de TEOS conduisant à l'encapsulation de la DSDH dans une matrice de silice pure. Ces conditions d'immobilisation ne permettent pas de mesurer une activité catalytique (par oxydation du NADH devant être produit par la protéine pendant l'oxydation du sorbitol). L'influence de l'introduction de différents additifs dans le sol sur l'activité enzymatique a ensuite été étudiée. Il a ainsi été montré que l'introduction de polyélectrolyte positivement chargés au sein de la couche mince sol-gel permettait d'observer une bonne activité de la DSDH vis-à-vis de l'oxydation du D-sorbitol.

La bioencapsulation sol-gel a ensuite été obtenue par électrochimie. L'électrodépôt sol-gel est basé sur la modulation électrochimique du pH à la surface de l'électrode qui conduit à une transition sol-gel rapide seulement à proximité de l'électrode et à la formation de la couche mince. Le rôle des polyélectrolytes mis précédemment en évidence a été confirmé et la composition du sol ainsi que les paramètres d'électrogénération (temps et potentiel d'électrolyse) ont été optimisés. Il a été observé que ce procédé d'électrogénération sol-gel était parfaitement adapté à l'encapsulation de la DSDH et à la co-immobilisation avec la diaphorase (cette dernière protéine catalysant la régénération du cofacteur enzymatique en présence d'un médiateur redox). Enfin, le protocole optimal d'électrogénération a été appliqué à la fonctionnalisation contrôlée d'électrodes d'or macroporeuses présentant une grande surface électroactive.

Chapter III. Feasibility of dehydrogenase encapsulation in sol-gel matrix

In this chapter, the work focuses on the immobilization of the active dehydrogenase on the electrode surface. Here, sol-gel is chosen as the matrix for the D-sorbitol dehydrogenase (DSDH) encapsulation, which is expected to be likely to provide suitable environment for bioencapsulation. First of all, the feasibility of DSDH encapsulation in sol-gel film is evaluated by drop-coating (see section 2). DSDH encapsulation in pure silica thin films resulted in undetectable electrochemical signal. Then, the influence of polyelectrolyte (PE) additives on the sol-gel encapsulation of dehydrogenases has been evaluated by drop-coating. DSDH was found to be very sensitive to the silica gel environment and the addition of a positively-charged polyelectrolyte was necessary to ensure effective operational behavior of the biomolecules. Since the suitable sol-gel environment for DSDH encapsulation has been found by drop-coating, we then investigate the electrochemically-assisted deposition of sol-gel thin films for DSDH encapsulation (see section 3). This was achieved via the electrolysis of a hydrolyzed sol containing the biomolecules to initiate the polycondensation of silica precursors upon electrochemically-induced pH increase at the electrode/solution interface. The composition of the sol and the conditions for electrolysis have been optimized with respect to the intensity and the stability of the electrochemical response to D-sorbitol oxidation. The electrochemically-assisted deposition of silica thin films was found to be a good strategy for DSDH immobilization as well as DSDH and diaphorase co-immobilization. At the end, this process has been extended to macroporous electrodes exhibiting a much bigger electroactive surface area.

1. Introduction

Dehydrogenases are interesting enzymes for electrosynthesis applications, especially for the production of rare sugars as building blocks for pharmaceutical and food industry [1]. One of the main requirement for electrosynthesis is the stable immobilization of a large amount of active proteins on the electrode surface of the reactor [2, 3]. The encapsulation of proteins in a silica matrix using the sol-gel process is known to prevent their denaturation and to keep these proteins active for a long time, in some case longer than in solution, and can also allow the use of some enzymes in rather harsh conditions of pH and temperature [4]. When tetraethoxysilane (TEOS) is used as silica precursors, the hydrolysis of the ethoxy groups leads to a significant amount of ethanol potentially harmful for the enzyme. Ethoxy groups can be replaced by methoxy groups, to produce methanol that was reported to be less toxic for the enzyme [5]. Alcohol molecules can also be removed by solvent evaporation [6] and other sol-gel routes can also be involved in order to prevent the presence of any alcohol molecules in the starting sol [7]. A good example of this last strategy was reported recently for the encapsulation of horseradish peroxidase (HRP) in silica thin films obtained by electrochemically-assisted deposition with a sol based on ammonium hexafluorosilicate [8]. A favorable environment can also be obtained by the introduction of additives into the sol [9]. Recent efforts have been made to optimize the process by controlling the porosity of the material and the chemical environment of trapped species. This notably involved the use of biocompatible silane precursors, protein-stabilizing additives, charged polymers, or sugars and aminopeptides [4, 10, 11].

For electrochemical applications, the silica thin films can be effectively deposited on the surface of a flat electrode by the conventional sol-gel method using the controlled evaporation of the solvent by dip-coating, drop-coating, etc [12]. This has been largely exploited to design amperometric biosensor devices [13]. In the particular case of electro-enzymatic synthesis, the electroactive surface area of the reactor has to be increased in order to allow high flux of substrate to be oxidized or reduced. This can be achieved, e.g., by the use of macroporous electrodes exhibiting very high surface areas [14, 15]. However, coating such porous electrodes in a controlled way with an enzyme-doped silica gel is somehow difficult with the evaporation methods cited above because they are mostly restricted to flat surfaces [16]. As an alternative, the silica layer can be produced at porous electrode surfaces by a local

modulation of pH [17]. This is achieved by a controlled electrolysis of the pre-hydrolyzed sol that induces the rapid gelification of the thin film. The possible application of the electrochemically-assisted sol-gel deposition to bio-encapsulation was shown recently by some research groups, using glucose oxidase as a model enzyme [18, 19].

It is also essential for electrosynthesis application to ensure a very smooth regeneration of the cofactor, especially if the cofactor is successfully immobilized with the protein(s), to prevent non-controlled oxidation of the expensive NADH (or reduction of NAD^+). Diaphorase catalyzes this cofactor regeneration in the presence of a molecular mediator, for example ferrocene species for oxidation or methylviologen for reduction [20]. The co-immobilization of both dehydrogenase and diaphorase in active forms into a thin silica film would allow the reactor to perform alternatively oxidation or reduction reactions by "simply" changing the mediator system and the applied potential [21, 22]. For this reason the well-controlled deposition of such active bio-composite layers in macroporous electrodes would be of great value for bioelectrocatalytic application.

In this work, we used DSDH as model enzyme to evaluate the feasibility of dehydrogenase encapsulation in sol-gel film. First, we have evaluated the interest of various polyelectrolytes in combination to silica films for DSDH encapsulation (section 2). We have chosen positively-charged polyelectrolytes because of expected favorable interactions with the negatively-charged enzyme surface [23]. Comparing the electrochemical responses observed in the presence and absence of these additives allowed to evidence the critical role played by the polyelectrolyte in enhancing cofactor regeneration. Then, we show the electrochemically-assisted deposition of silica-based thin films for DSDH immobilization as well as DSDH and diaphorase co-immobilization (section 3). The process and the sol composition have been optimized on flat glassy carbon electrodes before being applied to macroporous gold electrodes. The electrodeposited bio-composite containing both DSDH and diaphorase has been tested for electrochemical oxidation of D-sorbitol and a comparison was made between flat and macroporous gold electrodes.

2. Critical effect of polyelectrolytes on the electrochemical response of dehydrogenases entrapped in sol-gel thin films

2.1 Preliminary observations

D-sorbitol dehydrogenase (DSDH) needs electron transfer cofactors ($NADH/NAD^+$) for its enzymatic activity. A large amount of work has been done over the past years in order to decrease the overpotentials for the electrochemical detection of this cofactor, especially when operating in oxidation mode [24]. For simplicity, we first considered the direct oxidation of NADH (i.e., without mediator) to evaluate the activity of the enzyme encapsulated into the sol-gel matrix to be tested. The overall reaction scheme is shown on ***Figure III-1***. The sol-gel film contains encapsulated DSDH and the cofactor is present in solution (typically at a concentration of 1 mM) to which various concentrations of D-sorbitol were added. DSDH catalyses the oxidation of D-sorbitol into fructose and simultaneously NAD^+ is reduced into NADH. The equilibrium of this enzymatic reactions strongly favors the substrate (D-sorbitol) rather than the product (fructose) side because of the very low formal potential of the NAD^+/NADH redox couple (-560 mV versus saturated calomel electrode, pH 7.0, 25°C). Here, the electrochemical oxidation of NADH at the electrode surface pushes the reaction to the product side. The reduced form of the cofactor can be detected electrochemically on glassy carbon. In our experimental conditions, a well-defined oxidation peak was observed on bare glassy carbon electrode (GCE) around +0.7 V (versus Ag/AgCl reference electrode).

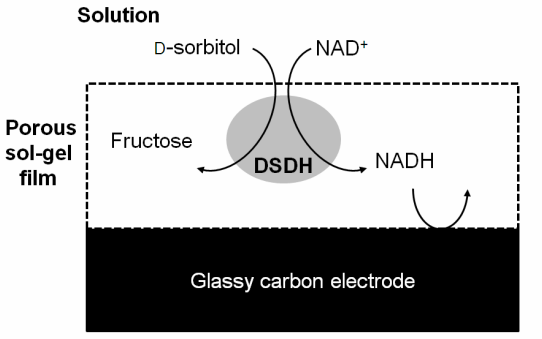

Figure III-1. *Enzymatic and electrochemical reactions occurring on the gel-enzyme modified GCE.*

2.1.1 Enzyme encapsulation in pure silica films

The encapsulation of DSDH was first evaluated with using pure silica thin films (i.e., without any additive). ***Figure III-2*** reports the electrochemical characterization of the film deposited by drop-coating on GCE. It is shown that the addition of D-sorbitol into the solution does not lead to noticeable modification of the current response and no peak current can be observed at the potential of NADH oxidation. Obviously, the enzyme does not exhibit electrochemically detectable activity when encapsulated into the pure silica layer. The actual sol contains a certain amount of alcohol that could be harmful for the enzyme (possible denaturation). Other sol-gel protocols have thus been tested: alcohol evaporation before enzyme encapsulation, use of other silica precursors (aqueous silicates or TMOS instead of TEOS). In all cases, the biocomposite films deposited on GCE did not reveal any measurable electroactivity. Several hypotheses can be proposed to explain the absence of response: (1) DSDH was not successfully incorporated into the sol-gel matrix; (2) enzyme entrapment was successful but led to loss in its biological activity; (3) DSDH was successfully entrapped in an active form but lack of effective electrochemical transduction made the detection not visible.

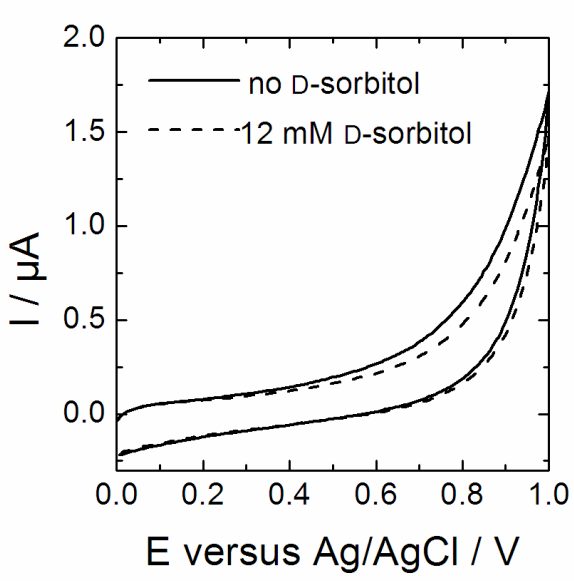

Figure III-2. *Cyclic voltammograms obtained using GCE modified with a silica/DSDH film in the absence (dashed line) and in the presence (plain line) of 12 mM D-sorbitol. The measurements have been performed in 0.1 M Tris-HCl buffer solution (pH 9) containing 1 mM NAD^+. Potential scan rate was 50 mV/s.*

2.1.2 UV monitoring of the enzyme activity in gel monoliths

In order to distinguish between the above hypotheses, DSDH was encapsulated in sol-gel-derived monoliths and its biological activity was monitored by UV spectroscopy via NADH generation upon addition of D-sorbitol in the medium. The biomaterial was prepared according to a protocol reported by Miller et al. [25], requiring notably a rather long aging period (6 days at 4°C). Significant shrinkage of the monolith occurred during gelification. The solid was then washed three times in 3 mL phosphate buffer solution in order to remove weakly encapsulated enzymes. It was then introduced into a solution containing 0.36 mM NAD^+ and 5 mM D-sorbitol. The activity of encapsulated DSDH can be evidenced by UV monitoring of the solution phase at 340 nm (maximum absorbance for NADH detection). ***Figure III-3*** shows the variation of generated NADH concentrations versus the contact time between the D-sorbitol solution and the enzyme-entrapped gel. As shown, DSDH was still active when encapsulated into the sol-gel silica material (see curve "b" in ***Figure III-3***) but the response was much slower and much lower than that of free enzyme in solution (compare with inset in ***Figure III-3***) as only 20 % of NAD^+ have been transformed after 6 hours of reaction. A blank experiment (curve "a" in ***Figure III-3***) confirms that UV response was indeed due to NADH generation originating from the activity of encapsulated DSDH.

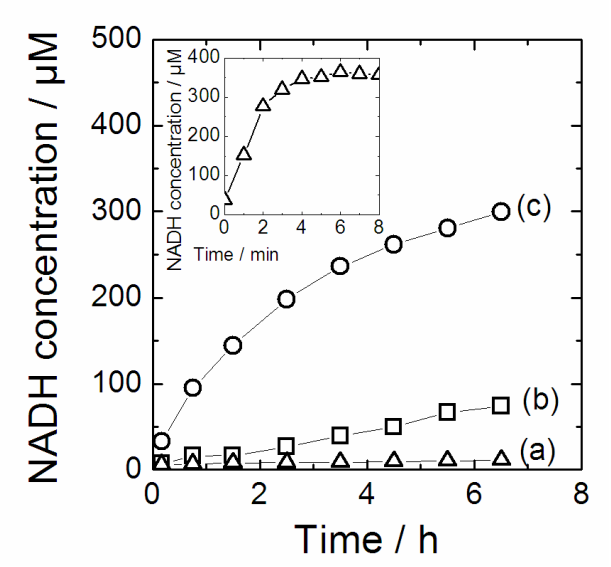

Figure III-3. *Evolution of the NADH concentration in solution (a) in the absence of enzyme encapsulated silica gel and in the presence of a gel monolith containing (b) only DSDH and (c) both DSDH and PDDA (1.7 % w/w) . Experiments were performed in 0.1M pH 9.0 Tris-HCl buffer solution containing 0.36 mM NAD^+ and 5 mM D-sorbitol. NADH concentration was determined by UV absorbance at 340 nm. Inset: free enzyme in solution.*

The pH of the sol used for the enzyme encapsulation was comprised in between 5 and 7. In these conditions, negative charges are present on the silica surface due to silanol deprotonation (the point of zero charge of silica is reported to be in the range 2-3 [26]). The isoelectric point of DSDH is 4.3 [27]. During the protein encapsulation, the interaction between the silica matrix and the protein seems to be not so favorable in the pH conditions used here. The above sol-gel entrapment and UV monitoring experiments have thus been repeated on the basis of monoliths prepared in the presence of a positively-charged polyelectrolyte (PDDA) likely to act as a stabilizing intermediate between the enzyme and the silica surface. Results presented in ***Figure III-3*** (curve "c") show that this is indeed the case as a much higher activity was observed with the gel containing PDDA for which almost 90 % of NAD^+ have reacted after the same period of time (6 h). It is noteworthy that the process is still much slower than for the free enzyme in solution, but the presence of PDDA in the sol-gel encapsulation matrix provides definite advantage in comparison to undoped silica.

2.2 Interest of additives for DSDH encapsulation onto electrode surfaces

2.2.1 Sol-gel matrices

The above results suggest that the presence of positively-charged moieties in the silica/DSDH biocomposite would be helpful to improve the enzyme activity and thereby to enhance the electrochemical response of GCE covered with such biocomposite films. We have evaluated two ways to introduce positive charges in the material: (1) the resort to a positively-charged organosilane (i.e., protonated aminopropyltriethoxysilane, APTES) and (2) the addition of positively-charged polyelectrolytes.

Figure III-4A shows the typical response of a bio-composite film deposited on GCE from a sol made of 50 mol% APTES relative to the total content of precursor (TEOS+APTES), for increasing D-sorbitol concentrations in the solution. The modified electrode is now sensitive to the addition of the substrate in the 2 to 12 mM concentration range. The signals correspond to the oxidation of NADH produced by the enzyme encapsulated into the film. They are however less well-defined and positively-shifted (by ca. 100-150 mV) in comparison to NADH oxidation on bare GCE (inset in ***Figure III-4A***). This suggests that the presence of the silica film induces some resistance to charge transfer kinetics. One can conclude from this first series of experiments that favorable electrostatic interactions between DSDH and the aminopropyl-functionalized silica matrix (point of zero charge = 9.8 [28]) is beneficial for

getting electrochemically detectable enzymatic activity. The positive charges held by the aminopropyl groups could also interact with NAD^+ (which is also negatively charged), bringing DSDH and NAD^+ together and allowing a higher net production of NADH [29, 30].

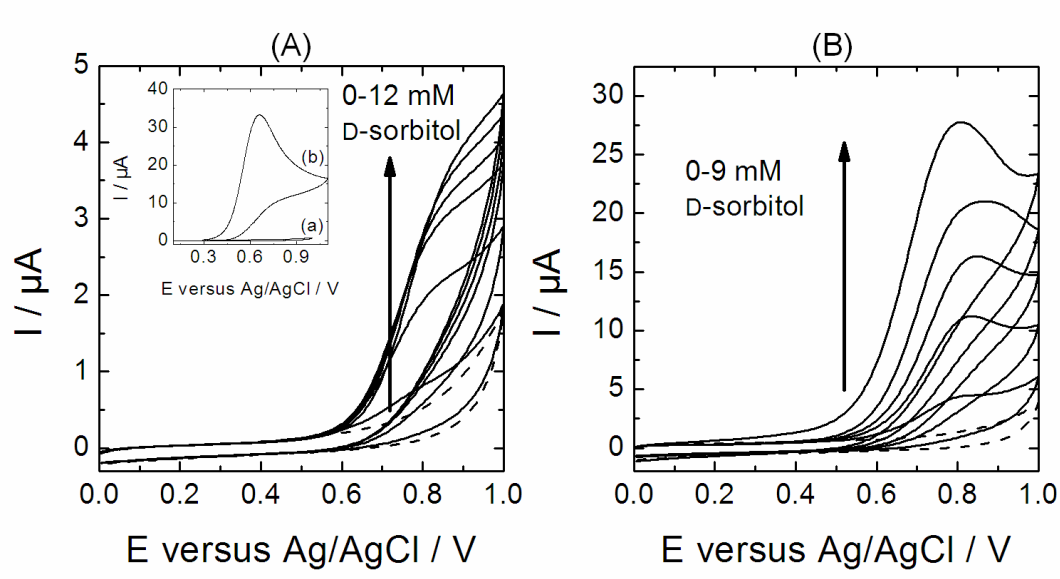

Figure III-4. *Influence of additives (**A**, 50 mol % APTES; **B**, 5 % w/w PDDA) introduced into the synthesis sol on the electrochemical response of DSDH-silica composite films on GCE, as measured by cyclic voltammetry in the presence of increasing concentrations of D-sorbitol. Cyclic voltammogram for solution-phase NADH (curve "a" without NADH and curve "b" with 5mM NADH) at bare GCE has been added as inset in part A of the figure. Potential scan rate 50 mV/s. Others conditions as in Figure III-2.*

Figure III-4B shows that even more impressive behavior can be obtained when using a polyelectrolyte (i.e., 5% PDDA) as additive in the starting sol. A well-defined electrochemical response was observed, increasing regularly by increasing the D-sorbitol concentration from 1 to 9 mM, in the same conditions as those applied for films prepared in the absence of PDDA (***Figure III-2.***). The signal corresponds to the oxidation of NADH produced by the enzyme encapsulated into the film. The measured peak currents (~30 µA for 9 mM D-sorbitol, ***Figure III-4B***), were largely superior to those reported when using APTES (~4µA for 10 mM D-sorbitol, ***Figure III-4A***). The interpenetrating PDDA-silica network thus provides a suitable microenvironment for DSDH encapsulation; it may also contribute to generate a more open structure than in pure silica, which would accelerate mass transport of the various reagents (substrate and cofactors). The key parameter seems however to be the favorable electrostatic interactions originating from the positive charges of the polymer additive, as confirmed by comparing the results obtained for various polyelectrolytes, i.e., three positively-charged

compounds in the condition of encapsulation (PDDA, PAA and PEI) and one displaying negative charges (Nafion). This is illustrated in ***Figure III-5,*** showing the variation of peak currents versus the concentration of D-sorbitol for the different polyelectrolytes. The encapsulation of alcohol dehydrogenase in Nafion membrane has been reported [31], but here the introduction of this negatively charged polyelectrolyte into the sol, led to inactive electrode as no NADH can be detected when increasing the substrate concentration in the solution (curve "a"). At the opposite, all polyelectrolytes bearing positive charges gave rise to good sensitivity of the modified electrode to the enzymatic substrate, the use of PDDA (curve "d") being somewhat more efficient than PEI (curve "b") or PAA (curve "c"). These results support the aforementioned assumption concerning the need of positive charges into the gel for ensuring good encapsulation of DSDH in an active form.

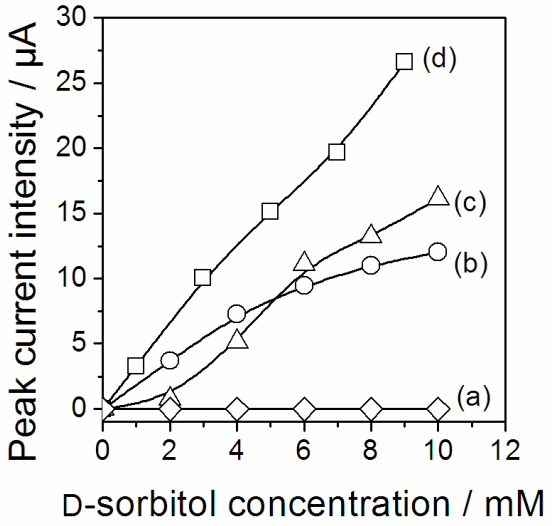

Figure III-5. *Variation in peak currents for NADH oxidation versus the d-sorbitol concentration measured with films prepared with TEOS as silica precursor and (a) Nafion, (b) PEI, (c) PAA and (d) PDDA as polyelectrolyte (5% w/w). Other conditions as in Figure III-2.*

2.2.2 Extension to chitosan and chitosan sol/gel composites

Chitosan is produced by deacetylation of chitin bio-polymer. This reaction allows generating a certain fraction of amine functions that makes the polymer soluble and suitable for bio-encapsulation [32]. This property has been advantageously used for electroanalytical purposes [33]. One observed in the previous section that doping silica sol-gel films with polymers bearing protonated amine or ammonium groups was essential for improving the enzymatic activity of DSDH immobilized on GCE. We have thus evaluated if chitosan, in

combination with silica gel, could provide this favorable environment because of the amine groups it holds. ***Figure III-6A*** shows the typical response observed with a chitosan-silica gel composite with encapsulated DSDH. The electrode was first tested with cyclic voltammetry in a Tris-HCl buffer solution containing 1 mM NAD^+ (dashed line) and, as expected, no anodic peak was observed. More surprising was the absence of signal upon addition of D-sorbitol from 2 to 8 mM in the medium, suggesting that no NADH was produced by the DSDH enzyme (only a decrease in background currents was observed). It was necessary to introduce PDDA in addition to chitosan in the biocomposite film to observe the production of NADH in the presence of D-sorbitol (***Figure III-6B***). The measured currents are in the same magnitude as those observed with silica gel/polyelectrolyte composites (***Figure III-6B***).

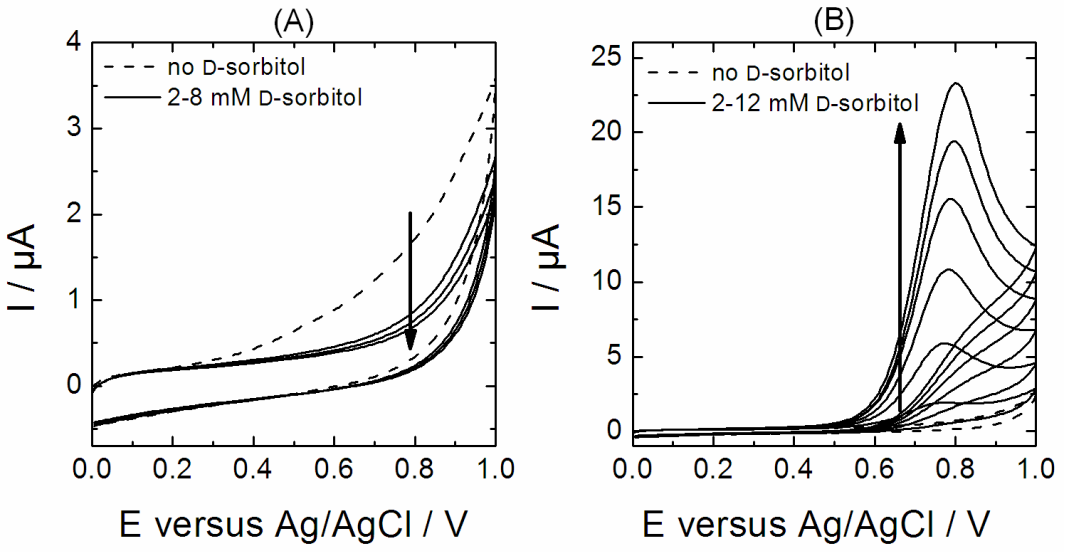

Figure III-6. *Cyclic voltammograms obtained at GCE modified with (A) a chitosan/silica/DSDH film and (B) a chitosan/silica/PDDA/DSDH film. Measurements have been performed in the absence (dashed line) and in the presence (plain line) of D-sorbitol, up to 12 mM. Potential scan rate 50 mV/s. Other conditions as in Figure III-2.*

Sol-gel-free chitosan films as encapsulation matrices for DSDH were finally tested, but no significant change in the voltammetric behavior was observed: no response to D-sorbitol in the absence of PDDA in the film (***Figure III-7A***) and good response to increasing concentrations of this substrate in the PDDA-doped film electrode (***Figure III-7B***). The only small difference with sol-gel and chitosan-sol-gel layers was a slightly better sensitivity for pure chitosan film. This clearly confirms the critical effect of polyelectrolytes on the electrochemical responses of encapsulated DSDH. The same conclusion was drawn when

using another enzyme of the same family (galactitol dehydrogenase, GatDH, with hexanediol as substrate), as well as when operating with these enzymes in reduction instead of oxidation, using hydroxyaceton (GatDH) or fructose (DSDH) as substrates (data not shown).

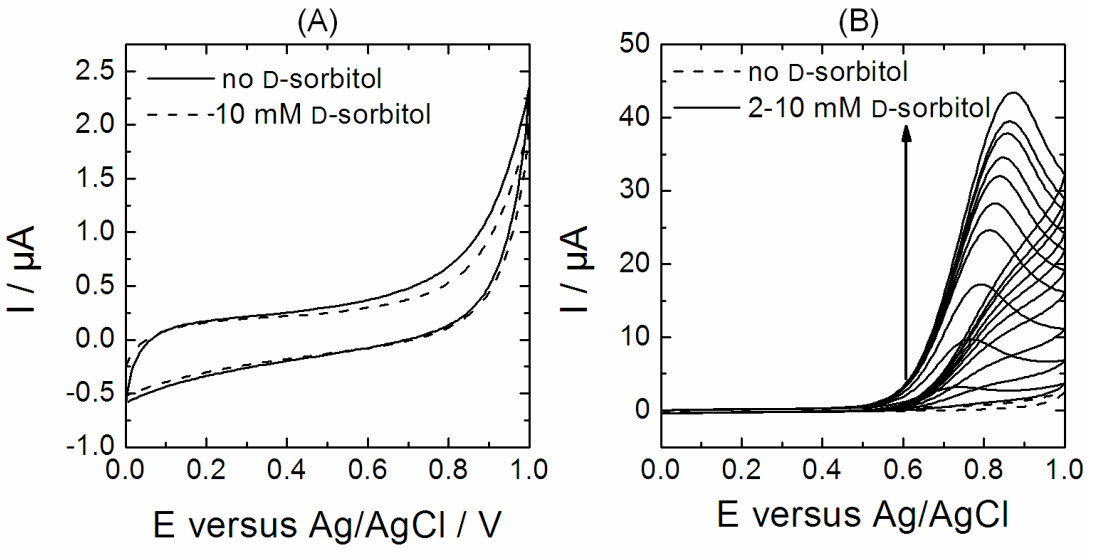

Figure III-7. *Cyclic voltammograms obtained at GCE modified with (A) a chitosan/DSDH film and (B) a chitosan/PDDA/DSDH film. Measurements have been performed in the absence (dashed line) and in the presence (plain line) of* D*-sorbitol, up to 10 mM. Potential scan rate 50 mV/s. Other conditions as in Figure III-2.*

2.3 Factors affecting the electrode response

2.3.1 Sol composition

The sol composition has been optimized in order to define conditions leading to the highest electrochemical response. Both polyelectrolyte (PDDA has been selected because it gave rise to best results among others, see ***Fig. III-5***) and precursor (TEOS) concentrations have been found to affect significantly the film electrode response (***Figure III-8***).

Figure III-8A shows the influence of PDDA content into the starting sol. As already discussed above, the absence of PDDA led to inactive films since no NADH was detected in the presence of D-sorbitol (***FigureIII-2***). Addition of PDDA, even in few amounts (e.g., 1.7 %) resulted in significant electrochemical signals, the intensity of which increasing up to 5 % and decreasing then quite regularly for higher polyelectrolyte contents (up to 10 %). All electrodes displayed well-defined voltammetric peaks for NADH oxidation. This trend leading to an

optimal value of 5 % can be explained by the role played by PDDA, acting somewhat as "macromolecular glue" between the enzyme and silica surfaces, too low or too high contents of this additive contributing to unbalance the stabilizing effect. Another explanation can be found in the concentration-dependent effect of polycationic macromolecules on biosilication, in providing a favorable interaction with silica precursors during the sol-gel process that contributes to the gelification [7]. They can also induce modification in the texture of the final material [34], which would affect mass transport processes in the biocomposite and, therefore, the rate of cofactor generation/regeneration.

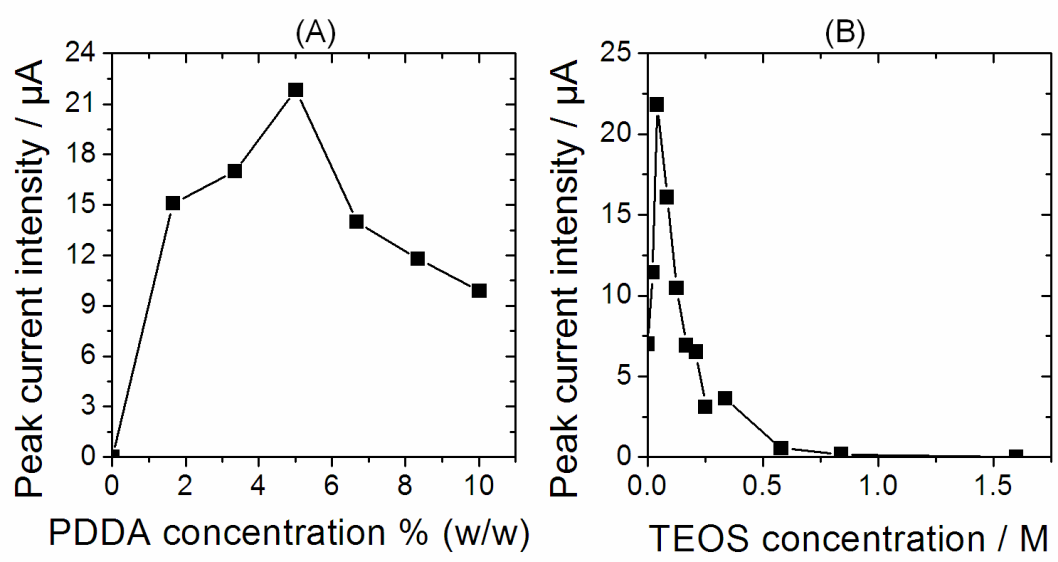

Figure III-8. *Variation of peak currents sampled at DSDH-doped sol-gel modified GCE in the presence of 8 mM D-sorbitol, as a function of (A) the amount of PDDA in the starting sol prepared with 42 mM TEOS and (B) the TEOS concentration initially introduced in the synthesis medium, in the presence of 5 % PDDA. Other conditions are the same as in Figure III-2.*

The concentration of TEOS in the starting sol has a strong influence on the electrochemical response of the resulting bio-composite films (***Figure III-8B***). One has first to mention that a DSDH-doped film deposited with PDDA only (5 % w/w in the starting solution), in the absence of silica precursor, gave already rise to a well-defined response but it was not stable with time (see data and discussion below) because only electrostatic interactions are responsible for enzyme immobilization onto the electrode surface. The addition of small amounts of TEOS led to an increase of both the mechanical stability of the film and the

intensity of the electrode response. Gelification and silica formation around the PDDA/enzyme assembly contributes to stabilize the biocomposite and to prevent fast leaching of the protein into the solution. A maximum current was observed for a TEOS concentration of 42 mM. The use of higher concentrations of the silica precursor in the starting sol induced then a dramatic drop in the electrochemical response, the film resembling more and more to a PDDA-free silica layer, in agreement with what was observed with pure silica gels (***Fig. III-2***). No noticeable response can be detected when using TEOS concentrations above 1 M. The electrochemical response is not only related to the enzyme activity but also strongly dependent on the diffusion of both D-sorbitol substrate and NAD^+ cofactor inside the film. While a low concentration of silica precursor induced the formation of a rather porous matrix, suitable for both encapsulation and diffusion, increasing TEOS concentrations led to densification of the silica matrix and thicker films [35], which became less suitable for fast diffusion of species from the solution to the enzyme and from the enzyme to the electrode surface.

2.3.2 Stability with time

Both composition of the film and type of additives have been found to affect significantly the operational and long-term stability of the biocomposite electrodes. This has been studied for three typical cases (PDDA/DSDH, Chitosan/PDDA/DSDH, and Silica/PDDA/DSDH films on GCE) and variations in the relative peak currents of the modified electrodes to 6 mM D-sorbitol in the presence of 1 mM NAD^+ are shown in ***Figure III-9***. The relative current values are given versus the peak height measured during the first cycle, about 1 min after the electrode was placed in solution. Let's first consider the short-term operational stability (***Figure III-9A***). With the Silica/PDDA/DSDH composite (curve "c") an increase in peak current intensity *ca.* 65% was first observed, which can be due to changes originating from the film hydration (dissolution/precipitation of silica can occur and the presence of PDDA can influence strongly this silication process [7]). After this initial step, the current reached more stable values, yet continuing to increase slowly with time, varying from 1.65 to 1.8 for the last 3 h of the experiment. Immobilization of DSDH in a pure PDDA film, in the absence of silica precursor, also allowed measuring a current response when the electrode was introduced in solution but this was not stable in successive measurements (increase in the first 30 min of experiment and then continuous decrease down to the initial value). This can be due to lack of mechanical stability of the film, with progressive leaching of the enzyme in solution. Despite

chitosan is known to be a suitable matrix for bio-encapsulation [33], the last system Chitosan/PDDA/DSDH gave rise to even more variable response, starting with a sharp increase in peak currents and following with dramatic decrease in the signal intensity after 30 min of use.

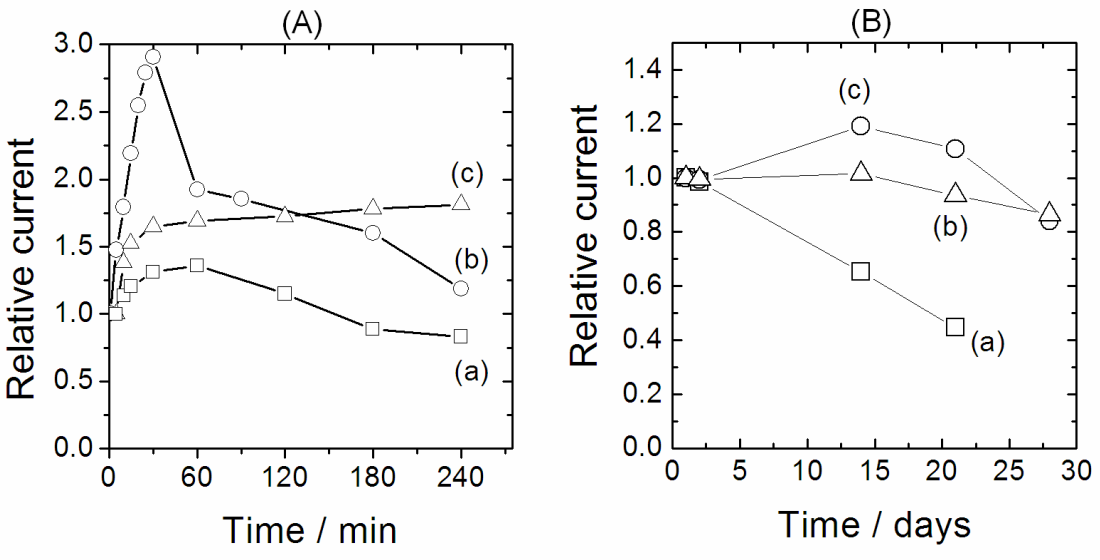

Figure III-9. *Evolution of the relative peak currents recorded for successive analyses of 6 mM D-sorbitol solutions (in the presence of 1 mM NAD^+) at distinct periods of time, using various DSDH-doped film electrodes: (A) short-term measurements have been made with GCE modified with (a) PDDA/DSDH film, (b) chitosan/PDDA/DSDH film, and (c) silica/PDDA/DSDH film; (B) long-term measurements have been made with GCE modified with (a) silica/PAA/DSDH film, (b) silica/PEI/DSDH film, and (c) silica/PDDA/DSDH film. Other conditions as in Figure III-2.*

For all electrodes, a reorganization/modification of the film resulted in an enhancement of the electrochemical response during the first minutes. This probably arises from easier diffusion of the substrate and cofactor species into the composite matrix. However, after this first step, only the sol-gel-derived film resulted in steady-state values of peak currents, all other systems underwent significant degradation of the electrochemical response. This can be ascribed to the rigid character of the inorganic network likely to ensure more durable bio-encapsulation, which appears promising for bio-electrochemical applications.

The long-term stability of the best systems (sol-gel based biocomposite film electrodes with added polyelectrolytes) has been also considered. ***Figure III-9B*** shows the evolution of the electrode response during almost 1 month for three electrodes prepared with combining positively charged polyelectrolytes (PAA, PEI and PDDA) with silica precursors for the

enzyme encapsulation. The worst stability was observed with PAA (curve "a") for which current response of the electrode was found to drop by 50 % within three weeks. PEI (curve "b") displayed a rather stable electrochemical response as the measured peak currents did not change significantly during the first 15 days of investigation and then decreased by less than 15 % in the second half of the month. Finally, the behavior of the electrode prepared with PDDA (curve "c") resembles to that prepared with PEI, being slightly less stable, as its response was maximum after 15 days and decreased somewhat afterwards, suggesting some lack of long-term stability.

3. Electrochemically-assisted deposition of sol-gel bio-composite with co-immobilized dehydrogenase and diaphorase

3.1. Feasibility of the electrochemically-assisted deposition

The electrochemically-assisted deposition of silica thin films involves the local perturbation of the pH at the electrode solution interface. Starting from a stable sol, slightly acidic, the electrochemically-induced pH increase allows a fast gelification only at the electrode surface. The electrolysis of the sol at -1.3 V leads to the rapid formation of the thin sol-gel bio-composite layer. All films that are displayed in ***Figure III-10*** have been prepared using 60 s electrolysis. ***Figure III-10A*** shows the electrochemical response of the DSDH-modified electrode to successive addition of D-sorbitol in the solution from 1 to 8 mM. Before addition of this enzymatic substrate, no electrochemical signal could be observed between 0 and 1 V. A well defined voltammetric signal with a peak potential located between 0.7 and 0.8 V (versus Ag/AgCl reference electrode) appears when D-sorbitol is added to the solution and this signal increases with the D-sorbitol concentration. It corresponds to the electrochemical oxidation of the NADH cofactor produced by the encapsulated DSDH while oxidizing D-sorbitol. Here the enzymatic cofactor is directly detected at the glassy carbon electrode without using electron mediator. ***Figure III-10B*** confirms the results observed in ***Figure III-10A***, with the same enzyme, but for the reduction of fructose. No electrochemical signal could be observed in the absence of fructose. The addition of fructose from 1 to 8 mM produces well defined electrochemical responses with a peak potential close to -1.1 V versus Ag/AgCl

reference electrode. This signal corresponds to the reduction of the NAD^+ cofactor produced by DSDH in the presence of fructose. The electrode was here sensitive to the concentration of fructose from 1 to 8 mM. DSDH immobilized in electrogenerated silica film is thus active in both oxidation and reduction sides.

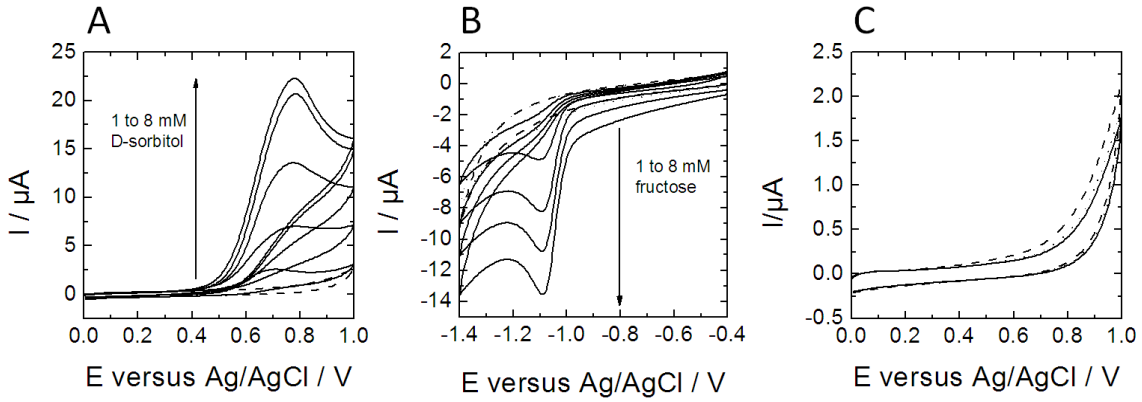

Figure III-10. *Electrochemical responses to D-sorbitol (A) and to fructose (B) measured at GCE modified by DSDH with using sol-gel E-AD. E-AD was done at -1.3 V for 60 s from a sol containing 0.17 M TEOS, 3.3 mg/mL DSDH and 6.7% PDDA. (A) Responses in the absence of D-sorbitol (dashed line) and in the presence of D-sorbitol from 1 to 8 mM (solid lines). CVs were done in Tris-HCl buffer (pH 9) containing 1 mM NAD^+ (B) Responses in the absence of fructose (dashed line) and in the presence of fructose from 1 to 8 mM (solid lines). CVs were done in 0.1 M phosphate buffer (pH 6.5) containing 1 mM NADH. (C) Blank experiments have been performed in tris-HCl buffer (pH 9.0) containing 1 mM NAD^+ and 6mM D-sorbitol with GCE modified by a film prepared with the same procedure as (A) but in the absence of the protein (solid line) or PDDA (dotted line) or prepared with the same sol (with protein and PDDA) but without applying the electrolysis potential for the EAD (dashed line).*

Figure III-10C shows several blank experiments (CV in the presence of 6 mM D-sorbitol) with films prepared in the absence of DSDH (plain line), in the absence of polyelectrolyte (dotted line), or by using the same sol and the same protocol as for the electrode presented in ***Figure III-10A***, but without applying the electrolysis step (dashed line). In all three cases, no electrochemical signal was observed. The later blank experiment (no electrolysis) demonstrates that the electrode response observed in ***Figure III-10A*** is only due to the DSDH protein encapsulated in a silica film that has been produced by electrochemistry and neither to any non specific protein adsorption nor gel deposition by evaporation that might have occurred in the course of the electrode preparation. Electrode modification is totally controlled by the electrochemically-assisted sol-gel deposition. Moreover the blank experiment performed in the absence of protein confirms that the signal observed around 0.7-

0.8 V is effectively due to the NADH produced by the encapsulated enzyme, demonstrating thus the operational activity of the biomolecules once immobilized. Finally the critical role of PDDA on the DSDH activity is confirmed as no polyelectrolyte in the silica film means no detectable enzymatic activity. In the conditions of electrochemically-assisted deposition, negative charges are present on the silica surface due to silanol deprotonation (the point of zero charge of silica is reported to be in the range 2–3 [26]). The isoelectric point of DSDH is 4.3 [27]. During the protein encapsulation, the interaction between the silica matrix and the protein seems to be not so favourable. The positively charged polyelectrolyte (PDDA) is likely to act as a stabilizing intermediate between the enzyme and the silica surface.

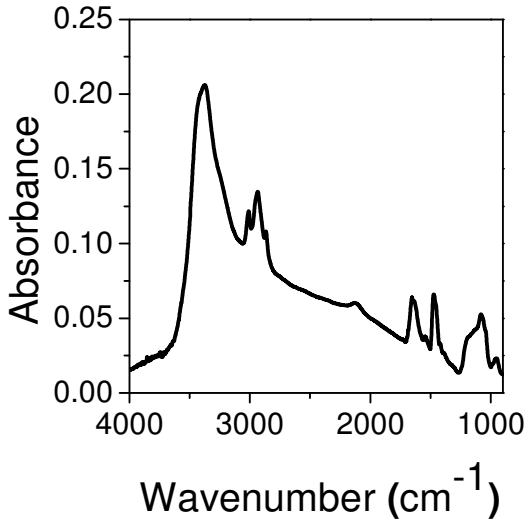

Figure III-11*. FTIR spectrum measured on a thin biocomposite film deposited on indium tin oxide electrode by sol-gel E-AD at -1.3 V for 10 s from a sol containing 0.17 M TEOS, 3.3 mg/mL DSDH and 6.7% PDDA.*

Figure III-11 shows the FTIR spectrum, which has been obtained on a thin film deposited on indium tin oxide electrode by sol-gel electrochemically-assisted deposition at -1.3 V for 10 s from the same sol as reported in ***Figure III-10*** (60 s electrochemically-assisted deposition led to a signal saturation, so shorter electrolysis time was necessary). Background measurement was done on unmodified ITO electrode. As expected the different bands related to the silica network (~1000-1200 cm^{-1}) and the surface silanol groups Si-OH (~900-1000 cm^{-1}), the amide I and II bands of the proteins (1653 and 1538 cm^{-1}), the band from the ammonium groups of PDDA (1474 cm^{-1}), and the C-H stretching bands of both PDDA and proteins (~2800-3050 cm^{-1}) were distinctively observed on the same spectrum. So the FTIR

measurement supports the observation made by cyclic voltammetry and indicates that PDDA and proteins are indeed co-encapsulated in the electrodeposited silica network.

3.2 Optimization of the electrode response

The effect of sol composition has been thoroughly studied and the three major parameters of the sol, i.e. the DSDH concentration (***Figure III-12A***), the PDDA concentration (***Figure III-12B***) and the TEOS concentration (***Figure III-12C***) have been varied and their influence on the electrochemical response of the resulting film to 6 mM D-sorbitol has been studied. The quantity of protein introduced into the sol has a strong influence on the electrode response, a rapid increase was observed from 0.3 to 2.5 mg/mL, which started to level off for 3.3 mg protein/mL of sol. Higher concentrations of protein cannot be used for this process due to a rapid gelification of the sol (proteins or buffer of the suspension facilitate the sol-gel transition). PDDA concentration has also a dramatic influence on the electrode response. In the absence of PDDA, no signal could be measured (see ***Figure III-12B***). The electrode became active in the presence of 1.8 % polyelectrolyte and the electrode response increased then regularly with increasing the polyelectrolyte concentration up to 6.7 %. As for the protein content, a higher quantity of PDDA is difficult to handle as it facilitates also the gelification of the sol before application of the electrolysis potential. The influence of TEOS concentration follows a different trend as it induces first an increase in the electrode response, passes through a maximum and then decreases. The optimal signal was observed for 0.17 M TEOS in the sol. We can assume that the deposition rate is too slow for low TEOS concentrations [35] inducing thereby less efficient protein encapsulation. On the other hand, a higher TEOS concentration can lead to hindered mass transport (see the next section) as a result of thicker films that limit the efficiency of the bio-electrode (restricted diffusion of the reactants). Deposition time has also a strong influence on the electrode response. ***Figure III-12D*** shows the effect of the time of electrolysis on the electrode response for sols containing (a) 1.67, (b) 3.35 and (c) 6.7 % PDDA. For high polyelectrolyte concentration, the optimal deposition time was found to be 60 s (3.35 and 6.7 %, curves a&b) and a higher time was observed with lower PDDA content (about 120 s for 1.67 %, curve c). It can be assumed that the quantity of encapsulated protein increases with increasing the deposition time, but film thickness probably becomes a significant limitation for too long deposition times.

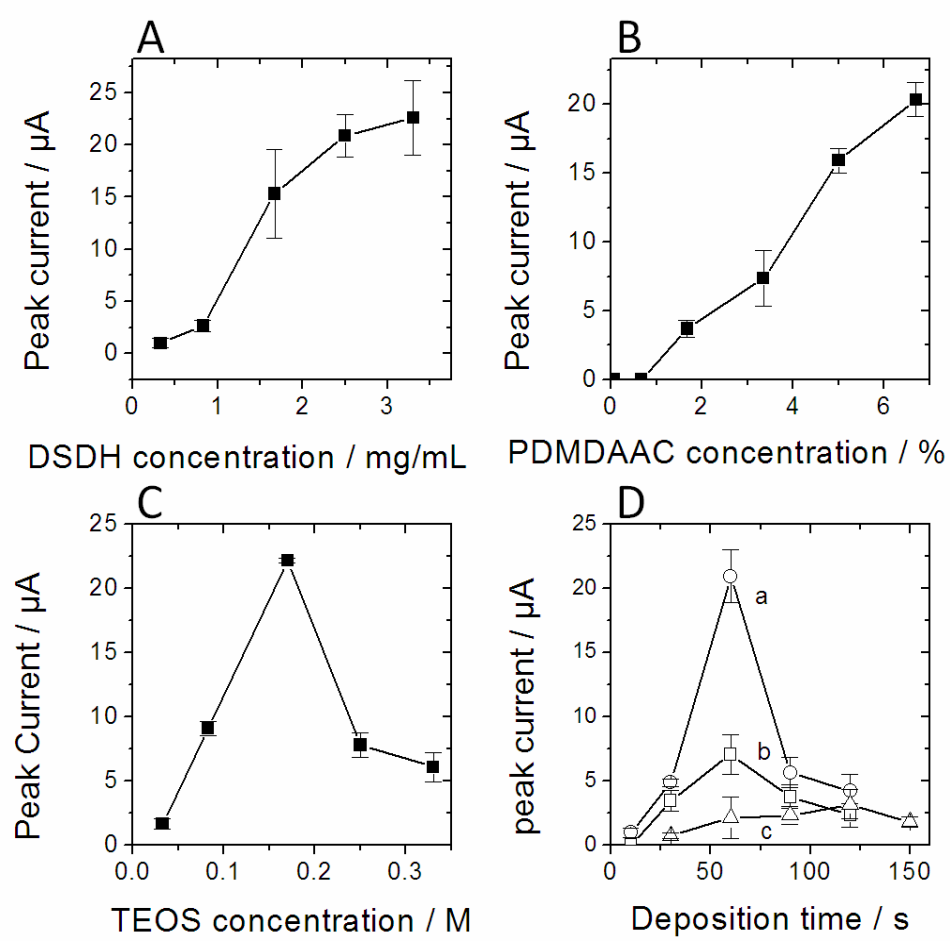

Figure III-12. *Influence of DSDH concentration (A), PDDA (B), deposition time (C) and TEOS concentration (D) on the peak current response measured at glassy carbon electrodes modified by an electrodeposited silica films with encapsulated DSDH. (A) The electrodes were prepared with 0.17 M TEOS sol, 6.7% PDDA and different concentrations of DSDH from 0.33 mg/mL to 3.3 mg/mL. The electrochemically-assisted deposition was done at -1.3 V for 60 s. (B) The electrodes were prepared with 0.17 M TEOS sol, 3.3 mg/mL DSDH and different concentrations of PDDA from 0 to 6.7 %. The electrochemically-assisted deposition was done at -1.3 V for 60 s. (C) The electrodes were prepared with a sol containing 3.3 mg/mL DSDH, 6.7 % PDDA and different concentrations of TEOS. The electrochemically-assisted deposition was done at -1.3 V for 60 s. (D) The electrodes were prepared with 0.17 M TEOS sol, 3.3 mg/mL DSDH and different concentrations of PDDA from 1.67 to 6.7 %. The electrochemically-assisted deposition was performed at -1.3 V for different deposition time from 10 to 150 s. For all experiments, cyclic voltammetry has been performed in 0.1 M Tris-HCl buffer (pH 9.0) containing 1 mM NAD^+ and 6 mM D-sorbitol. Potential scan rate was 50 mV/s.*

The influence of TEOS concentration and deposition time are evidenced by measuring the film thickness (by using the sheaforce mode of a SECM operating as a profilometer). TEOS concentration has a dramatic influence on the film thickness. As it is shown in ***Figure III-13A*** the film thickness increase with TEOS concentration, in agreement with what has been assumed from ***Figure III-12C***. Deposition time has also a strong influence on the film thickness. ***Figure III-13B*** shows the effect of the time of electrolysis on the film thickness. Only 0.2 µm variation is observed from 30s to 60s, and thicknesses increase rapidly beyond 1 µm from 60s to 90s.

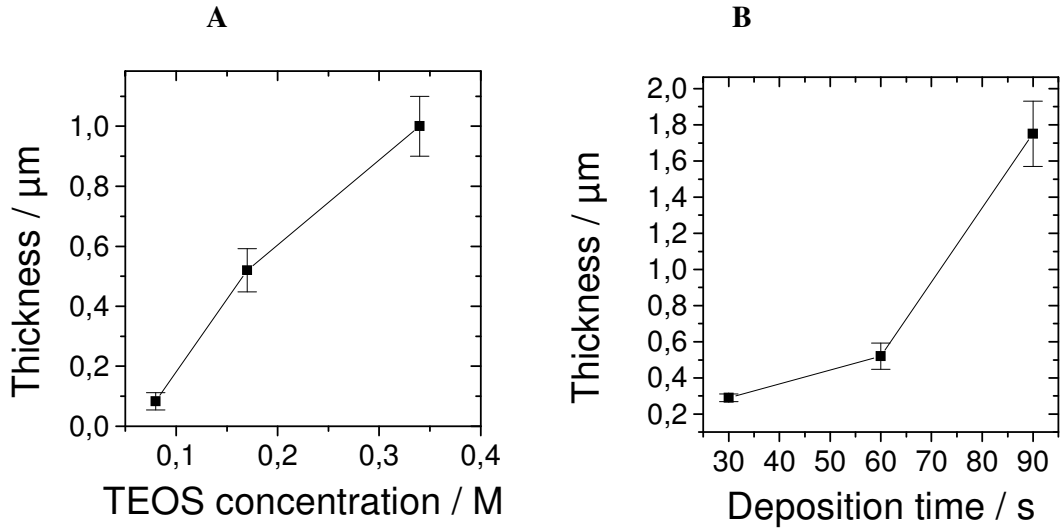

Figure III-13. *Corresponding variations of film thickness with (A) TEOS concentration; (B) deposition time, as determined by SECM. (A)E-AD was done at -1.3 V for 60 s with a sol containing 3.3 mg/mL DSDH, 6.7% PDDA and different concentrations of TEOS. (B) E-AD was done at -1.3 V for different deposition time from 30 to 90 s with a sol containing 0.17M TEOS, 3.3 mg/mL DSDH and 6.7% PDDA.*

Figure III-14 reports some SEM pictures of films prepared with the optimal sol composition (A) or containing less protein (B) or less PDDA (C). Optimal composition leads to a film with a homogenous texture (***Figure III-14A***). Only few filaments about 1-2 µm long, probably due to PDDA can be observed on the top of the film. Changing the composition of the sol does not change significantly the texture of the silica gel layer (the surface of all electrodes is covered by a sol-gel film). However, using a lower protein concentration leads to the presence of more filaments on the surface (***Figure III-14B***). In the presence of lower PDDA concentration, these filaments disappeared and some aggregates can be observed (***Figure III-14C***). We suppose that these aggregates are due to proteins that are not protected

by the PDDA. The optimal sol composition that has been determined using only electrochemical measurements leads also to the more homogeneous sol-gel biocomposite, showing a good incorporation of both protein and polyelectrolyte.

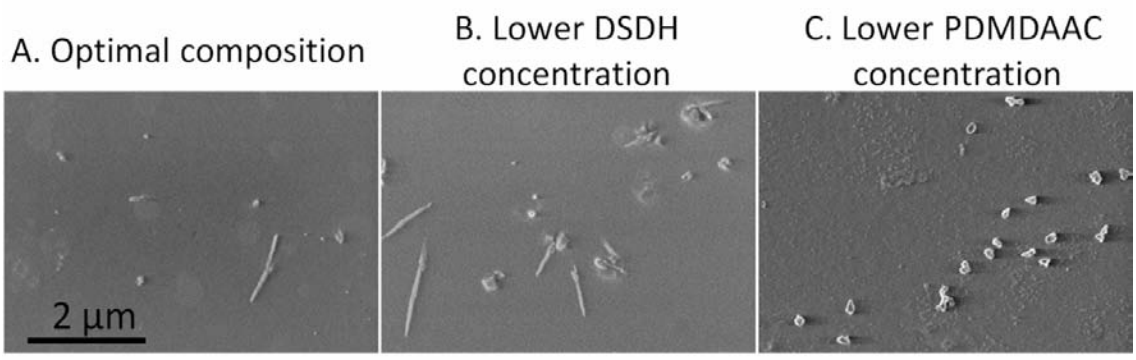

Figure III-14. *SEM image of different films prepared by sol-gel electrochemically-assisted deposition at -1.3 V for 60 s from a sol containing (A) 0.17 M TEOS, 3.3 mg/mL DSDH and 6.7% PDDA; (B) 0.17 M TEOS, 3.3 mg/mL DSDH and 3.35 % PDDA; (C) 0.17 M TEOS, 1.65 mg/mL DSDH and 6.7% PDDA.*

3.3. Relationship between the reactivity, the permeability and the film stability

All the optimization steps reported in the previous section have been made in order to obtain the highest electrochemical response as possible. When considering electrosynthesis applications it is critical to have an intense electrochemical response, but it is also critical to get sufficient long-term stability of the electrode, at least at a time scale compatible with industrial processes. The quantity of TEOS in the starting sol has in principle an influence on the permeability of the layer [35]. Linear sweep voltammetry for ferrocenedimethanol (Fc) oxidation has been performed at a rotating disc electrode with a bare glassy carbon electrode (GC) and GC covered by thin silica films prepared with sols containing 0.08, 0.17 and 0.33 M TEOS. This experiment allows the estimation of the effective kinetic of the heterogeneous electron transfer reaction (k_{eff}) for the chosen electrochemical reaction. This constant can be affected by the film permeability, the eventual defects in the layer and the thickness of the electrodeposited films. Here, k_{eff} decreases regularly from 0.039 to 0.033 $cm.s^{-1}$ when

increasing the TEOS concentration in the starting sol from 0.08 to 0.33 M (see ***Figure III-15A***).

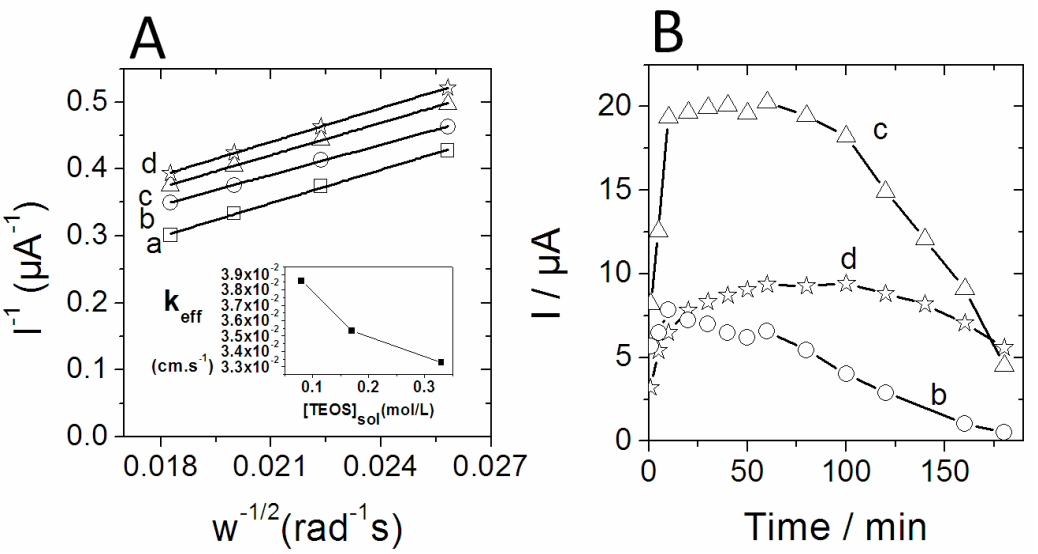

Figure III-15. *(A) 1/I versus $1/w^2$ measured in the presence of 0.05 mM Ferrocenedimethanol with (a, squares) bare glassy carbon electrode and electrodes modified by a thin film prepared from a sol containing various TEOS concentration: (b, circles) 0.08 M, (c, triangles) 0.17 M and (d, stars) 0.33 M. Steady state current was measured by linear sweep voltammetry with using a potential scan rate of 20 mV/s. (B) Evolution of the peak current response of glassy carbon electrode modified by film (b), (c) and (d) in the presence of 1mM NAD^+ and 6 mM D-sorbitol in 0.1 M Tris-HCl buffer (pH 9). All electrodes have been prepared by electrochemically-assisted deposition at -1.3 V for 60 s from a sol containing 6.7% PDDA, 3.3 mg/mL DSDH and various concentrations of TEOS (see above). Potential scan rate 50 mV/s.*

The electrode response stability is also very sensitive to the TEOS concentration in the starting sol. Successive CV measurements have been performed with the same electrodes prepared from sols containing 0.08 , 0.17 and 0.33 M TEOS respectively (see ***Figure III-15B***). The highest response was observed for films prepared with 0.17 M TEOS (curve c) and it was stable for more than 1 hour in solution and then decreased rapidly during the next hour of operation. A higher TEOS concentration (0.33M) (curve d) leads to a lower electrochemical response and to significantly improved electrode stability during the 3 hours of operation. Lowering TEOS concentration (0.08 M) (curve b) leads then to both lowest response and to the worst electrode stability. To conclude, the quantity of TEOS in the starting sol is a critical parameter that has to be carefully tuned, in connection with other sol

constituents, to get the best compromise between electrochemical response and electrode stability.

3.4. Comparison of the enzyme activity into the film and in solution

The variation of the electrochemical response for increasing concentrations of D-sorbitol into the solution has been studied (see ***Figure III-16***). The measurements have been done during the one hour for which the electrode gave a stable electrochemical response. In these conditions, the peak current intensity increases regularly with the D-sorbitol concentration up to 10 mM and starts to level off for higher concentrations. We can extract from these data a K_m value of about 3 mM, slightly lower than the K_m of about 6 mM observed for the same protein in solution [36]. The electrochemically-assisted deposition allows thus maintaining an enzymatic activity similar as in solution, with a small improvement due to the encapsulation in the silica gel.

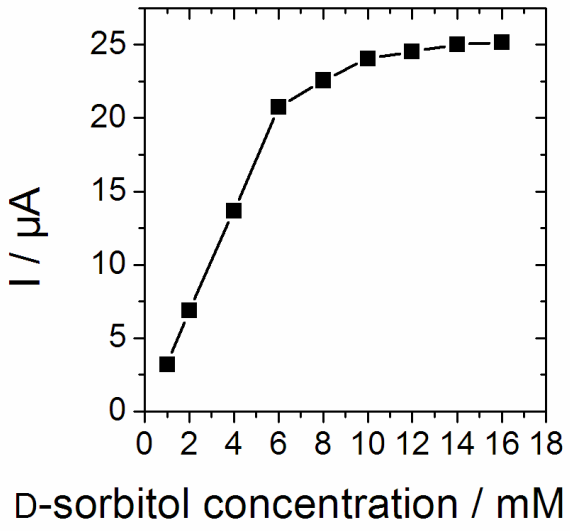

Figure III-16. *Peak current response versus D-sorbitol concentration measured with a glassy carbon electrode that has been modified by a thin silica film with encapsulated DSDH. The film was prepared with a sol containing 0.17 mM TEOS, 6.7 % PDDA and 3.3 mg/mL DSDH. The electrochemically-assisted deposition was done by applying -1.3 V for 60 s. All cyclic voltammograms have been performed at 50 mV/s, in the presence of 1 mM NAD^+ and different D-sorbitol concentrations in Tris-HCl buffer (pH 9).*

pH is known to affect strongly the enzymatic activity of DSDH [36]. ***Figure III-17*** shows the influence of pH on the electrochemical response for both reduction of fructose (***Figure***

III-17A) and oxidation of D-sorbitol (***Figure III-17B***), from measurements carried out with glassy carbon electrodes covered by the thin silica gel layer with encapsulated DSDH. A sharp increase in the electrode response is observed for fructose reduction around pH 6.5 (phosphate buffer), followed by a sharp decrease above this optimum value. With the oxidation of D-sorbitol, the electrode response increases more regularly from pH 6 to 9 and decreases slightly at pH 10. The behavior of DSDH in the silica layer is very comparable with the data coming from protein activity in solution with an optimal pH of 6.5 for the reduction of fructose and an optimal oxidation of D-sorbitol at pH 9, suggesting again that the electrogenerated silica layer offers a good environment for DSDH encapsulation onto the electrode surface. The immobilized protein exhibits good activity, similar as the free enzyme in solution concerning both the enzymatic kinetics and the sensitivity to pH.

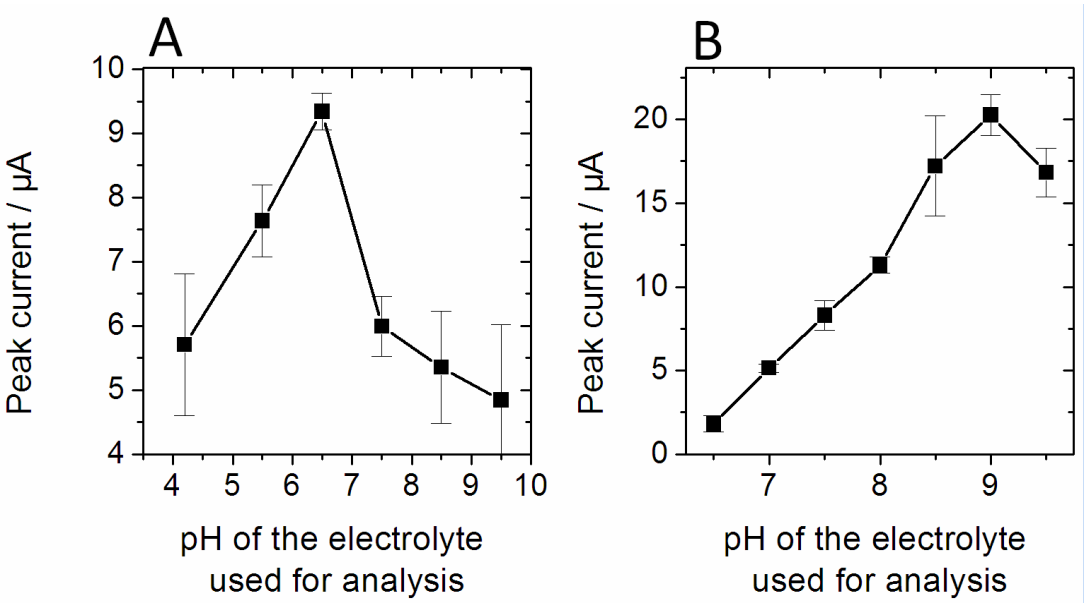

Figure III-17. *Evolution of the peak current response versus the pH for (A) reduction of 6 mM fructose in 0.1 M Tris-HCl buffer with 1 mM NADH and (B) oxidation of 6 mM D-sorbitol in 0.1 M tris-HCl buffer with 1 mM* NAD^+*. The modified glassy carbon electrode was prepared with a sol containing 0.17 mM TEOS, 6.7 % PDDA and 3.3 mg/mL DSDH. The electrochemically-assisted deposition was done by applying -1.3 V for 60 s. All cyclic voltammograms have been performed 50 mV/s potential scan rate.*

3.5. Co-immobilization of DSDH and diaphorase

The direct electrochemical detection of NADH, occurring at high potential compared to E_0, induces uncontrolled oxidation and rapid deactivation of the bio-molecule. A large number of studies have been and are still devoted to the electro-catalytic oxidation of NADH that allows

decreasing this over-potential. An elegant and very versatile regeneration can be obtained with using diaphorase. An additional electron mediator is then used to transfer the electrons from this protein to the electrode. Interestingly, the same diaphorase can be used for both NADH oxidation and NAD^+ reduction. Among others, ferrocene species can be used for mediating electron transfer for the oxidation of NADH and methylviologen can be used for the reduction of NAD^+ [20].

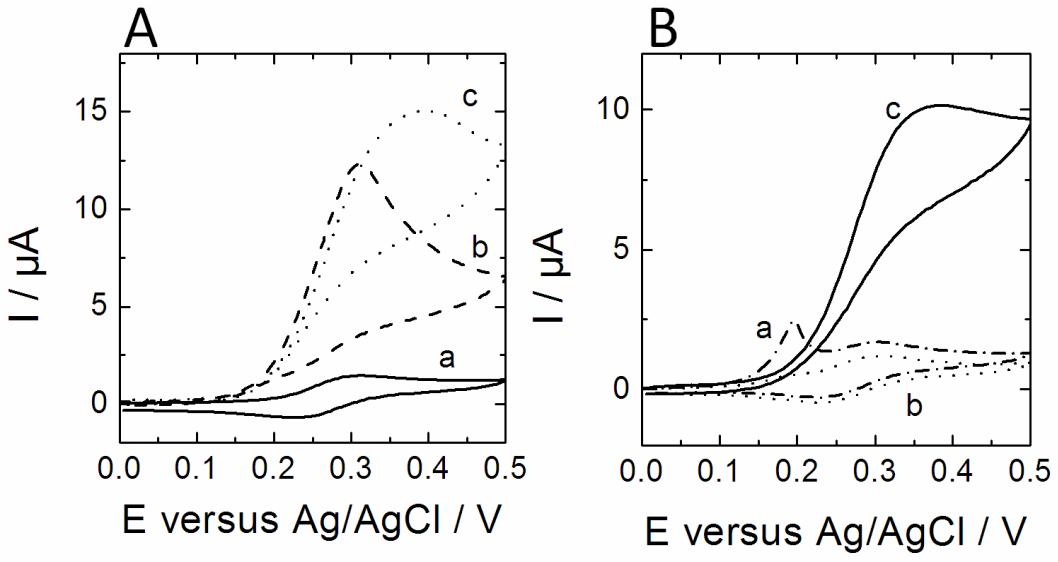

Figure III-18. *Electrochemical behavior of glassy carbon electrode modified by a silica thin film with encapsulated diaphorase. (A) Electrode response in the absence (a) and in the presence of 1 mM (b) and 2 mM (c) NADH. (B) Evolution of the electrode response to 0.4 mM NADH at pH 7 (a), 8 (b) and 9 (c). Films have been deposited by electrolysis at -1.3 V for 60 s with a sol containing 6.7 % PDDA, 0.17 M TEOS sol and 0.83 mg/mL diaphorase. Cyclic voltammograms have been performed in 0.1 M Tris-HCl buffer, in the presence of 0.1 M ferrocenedimethanol (and different NADH concentrations). Potential scan rate was 50 mV/s.*

The encapsulation of diaphorase inside the electrodeposited silica gel has thus been investigated. ***Figure III-18A*** shows the typical electro-catalytic response of the silica-diaphorase film electrode to NADH addition in solution using ferrocenedimethanol as electron mediator. In the absence of NADH, only the reversible electrochemical signal of ferrocene is observed. The addition of 1 mM NADH induces a strong modification of the electrochemical response, the anodic current increased by a factor 8 while the cathodic signal disappeared. A second addition of NADH leads to an additional anodic peak current increase. Control experiments have confirmed that in our conditions ferrocenedimethanol does not allow the direct catalytic oxidation of NADH, in agreement with the literature [37] and could only be obtained with the active diaphorase. The pH has a very strong influence on the

catalytic oxidation of NADH (***Figure III-18B***). At pH 7, the presence of NADH induced a complex cyclic voltammogram with a sharp oxidation peak at about 0.2 V and an additional peak shaped signal, very similar to the initial CV of ferrocenedimethanol in the absence of NADH (***Figure III-18B curve a***). The signal became much simpler at pH 8 but no significant catalysis could be observed (***Figure III-18B curve b***). At pH 9, the electro-catalysis was observed as discussed before (***Figure III-18B curve c***).

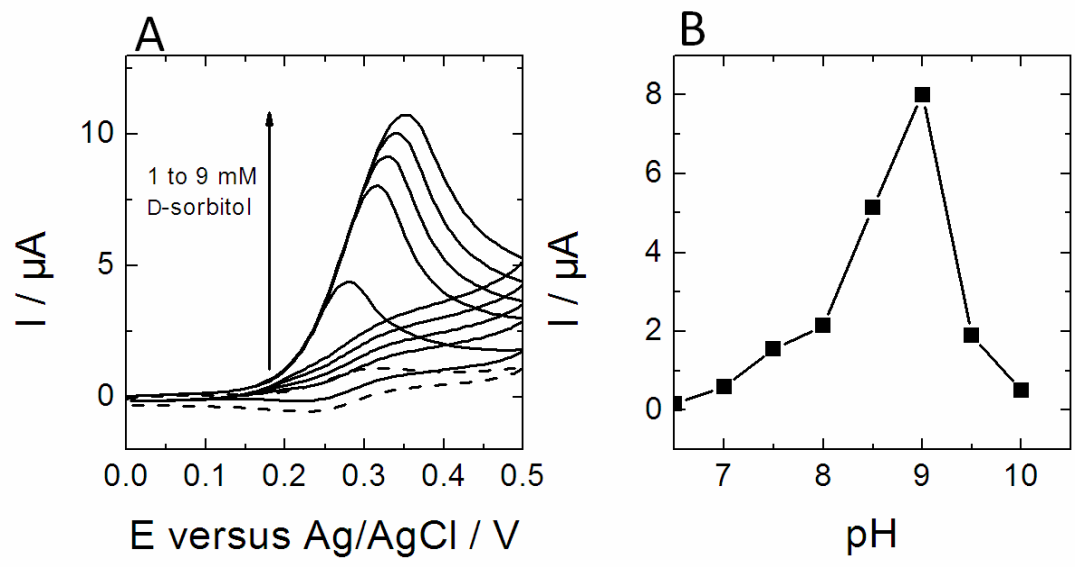

Figure III-19. *Electrochemical behavior of glassy carbon electrodes modified by a silica film with co-encapsulated DSDH and diaphorase. (A) Evolution of the electrode response to increasing concentration of D-sorbitol from 1 to 9 mM. The measurement was done at pH 9. (B) Evolution of the peak current response to 6 mM D-sorbitol from pH 6 to 10. Films have been deposited by electrolysis at -1.3 V for 60 s with a sol containing 6.7 % PDDA, 0.17 M TEOS sol and 0.83 mg/mL diaphorase. The cyclic voltammograms have been performed in 0.1 M Tris-HCl buffer in the presence of 1 mM* NAD^+ *and 0.1 mM ferrocendimethanol. Potential scan rate was 50 mV/s.*

Finally, the co-encapsulation of DSDH and diaphorase was evaluated. The protocol for the electrode preparation is rather simple; the two proteins are mixed together inside the sol and are encapsulated in one step into the silica gel layer during the electrochemically-assisted deposition. ***Figure III-19A*** shows the electrochemical response of the bi-enzyme composite to the addition of D-sorbitol in solution. The oxidation of D-sorbitol by DSDH leads to the production of NADH inside the film. NADH reacts with diaphorase and the electrochemically generated ferricinium ions to produce NAD^+ and ferrocene species that can be re-oxidized in the electrocatalytic scheme. The electrocatalytic current increases with the addition of D-sorbitol from 1 to 9 mM. ***Figure III-19B*** shows the influence of pH on the bi-enzyme system,

giving rise to a similar trend as for DSDH alone, with an optimal pH value located around pH 9. Note that the bi-enzyme system is much more sensitive to small pH variations, which is illustrated by a current decrease by 75 % when passing from pH 9 to pH 9.5 or pH 8. This influence of pH is mainly due to the strong effect of pH on the diaphorase activity (***Figure III-19B***). The co-immobilization of DSDH and diaphorase does not prevent the efficient communication between the two proteins. NADH can diffuse from one enzymatic center to the other for efficient bioelectrocatalysis. The electrochemically-assisted silica gel deposition is thus an effective method for the elaboration of complex enzymatic layers on electrode surfaces.

3.6. Extension to the particular case of macroporous electrodes

Macroporous electrodes display pores of about 440 nm with well defined interconnections allowing good mass transport [38]. They were obtained by gold electrodeposition inside an opal network of silica beads. The height of the different gold macroporous electrodes were 220 nm for one half layer of gold and 660 nm for three half layers (***Figure III-20***).

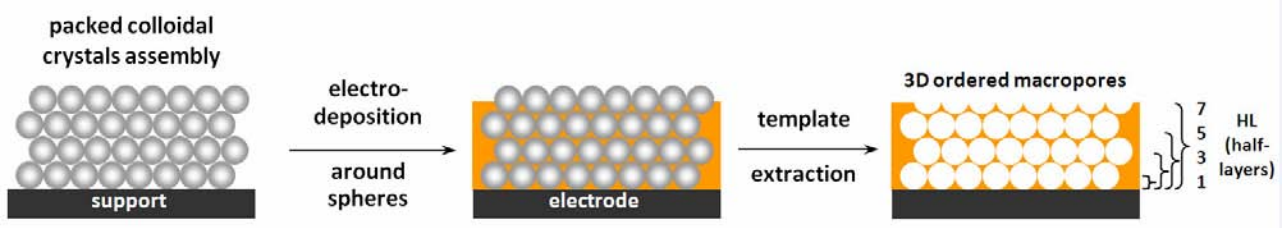

Figure III-20*. Preparation of the macroporous gold electrode by electrodeposition through nanospheres assembly.*

To further point out the interest of the electrochemically-assisted deposition method for bioelectrocatalysis purposes, the above approach was extended to macroporous electrodes displaying a much larger electroactive surface area in comparison to the geometric one (***Figure III-21B*** to ***21C***) and compared to flat gold electrode (***Figure III-21A***). The electrolysis of the sol does not occur on gold at the same potential as for glassy carbon. A potential of -1.3 V versus the Ag/AgCl reference electrode was used in previous optimization on glassy carbon but only -1.1 V was necessary for macroporous electrodes in order to trigger the sol-gel deposition.

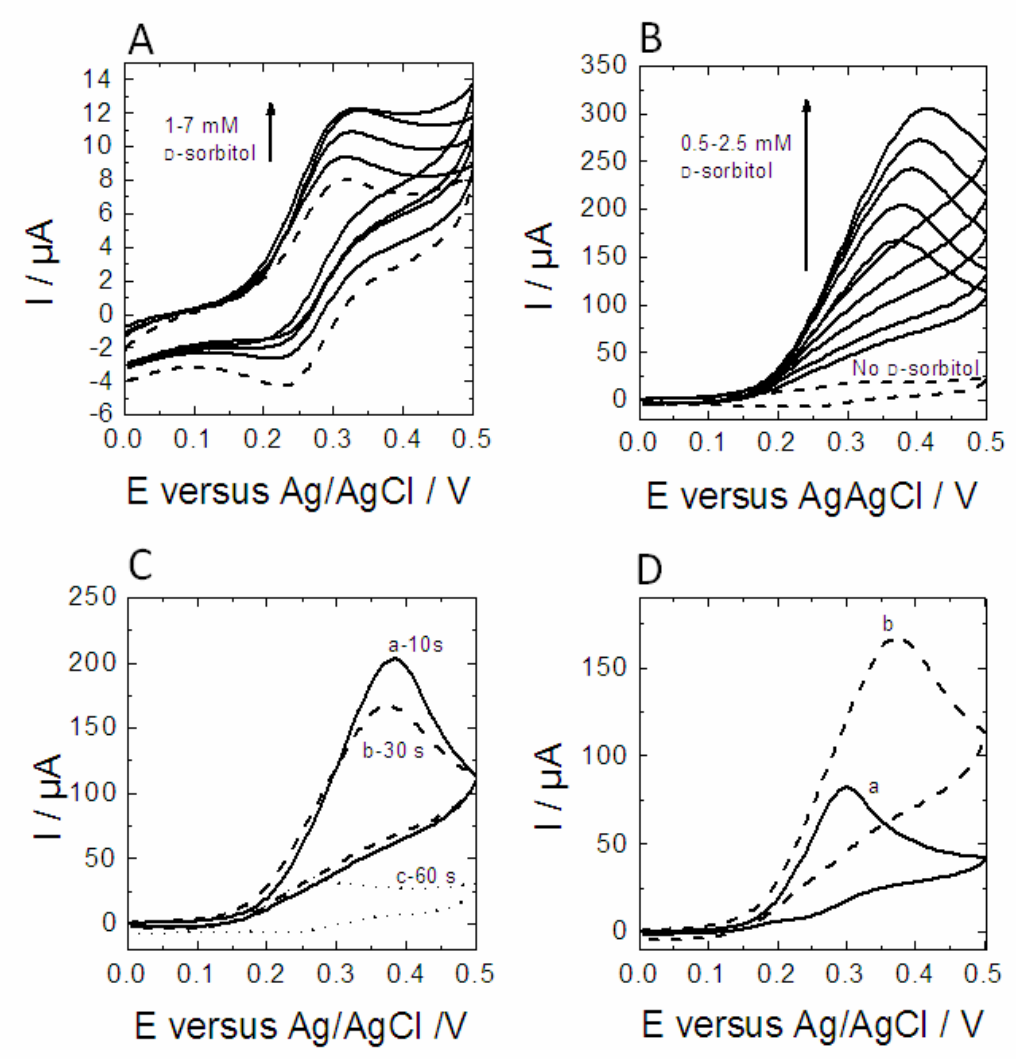

Figure III-21. *Electrochemical behavior of flat and macroporous gold electrodes modified by silica films with co-encapsulated DSDH and diaphorase. (A) Evolution of the flat gold electrode response to increasing concentrations of D-sorbitol from 1 to 7 mM. Dashed curves show the electrode response in the absence of D-sorbitol. (B) Evolution of the macroporous gold electrode response to increasing concentrations of D-sorbitol from 0.5 to 2.5 mM. Dashed curves show the electrode response in the absence of D-sorbitol. The measurement was done with a macroporous electrode of 660 nm thickness (three half layers) modified with using 30 s electrolysis. (C) Evolution of the peak current response to 0.5 mM D-sorbitol with modified electrodes prepared when using different electrolysis times from 10 s to 60 s (curves a to c). The measurements were done with a macroporous electrode of 660 nm thickness (three half layers). (D) Evolution of the peak current response to 0.5 mM D-sorbitol with macroporous electrodes displaying one half layer (a) and three half layers (b). Films were obtained when using 30 s electrolysis. (A-D) All films have been deposited by electrolysis at -1.1 V with a sol containing 6.7 % PDDA, 0.17 M TEOS sol and 0.83 mg/mL diaphorase. The cyclic voltammograms have been performed in 0.1 M Tris-HCl buffer at pH 9 in the presence of 1 mM NAD^+ and 0.1 mM ferrocendimethanol. Potential scan rate was 50 mV/s.*

Figure III-21A displays the response to D-sorbitol obtained with a flat gold electrode modified by the electrogenerated silica film with encapsulated DSDH and diaphorase. The electrode was found to be sensitive to successive additions of D-sorbitol, as shown by the increase in peak current intensity for the oxidation of ferrocenedimethanol. The addition of 1 mM D-sorbitol led here to 16 % peak current increase. By comparison, a much higher response was observed when doing the same experiment with a macroporous electrode (three half layers) modified in the same conditions by the bio-composite layer (***Figure III-21B***), and the peak current intensity was increasing by 1000 % when adding 1 mM D-sorbitol in the solution. The macroporous texture of the gold electrode improves thus significantly the catalytic efficiency of the sol-gel biocomposite.

As for flat electrodes, deposition time also has a strong effect on the functionalized macroporous electrode response (***Figure III-21C***). Optimal deposition time was 60 s with bare glassy carbon electrodes. Here the best response was observed when using 10 s electrolysis. 30 s and 60 s electrolysis led then to lower electrode responses. The electrode response of a modified bare electrode is a compromise between the amount of active enzyme deposited on the electrode surface and the hindered diffusion into the silica layer. The thicker the film, the higher is the diffusion limitation. In macroporous electrodes the situation is even more complex as the pore interconnections can be rapidly blocked by the electrogenerated silica gel layer. Low deposition times are here needed to prevent the rapid macropore clogging.

Finally the influence of the number of half layer of the gold macropores electrode was examined. Electrodes with one (a) and three half layers of gold (b) have been modified by using 30 s electrolysis of the sol containing both DSDH and diaphorase (***Figure III-21D***). The electrochemical response increases significantly from one half layer to three half layers when detecting 1 mM D-sorbitol. This result is consistent with recent observations made with macroporous electrodes modified by a thin silica film containing hemoglobin [17] in which it was shown that the electrochemical signal of hemoglobin as well as the catalytic current for H_2O_2 detection is increasing significantly with increasing the number of half-layer from 3 to 9. However, the direct transposition of the results from this previous study to the present work is not possible because the compositions of the sols are very different. The sol used for hemoglobin encapsulation contained much less silane precursors (13.6 mM TEOS) than the

sol used here for DSDH and diaphorase encapsulation (0.17M). In addition, the sol we developed for dehydrogenase is complex to handle with the macroporous electrodes because of the presence of the polyelectrolyte.

These experiments point out the interest and the complexity of surface modification of such porous material with an elaborated sol-gel biocomposite. Additional optimization will be necessary to carefully control the film deposition inside the macropores. The optimal thickness of the macroporous electrode will also have to be defined with respect to the application in electrosynthesis.

4. Conclusion

The first part of the work has pointed out the importance of adding positively-charged polyelectrolytes into sol-gel-derived films doped with dehydrogenase enzymes for providing a good environment for encapsulation of the biomolecules in an active form. Among the tested additives, PDDA offered the best results. The improved behavior in the presence of polyelectrolyte was also observed for other kinds of thin films (i.e., based on chitosan). Then, electrochemically-assisted deposition of silica gel layer has been successfully adapted to the encapsulation of DSDH. The encapsulated DSDH enzyme is likely to either oxidize D-sorbitol and produce simultaneously NADH inside the silica gel layer or reduce fructose and generate NAD^+. The functional layer has been successfully deposited in macroporous gold electrodes and applied for the oxidation of D-sorbitol. When deposited in the same conditions and in the presence of the same concentration of D-sorbitol, the catalytic current increased much more with a macroporous electrode (1000 %) in comparison with a flat gold electrode (16 %). The macroporous texture of the gold electrode improves thus significantly the catalytic efficiency of the sol-gel biocomposite. The next step(s) of this work will be the immobilization of the electron-mediator and the enzymatic cofactor inside the silica gel matrix for application in zero-waste electrosynthesis.

References

[1] Kornberger, P.; Giffhorn, F.; Kohring, G. W., In Encyclopedia of Industrial Biotechnology, Bioprocess, Bioseparation, and Cell Technology (Ed: M.C. Flickinger) Vol. 3, Wiley, Hoboken, NJ, USA, **2010**, 1888-1898.

[2] Kohlmann, C.; Märkle, W.; Lütz, S., Electroenzymatic Synthesis. *J. Mol. Cat. B* **2008**, *51*, 57-72.

[3] Wichmann, R.; Vasic-Racki, D., Cofactor regeneration at the lab scale. *Adv. Biochem. Engin./Biotechnol* **2005**, *92*, 225-260.

[4] Avnir, D.; Coradin, T.; Lev, O.; Livage, J., Recent bio-applications of sol-gel materials. *J. Mater. Chem.* **2006**, *16(11)*, 1013-1030.

[5] Williams, A. K.; Hupp, J. T., Sol-gel-encapsulated alcohol dehydrogenase as a versatile, environmentally stabilized sensor for alcohols and aldehydes. *J. Am. Chem. Soc.* **1998**, *120(18)*, 4366-4371.

[6] Ferrer, M. L.; Del Monte, Franciscol; Levy, David. A Novel and Simple Alcohol-Free Sol-Gel Route for Encapsulation of Labile Proteins. *Chem. Mater.* **2002**, *14(9)*, 3619-3621.

[7] Coradin, T.; Livage, J., Aqueous Silicates in Biological Sol-Gel Applications: New Perspectives for Old Precursors. *Acc. Chem. Res.* **2007**, *40(9)*, 819-826.

[8] Yang, S.; Jia, W.; Qian, Q.; Zhou, Y.; Xia, X., Simple Approach for Efficient Encapsulation of Enzyme in Silica Matrix with Retained Bioactivity. *Anal. Chem.* **2009**, *81(9)*, 3478-3484.

[9] Brennan, J. D., Biofriendly Sol-Gel Processing for the Entrapment of Soluble and Membrane-Bound Proteins: Toward Novel Solid-Phase Assays for High-Throughput Screening. *Acc. Chem. Res.* **2007**, *40(9)*, 827-835.

[10] Besanger, Travis R.; Brennan, John D. Entrapment of membrane proteins in sol-gel derived silica. *J. Sol-Gel Sci. Technol.* **2006**, *40(2/3)*, 209-225.

[11] Pchelintsev, N. A.; Neville, F.; Millner, P. A. Biomimetic silication of surfaces and its application to preventing leaching of electrostatically immobilized enzymes. *Sens. Actuators B* **2008**, *135(1)*, 21-26.

[12] Brinker, C. J.; Scherer, G.W., **1990**. Sol-Gel Science, Academic, Press, San Diego.

[13] Walcarius, A.; Collinson, M. M., Analytical chemistry with silica sol-gels: traditional routes to new materials for chemical analysis. *Annual Rev. Anal. Chem.* **2009**, *2*, 121-143.

[14] Bartlett, P. N.; Baumberg, J. J.; Birkin, Peter R.; Ghanem, M. A.; Netti, M. C., Highly Ordered Macroporous Gold and Platinum Films Formed by Electrochemical Deposition through Templates Assembled from Submicron Diameter Monodisperse Polystyrene Spheres. *Chem. Mater.* **2002**, *14(5)*, 2199-2208.

[15] Ben-Ali, S.; Cook, D. A.; Bartlett, P. N.; Kuhn, A., Bioelectrocatalysis with modified highly ordered macroporous electrodes. *J. Electroanal. Chem.* **2005**, *579(2)*, 181-187.

[16] Sanchez, C.; Boissiere, C.; Grosso, D.; Laberty, C.; Nicole, L., Design, Synthesis, and Properties of Inorganic and Hybrid Thin Films Having Periodically Organized Nanoporosity. *Chem. Mater.* **2008**, *20(3)*, 682-737.

[17] Qu, F.; Nasraoui, R.; Etienne, M.; Saint Come, Y. B.; Kuhn, A.; Lenz, J.; Gajdzik, J.; Hempelmann, R.; Walcarius, A., Electrogeneration of ultra-thin silica films for the functionalization of macroporous electrodes. *Electrochem. Commun. 2011*, *13(2)*, 138-142.

[18] Nadzhafova, O.; Etienne, M.; Walcarius, A., Direct electrochemistry of hemoglobin and glucose oxidase in electrodeposited sol-gel silica thin films on glassy carbon. *Electrochem. Commun.* **2007**, *9(5)*, 1189-1195.

[19] Jia, W.; Wang, K.; Zhu, Z.; Song, H.; Xia, X., One-step immobilization of glucose oxidase in a silica matrix on a Pt electrode by an electrochemically induced sol-gel process. *Langmuir* **2007**, *23(23)*, 11896-11900.

[20] Takagi, K.; Kano, K.; Ikeda, T., Mediated bioelectrocatalysis based on NAD-related enzymes with reversible characteristics. *J. Electroanal. Chem.* **1998**, *445(1-2)*, 211-219.

[21] Kashiwagi, Y.; Yanagisawa, Y.; Shibayama, N.; Nakahara, K.; Kurashima, F.; Anzai, J.; Osa, T., Preparative, electroenzymatic reduction of ketones on an all components-immobilized graphite felt electrode. *EIectrochim. Acta* **1997,** *42(13-14)*, 2267-2270.

[22] Osa, T.; Kashiwagi, Y.; Yanagisawa, Y., Electroenzymic oxidation of alcohols on a poly(acrylic acid)-coated graphite felt electrode terimmobilizing ferrocene, diaphorase and alcohol dehydrogenase. *Chem. Letters,* **1994**, *2*, 367-370.

[23] Shi, H.; Song, Z.; Huang, J.; Yang, Y.; Zhao, Z.; Anzai, J.; Osa, T.; Chen, Q., Effects of the type of polycation in the coating films prepared by a layer-by-layer deposition

technique on the properties of amperometric choline sensors. *Sens. Actuators B* **2005**, *109(2)*, 341-347.

[24] Gorton, L.; Bartlett, P.N. in Bioelectrochemistry eds. P.N. Bartlett, John Wiley & Sons Ltd, Chichester, UK. **2008**, p; 157.

[25] Miller, J. M.; Dunn, B.; Valentine, J. S.; Zink, J. I., Synthesis conditions for encapsulating cytochrome c and catalase in SiO_2 sol-gel materials. *J. Non-Cryst. Solids* **1996**, *202(3)*, 279-289.

[26] Persello, J., in Adsorption on silica surfaces, ed. E. Papirer, Surf. Sci. Ser. **2000**, 90, Marcel Dekker, New York, pp.317-318.

[27] Schneider, K. H.; Giffhorn, F., Purification and properties of a polyol dehydrogenase from the phototrophic bacterium Rhodobacter sphaeroides. *Eur. J. Biochem.* **1989**, **184(1)**, 15-19.

[28] Koopal, L. K.; Yang, Y.; Minnaard, A. J.; Theunissen, P. L. M.; Van Riemsdijk, W. H., Chemical immobilization of humic acid on silica. *Colloids Surf. A* , **1998**, *141(3)*, 385-395.

[29] Dominguez, E.; Lan, H. L.; Okamoto, Y.; Hale, P. D.; Skotheim, T. A.; Gorton, L.; Hahn-Haegerdal, B. Reagentless chemically modified carbon paste electrode based on a phenothiazine polymer derivative and yeast alcohol dehydrogenase for the analysis of ethanol. *Biosensors Bioelectron.* **1993**, *8(3-4)*, 229-237.

[30] Shu, H. C.; Mattiasson, B.; Persson, B.; Nagy, G.; Gorton, L.; Sahni, S.; Geng, L.; Boguslavsky, L.; Skotheim, T., A reagentless amperometric electrode based on carbon paste, chemically modified with D-lactate dehydrogenase, NAD^+, and mediator containing polymer for D-lactic acid analysis. I. Construction, composition, and characterization. *Biotechnol. Bioeng.* **1995**, *46(3)*, 270-279.

[31] Karyakin, A. A.; Karyakina, E. E.; Gorton, L.; Bobrova, O. A.; Lukachova, L. V.; Gladilin, A. K.; Levashov, A. V. Improvement of Electrochemical Biosensors Using Enzyme Immobilization from Water-Organic Mixtures with a High Content of Organic Solvent. *Anal. Chem.* **1996**, *68(24)*, 4335-4341.

[32] Yang, Y. M.; Wang, J. W.; Tan, R. X. Immobilization of glucose oxidase on chitosan-SiO_2 gel. *Enzyme and Microbial Technology* **2004**, *34(2)*, 126-131.

[33] Dai, H.; Wu, X.; Xu, H.; Wang, Y.; Chi, Y.; Chen, G., A highly performing electrochemiluminescent biosensor for glucose based on a polyelectrolyte-chitosan modified electrode. *Electrochim. Acta* **2009**, *54(19)*, 4582-4586.

[34] Coradin, T.; Durupthy, O.; Livage, J., Interactions of Amino Containing Peptides with Sodium Silicate and Colloidal Silica: A Biomimetic Approach of Silicification. *Langmuir* **2002**, *18(6)*, 2331-2336.

[35] Goux, A.; Etienne, M.; Aubert, E.; Lecomte, C.; Ghanbaja, J.; Walcarius, A., Oriented Mesoporous Silica Films Obtained by Electro-Assisted Self-Assembly (EASA). *Chem. Mater.* **2009**, *21(4)*, 731-741.

[36] Schauder, S.; Schneider, K. H.; Giffhorn, F., Polyol metabolism of Rhodobacter sphaeroides: biochemical characterization of a short-chain sorbitol dehydrogenase. *Microbiology* **1995**, *141*, 1857-1863.

[37] Matsue, T.; Suda, M.; Uchida, I.; Kato, T.; Akiba, U.; Osa, T., Electrocatalytic oxidation of NADH by ferrocene derivatives and the influence of cyclodextrin complexation. *J. Electroanal. Chem. Inter. Electrochem.* **1987**, *234(1-2)*, 163-73.

[38] Szamocki, R.; Velichko, A.; Muecklich, F.; Reculusa, S.; Ravaine, S.; Neugebauer, S.; Schuhmann, W.; Hempelmann, R.; Kuhn, A., Improved enzyme immobilization for enhanced bioelectrocatalytic activity of porous electrodes. *Electrochem. Commun.* **2007**, *9(8)*, 2121-2127.

Chapitre IV. Co-immobilisation d'une déshydrogénase et du cofacteur enzymatique NAD^+ au sein de la matrice sol-gel

L'immobilisation du cofactor enzymatique NAD^+ au sein de la matrice sol-gel a été étudiée en présence de DSDH et de diaphorase co-encapsulés au sein de cette même matrice. Dans cette configuration, le cofacteur doit avoir suffisamment de mobilité pour se déplacer du centre enzymatique de la DSDH au centre enzymatique de la diaphorase. Un médiateur électrochimique, le ferrocenedimethanol, permet alors la communication électronique entre la diaphorase et la surface de l'électrode. La faisabilité de cette étude a tout d'abord été menée en préparant la couche mince sol-gel par évaporation du sol initial. Différentes stratégies d'immobilisation du cofacteur ont alors été étudiées : (1) la simple encapsulation du NAD^+ dans la matrice sol-gel, seul ou en présence de nanotubes de carbone ; (2) l'encapsulation d'un dérivé du NAD^+ à haut poids moléculaire (NAD-dextran) ; (3) la fixation chimique du NAD^+ à la matrice silicatée via sa condensation sur le groupement époxy du glycidoxypropylsilane au cours du processus sol-gel (cette réaction a alors été suivie par spectroscopie infrarouge). Cette dernière approche s'est révélée être la plus intéressante en terme de réponse électrochimique et de stabilité du signal bioélectrocatalytique. Cette même approche a ensuite été étendue pour la génération électrochimique de couches minces sol-gel pour la co-immobilisation de la DSDH, de la diaphorase et du cofacteur NAD^+. Cette expérience est alors applicable aux électrodes planes (carbone vitreux ou or) et aux électrodes macroporeuses.

Chapter IV. Co-immobilization of dehydrogenase and cofactor in sol-gel matrix

In this chapter, successful strategies for dehydrogenase and cofactor co-immobilization in sol-gel films have been developed by both drop-coating and electrochemically-assisted deposition. First of all, we compare various strategies directed to the durable immobilization of NAD^+/NADH cofactors in biocompatible sol-gel matrices encapsulating a bi-enzymatic system (a dehydrogenase and a diaphorase, this latter being useful to the safe regeneration of the cofactor), which were deposited by drop-coating as thin films onto glassy carbon electrode surfaces. These strategies are (1) the "simple" entrapment of NAD^+ in the sol-gel matrix, alone or in the presence of carbon nanotubes; (2) the formation of interpenetrated organic-inorganic networks using a high molecular weight NAD derivative (NAD-dextran); (3) the chemical attachment of NAD^+ to the silica matrix using glycidoxypropylsilane in the course of the sol-gel process (in smooth chemical conditions). The third approach based on chemical bonding of the cofactor (which was checked by infrared spectroscopy) led to much better performance in terms of long-term stability of the electrochemical response. The co-immobilization of DSDH, diaphorase (DI) and NAD^+ was then obtained by electrochemically-assisted deposition. Finally, the functional layer has been successfully deposited in macroporous gold electrodes and applied for the oxidation of D-sorbitol.

1. Introduction

The main difficulty to fabricate reagentless dehydrogenase-based bioelectrodes is that the cofactor must be immobilized and regenerated in a stable and active way. In most studies, the native cofactor is added to the starting electrolyte before the enzymatic reaction. Despite the good performance of these methods, a maybe drawback exists: the operation is not only complicated but also involves high cost because the expensive cofactor cannot be reused. One way to overcome this problem is to co-immobilize cofactor and dehydrogenase in the sensing layer, but the difficulty is that the water soluble cofactor is a relatively small molecule, so is likely to diffuse away from the electrode surface into the solution, thus limiting the long-time durability of the modified electrode. Different strategies have been proposed for cofactor immobilization on electrode surfaces. The simple encapsulation leads to rapid leaching of the cofactor in the solution during the electrochemical operation and can only be considered for disposable sensors [1]. One possibility to improve the stability of the immobilization is the chemical attachment of the cofactor to a macromolecule that can be encapsulated or immobilized on the electrode without leaching. Dextran [2, 3, 4], PEG [5], Chitosan [6], and PEI [7], have been reported to allow this cofactor immobilization for biosensor applications. The stability of some systems has been studied and the bio-electrode can in some cases be operating for several days. One limitation of this approach comes from the rather complex modification, especially if proteins [6] or mediator [7] are also immobilized on the same macromolecule. This induces a significant cost and limits the number of functionalized groups in the layer; More recently the adsorption of NAD^+ on carbon nanotubes was also proposed as a new strategy for the biomolecules immobilization [8]. Up to now, sol-gel chemistry was only used for enzyme and mediator immobilization [1, 9, 10], and was not considered for durable cofactor immobilization.

During operation of bioelectrodes containing coimmobilized dehydrogenase and cofactor, the cofactor must be detected or regenerated electrochemically and this operation has to be done with using a mediator. The demand for electrocatalytic detection of NAD^+ cofactor comes from the nature of this molecule, free diffusing in the living cell and for which a high electrochemical overpotential is observed for both oxidation and reduction reactions. The molecule is protected from side reaction, but the direct electrochemical detection at high

overpotential can lead to the irreversible degradation of the compound and to the simultaneous detection of interfering species. Many strategies for electrocatalytic detection of the cofactor have been developed. Organic mediators [11,12, 13, 14, 15] , carbon nanotubes (CNTs) [10,16,17,18,19] or even gold nanoparticles [20] have been proposed to recycle the NADH back to the enzymatically active NAD^+. The cofactor can also be efficiently regenerated by the use of diaphorase in the presence of several molecular mediators, metal complexes [21, 22], quinones and flavins [23, 24], and also viologens [25]. This later approach being very appealing when smooth cofactor regeneration is needed for improving the long term stability of the device, notably if NAD^+ is immobilized for reagentless device. In this study, we will use diaphorase (DI) in combination with ferrocenedimethanol for cofactor regeneration.

We have compared here different strategies for cofactor immobilization in sol-gel matrix, i.e. simple encapsulation of the native cofactor, encapsulation of NAD-Dextran, adsorption on carbon nanotubes introduced in the sol-gel matrix and finally the use of glycidoxypropylsilane (GPS) as additive. This later molecule displays an epoxide ring susceptible to react with the adenine moieties of the cofactor. According to the literature, such coupling has to be prepared in basic solution in order to get the most active biomolecules [26], but sol-gel bio-encapsulation can only be obtained in neutral conditions. We will show here that despite this limitation, the confinement of the linked cofactor in the sol-gel matrix with using GPS allows good activity to be detected with high stability. Evidence of reaction between cofactor and GPS were obtained by FTIR. The co-encapsulation of DSDH and NAD was then evaluated by electrochemically-assisted deposition. The process and the sol composition have been optimized on flat glassy carbon and gold electrodes before being applied to macroporous gold electrodes. At the end, the electrodeposited bio-composite containing DSDH, diaphorase and cofactor has been tested for the electrochemical oxidation of D-sorbitol and a comparison was made between flat and macroporous gold electrodes.

2. Co-immobilization of dehydrogenase and cofactor in sol-gel matrix by drop-coating

Figure IV-1 describes the reaction pathway used in this work. Oxidation of the enzymatic substrate by the immobilized dehydrogenase induces NAD^+ reduction to NADH. Diaphorase catalyses then the oxidation of NADH back to NAD^+. Electron transfer from the diaphorase to the glassy carbon electrode surface is carried out by ferrocene species that are introduced in the solution. The main technological barrier is the durable immobilization of the cofactor in an active form, the comparison of the various approaches proposed here to overcome this limit will be made with the redox mediator in solution.

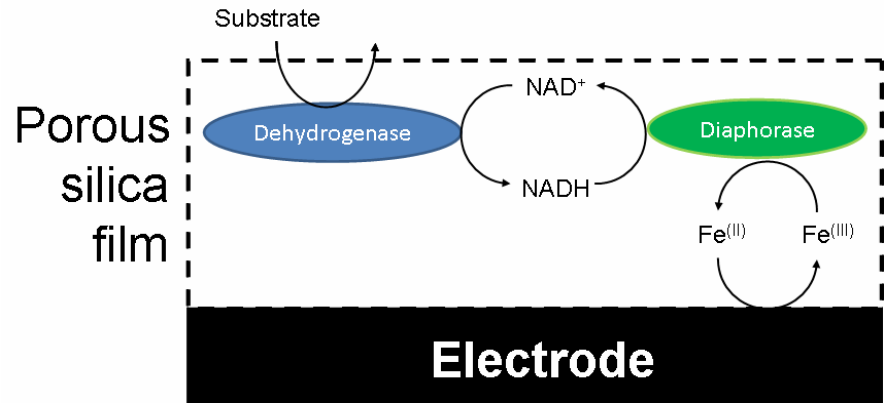

Figure IV-1. *Illustration of the electrochemical pathway used for the detection of the dehydrogenase enzymatic substrate.*

2.1. "Simple" physical entrapment of the cofactor in the sol-gel film

A straightforward way to associate the cofactor to the biocomposite layer is its addition to the starting sol so that, after gelification, it would be physically entrapped in the silica matrix. In **chapter III** dealing with the encapsulation of D-sorbitol dehydrogenase and diaphorase in sol-gel matrices, we have demonstrated the critical effect of positively-charged polyelectrolyte on the electrochemical activity of the sol-gel biocomposite. Several polyelectrolytes were tested, polydimethyldiallylammonium (PDDA), polyallylamine (PAA) and polyethyleneimine (PEI) and they all allow efficient protein immobilization characterized

by good catalytic responses when the NAD^+ cofactor was introduced in solution, freely diffusing in the sol-gel matrix. In the present work, NAD^+ was encapsulated into the sol-gel film.

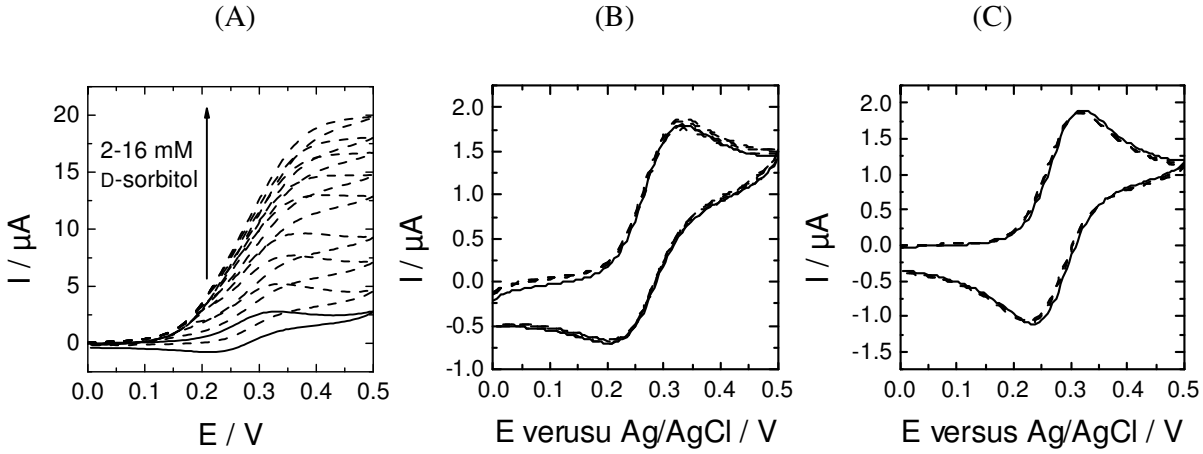

Figure IV-2. *Cyclic voltammograms obtained with (A) GCE/TEOS/PEI/(DSDH+DI)/NAD^+; (B) GCE/TEOS/PDDA/(DSDH+DI)/NAD^+ and (C) GCE/TEOS/PAA/(DSDH+DI)/NAD^+ in the absence of D-sorbitol (solid lines) and in the presence of D-sorbitol from 2 to 16 mM. All cyclic voltammograms have been performed in Tris-HCl buffer (pH 9) containing 0.1 mM FDM. Potential scan rate was 50 mV/s.*

Figure IV-2A shows the electrochemical response obtained with the modified electrode prepared with PEI as polyelectrolyte additive. Before addition of D-sorbitol, a well defined electrochemical signal due to ferrocenedimethanol could be measured (plain line). The addition of D-sorbitol in the solution from 2 to 16 mM led to a significant increase in the current response (dashed lines) and typical S-shape curves expected for a bio-catalytic process. The same experiment was performed with PDDA or PAA as additive, but no electrochemical activities were observed (see ***Figure IV-2B&C***).

PEI was already reported in the literature to allow efficient immobilization of several dehydrogenase, alcohol [27], D-lactate [28], or glucose dehydrogenase [29]. The effect of PEI for co-immobilization could be explained by the formation of "conjugates" by electrostatic attraction among the cationic polymer and the negatively charged dehydrogenase and NAD^+. These "conjugates" could make the enzyme more rigid and stable against unfolding, presenting a more stable conformation, which also could enrich the cofactor in the vicinity of

dehydrogenase. In principle, various polyelectrolytes can be used to ensure the biological activity of DSDH and DI enzymes, such as PDDA, PAA or PEI, which gave rise to good catalytic responses when NAD^+ was introduced in solution. In the present case, the cofactor was part of the sol-gel film and only PEI gave rise to well-defined bioelectrocatalytic responses (***Figure IV-2A***) whereas no response to D-sorbitol could be observed when using PDDA or PAA additives (***Figure IV-2B&C***). The reason for such behavior/difference is not clear because favorable electrostatic interactions are expected in all cases, but comparison between ***Figure IV-2A*** and ***Figure IV-2B*** and ***2C*** clearly demonstrates the crucial role of PEI to ensure cofactor entrapment in an active form in the films whereas other polyelectrolytes did not. A possible explanation can be related to the fact that PEI is a branched polyelectrolyte while the others are linear macromolecules.

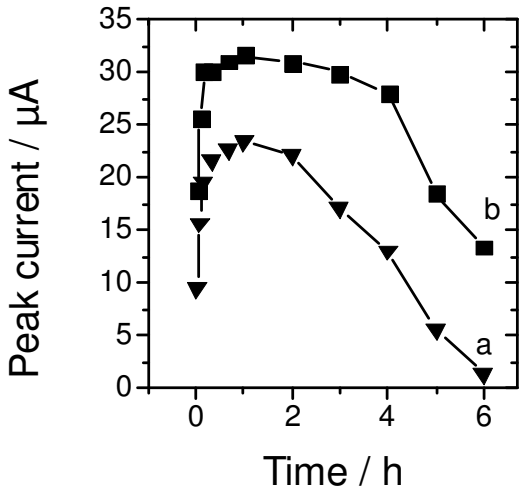

Figure IV-3. *Evolution of the peak current intensity recorded for successive analyses of 10 mM D-sorbitol solutions at distinct periods of time, using GCE modified with the same sol as Figure IV-2A, (a) in the absence and (b) in the presence of SWCNTs. All cyclic voltammograms have been performed in Tris-HCl buffer (pH 9) containing 0.1 mM FDM. Potential scan rate was 50 mV/s.*

One can evaluate the stability of this simple encapsulation procedure by recording successive cyclic voltammograms in the presence of 10 mM D-sorbitol (Fig. 1B, curve a). As shown, the electrode response increased rapidly during the first hour in solution, suggesting a necessary equilibration period, and then reached a maximum value that was somehow stable up to 2 hours in solution. After this time, the electrode response was decreasing rapidly and was almost suppressed after 6 hours in solution. Such decrease is explained by the progressive

leaching of the weakly bonded NAD^+ species in solution, being therefore no more available for the biocatalytic event. This explanation is also supported by the faster signal decrease when operating under convective conditions (response vanishing in less than 2 hours). So, in spite of exhibiting a rather good bioelectrocatalytic response, the system based on the simple encapsulation of NAD^+ into the sol-gel biocomposite (*GCE/TEOS/PEI/(DSDH+DI)/NAD*$^+$) does not allow to get long-term stability.

2.2. Effect of carbon nanotubes on the electrode stability

One knows from a recent report by Zhou et al. [8] that noncovalent attachment of NAD^+ to carbon nanotubes is possible by taking advantage of the strong π-π stacking interaction between the adenine moiety in the NAD^+ molecule and the nanotube surface. We have thus evaluated if such interaction could contribute to improve the long-term stability of cofactor immobilization in our sol-gel biocomposites. In the present case, however, it was necessary to use carboxylate-functionalized SWCNTs because crude carbon nanotubes cannot be easily dispersed in the water-based sols utilized here.

The first straightforward attempt was to incorporate SWCNTs in the starting sol containing all other ingredients (TEOS, PEI, enzymes, NAD^+) so that they are expected to be dispersed in the final sol-gel biocomposite film deposited on GCE and likely to hold the cofactor by adsorption. Typical response of *GCE/TEOS/PEI/SWCNT/(DSDH+DI)/NAD*$^+$ to successive detections of 10 mM D-sorbitol is illustrated in ***Figure IV-3*** (curve b). As shown, the voltammetric signals were slightly larger (by *ca.* 30 %) than in the absence of SWCNT, as well as some improved stability (almost constant response for 4 hours) but not at long time (> 50 % lost in sensitivity between 4 and 6 hours of use). The larger signal intensities can be explained by the increase in the electroactive surface area of the bio-electrode as a result of the introduction of SWCNT, but the fact that such increase remains rather small also suggests poor electrical interconnection, possibly due to the deposition of insulating sol-gel material on the surface of the individual nanotubes during the film formation.

In a second step, experiments have been performed by adsorbing first the cofactor to carbon nanotubes (to get NAD-SWCNT) and introducing them afterwards in the biocomposite sol-gel matrix without any additional "free" NAD^+. The resulting system (*GCE/TEOS/PEI/(DSDH+DI)/NAD-SWCNT*) led however to a limited electrochemical

activity (about 10 times lower electrochemical response) (***Figure IV-4***), probably because the quantity of cofactor introduced by this route was rather low, and the stability of the cofactor immobilization was not significantly improved by comparison with the previous route.

So, even if carbon nanotubes provides some improvements, the long-term operational stability was not yet satisfactory.

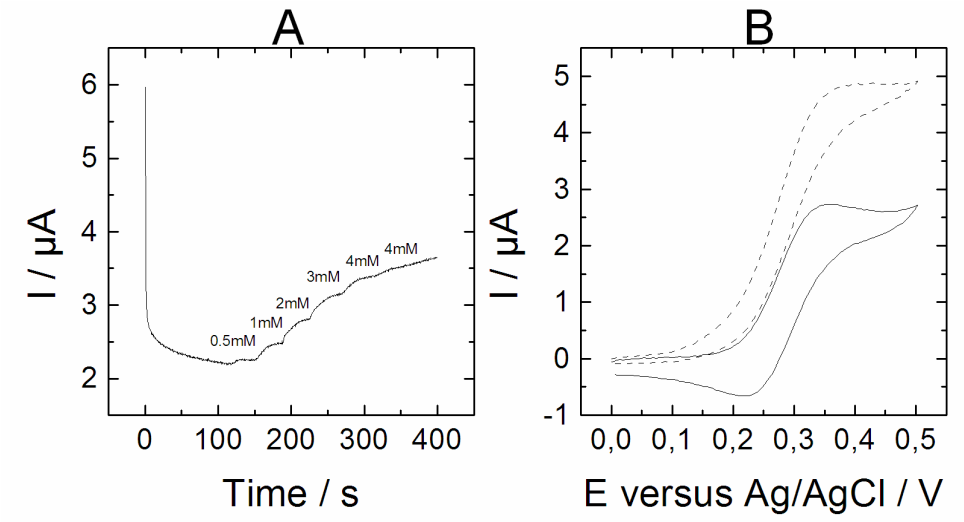

Figure IV-4. *(A) Chronoamperogram recorded at 0.4 V with GCE modified with GCE/TEOS/PEI/(DSDH+DI)/SWCNT-NAD film to successive additions of D-sorbitol from 0.5 to 14.5 mM; (B) Cyclic voltammograms measured with the same electrode as (A) in the absence of D-sorbitol and in the presence of 14.5 mM D-sorbitol. Measurements have been performed in Tris-HCl buffer (pH 9) containing 0.1mM FDM.*

2.3. Encapsulation of NAD-Dextran

Chemical attachment of the cofactor to a macromolecule is the most usual protocol for their immobilization on electrode surface [5,6,7]. Cofactor immobilization via the formation of interpenetrated organic-inorganic networks using a high molecular weight NAD^+ derivative (NAD-dextran) was also tested. The commercially available NAD-Dextran compound is indeed known to be active when associated to dehydrogenases [2,3,4]. The macromolecule was introduced in the sol-gel matrix following a similar protocol as previous experiments. ***Figure IV-5A*** reports the typical response when increasing concentrations of D-sorbitol were introduced in the solution. The catalytic current increased regularly up to 16 mM, confirming the good behavior of this system. The stability of the electrode response was again evaluated by successive cyclic voltammograms in the presence of 10 mM D-sorbitol (***Figure IV-5B***).

The electrode response increased during the first hour of experiment and was then stable for more than 6 hours. This experiment was performed with using ferrocenedimethanol in solution as electron mediator between DI and the electrode surface for recycling the immobilized cofactor.

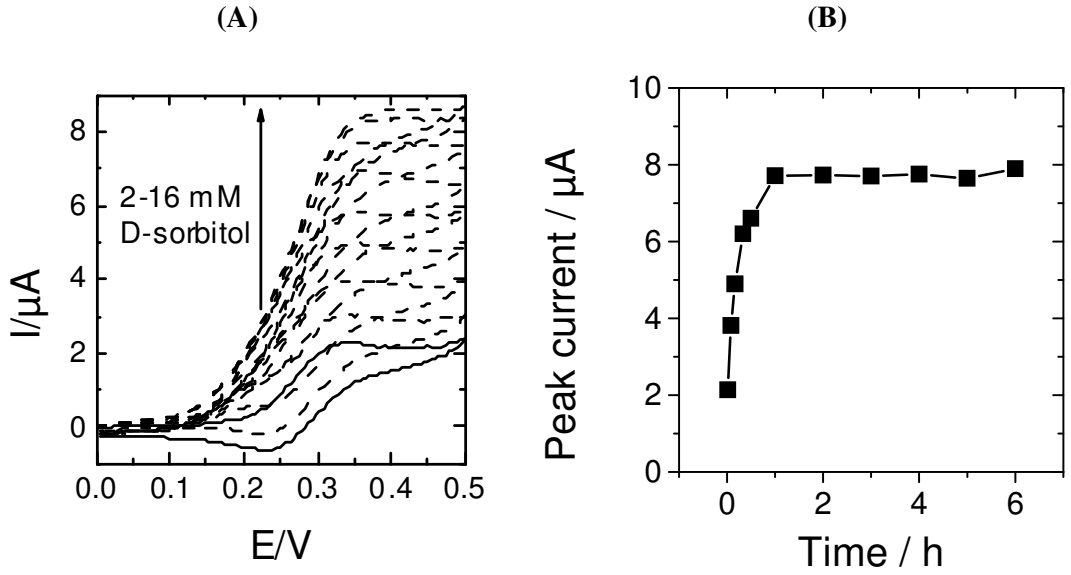

Figure IV-5. *(A) Cyclic voltammograms obtained with GCE/TEOS/PEI/(DSDH+DI)/NAD-dextran in the absence of D-sorbitol (solid lines) and in the presence of D-sorbitol from 2 to 16 mM (dashed line). (B) Evolution of the peak current intensity recorded for successive analyses of 10 mM D-sorbitol solutions at distinct periods of time, using GCE modified with the same sol as (A). Cyclic voltammograms have been performed in Tris-HCl buffer (pH 9) containing 0.1 mM FDM. Potential scan rate was 50 mV/s.*

2.4. Covalent attachment to the silica matrix with Glycidoxypropylsilane

Glycidoxypropyl-trimethoxysilane (GPS) is a well known compound in sol-gel chemistry, widely used as adhesive layer in composite material, and can find application as part of protective coatings. This compound was recently proposed separately for chemical attachment of cofactor of silica nanoparticles [30] or protein immobilization into macroporous silica monolith [31]. Both approaches used first chemical grafting of the GPS on the silica substrate before taking advantage of the epoxide ring for further functionalization with the enzyme or the cofactor. GPS was also successfully used as silica precursor for the encapsulation of enzymes [32, 33]. In these previous reports, however, no attempt was made to get *in situ*

functionalization in a one-pot reaction and no discussion was provided on the question if, or how, the epoxy ring participates effectively to the immobilization process.

According to the literature, coupling an epoxy ring with the adenine moieties of the cofactor should be made in basic medium in order to get the most active biomolecules [26], but such conditions are prevented here as sol-gel bio-encapsulation can only be obtained in neutral conditions. We will show hereafter that despite this limitation, the confinement of the linked cofactor in the sol-gel matrix with using GPS allows good activity to be detected with high stability. Evidence of reaction between NAD^+ and GPS can be obtained indirectly by electrochemistry and directly by infrared spectroscopy.

2.4.1 Electrochemical evidences of NAD^+ immobilization

Here GPS was first let to react with NAD^+ for at least 12 hours, before to be introduced as NAD-GPS educt into the sol that was deposited on the electrode surface along with other components (TEOS, PEI, enzymes). First of all, GPS provides to the film a very good adhesion to the glassy carbon electrode surface, because of the adhesive properties of this organosilane [34]. Typical amperometric and voltammetric responses of *GCE/TEOS/PEI/(DSDH+DI)/NAD-GPS* are reported in ***Figure IV-6A***. Note that in this experiment the electron mediator (ferrocenedimethanol) was not immobilized on the electrode surface but simply introduced in solution. In these conditions a good electrocatalysis could be observed as shown by the increase in current upon successive additions of D-sorbitol from 0.5 to 15.5 mM. CV curves in the presence of 15.5 mM D-sorbitol also display the typical curve of electrocatalytic detection (inset of ***Figure IV-6A***).

Figure IV-6B compares the response of bioelectrodes prepared with and without GPS (*i.e.*, *GCE/TEOS/PEI/(DSDH+DI)/NAD-GPS* and *GCE/TEOS/PEI/(DSDH+DI)/NAD*$^+$, respectively) to 2 mM D-sorbitol. Both electrodes showed comparable current response around 6 µA at the beginning of the experiment but, while the amperometric signal of the bioelectrode prepared with GPS kept a rather stable value for *ca.* 14 hours of continuous reaction (curve a), that prepared without GPS showed very low stability as the bioelectrocatalytic response decreased dramatically during the first hour of the experiment and totally vanished after 5 hours (curve b). The current value of *ca.* 2.5 µA remaining at that time corresponds only to that of ferrocene (FDM) species in solution (which is even lower than that recorded in a control experiment made on bare GCE (about 3µA)).

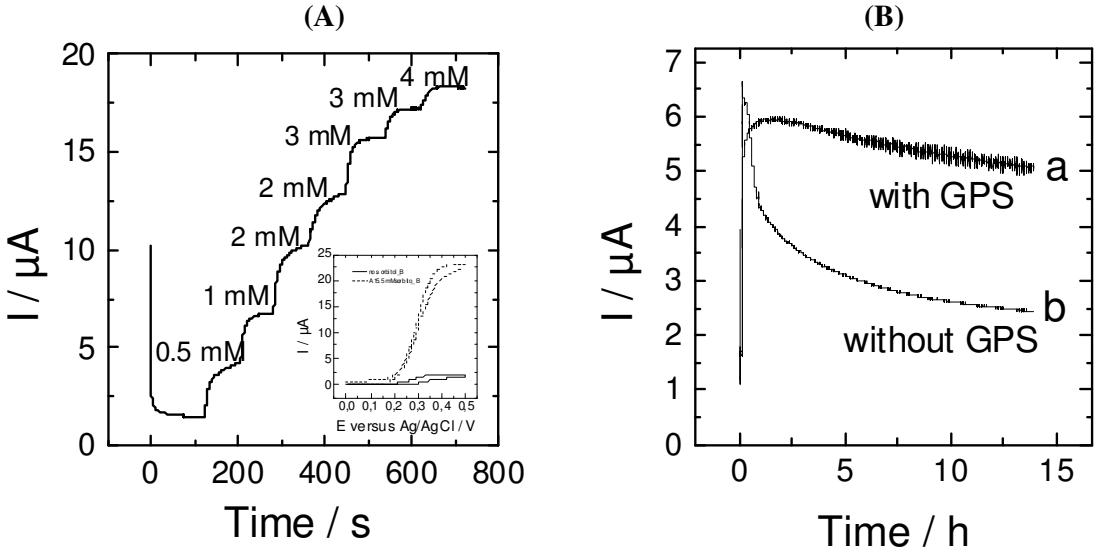

Figure IV-6. *(A) Chronoamperograms recorded at 0.4 V with GCE/TEOS/PEI/(DSDH+DI)/ NAD-GPS film to successive additions of D-sorbitol; Inset plot: Cyclic voltammograms in the absence of D-sorbitol and in the presence of 15.5 mM D-sorbitol. (B) Chronoamperograms recorded at 0.4 V with (a) GCE/TEOS/PEI/(DSDH+DI)/NAD-GPS (i.e. in the presence of GPS) and (b) GCE/TEOS/PEI/(DSDH+DI)/NAD$^+$ (i.e. in the absence of GPS). Measurements have been performed for 14 hours under convective conditions in 0.1 M Tris-HCl buffer (pH 9) containing 0.1 mM FDM and 2 mM D-sorbitol.*

2.4.2 ATR-FTIR spectroscopy

2.4.2.1 ATR-FTIR monitoring of GPS hydrolysis

Because the methoxy groups of GPS can easily hydrolyze in aqueous media, it was important to identify the characteristic spectral features occurring during the hydrolysis reaction before the analysis of the spectra in the presence of NAD^+. All spectra are discussed in the more useful 1800-700 cm^{-1} region.

Figure IV-7 shows the time-evolution of the ATR-FTIR spectra during 18 hours GPS hydrolysis in Tris-HCl buffer at pH=7.5. This figure shows also the ATR-FTIR spectrum of GPS in water after 1 h 40 min hydrolysis. The bands assignment was made according to the literature [35, 36].

The more interesting bands against hydrolysis of GPS are discussed below. In the spectrum of pure GPS (***Figure IV-8***), broad, poorly resolved bands are centered at 1076 cm^{-1}. They are mainly assigned to C-O, Si-O stretching modes of glycidoxy and methoxy groups. Their

intensities decreased with the increase of the hydrolysis of GPS. At the same time, two bands at 1095 and 1016 cm^{-1} appeared (***Figure IV-7&8***). They are two major bands of the hydrolyzed GPS spectrum (***Figure IV-7(k)***), and they are assigned to Si-O-Si stretching modes of open chains and trimers of hydrolyzed GPS, respectively. Another group of bands absorbing below 850 cm^{-1} disappears with increasing hydrolysis, and are characteristic of non hydrolyzed GPS. They are mainly assigned to Si-C, Si-O, C-C stretching modes.

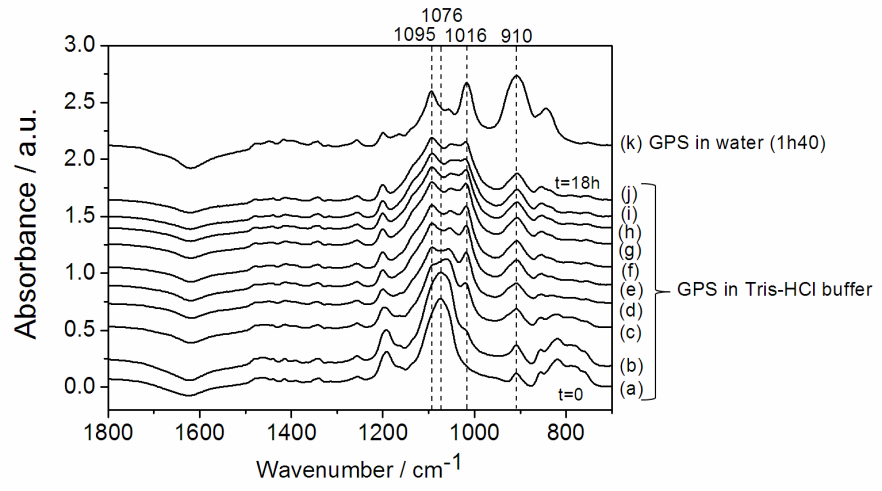

Figure IV-7. *(a)-(j) Time evolution of ATR-FTIR spectra during 18 hours GPS hydrolysis in Tris-HCl buffer (pH=7.5) on a diamond ATR crystal (one spectrum every 2 hours). (k) ATR-FTIR spectrum of GPS in water after 1 h 40 min. hydrolysis on a diamond crystal. Offsets of spectra are used for clarity.*

One interesting band absorbs at 911 cm^{-1}. It is characteristic of the epoxide group and it was assigned to C-O, C-C stretchings and C-O torsion modes of this little cycle. One can note that the wavenumber of this band do not change in the course of hydrolysis. However, one can observe a quite big intensity increase with the increase of hydrolysis time. This is probably due a drastic change in the polarity of GPS with hydrolysis that leads to higher transition moments for these vibrational modes. This led us to conclude that the epoxide group did not open in the Tris-HCl buffer used in the study. The hydrolysis reaction in Tris-HCl buffer is also slower than in pure water, since after 18 hours of reaction the spectrum shows a mixture of the spectra of pure GPS and hydrolyzed GPS (***Figure IV-7 (a, j, k)***). It was probably because of some protecting interactions between the $Si(OCH_3)_3$ group of GPS and the amino or hydroxide groups of the Tris molecule.

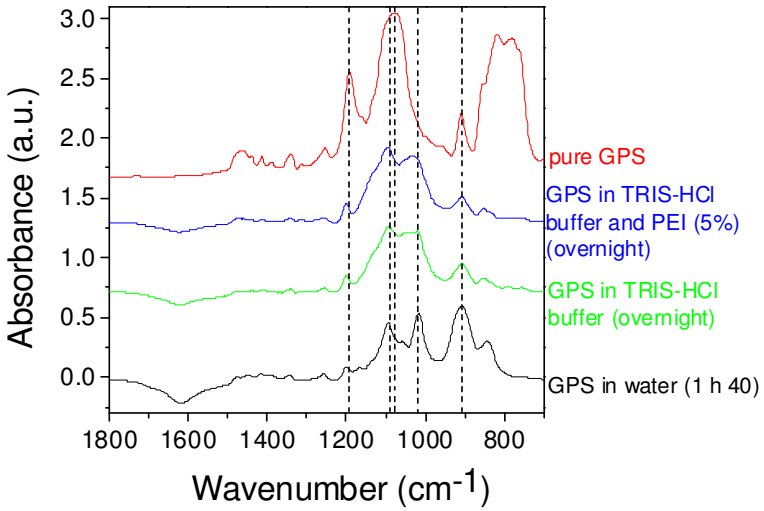

Figure IV-8. *ATR-FTIR spectra on a diamond ATR crystal of (a) pure GPS, (b) GPS and PEI(5%) after about 15 h in Tris-HCl buffer (pH=7.5), (c) GPS after about 14 hours in Tris-HCl buffer, (d) GPS after 1h40 in pure water and (e) and 5 % PEI in Tris-HCl buffer at pH 7.5. Offsets of spectra are used for clarity.*

2.4.2.2 ATR-FTIR spectrum of NAD^+

Figure IV-9 shows the spectrum of NAD^+ in Tris-HCl buffer with main group assignments determined according to the literature [37, 38, 39, 40, 41] .

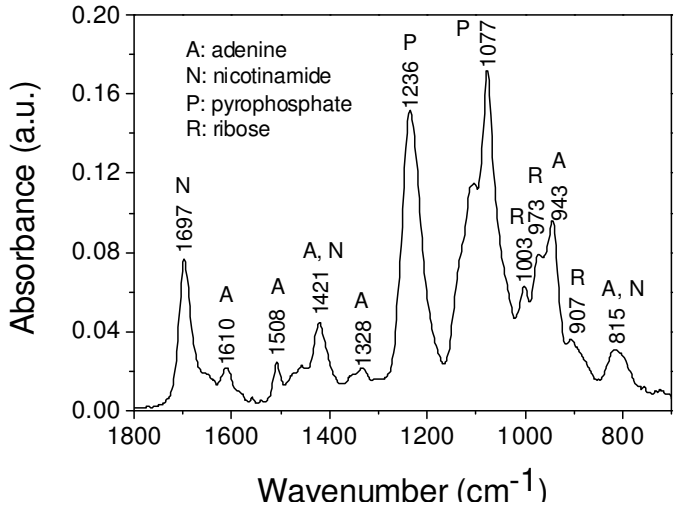

Figure IV-9. *ATR-FTIR spectrum of NAD^+ (0.3 M) in Tris-HCl buffer (pH=7.5) on a diamond ATR crystal.*

2.4.2.3 Evidence of reaction between cofactor and GPS

Figure IV-10 shows the time-evolution of the ATR-FTIR spectra during 18 hours reaction of GPS with NAD^+ (1:1 molar ratio) in Tris-HCl buffer. Here, C=O stretching band at 1696 cm^{-1} from the nicotinamide of NAD^+ does not change during the course of the reaction. It can be concluded that this group do not react with GPS (such reaction would have prevented electrocatalytic activity). Weak bands that absorb between 1370 and 1310 cm^{-1} are characteristic of the adenine part of NAD^+ [39]. The profile of these weak, poorly resolved bands change with increasing time. This suggested that the adenine group react with GPS, but it is not possible to identify precisely the reacting bonds.

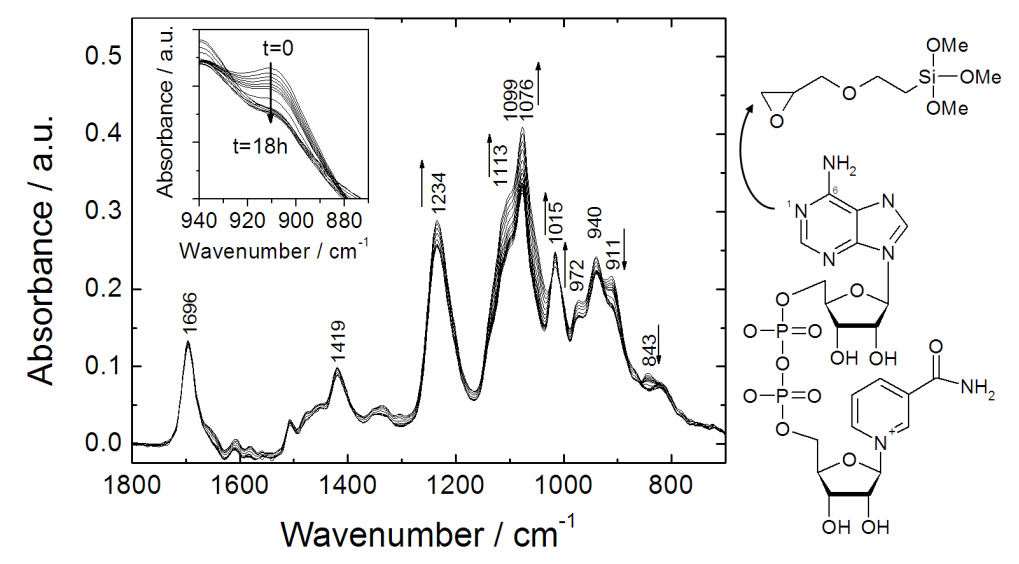

Figure IV-10. *Time evolution of ATR-FTIR spectra during 18 hours reaction of GPS (0.3 M) with NAD^+ (0.3 M) in Tris-HCl buffer (pH=7.5) on a diamond ATR crystal (one spectrum every 5 min. during 30 min. then at 1 h, 2 h, 3 h, 5 h, 8 h, 11 h, 14 h, 18 h of reaction). Inset plot shows a detail of this spectrum between 870 and 940 cm^{-1}. The scheme shows the possible reaction between N-1 of NAD^+ and the epoxide ring of GPS.*

The intensity of the bands between 1300 and 1000 cm^{-1} increases with increasing time. Even though GPS was already partly hydrolyzed when FTIR monitoring started (bands around 1100 and at 1015 cm^{-1}), it shows the continuing hydrolysis and rearrangement of hydrolyzed species during the time of the reaction monitoring (note that PO_2 elongation from phosphate groups can also be found in this region).

One interesting spectral feature is the intensity decrease of the band at 911 cm^{-1} that is assigned to the epoxide group of GPS. It shows that this group is opened when in the presence of NAD^+ while no opening of this epoxide ring was observed in Tris-HCl buffer alone (***Figure IV-7.***). The intensity of this band decreases during 8 hours of reaction, and then stays almost constant showing the end of the reaction. After 8 hours, a residual weak band stays with constant intensity on the spectrum. It is due to a ribose νC-C mode from NAD^+ (see ***Figure IV-9***).

According to previous work from Fuller et al [26], the conditions that were used here should lead to the alkylation of NAD^+ at position N-1 (see scheme on ***Figure IV-10***). This compound displays very low activity with dehydrogenase [42]. For optimal enzymatic activity, the cofactor should better be attached through the C-6 amino group rather than the N-1 ring nitrogen. This is usually obtained in basic medium using hours of reaction. But such condition cannot be used here as it would induce a rapid gelification and would make impossible the further encapsulation of proteins. Despite this possible limitation, the high concentration of NAD^+ and the confinement inside the gel at close distance to the proteins (dehydrogenase and diaphorase) allows measuring good enzymatic activity with DSDH (***Figure IV-6.***).

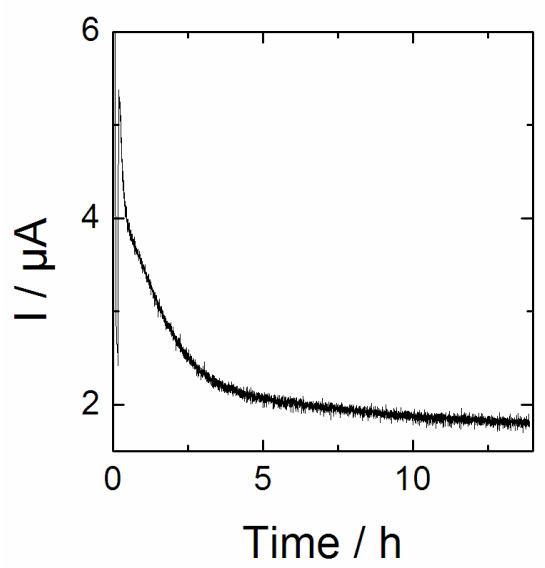

Figure IV-11. *Experiment of chronoamperometry recorded at 0.4 V with GCE/TEOS/PEI/(DSDH+DI)/NADH+GPS (i.e. replacing NAD^+ by NADH and following the same protocol). Measurements have been performed for 14 hours under convective conditions in 0.1 M Tris-HCl buffer (pH 9) containing 0.1 mM FDM and 2 mM D-sorbitol.*

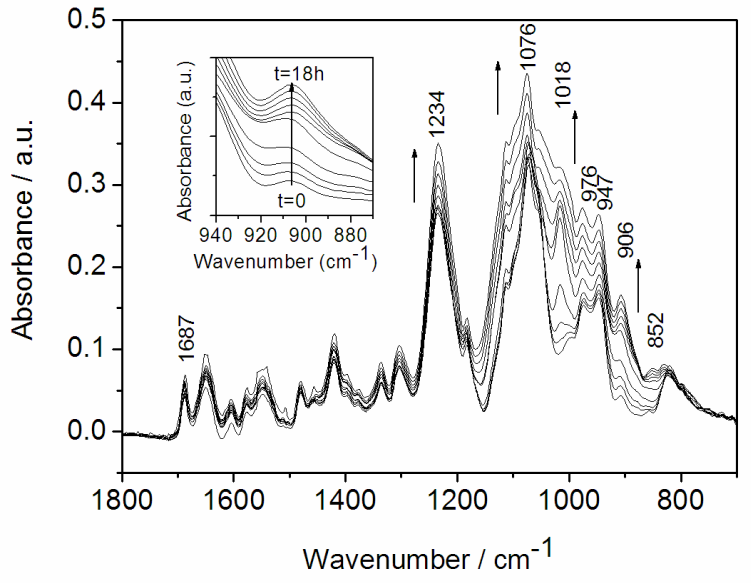

Figure IV-12. *Time evolution of the ATR-FTIR spectra during the 18 hours reaction of GPS (0.3 M) with NADH (0.3 M) in Tris-HCl buffer (pH=7.5) on a diamond ATR crystal (one spectrum at 0, 15, 30 min and at 1, 2, 5, 8, 11, 14 and 18 h of reaction). Inset plot shows a detail of the same spectra between 940 and 870 cm^{-1}.*

A final control experiment was made by replacing NAD^+ by NADH for the reaction with GPS following the same protocol. Indeed, the electrochemical biosensor/bioreactor is expected to operate independently on the initial form of the cofactor (because the required form is continuously regenerated via the electron mediator). This time, no decrease was observed at 911 cm^{-1} (***Figure IV-12***). At the opposite, the band ascribed to GPS was slightly increasing due to the hydrolysis of alkoxysilane moieties. A similar effect was observed during the simple hydrolysis of GPS in Tris-HCl buffer (***Figure IV-7***). The reduced form of the cofactor did not react with the epoxide ring in the smooth condition of the sol-gel protocol. This absence of alkylation was confirmed by electrochemical measurements. The electrode was responding to D-sorbitol additions, but the electrochemical response was not stable and disappeared in less than 3 hours (***Figure IV-11***). This trend is comparable to the one observed with the film prepared in the absence of GPS (***Figure IV-6B***, curve b).

In addition to the attachment of the cofactor, the different components participate to the good stability of the sol-gel film. By comparison, PEI was here replaced by PDDA. As mentioned in the first section of the discussion, this later polyelectrolyte did not lead to

electrocatalytic activity when NAD^+ is present in the film. In addition, it was observed that PDDA led to swelling films with limited stability (few hours). Only the association between PEI and GPS permitted to obtain good film stability with good catalytic activity. FTIR was also used to monitor an eventual reaction between PEI and GPS but no evidence of coupling between them could be observed by following the intensity of the signal at 911 cm^{-1}(***Figure IV-8)***. Contrarily to PAA or PDDA that are linear polymer, PEI is a branched polymer and we suppose it can be better distributed in the sol-gel layer. This would be the main explanation of the good stability of this bio-organic-inorganic hybrid sol-gel layer, but reaction between PEI and GPS can not be totally exclued during drying and aging that were not monitored by FTIR.

3. Co-immobilization dehydrogenase and cofactor in electrodeposited sol-gel thin film

It was demonstrated in section 2 of this chapter that dehydrogenase and cofactor can be readily co-immobilized in silica sol-gel films on electrode surfaces, showing effective bio-electrochemical activity if using PEI and GPS as additive in the sol, but those works were performed using drop-coating to deposit sol-gel films. In the present section, this approach has been extended to electrochemically-assisted deposition of the sol-gel layer.

3.1 The feasibility on GCE

First of all, the co-immobilization of DSDH, DI and NAD-GPS by electrochemically-assisted deposition is evaluated on glassy carbon electrode. ***Figure IV-13*** displays the response to D-sorbitol obtained with a GCE electrode modified by the electrogenerated silica film with encapsulated DSDH, diaphorase and GPS functionalized cofactor (NAD-GPS). Before addition of D-sorbitol, a well defined electrochemical signal due to ferrocenedimethanol could be observed (plain line). The addition of D-sorbitol in the solution from 2 to 6 mM led to a significant increase in the current response (dashed lines). The electrochemically-assisted silica gel deposition is thus an effective method for the co-immobilization of DSDH and NAD on electrode surfaces. Note that PEI was here used as polyelectrolyte for stabilizing the protein in the sol-gel film.

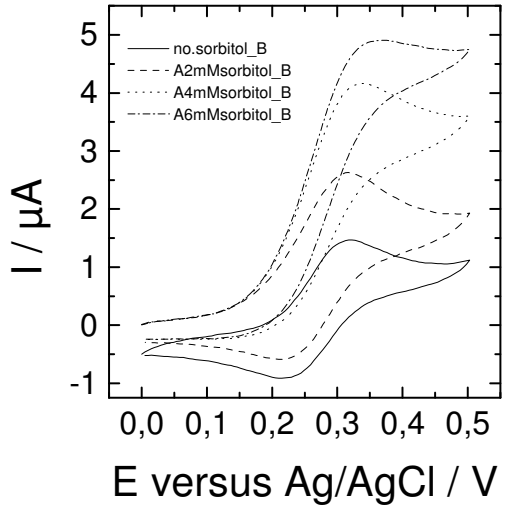

Figure IV-13. *Cyclic voltammograms obtained using GCE modified by TEOS/NAD-GPS/PEI/(DSDH+DI) film in the absence and presence of D-sorbitol. Films have been deposited by electrolysis at -1.3 V for 60 s with a sol containing 0.15M TEOS, 14 mM NAD-GPS, 2.3 mg/mL DSDH, 0.76 mg/mL DI and 1.5% PEI. Cyclic voltammograms have been performed in 0.1 M Tris-HCl buffer, in the presence of 0.1m M FDM. Potential scan rate was 50 mV/s.*

3.2 The feasibility on flat gold electrode

The co-immobilization of DSDH, DI and NAD-GPS by electrochemically-assisted deposition was then evaluated on flat gold electrode. ***Figure IV-14*** displays the response to D-sorbitol obtained with a flat gold electrode modified by the electrogenerated silica film with encapsulated DSDH, diaphorase and NAD-GPS.

We first started with the same conditions as used for the experiment on glassy carbon (***Figure IV-13***), but these conditions did not allow to be extended to gold electrode without changing. It was in fact necessary to introduce a small amount of PDDA in the sol for improving the adhesion of the film on the gold electrode. ***Figure IV-14*** shows the electrochemical response obtained with the modified electrode prepared with both PEI and PDDA as polyelectrolyte additive. Before addition of D-sorbitol, a well defined electrochemical signal due to ferrocenedimethanol could be observed. The addition of D-sorbitol in the solution from 2 to 10 mM led to a significant increase in the current response. The co-immobilization of DSDH and GPS-NAD on gold electrode surfaces was properly achieved by using both PEI and PDDA as polyelectrolyte additive.

Cofactor immobilization together with DSDH and diaphorase was successfully achieved in sol-gel film prepared by electrodeposition. As for the proteins, the appropriate choice of polyelectrolyte and concentration in the sol was critical for getting the optimal film deposition and electrocatalytic activity. A combination of PEI and PDDA was used for electrochemically-assisted deposition of this sol-gel biocomposite with co-immobilized DSDH, diaphorase and cofactor on gold surface. Such process has been also applied to the functionalization of macroporous electrodes.

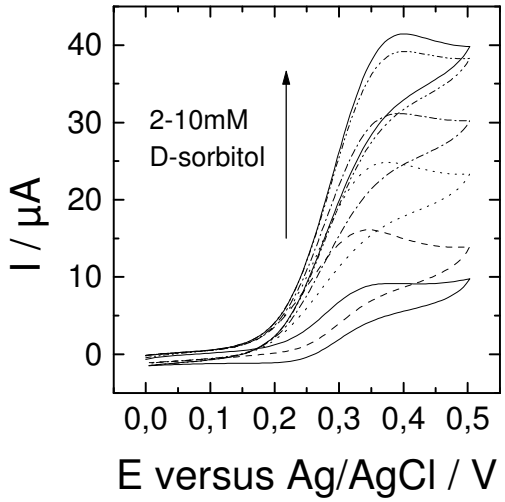

Figure IV-14. *Cyclic voltammograms obtained using gold electrode modified by TEOS/NAD-GPS/PEI/PDDA/(DSDH+DI) film in the absence and presence of D-sorbitol. Films have been deposited by electrolysis at -1.3 V for 60 s with a sol containing 0.15M TEOS, 14 mM NAD-GPS, 2.3 mg/mL DSDH, 0.76 mg/mL DI and 1 % PEI and 0.5% PDDA. Cyclic voltammograms have been performed in 0.1 M Tris-HCl buffer, in the presence of 0.1m M FDM. Potential scan rate was 50 mV/s.*

3.3 Extension to the macroporous gold electrode

The above approach was extended to macroporous gold electrode displaying a much larger electroactive surface area in comparison to the geometric one. A deposition condition -1.3 V, 60 s (versus the Ag/AgCl reference electrode) was used in previous experiment. Despite the good catalytic response was obtained on the flat gold electrode, the deposited sol-gel film was rather thick. In macroporous electrodes the situation is even more complex as the pore interconnections can be rapidly blocked by the electrogenerated silica gel layer. Low potential and deposition times are here needed to prevent the rapid macropore clogging. Here, films have been deposited by electrolysis at -1.1 V for 30 s. ***Figure IV-15A*** displays the response to

D-sorbitol obtained with a flat gold electrode modified by the electrogenerated silica film with encapsulated DSDH, DI and NAD-GPS. The electrode was found to be sensitive to successive additions of D-sorbitol, as shown by the increase in peak current intensity for the oxidation of ferrocenedimethanol. By comparison, a much higher response was observed when doing the same experiment with a macroporous gold electrode (three half layers) modified in the same conditions by the bio-composite layer (***Figure IV-15B***). The macroporous texture of the gold electrode improves thus significantly the catalytic efficiency of the sol-gel biocomposite. These experiments point out the feasibility of surface modification of such porous material with an electrodepostied sol-gel biocomposite with co-immobilized NAD^+, DSDH and diaphorase.

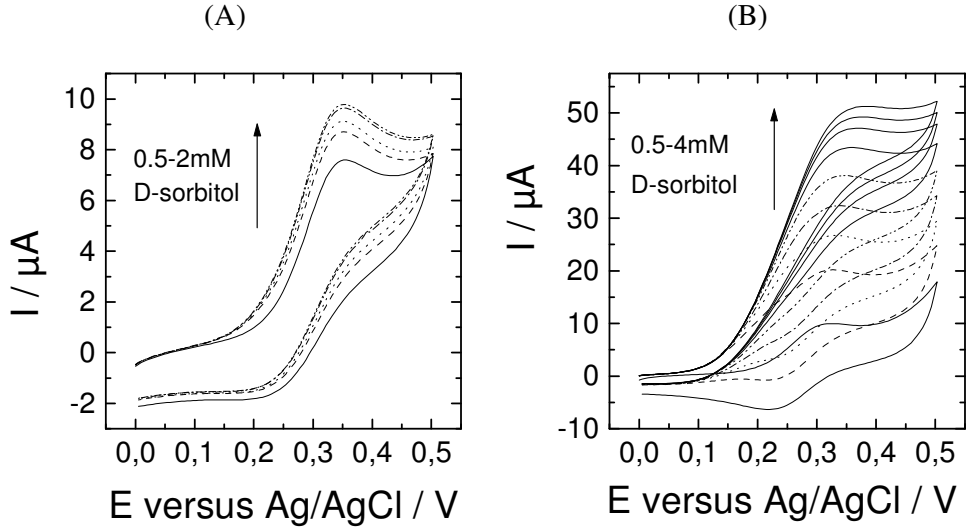

Figure IV-15. *Cyclic voltammograms obtained using (A) flat and (B) macroporous (660 nm, three half layers) gold electrode modified by TEOS/NAD-GPS/PEI/PDDA/(DSDH+DI) film in the absence and presence of D-sorbitol. Films have been deposited by electrolysis at -1.1 V for 30 s with a sol containing 0.15M TEOS, 14 mM NAD-GPS, 2.3 mg/mL DSDH, 0.76 mg/mL DI and 1 % PEI and 0.5%. Cyclic voltammograms have been performed in 0.1 M Tris-HCl buffer, in the presence of 0.1m M FDM. Potential scan rate was 50 mV/s.*

4. Conclusion

A successful strategy for dehydrogenase, diaphorase and cofactor co-immobilization in sol-gel films has been developed. It involves the chemical bonding of NAD^+ to the epoxide group of glycidoxypropylsilane (GPS) before co-condensation of the organoalkoxisilane with tetraethoxysilane in the presence of the proteins (dehydrogenase and diaphorase) and a

polyetheleneimine additive (PEI). All the operations are done in smooth conditions compatible with the sol-gel bio-encapsulation process. By comparison with the simple encapsulation of NAD^+ or NAD-dextran or adsorption of NAD^+ on carbon nanotubes, the strategy with GPS is cheaper, simpler to implement and leads to more stable sol-gel films. The electrode shows good stability under stirring for more than 14 hours. The sol-gel biocomposite can be deposited on the electrode surface either by evaporation of the sol or by sol electrolysis (i.e. electrochemically-assisted deposition). Finally, the functional layer has been successfully deposited in macroporous gold electrodes and applied for the oxidation of D-sorbitol. The macroporous texture of the gold electrode improves significantly the catalytic efficiency of the sol-gel biocomposite in comparison with a flat gold electrode. By comparison with the methods previously employed, the strategy that is described here offers a simple, cheap and clean way but effective approach to the development of integrated dehydrogenase-based bio-electrochemical devices.

References

[1] Noguer, Th.; Szydlowska, D.; Marty, J.-L.; Trojanowicz, M., Sol-gel immobilization of aldehyde dehydrogenase and NAD^+ on screen-printed electrodes for designing of amperometric acetaldehyde biosensor. *Polish J. Chem.* **2004**, *78(9)*, 1679-1689.

[2] Leca, B.; Marty, J.-L., Reusable ethanol sensor based on a NAD^+ -dependent dehydrogenase without coenzyme addition. *Anal. Chim. Acta*, **1997**, *340 (1-3)*, 143-148.

[3] Leca, B.; Marty, J. -L., Reagentless ethanol sensor based on a NAD-dependent dehydrogenase. *Biosens. Bioelectron.* **1997**, *12(11)*, 1083–1088.

[4] Montagnk, M.; Marty, J. -L., Bi-enzyme amperometric D-lactate sensor using macromolecular NAD^+. *Anal. Chim. Acta*, **1995,** *315(3)*, 297-302.

[5] Mak, K. K. W., Wollenberger, U, Scheller, F. W., Renneberg, R. An amperometric bi-enzyme sensor for determination of formate using cofactor regeneration. *Biosens. Bioelectron.* **2003**, 18(9), 1095-1100.

[6] Zhang, M.; Mullens C.; Gorski, W., Coimmobilization of dehydrogenases and their cofactors in electrochemical biosensors. *Anal. Chem.* **2007**, *79(6)*, 2446-2450.

[7] Zheng, H.; Zhou, J.; Zhang, J.; Huang, R.; Jia, H.; Suye, S., Electrical communication between electrode and dehydrogenase by a ferrocene-labeled high molecular-weight cofactor derivative: application to a reagentless biosensor. *Microchim Acta* **2009,** 165(1-2), 109–115.

[8] Zhou, H.; Zhang, Z.; Yu, P.; Su, L.; Ohsaka, T.; Mao, L., Noncovalent attachment of NAD^+ cofactor onto carbon nanotubes for preparation of integrated dehydrogenase-based electrochemical biosensors. *Langmuir* **2010**, *26(8)*, 6028–6032.

[9] Lin, C. L.; Shih, C. L.; Chau, L. K. Amperometric L-Lactate Sensor Based on Sol-Gel Processing of an Enzyme-Linked Silicon Alkoxide. *Anal. Chem.* **2007**, *79(10)*, 3757-3763.

[10] Wooten, M.; Gorski, W., Facilitation of NADH Electro-oxidation at Treated Carbon Nanotubes. *Anal. Chem.* **2010**, 82(4), 1299–1304.

[11] Tse, D. C.; Kuwana, T., Electrocatalysis of dihydronicotinamide adenosine diphosphate with quinones and modified quinone electrodes. *Anal. Chem.* **1978**, *50(9)*, 1315–1318.

[12] Carlson, B. W.; Miller, L. L., Mechanism of the oxidation of NADH by quinones. Energetics of one-electron and hydride routes. *J. Am. Chem. Soc.* **1985**, *107(2),* 479–485..

[13] Antiochia, R.; Gallina, A.; Lavagnini, I.; Magno, F., Kinetic and thermodynamic aspects of NAD-related enzyme-linked mediated bioelectrocatalysis. *Electroanalysis* **2002**, *14(18)*, 1256–1261.

[14] Kitani, A.; So, Y. H.; Miller, L. L., Electrochemical study of the kinetics of NADH being oxidized by diimines derived from diaminobenzenes and diaminopyrimidines. *J. Am. Chem. Soc.* **1981**, *103(25)*, 7636–7641.

[15] Kitani, A.; Miller, L. L., Fast oxidants for NADH and electrochemical discrimination between ascorbic acid and NADH. *J. Am. Chem. Soc.* **1981**, *103(12)*, 3595–3597.

[16] Zhou, M.; Shang, L.; Li, B.; Huang, L.; Dong, S. Highly ordered mesoporous carbons as electrode material for the construction of electrochemical dehydrogenase- and oxidase-based biosensors. *Biosens. Bioelectron.* **2008**, *24(3)*, 442–447.

[17] Wang, Y.; Iqbal, Z.; Mitra, S., Rapidly Functionalized, Water-Dispersed Carbon Nanotubes at High Concentration. *J. Am. Chem. Soc.* **2006**, *128(1)*, 95-99..

[18] Kachoosangi, R. T.; Musameh, M. M.; Abu-Yousef, I.; Yousef, J. M.; Kanan, S. M.; Xiao, L.; Davies, S. G.; Russell, A.; Compton, R. G. Carbon Nanotube-Ionic Liquid Composite Sensors and Biosensors. *Anal. Chem.* **2009**, *81(1)*, 435–442.

[19] Moore, R. R.; Banks, C. E.; Compton, R. G. Basal plane pyrolytic graphite modified electrodes: comparison of carbon nanotubes and graphite powder as electrocatalysts. *Anal. Chem.* **2004**, *76(10)*, 2677–2682.

[20] Jena, B. K.; Raj, C. R. Electrochemical Biosensor Based on Integrated Assembly of Dehydrogenase Enzymes and Gold Nanoparticles. *Anal. Chem.* **2006**, *78(18)*, 6332-6339.

[21] Tsujimura, S.; Kano, K.; Ikeda, T. Electrochemical oxidation of NADH catalyzed by diaphorase conjugated with poly-1-vinylimidazole complexed with Os(2,2'-dipyridylamine)2Cl. *Chem. Lett.* **2002**, *10*, 1022-1023.

[22] Nikitina, O.; Shleev, S.; Gaydab, G.; Demkiv, O.; Gonchar, M.; Gorton, L.; Csoregi, E.; Nistor, M. Bi-enzyme biosensor based on NAD^+- and glutathione-dependent recombinant formaldehyde dehydrogenase and diaphorase for formaldehyde assay. *Sens. Actuators B* **2007**, *125(1)*, 1–9.

[23] Matsue, T.; Yamada, H.; Chang, H. C.; Uchida, I.; Nagata, K.; Tomita, K., Electron transferase activity of diaphorase (NADH: acceptor oxidoreductase) from Bacillus stearothermophilus. *Biochim. Biophys. Acta* **1990**, *1038(1)*, 29–38.

[24] Takagi, K.; Kano, K.; Ikeda, T., Mediated bioelectrocatalysis based on NAD-related enzymes with reversible characteristics. *J. Electroanal. Chem.* **1998**, *44(1-2)*, 211–219.

[25] Ogino,Y.; Takagi, K.; Kano, K.; Ikeda, T., Reactions between diaphorase and quinone compounds in bioelectrocatalytic redox reactions of NADH and NAD^+. *J. Electroanal. Chem.* **1995**, *396(1-2)*, 517–524.

[26] Fuller, C. W.; Rubin, J. R.; Bright, H. J. A simple procedure for covalent immobilization of NADH in a soluble and enzymically active form. *Eur. J. Biochem.* **1980,** *103(2)*, 421 -430.

[27] Dominguez, E.; Lan, H. L.; Okamoto, Y.; Hale, P. D.; Skotheim, T. A.; Gorton, L. A carbon paste electrode chemically modified with a phenothiazine polymer derivative for electrocatalytic oxidation of NADH. Preliminary study. *Biosens. Bioelectron.* **1993**, *8(3-4)*, 167-175.

[28] Shu, H. C.; Mattiasson, B.; Persson, B.; Nagy, G.; Gorton, L.; Sahni, S.; Geng, L.; Boguslavsky, L.; Skotheim, T., A reagentless amperometric electrode based on carbon paste, chemically modified with D-lactate dehydrogenase, NAD^+, and mediator containing polymer for D-lactic acid analysis. I. Construction, composition, and characterization. *Biotechnol. Bioengin.* **1995**, *46(3)*, 270-279.

[29] Teramoto, M.; Nishibue, H.; Okuhara, K.; Ogawa, H.; Kozono, H.; Matsuyama, H.; Kajiwara, K., Effect of addition of polyethyleneimine on thermal stability and activity of glucose dehydrogenase. *App. Microbiol. Biotechnol.* **1992**, *38(2)*, 203-208.

[30] Liu, W.; Zhang, S.; Wang, P., Nanoparticle-supported multi-enzyme biocatalysis with in situ cofactor regeneration. *J. Biotechnol.* **2009**, *139(1)*, 102-107.

[31] Brun, N.; Garcia, A. B.; Deleuze, H.; Achard, M.-F.; Sanchez, C.; Durand, F.; Oestreicher, V.; Backov, R.; *Chem. Mater.* **2010**, *22*, 4555–4562.

[32] Barsan, M. M.; Klincar, J.; Batic, M.; Brett, C. M. A. Design and application of a flow cell for carbon-film based electrochemical enzyme biosensors. *Talanta* **2007**, *71(5)*, 1893-1900.

[33] Chiorcea-Paquim, A.; Pauliukaite, R.; Brett, C. M. A.; Oliveira-Brett, A. M., AFM nanometer surface morphological study of in situ electropolymerized neutral red redox mediator oxysilane sol-gel encapsulated glucose oxidase electrochemical biosensors. *Biosens. Bioelectron.* **2008**, *24(2)*, 297-305.

[34]Atanacio, A. J.; Latella, B. A.; Barbe, C. J.; Swain, M. V., Mechanical properties and adhesion characteristics of hybrid sol-gel thin films. *Surf. Coat. Technol.* **2005**, *192(2-3)*, 354-364

[35] Bellamy L. J. "The infra-red spectra of complex molecules" Chapman and Hall Ltd, London (1975).

[36] Sapic I. M.; Bistricic L.; Volovsek V.; Dananic V.; Furic K. DFT study of molecular structure and vibrations of 3-glycidoxypropyltrimethoxysilane. *Spectrochim. Acta A*, **2009**, *72(4)*, 833-40.

[37] Mathlouthi, M.; Seuvre, A.M. ; Koenig, J. L., FT-IR and laser-Raman spectra of constituents of nucleic acids. Part I. FT-IR and laser-Raman spectra of D-ribose and 2-deoxy-D-erythro-pentose ("2-deoxy-D-ribose"). *Carbohydr. Res.* **1983**, *122(1)*, 31-47.

[38] Mathlouthi, M.; Seuvre, A.M. ; Koenig, J. L., FTIR and laser-Raman spectra of constituents of nucleic acids. Part II. FTIR and laser-Raman spectra of adenine and adenosine. *Carbohydr. Res.* **1984**, *131(1)*, 1-15.

[39] Nadolny, C.; Zundel, G., Protonation, conformation and hydrogen bonding of nicotinamide adenine dinucleotide - an FT-IR study. *J. Molec. Struct.* **1996**, *385(2)*, 81-87.

[40] Bellamy L. J. "The infra-red spectra of complex molecules" Chapman and Hall Ltd, London (1975).

[41] Sapic I. M., L. Bistricic, V. Volovsek, V. Dananic, K. Furic, Spectrochim. Acta Part A 72 (2009) 833-840.

[42] CARL W. FULLER+ AND HAROLD J. BRIGHT, THE JOURNAL OF BIOLOGUXL CHEMISTRY, Vol. 252, No. 19, Issue of October 10, pp. 6631-6639, 1977

Chapitre V. Immobilisation du médiateur électrochimique au sein de la matrice sol-gel et co-immobilisation avec la déshydrogénase et le cofacteur NAD^+

Dans ce chapitre sont présentés les travaux menés pour immobiliser le médiateur électrochimique au sein de la matrice sol-gel afin d'établir la communication électronique entre le centre redox de la diaphorase et l'électrode. Les médiateurs utilisés sont soit des groupements ferrocène liés chimiquement à la poly(ethyleneimine) ou à une fonction silane (qui peut alors être introduite dans la matrice sol-gel par co-condensation) ou un polymère d'osmium fournit par le groupe du Prof. Schuhmann de la Ruhr-Universität (Bochum, Allemagne). Nous avons observé que le glycidoxypropylsilane (GPS) utilisé pour fixer chimiquement le cofacteur à la matrice de silice permettait également d'améliorer la stabilité de la fixation du médiateur électrochimique. La co-immobilisation de la DSDH, de la diaphorase, du cofacteur NAD^+ et du médiateur électrochimique a alors été étudiée, tout d'abord en déposant la couche mince sol-gel par évaporation du sol et enfin en utilisant le procédé d'électrogénération sol-gel. Alors que l'évaporation permet la formation de couches minces dans lesquels tous les éléments encapsulés peuvent communiquer entre eux efficacement, l'électrogénération induit une perte d'activité du médiateur électrochimique et donc une absence d'activité bioélectrocatalytique.

Chapter V. Mediator immobilization in sol-gel matrix and co-immobilization with dehydrogenase and cofactor

In this chapter, diaphorase has been used in addition to the dehydrogenase in order to ensure the safe regeneration of the NAD^+ cofactor, using ferrocene species or osmium polymer as electron shuttles between the diaphorase and the electrode. First of all, the immobilization of ferrocene species and osmium polymer in sol-gel matrix was studied. The influence of GPS as additives for the mediator immobilization was described. Then, the feasibility of co-immobilization base on sol-gel film was evaluated by one step drop-coating. In addition, electrochemically-assisted deposition of sol-gel thin film to co-immobilize dehydrogenase, diaphorase, the cofactor NAD^+ and an electron mediator was also investigated.

1. Introduction

Near 300 dehydrogenases are known to catalyze the oxidation of a variety of substrates. However, there are some difficulties in the development of dehydrogenase-based reagentless devices because of the high over-potential for the direct oxidation of NADH that results in the formation of non-active form of cofactors. Some of these difficulties can be minimized through the use of redox mediators that shuttle electrons between the cofactor and the electrode surface [1]. The oxidation of NADH can also be achieved using the enzyme diaphorase (DI). The association of diaphorase with mediators to regenerate cofactor at the electrode surface has already been reported [2, 3, 4]. The regeneration of cofactor with the participation of diaphorase ensures that only enzymatically active cofactors are produced selectively. Mediator is necessary because the diaphorase shows only very slow rates of electron transfer to electrode surfaces [5]. Ferrocene species [3] are by far the most common among the mediators used in combination with diaphorase for cofactor regeneration. Osmium redox polymers have also been proposed recently for such applications [4].

The difficulty to elaborate reagent free device comes from the development of a suitable matrix in which all component of the electrochemical detection are immobilized in a stable form, i.e. the enzyme(s), the cofactor and the electrocatalytic system for cofactor detection and regeneration. Sol-gel materials are known to have very promising features as immobilization matrices, because they can be prepared at room temperature and can retain the catalytic activity of the biomolecules [6, 7, 8]. By changing the experimental conditions of the sol-gel process, gel structures with related characteristics can be obtained. A very large number of enzymes have been trapped within sol-gel films, showing that they usually retain their catalytic activity and can even be protected against degradation [9, 10, 11]. Moreover, during the sol-gel process, additional substances such as redox mediators, e.g. Ruthenium complex [12], toluidine blue [13], thionin [14], or ferrocene [15], can also be easily incorporated into the final structure. Despite the long history of using sol-gel material for enzymes immobilization and mediator immobilization, no work has been reported regarding the co-immobilization of enzyme, cofactor and mediator by using a sol-gel material to construct this reagentless device.

In this work, a series of strategies allowing dehydrogenase, cofactor and electron mediator co-immobilization in sol-gel thin films have been investigated. As illustrated on ***Scheme V-1***,

oxidation of the enzymatic substrate by the immobilized dehydrogenase induces NAD^+ reduction to NADH. Diaphorase catalyses then the oxidation of the immobilized NADH back to NAD^+ and the electron transfer from the diaphorase to the glassy carbon electrode surface is carried out by the immobilized mediators. These mediator species can be ferrocene species (ferrocene linked to a poly(ethylenimine) or a ferrocene-silane) or an osmium polymer. First of all, the immobilization ferrocene species and osmium polymer in the sol-gel matrix are shown. The influence of glycidoxypropylsilane (GPS) as additive to improve the long term stability of the mediator immobilization is studied. Then, the feasibility of co-immobilization of dehydrogenase, diaphorase and cofactor in the sol-gel film is evaluated by one step drop-coating. Attempt to perform this co-immobilization by electrochemically-assisted sol-gel deposition is finally presented.

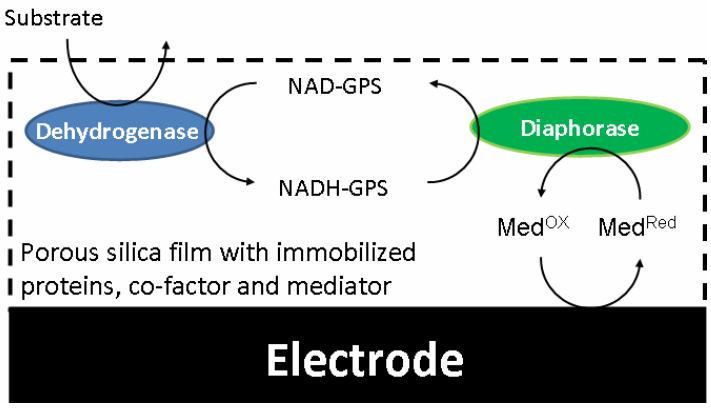

Scheme V-1. *Illustration of the electrochemical pathway used for the detection of the dehydrogenase enzymatic substrate.*

2. Fc-PEI as co-immobilized mediator

Ferrocene (Fc) species are commonly used in combination with diaphorase for cofactor regeneration. The great interest in ferrocene derivatives originates from their fast electron transfer properties, their pH-independent redox potentials, and their efficient electrochemical reversibility [16]. In this process, NADH reacts with diaphorase and the electrochemically generated ferricinium ions to produce NAD^+ and ferrocene species that can be re-oxidized in the electrocatalytic scheme (see ***Scheme V-1***).

2.1 Co-immobilization in drop-coated sol-gel film

2.1.1 Effect of GPS on Fc-PEI immobilization

The ferricinium ion is much more soluble than ferrocene itself [17]. Therefore, the main problem in using Fc is a gradual leakage, from the electrode surface, of the mediator via its oxidized form. One way to overcome the above problem is attaching the Fc to a polymer. Poly(ethylenimine) (PEI) is an attractive candidate to serve as a redox polymer backbone for a high degree of functional density on the polymer to facilitate modification and high segmental mobility. Liu et al. coupled ferrocene carboxaldehyde to PEI and incorporated these redox polymers into polyelectrolyte multilayer films via a layer-by-layer deposition technique [18]. Hodak et al. reported the redox mediation of glucose oxidase (GOx) in a self-assembled structure of cationic protonated poly-(allylamine) modified by ferrocene (PAA-Fc) and anionic GOx deposited electrostatically layer-by-layer on negatively charged alkanethiol-modified Au surfaces [19]. Zheng et al. prepared PEI with attaching both the redox mediator (ferrocene) and the native cofactor (NAD^+), and then the modified polymer was immobilized with the NAD-dependent dehydrogenase to construct reagentless amperometric biosensor [20]. Here, the synthesized Fc-PEI is introduced into the sol-gel matrix to construct the mediator modified electrode with the idea to form an interpenetrated organic-inorganic hybrid ensuring durable immobilization of the mediator. ***Figure V-1A*** shows cyclic voltammograms recorded with a GCE modified by TEOS sol-gel film containing Fc-PEI. A well-defined CV signal can be observed, but it is not stable on multiple potential scan due to the rapid leaching of the mediator. Unfortunately, the leakage of Fc from the electrode can not be prevented by the chemical attachement of Fc to PEI.

The chemical structure of the alkoxysilane precursors and the composition of the sol-gel mixture influenced the roughness, the size and the distribution of pores in the sol-gel films, which are important criteria for both efficient enzyme and mediator encapsulation. It is reported that the formation of sol-gel from GPS precursor comparing with the other (organol)alkoxyoxysilane precursors lead to the formation of a more uniform thin film with smaller pores [21, 22], which would allow stable enzyme and mediator immobilization. Here, we try to introduce GPS inside the sol-gel matrix to improve the stability of mediator immobilization with the idea to encapsulate more effectively Fc-PEI to the structure via favourable interaction between amino group and epoxide function of GPS. ***Figure V-1B*** shows cyclic voltammograms recorded with a GCE modified by TEOS/GPS sol-gel film containing Fc-PEI. In this case, the stability of the electrochemical response upon multisweep is satisfactory, which can maintain several potential scans without degradation. Using GPS as additive in TEOS sol-gel matrix can indeed enhance the stability of the Fc-PEI immobilization.

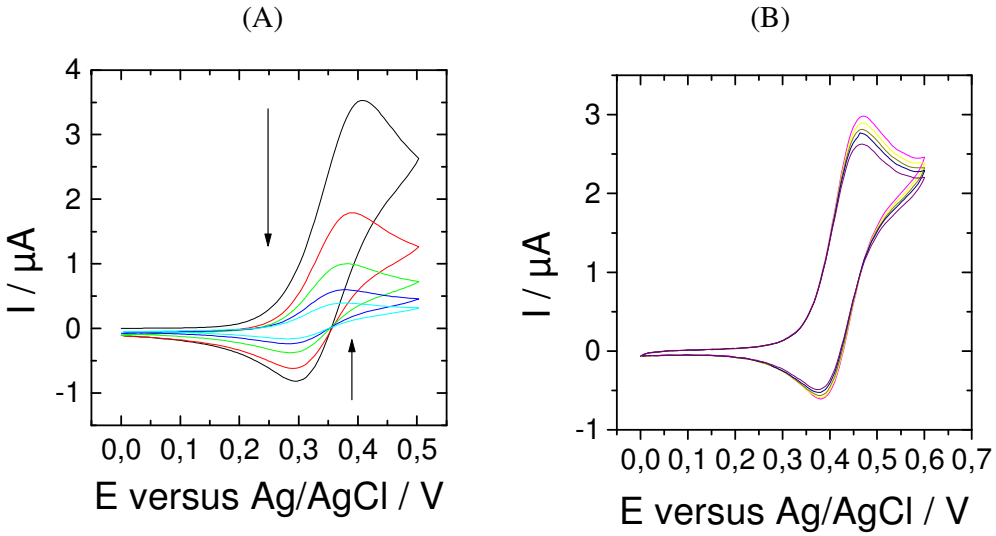

Figure V-1*. Cyclic voltammograms recorded with a GCE modified by drop-coated (A) TEOS/PEI/Fc-PEI;(B) TEOS/GPS/PEI/Fc-PEI film in the 0.1 M Tris-HCl buffer (pH 9) at a scan rate of 50 mV/s, scan cycle, 5.*

2.1.2 Co-immobilization of Fc-PEI, DSDH, DI and cofactor

Here, the co-immobilization of Fc-PEI, cofactor, DSDH and diaphorase inside the silica gel has been investigated. Fc-PEI, GPS functionalized cofactor (NAD-GPS), DSDH and

diaphorase are mixed together inside sol. All these components are encapsulated in one step into the silica gel layer by drop-coating to get *TEOS/GPS/Fc-PEI/NAD-GPS/DSDH/DI* film modified electrode.

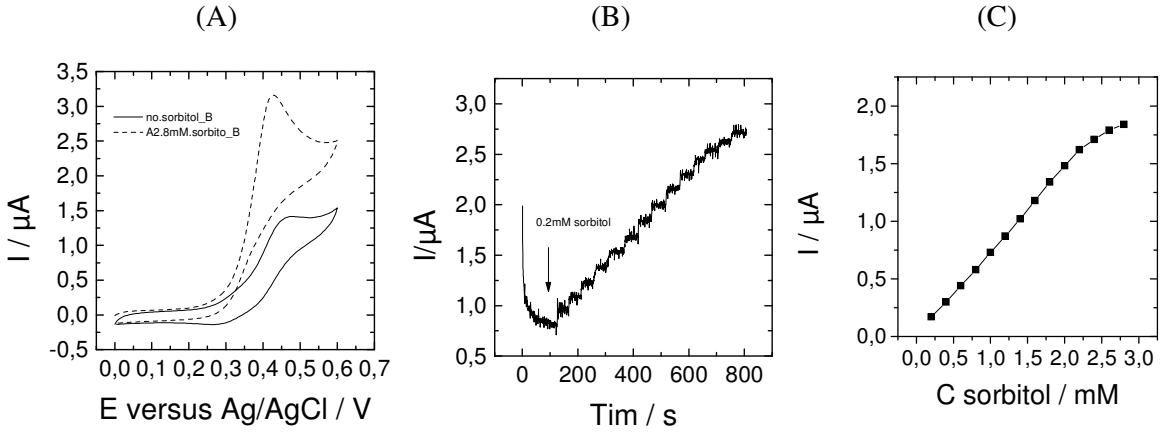

Figure V-2. *(A) Cyclic voltammograms recorded at GCE modified with TEOS/GPS/Fc-PEI/NAD-GPS/DSDH/DI film in the absence of D-sorbitol and in the presence of 2.8 mM D-sorbitol. (The film was prepared with a sol containing 0.077 M TEOS, 0.0385MGPS, 14 mM NAD-GPS, 2.3 mg/mL DSDH, 0.76 mg/mL DI and Fc-PEI by drop-coating); (B) Amperometric responses recorded at an applied potential of 0.4 V to successive additions of 0.2mM D-sorbitol in stirred solution. (C) Corresponding calibration plot. All measurements were performed in the 0.1 M Tris-HCl buffer (pH 9).*

Figure V-2A shows the electrochemical response of the film to the addition of D-sorbitol in solution. In the absence of D-sorbitol, only the electrochemical signal of ferrocene is observed. The addition of D-sorbitol induces an increase of the anodic current and a decrease of the cathodic current. It corresponds to the electrochemical oxidation of the NADH cofactor produced by the encapsulated DSDH while oxidizing D-sorbitol. Here the enzymatic cofactor is detected at the diaphorase modified GCE by using ferrocene as electron mediator. NADH reacts with diaphorase and the electrochemically generated ferricinium ions to produce NAD^+ and ferrocene species that can be re-oxidized in the electrocatalytic scheme. ***Figure V-2B*** shows amperometric responses of the modified electrode to D-sorbitol in a stirred solution. An increasing electrocatalytic response is obtained upon the addition of 0.2 mM D-sorbitol. The electrocatalytic response is about three times lower with the mediator inside the film by comparison with the response with the mediator in solution (***Figure IV-6***). ***Figure V-2C*** shows the corresponding calibration plot, the current intensity increases regularly with the D-sorbitol concentration up to 2.2 mM and starts to level off for higher concentrations.

We have here studied the electrode stability (***Figure V-3***). The response to 2 mM D-sorbitol of electrodes prepared the same way, with (curve a) and without GPS (curve b) are monitored during 14 hours. In the absence of GPS, the electrode current decreases dramatically during the first 500 s (before the addition of D-sorbitol), due to the rapide loss of Ferrocene and NAD^+ in the solution. After the addition of D-sorbitol, only faintly visible current increase is obtained, that reach quickly a current value close to zero. At the opposite, the electrode prepared with GPS display a very good stability, and just a limited (few percents) decrease in current intensity was observed, possibly due to loss of enzymatic activity during the long operation. GPS has here two functions, it allows to chemically attach NAD^+ to the silica matrix and it stabilizes the overall assembly for improved long-term stability.

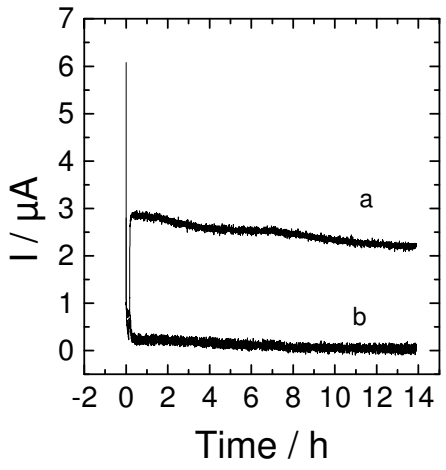

Figure V-3. *Chronoamperograms recorded at 0.4 V with GCE modified by (a) TEOS/GPS/Fc-PEI/NAD-GPS/DSDH/DI; (b) TEOS/Fc-PEI/NAD-GPS/DSDH/DI film. Measurements have been performed for 14 hours oxidation under convective conditions in 0.1 M Tris-HCl buffer (pH 9) containing 2 mM D-sorbitol.*

2.2 Co-immobilization in electrogenerated sol-gel films

2.2. Immobilization of Fc-PEI in electrodeposited sol-gel thin films

The electrochemically-assisted deposition of silica thin film involves the local increase of the pH that induces rapid gelification at the electrode surface. In order to develop a mediator immobilization method compatible to macroporous electrodes, we try to extend the previous droping/evaporation approach to the electrochemically-assisted deposition of sol-gel film. ***Figure V-4*** shows typical cyclic voltammograms recorded with a GCE modified by electrodeposited TEOS/GPS sol-gel film containing Fc-PEI. No electrochemical signal of

ferrocene was observed in the cyclic voltammograms. At the contrary to drop-coating, the electrodeposition involves a significant increase of pH during the gelification. It seems that these conditions limit the homogeneous incorporation of the ferrocene species in the sol-gel film, and limit strongly its electrochemical detection.

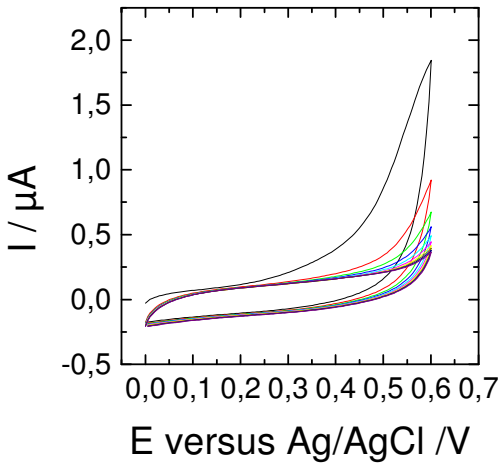

***Figure V-4**. Cyclic voltammograms recorded with a GCE modified by electrodeposited TEOS/GPS/PEI/Fc-PEI in the 0.1 M Tris-HCl buffer (pH 9) at a scan rate of 50 mV/s, scan cycle, 10. Films have been deposited by electrolysis at -1.3 V for 60 s with a TEOS/GPS sol containing Fc-PEI.*

2.2.2 Co-immobilization in electrodeposited sol-gel thin film

It has been demonstrated in chapter IV that dehydrogenase and cofactor can be readily encapsulated in electrochemically-assisted deposition of sol-gel films on electrode surfaces. Although the immobilization of Fc-PEI by electrodepostion was not successful, we here try to co-immobilize DSDH, NAD-GPS and Fc-PEI in electrochemically-assisted deposition sol-gel films. Indeed, the introduction of enzyme and cofactor in the starting sol solution may bring some changes of the film properties. However, only faintly visible electrochemical signal of ferrocene could be observed in the absence of D-sorbitol (***Figure V-5***). The addition of D-sorbitol did not induce any increase of the anodic current. Oppositely, the electrochemical signal of ferrocene decreased strongly.

Obviously the differences in gel texture/structure between the film obtained by drop-coating and electrodeposition lead to different electrochemical behaviour. In order to improve the incorporation of the ferrocene species in the electrogenerated sol-gel film, another strategy involving Fc-silane has been tested and is presented in the next section.

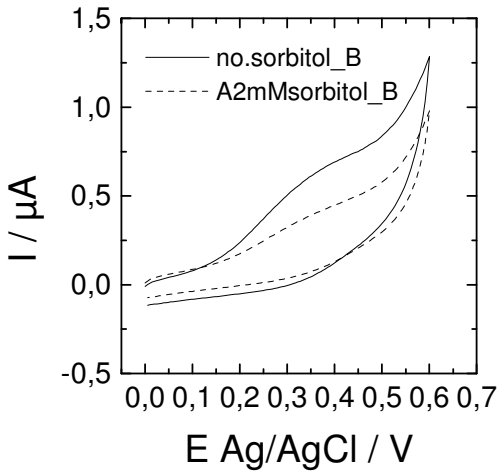

Figure V-5*. Electrochemical response of glassy carbon electrode modified by TEOS/GPS/PEI/Fc-PEI/NAD-GPS/DSDH/DI film in the absence and in the presence of D-sorbitol from 2mM to 4mM. Films have been deposited by electrolysis at -1.3 V for 60 s with a TEOS/GPS sol containing DSDH, DI, NAD-GPS and Fc-PEI. Cyclic voltammograms have been performed at 50 mV/s in 0.1 M Tris-HCl buffer.*

3. Fc-silane as co-immobilized mediator

The synthesis of sol-gel silica material [23, 24, 25] has become a vast area of research during the last few years. The silica framework can be synthesized in part from alkoxide precursors containing a nonhydrolyzable Si-C bond, i.e. $R_{4-x}Si(OR')_x$, where R represents the desired reagent or functional group. One of the possible applications of such materials in the development of sensors is the attachment of the redox material to the surface of electrode. Audebert et al. [25] developed a modified electrode from organic-inorganic hybrid gels formed by hydrolysis-polycondensation of some trimethoxysilylferrocenes. In this work, the used organic-inorganic hybrid gels contain ferrocene units covalently bonded inside a silica network. There is a great potential to study such ferrocene linked sol-gel silica material for mediated biosensor applications. Some works on ferrocene based sol-gel sensors are available [26, 27, 28]. Here, Fc-silane (see the top of ***Figure V-6***) comes to our consideration due to the problems of mediator immobilization through electrodepostion as demonstrated above. We expect Ferrocene functionalized with silane could improve mediator immobilization through electrodeposition. As previously, the first tests have been performed on the basis of drop-coated sol-gel film before to consider electrodeposition.

3.1 Co-immobilization in drop-coated sol-gel film

3.1.1 Effect of GPS on Fc-silane immobilization

Fc-silane serves as co-condensation precursors to functionalize the sol-gel films. One drawback of this Fc-silane was the limited solubility in the sol and the limited control on the quantity. ***Figure V-6*** shows a comparison of silane functionalized ferrocene immobilization in the presence and absence of GPS. In the absence of GPS (***Figure V-6A***), a well-defined oxidation/reduction peak coming from ferrocene was observed, but even if its stability on multiple potential scanning is improved in comparison with Fc-PEI, the long term stability was still not satisfactory. In the presence of GPS, the stability of the electrochemical response upon multisweep was further improved (***Figure V-6B***), and could be maintained on several potential scans without degradation. As previously discussed, GPS as additive in TEOS sol-gel matrix can greatly enhance the stability of the assembly.

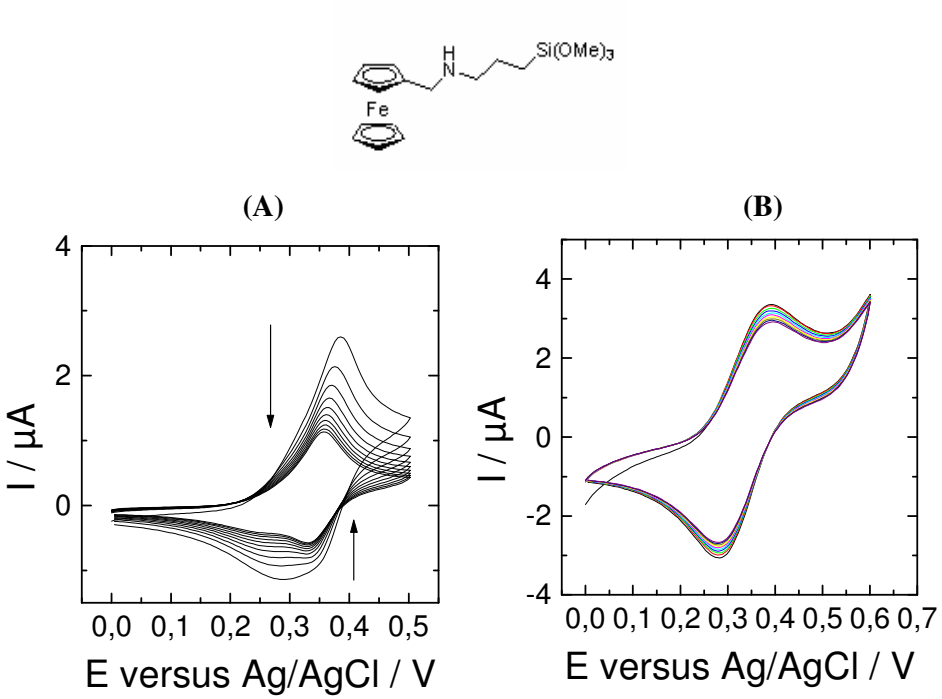

Figure V-6. *Cyclic voltammograms recorded with a GCE modified by drop-coated (A) TEOS/Fc-silane/PEI;(B) TEOS/GPS /Fc-silane/PEI film in the 0.1 M Tris-HClO_4 buffer (pH 9) at a scan rate of 50 mV/s, scan cycle, 10.*

3.1.2 Co-immobilization of Fc-silane, DSDH, DI and cofactor

The ferrocene-silane compound has been then associated with the other components of the reagentless device. First, a sol solution with Fc-silane as co-condensation precursors was prepared, then, GPS functionalized cofactor, DSDH and diaphorase were introduced into this

sol and drop-coated on GCE. ***Figure V-7A*** shows that it worked quite nicely with a well defined reversible electrochemical signal of ferrocene (plain line). It was found that the oxidation peak increase in the presence of 7 mM D-sorbitol and the reduction peak disappeared at the same time (dashed line). ***Figure V-7B*** shows amperometric responses of the modified electrode to D-sorbitol in a stirred solution. An increasing electrocatalytic response was observed upon addition of D-sorbitol in stirred solution. The immobilized ferrocene silane could transfer efficiently electron between the diaphorase and electrode for the catalytic oxidation of NADH.

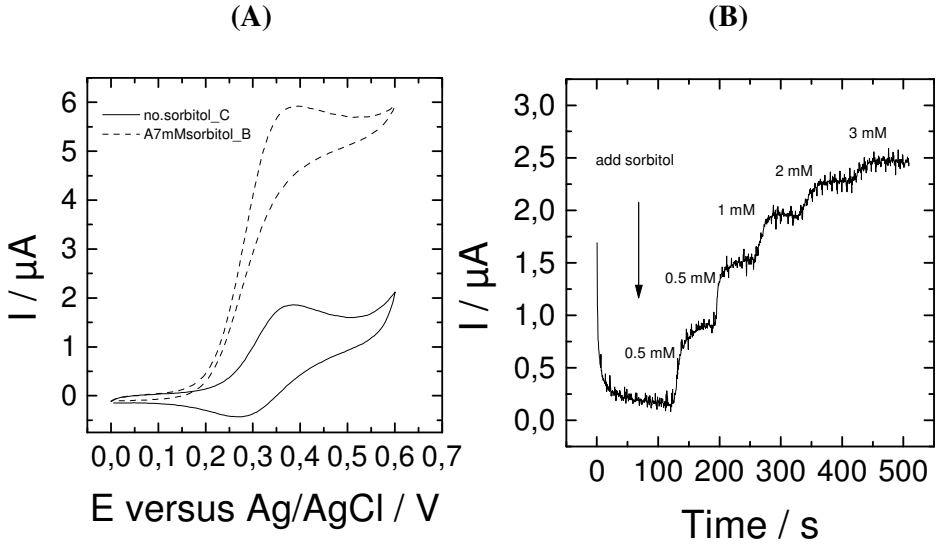

Figure V-7*. Cyclic voltammograms recorded with a GCE modified by drop-coated TEOS/GPS /Fc-silane/PEI/DSDH/DI/NAD-GPS film in the absence and in the presence of 7 mM D-sorbitol. Potential scan rate: 50 mV/s. (B) Amperometric responses recorded at an applied potential of 0.4 V to successive additions of different concentration of D-sorbitol in 0.1 M Tris-$HClO_4$ buffer (pH 9).*

3.2 Co-immobilization in electrogenerated sol-gel film

3.2.1 Immobilization of Fc-silane in electrodeposited sol-gel thin film

Although several reports on silylated ferrocene derivatives immobilized on electrode surfaces are available [25, 26, 27, 28], most of them were prepared by drop-coating or spin-coating. To our knowledge, no work has been reported regarding ferrocene-silane derivatives

immobilization through electrochemically-assisted deposition of silica sol-gel thin films. Here, electrochemically-assisted deposition of sol-gel film was applied for ferrocene-silane immobilization. The films have been deposited by electrolysis at -1.3 V for 60 s with a sol containing TEOS, GPS and Fc-silane. ***Figure V-8*** shows cyclic voltammograms recorded with a GCE modified by TEOS/GPS/Fc-silane sol-gel film. The obtianed film displayed a well-defined oxidation/reduction peak coming from ferrocene, and this signal was stable on multiple potential without significant degradation. Ferrocene-silane can be immobilized in the sol-gel thin film through electrodeposition

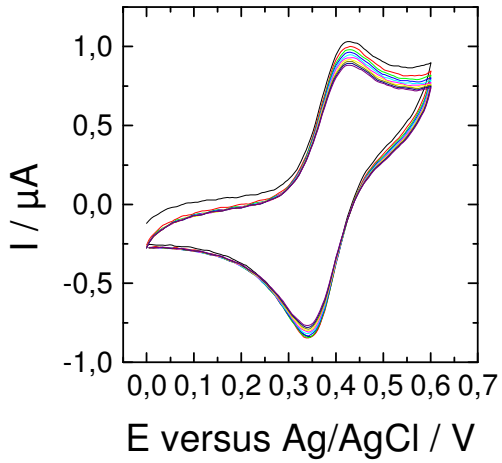

Figure V-8*. Cyclic voltammograms recorded with a GCE modified by electrodeposited TEOS/GPS/PEI/Fc-silane film in the 0.1 M Tris-$HClO_4$ buffer (pH 9) at a scan rate of 50 mV/s, scan cycle, 10. Films have been deposited by electrolysis at -1.3 V for 60 s with a TEOS/GPS sol with Fc-silane as co-condensation precursors.*

3.2.2 Co-immobilization in electrodeposited sol-gel thin film

Figure V-9 shows cyclic voltammograms recorded with a GCE modified by electrodeposited sol-gel film prepared with TEOS, GPS and Fc-silane and containing DSDH, DI and NAD-GPS. In the absence of D-sorbitol, the well reversible electrochemical signal of ferrocene was observed. However, the addition of D-sorbitol in the solution did not induce any increase of the anodic current.

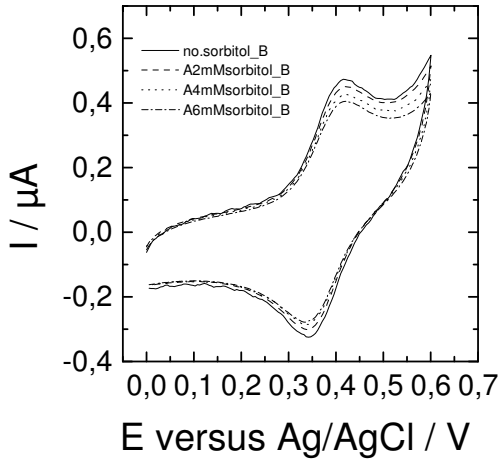

***Figure V-9**. Electrochemical response of glassy carbon electrode modified by TEOS/GPS /Fc-silane/PEI/DSDH/DI/NAD-GPS film in the absence and in the presence of D-sorbitol from 2 to 8 mM. Films have been deposited by electrolysis at -1.3 V for 60 s with a TEOS/GPS/Fc-silane sol containing DSDH, DI and NAD-GPS. Cyclic voltammograms have been performed at 50 mV/s in 0.1 M Tris-$HClO_4$ buffer.*

Good catalytic characteristic to D-sorbitol oxidation has been indicated in previous experiments with both proteins and cofactor immobilized in the electrodeposited sol-gel layer (Chapter IV section 3). In order to analyse this negative result, a similar film has been prepared without immobilized NAD^+ (*TEOS/GPS/Fc-silane/PEI/DSDH/DI/NAD-GPS*) (***Figure V-10).*** In this experiment, the enzyme and the mediator were co-immobilized on the electrode surface, and the cofactor was introduced into the solution before electrochemical experiments. In the absence of D-sorbitol, only the reversible electrochemical signal of ferrocene was observed. The addition of D-sorbitol into the solution does not lead to noticeable modification of the current response and no increase of peak current can be observed at the potential of NADH oxidation. Obviously, the co-immobilization of the enzymes and mediator in the sol-gel film by electrodepostion does not exhibit electrochemically detectable activity. The communication between of immobilized ferrocene and diaphorase was not sufficient to allow electro-catalysis. The different gel texture expected for film obtained by evaporation (drop-coating) or electrodeposition could explain the difference observed between these two kinds of electrode.

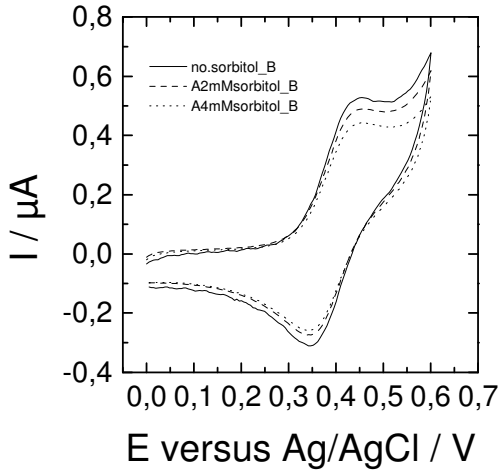

***Figure V-10**. Electrochemical response of glassy carbon electrode modified by TEOS /GPS /Fc-silane/PEI/DSDH/DI film in the absence and in the presence of D-sorbitol from 2 to 4mM. Films have been deposited by electrolysis at -1.3 V for 60 s. Cyclic voltammograms have been performed at 50 mV/s in 0.1 M Tris-$HClO_4$ buffer containing 1mM NAD^+.*

The co-immobilization of dehydrogenase, cofactor and electron mediator (Fc-PEI or Fc-silane) in sol-gel matrix by drop-coating was successful. However, such co-immobilization by by using electrogenerated sol-gel thin films was not possible. For Fc-PEI, no electrochemical signal of ferrocen was observed after the immobilization by electrodepostion. The incorporation of ferrocene in the electrogenerated sol-gel film could be improved by using Fc-silane, but no electrocatalysis was observed. These negative results obtained with ferrocene species in sol-gel electrodeposition led us to use different redox polymer for improving the connection between diaphorase and the electrode surface. Due to electrochemical reversibility, high electron transfer rate constant and stability of the Os-complexes, Osmium polymer has been recently proposed for such application and has been tested here.

4. Os-polymer as co-immobilized mediator

Flexible osmium redox polymers attracted the attention of a number of researchers due to the efficient electron shuttling properties combined with the polymeric structure, promoting a stable adsorption, as well as a possibility to immobilize the enzyme into multiple layers [29, 30] on the electrode surface. Osmium polymers can serve as mediator for a wide range of oxidases to fabricate biosensor, such as, glucose oxidase [31], lactate oxidase [32] and alcohol oxidase [33]. Osmium polymer as mediator can also be used to fabricate dehydrogenase

biosensor in combination with diaphorase [34, 35]. The principle of this mediator can be schematized as follows:

$$NADH + 2\,Os^{3+} \xrightarrow{DI} NAD^{+} + 2\,Os^{2+}$$

$$Os^{2+} \xrightarrow{electrode} Os^{3+} + e^{-}$$

The produced NADH is reoxidized to NAD^+ by DI with the concomitant reduction of the oxidized mediator (Os^{3+}) to the reduced mediator (Os^{2+}), which in turn is successively reoxidized at the electrode.

4.1 Co-immobilization in drop-coated sol-gel film

4.1.1 Effect of GPS on Os-polymer immobilization

One knows from literatures, osmium polymers as mediators have been immobilized on electrode surface to develop reagentless dehydrogenase biosensors. Riccarda et al. reported a biosensor based on glucose dehydrogenase (GDH) and diaphorase (DI) co-immobilized with NAD^+ into a carbon nanotube paste (CNTP) electrode modified with an osmium functionalized polymer [34]. The carbon nanotubes could be wrapped up in the Os-polymer molecules when they are mixed together in the paste and this combination could improve the transfer of electrons between the mediator and the electrode material itself. Olha et al. developed reagentless amperometric formaldehyde-selective biosensors based on the recombinant yeast formaldehyde dehydrogenase. In this method, the polymer layers simultaneously served as a matrix for keeping the negatively charged cofactors and glutathione in the bioactive layer [36].

Here, we tested four kinds of synthesized Os-polymer (see ***Figure II-2***) which were introduced into sol-gel matrix to construct the mediator modified electrode. All of them display similar electrochemical behaviours in the sol-gel matrix, so we only show the results of **compound 1** in this section. ***Figure V-11A*** shows cyclic voltammograms recorded with a GCE modified by TEOS based sol-gel film containing the Os-polymer. A well-defined oxidation/reduction peak coming from osmium could be observed, but it was not stable on multiple potential scan due to the low stability of the assembly. ***Figure V-11B*** shows cyclic voltammograms recorded with a GCE modified by a sol-gel prepared with TEOS and GPS

and containing the Os-polymer. As it was observed previously with Fc-PEI, the presence of GPS greatly improves the stability of the electrochemical response upon multisweep cyclic voltammograms, the signal being maintained several potential scans without significant degradation. We suppose that GPS helps to stabilize the redox polymer (Fc-PEI and Os-polymer) in the sol-gel environment. It also provides an improved electrochemical stability to the assembly.

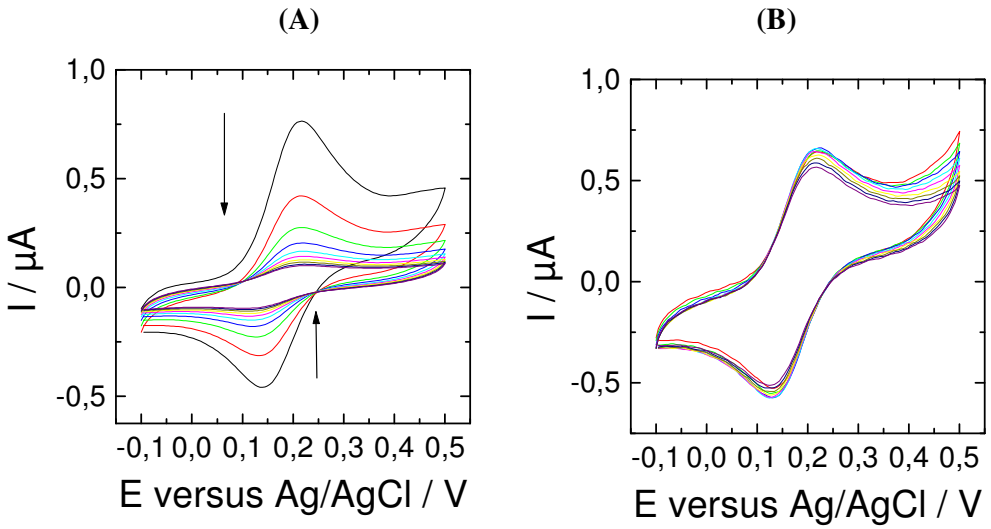

Figure V-11. *Cyclic voltammograms recorded with a GCE modified by drop-coated (A) TEOS/PEI/Os-polymer;(B) TEOS/GPS/PEI/Os-polymer film in the 0.1 M Tris-HCl buffer (pH 9) at a scan rate of 50 mV/s, scan cycle, 10.*

4.1.2 Immobilization of DI

The catalytic characteristic of the immobilized osmium was evaluated through the simple co-encapsulation of osmium and diaphorase. ***Figure V-12*** shows the typical electrocatalytic response of the *TEOS/GPS/PEI/Os-polymer/DI* film to NADH. In the absence of NADH, the reversible electrochemical signal of osmium was observed. The addition of 0.3 mM NADH induced a modification of the electrochemical response, the anodic current increased while the cathodic signal disappeared, and the anodic peak current continued to increase with the NADH concentration. Diaphorase kept good catalytic characteristic toward NADH inside the sol-gel film, and the immobilized osmium can efficiently transfer the electron between the electrode and the diaphorase.

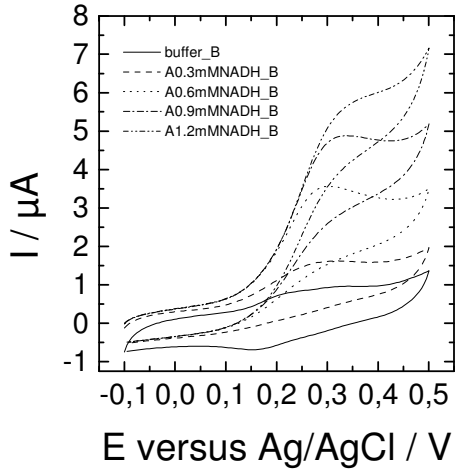

***Figure V-12**. Cyclic voltammograms recorded with a GCE modified by drop-coated TEOS/GPS/PEI/Os-polymer/DI film in the absence and presence NADH from 0.3 to 1.2mM. All cyclic voltammograms have been performed in Tris-HCl buffer (pH 9) at a scan rate of 50 mV/s.*

4.1.3 Co-immobilization of Os-polymer, DSDH, DI and cofactor

The co-encapsulation of osmium polymer, GPS functionalized cofactor (NAD-GPS), DSDH and diaphorase was evaluated with a drop-coated sol-gel film. ***Figure V-13*** shows the electrochemical response of the film to the addition of D-sorbitol in solution. These results are comparable to the result obtained with Fc-PEI. The oxidation of D-sorbitol by DSDH leads to the production of NADH inside the film. NADH reacts with diaphorase and the electrochemically generated NAD^+ and osmium species that can be re-oxidized in the electrocatalytic scheme. The electrocatalytic current increases with the addition of D-sorbitol from 2 to 6 mM. The co-immobilization of DSDH, DI, osmium polymer and NAD-GPS in sol-gel matrix does not prevent the efficient communication between them. NAD-GPS keep enough mobility to reach the enzymatic center of dehydrogenase, the dehydrogenase can catalyst the oxidation of D-sorbitol, and the DI/Osmium can decrease the overpotential of NADH detection for the smooth regeneration of the cofactor.

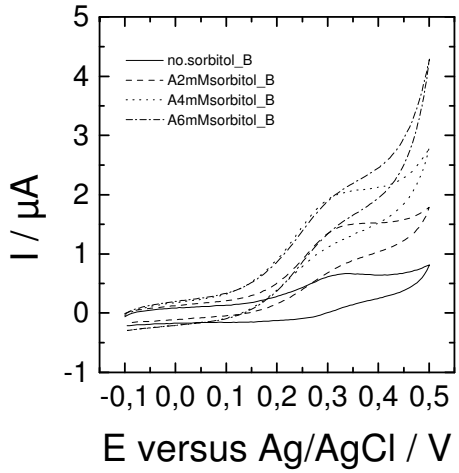

Figure V-13. *Cyclic voltammograms recorded with a GCE modified by drop-coated TEOS/GPS/PEI/Os-polymer/DSDH/DI/NAD-GPS film in the absence and presence D-sorbitol from 2 to 6mM. All cyclic voltammograms have been performed in Tris-HCl buffer (pH 9) at a scan rate of 50 mV/s.*

4.2 Co-immobilization in electrogenerated sol-gel film

4.2.1 Immobilization Os-polymer in electrodeposited sol-gel thin film

The encapsulation of Os redox polymer inside the electrodeposited silica gel has finally been investigated. ***Figure V-14*** shows cyclic voltammograms recorded with a GCE modified by electrodeposited TEOS/GPS sol-gel film containing Os-polymer. No electrochemical signal of osmium can be observed in the cyclic voltammograms, so that this way of sol-gel film formation does not seem to be an adequate strategy for Os-polymer immobilization.

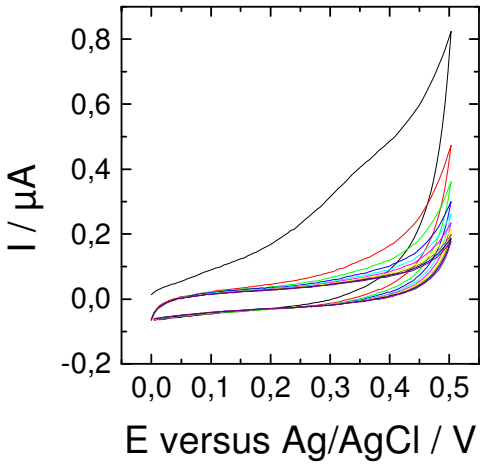

Figure V-14. *Cyclic voltammograms recorded with a GCE modified by electrodeposited TEOS/GPS/PEI/Os-polymer in the 0.1 M Tris-HCl buffer (pH 9) at a scan rate of 50 mV/s, scan cycle, 10. Films have been deposited by electrolysis at -1.3 V for 60 s with a TEOS/GPS sol containing Os-polymer.*

4.2.2 Co-immobilization in electrodeposited sol-gel thin film

The encapsulation of DSDH, DI, cofactor and Os redox polymer inside the electrodeposited silica gel led to a similar result and no visible electrochemical signals of Os neither before nor after the addition of D-sorbitol was observed (***Figure V-15***).

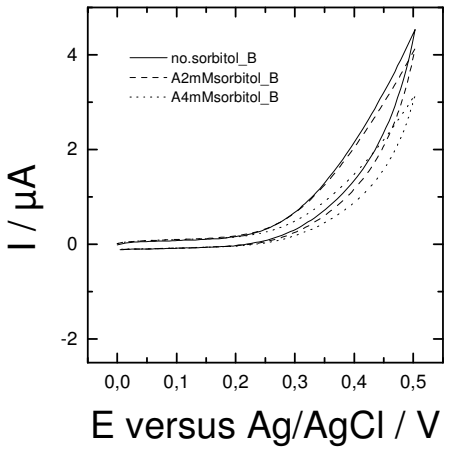

Figure V-15*. Electrochemical response of glassy carbon electrode modified by TEOS/GPS/PEI/Os/NAD-GPS/DSDH/DI film in the absence and in the presence of D-sorbitol from 2mM to 4mM. Films have been deposited by electrolysis at -1.3 V for 60 s with a TEOS/GPS sol containing DSDH, DI, NAD-GPS and Os-polymer. Cyclic voltammograms have been performed at 50 mV/s in 0.1 M Tris-HCl buffer.*

The conclusion for Os-polymer is the same as for ferrocene species. Co-immobilization of all components (dehydrogenase, cofactor and electron mediator) in the sol-gel films can be successfully achieved by using drop-coating. However, the co-immobilization by using electrogenerated sol-gel thin films was not so successful due to the same limitation with the mediator immobilization.

5. Conclusion

A series of strategies for dehydrogenase, cofactor and electron mediator co-immobilization in sol-gel thin films have been developed. First of all, ferrocene species (Fc-PEI and Fc-silane) or osmium polymers as mediators between diaphorase and the electrode have been successfully immobilized on the electrode within the sol-gel film, which allows the smooth regeneration of the cofactor. The importance of introducing GPS as an additive into the TEOS sol-gel-derived films has been pointed out with respect to mediator immobilization. GPS can greatly enhance the stability of the electrochemical response. Finally, successful co-

immobilization of all components (dehydrogenase, cofactor and electron mediator) in sol-gel films was achieved by using drop-coating. All the components were able to communicate inside the silica gel layer for efficient electro-catalytic oxidation of D-sorbitol. The electrode displayed good stability under stirring for more than 14 hours. However, such co-immobilization applied to electrochemically-assisted deposition of sol-gel thin films was not successful, revealing limitation with the mediator immobilization. An adequate distribution of the mediator in the sol-gel film could be achieved by drop-coating, allowing an efficient communication between the electrode and the protein. However, using the same sol, film prepared by electrodeposition did not display this property, and the electrocatalysis (for Fc-silane) or even the oxidation/reduction of the mediator (for Fc-PEI and osmium polymer) was not observed.

References

[1] Gorton, L.; Bartlett, P.N. Bioelectrochemistry: Fundamentals, Experimental techniques and Applications, Ed. P.N. Bartlett, John Wiley & Sons Ltd, Chichester, UK, 2008, 157-198.

[2] Ogino, Y.; Takagi, K.; Kano, K.; Ikeda, T., Reactions between diaphorase and quinone compounds in bioelectrocatalytic redox reactions of NADH and NAD^+. *J. Electroanal. Chem.* **1995**, 396(1-2), 517-524.

[3] Kashivagi, Y.; Osa, T., Electrocatalytic oxidation of NADH on thin poly(acrylic acid) film coated graphite felt electrode coimmobilizing ferrocene and diaphorase. *Chem. Lett.* **1993**, 677-680.

[4] Antiochia, R.; Gorton, L., Development of a carbon nanotube paste electrode osmium polymer-mediated biosensor for determination of glucose in alcoholic beverages. *Biosens. Bioelectron.* **2007**, *22(11)*, 2611-2617.

[5] Antiochia, R.; Cass, A. E. G.; Palleschi, G., Purification and sensor applications of an oxygen insensitive, thermophilic diaphorase. *Anal. Chim. Acta* **1997**, *345(1-3)*, 17-28.

[6] Polska, K.; Fiedurek, J.; Radzki, S., Bioencapsulation of biologically active compounds in matrixes obtained by sol-gel method and its application. *Biotecnologia* **2007**, *1*, 77-95.

[7] Gupta, R.; Chaudhury, N. K., Entrapment of biomolecules in sol-gel matrix for applications in biosensors: problems and future prospects. *Biosens. Bioelectron.* **2007**, *22(11)*, 2387-2399.

[8] Xu, Z.; Chen, X.; Dong, S., Electrochemical biosensors based on advanced bioimmobilization matrices. *Trends Anal. Chem.* **2006**, *25(6)*, 899-908.

[9] Williams, A. K.; Hupp, J. T., Sol-gel-encapsulated alcohol dehydrogenase as a versatile, environmentally stabilized sensor for alcohols and aldehydes. *J. Am. Chem. Soc.* **1998**, *120(18)*, 4366-4371.

[10] Yang, S; Lu, Y; Atanossov, P; Wilkins, E; Long, X., Microfabricated glucose biosensor with glucose oxidase entrapped in sol - gel matrix. *Talanta* **1998**, *47(3)*, 735-43.

[11] Lin C.; Shih C.; Chau L., Amperometric L-lactate sensor based on sol - gel processing of an enzyme -linked silicon alkoxide. *Anal. Chem.* **2007**, *79(10)*, 3757-3763.

[12] Salimi, A.; Pourbeyram, S.; Haddadzadeh, H., Sol-gel derived carbon ceramic composite electrode containing a ruthenium complex for amperometric detection of insulin at physiological pH. *J. Electroanal. Chem.* **2003**, *542*, 39-49.

[13] Thenmozhi, K.; Narayanan, S. S., Electrocatalytic reduction of nitrite ion on a toluidine blue sol-gel thin film electrode derived from 3-aminopropyl trimethoxy silane. *Electroanalysis* **2007**, *19(22)*, 2362-2368.

[14] Thenmozhi, K.; Narayanan, S. S., Surface renewable sol-gel composite electrode derived from 3-aminopropyl trimethoxy silane with covalently immobilized thionin. *Biosens. Bioelectron.* **2007**, *23(5)*, 606-612.

[15] Wang, J.; Collinson, M M., Electrochemical characterization of inorganiclorganic hybrid films prepared from ferrocene modified silanes. *J. Electroanal. Chem.* **1998**, *455(1-2)*, 127-137.

[16] Frew, J. E.; Hill, H. A., Electrochemical biosensors. *Anal. Chem.* **1987**, *59(15)*, 933A-944A.

[17] Ryabov, A. D.; Amon, A.; Gorbatova, R. K.; Ryabova, E. S.; Gnedenko, B. B., Mechanism of a "jumping off" ferricenium in glucose oxidase-D-glucose-ferrocene micellar electrochemical systems. *J. Phys. Chem.* **1995**, *99(38)*, 14072-7.

[18] Liu, A.; Kashiwagi, Y.; Anzai, J., Polyelectrolyte multilayer films containing ferrocene: Effects of polyelectrolyte type and ferrocene contents in the film on the redox properties. *Electroanalysis* **2003**, *15(13)*, 1139-1142.

[19] Hodak, J.; Etchenique, R.; Calvo, E. J.; Singhal, K.; Bartlett, P. N., Layer-by-Layer Self-Assembly of Glucose Oxidase with a Poly(allylamine)ferrocene Redox Mediator. *Langmuir* **1997**, *13(10)*, 2708-2716.

[20] Zheng, H.; Zhou, J.; Zhang, J.; Huang, R.; Jia, H.; Suye, S., Electrical communication between electrode and dehydrogenase by a ferrocene-labeled high molecular-weight cofactor derivative: application to a reagentless biosensor. *Microchim Acta* **2009,** 165(1-2), 109–115.

[21] Chiorcea-Paquim, A.; Pauliukaite, R.; Brett, C. M. A.; Oliveira-Brett, A. M., AFM nanometer surface morphological study of in situ electropolymerized neutral red redox mediator oxysilane sol-gel encapsulated glucose oxidase electrochemical biosensors. *Biosens. Bioelectron.* **2008**, *24(2)*, 297-305.

[22] Barsan, M. M.; Klincar, J.; Batic, M.; Brett, C. M. A., Design and application of a flow cell for carbon-film based electrochemical enzyme biosensors. *Talanta* **2007**, *71(5)*,

1893-1900.

[23] Lev, O.; Wu, Z.; Bharathi, S.; Glezer, V.; Modestov, A.; Gun, J.; Rabinovich, L.; Sampath, S., Sol-Gel Materials in Electrochemistry. *Chem. Mater.* **1997**, *9(11)*, 2354-2375.

[24] Wang, J.; Pamidi, P. V. A., Sol-Gel-Derived Gold Composite Electrodes. *Anal. Chem.* **1997**, *69(21)*, 4490-4494.

[25] Audebert, P.; Cerveau, G.; Corriu, R. J. P.; Costa, N., Modified electrodes from organic-inorganic hybrid gels formed by hydrolysis-polycondensation of some trimethoxysilylferrocenes. *J. Electroanal. Chem.* **1996**, *413(1-2)*, 89-96.

[26] Chut, S. L.; Li, J.; Tan, S. N., Reagentless amperometric determination of hydrogen peroxide by silica sol-gel modified biosensor. *Analyst* **1997**, *122(11)*, 1431-1434.

[27] Pandey, P. C.; Upadhyay, S.; Pathak, H. C. A new glucose sensor based on encapsulated glucose oxidase within organically modified sol-gel glass. *Sens. Actuators B* **1999**, *B60(2-3)*, 83-89.

[28] Pandey, P. C.; Upadhyay, S.; Pathak, H. C.; Tiwari, Ida; Tripathi, V. S. Studies on glucose biosensors based on nonmediated and mediated electrochemical oxidation of reduced glucose oxidase encapsulated within organically modified sol-gel glasses. *Electroanalysis* **1999**, *11(17)*, 1251-1258.

[29] Heller, A., Electron-conducting redox hydrogels: design, characteristics and synthesis. *Curr. Opin. Chem. Biol.* **2006**, *10(6)*, 664-672.

[30] Heller, A.; Feldman, B., Electrochemical Glucose Sensors and Their Applications in Diabetes Management. *Chem. Rev.* **2008**, *108(7)*, 2482-2505.

[31] Park, T.; Iwuoha, E. I.; Smyth, M. R.; MacCraith, B. D., Sol-gel-based amperometric glucose biosensor incorporating an osmium redox polymer as mediator. *Anal. Commun.* **1996**, *33(8)*, 271-273.

[32] Park, T.; Iwuoha, E. I.; Smyth, M. R.; Freaney, R.; McShane, A. J., Sol-gel based amperometric biosensor incorporating an osmium redox polymer as mediator for detection of L-lactate. *Talanta* **1997**, *44(6)*, 973-978.

[33] Alpeeva, I. S.; Vilkanauskyte, A.; Ngounou, B.; Csoeregi, E.; Sakharov, I. Y.; Gonchar, M.; Schuhmann, W., Bi-Enzyme Alcohol Biosensors Based on Genetically Engineered Alcohol Oxidase and Different Peroxidases. *Microchim. Acta* **2005**, *152(1-2)*, 21-27.

[34] Antiochia, R.; Gorton, L., Development of a carbon nanotube paste electrode osmium polymer-mediated biosensor for determination of glucose in alcoholic beverages.

Biosens. Bioelectron. **2007**, *22(11)*, 2611-2617.

[35] Nikitina, O.; Shleev, S.; Gayda, G.; Demkiv, O.; Gonchar, M.; Gorton, L.; Csoeregi, E.; Nistor, M., Bi-enzyme biosensor based on NAD^+- and glutathione-dependent recombinant formaldehyde dehydrogenase and diaphorase for formaldehyde assay. *Sens. Actuators B* **2007**, *B125(1)*, 1-9.

[36] Demkiv, O.; Smutok, O.; Paryzhak, S.; Gayda, G.; Sultanov, Y.; Guschin, D.; Shkil, H.; Schuhmann, W.; Gonchar, M., Reagentless amperometric formaldehyde-selective biosensors based on the recombinant yeast formaldehyde dehydrogenase. *Talanta* **2008**, *76(4)*, 837-846.

Chapitre VI. Immobilisation du médiateur électrochimique sur les nanotubes de carbone et co-immobillisation avec une déshydrogénase et le cofacteur NAD^+

Dans ce chapitre, différentes stratégies ont été développées pour élaborer un composite sol-gel/nanotubes de carbone permettant la co-immobilisation de la D-sorbitol déshydrogénase (DSDH), du cofacteur NAD^+ et du médiateur (et éventuellement de la diaphorase). Une configuration en bicouche a été utilisée consistant à immobiliser dans un premier temps les nanotubes de carbone fonctionnalisés et à déposer ensuite la couche mince sol-gel par évaporation du sol ou par électrogénération. Une attention particulière a été donnée à la co-immobilisation par électrochimie des différents éléments du système bioélectrocatalytique dans la mesure où cet objectif n'avait pu être atteint par électrogénération en une étape (chapitre V). Les nanotubes de carbones à parois simples (SWCNT) ou multiples (MWCNT) ont été fonctionnalisés par quatre protocoles différents pour leur donner des propriétés catalytiques intéressantes pour l'oxydation de NADH (ou la réduction du NAD^+) ; Ces protocoles sont (1) le traitement des nanotubes par micro-ondes (*MWCNT-μW*), (2) l'électropolymérisation du vert de méthylène (*MWCNT-PMG*), (3) le recouvrement des nanotubes par un polymère de type polyacrylate portant des complexes d'osmium(III) (*MWCNT-Os*), et (4) adsorption des complexes d'un complexe de rhodium (III) à la surface de nanotubes de carbone à paroi simple. Les électrodes de carbone vitreux fonctionnalisées par ces nanotubes de carbone présentes de bonnes propriétés catalytiques pour l'oxydation de NADH (1 et 2) ou la réduction de NAD^+ (4), ou l'oxydation de NADH en présence de diaphorase (3). Les films sol-gel ont ensuite été déposés à la surface de ces nanotubes de carbone by évaporation du sol ou par électrogénération afin d'obtenir la co-immobilisation de la DSDH (et de la diaphorase quand nécessaire) et du cofacteur NAD^+.

Chapter VI. Mediator immobilization on carbon nanotubes and co-immobilization with dehydrogenase and cofactor

In this chapter, various bilayers strategies based on CNTs/sol-gel matrix are developed for the fabrication of reagent free devices in attempting to overcome the problems encountered with mediator immobilization through one step electrodepostion (chapter V). Carbon nanotubes (CNTs) have been functionalized by four different protocols in order to provide them catalytic properties for NADH (or NAD^+) detection; they include (1) micro-wave treatment (*MWCNTs-μW*), (2) electrochemical deposition of poly(methylene green) (*MWCNTs-PMG*), (3) wrapping with a polyacrylate polymer holding osmium(III) complexes (*MWCNTs-Os*), and (4) adsorption a Rh (III) complex on SWCNTs. GCE electrodes modified with these functionalized CNTs show good electrochemical properties and allow the direct electrocatalytic detection of NADH (1 and 2) or NAD^+ (4), or the detection of NADH in the presence of diaphorase (3). To the last configuration, a sol-gel thin film has been further deposited on the carbon nanotube layer by drop-coating or by electrochemically-assisted deposition for encapsulation of D-sorbitol dehydrogenase (and diaphorase when necessary) and co-immobilization of the NAD^+ cofactor.

1. Introduction

The direct oxidation or reduction of cofactor on a bare electrode requires high overpotential, and usually leads to enzymatically inactive NAD-dimers and serious side reactions. However, only reversible cofactors recycling can guarantee the reagentless aspect of the bioelectrocatalytic devices. In order to overcome these inherent difficulties, a common approach is to confine the mediator at the electrode surface to facilitate the interfacial electron transfer kinetics.

The mediators for the regeneration of NAD^+ are diverse. Several mediators such as quinones [1, 2], oxometalates [3], ruthenium complexes [4], phenazines [5, 6] and phenoxazines [7, 8] quinonoid redox dyes have been proposed for NAD^+ regeneration. Traditionally, the mediators were directly adsorbed, electropolymerized or covalently bound onto the electrode surface [9, 10, 11]. The mediators for the regeneration of NADH are relatively few. The best systems to date fulfilling these requirements are tris(2,2'-bipyridyl) rhodium complexes [12, 13, 14] and substituted or non substituted (2,2'-bipyridyl) (pentamethylcyclopentadienyl)-rhodium complexes [15], and some others [16]. The mechanism of this electrocatalytic process has been largely studied and the effect of various parameters (e.g., solution composition, temperature) has been discussed in the literature [17, 18]. However, it might be surprising that not much effort was made to immobilize these mediators in an electrocatalytically-active form and further use it with immobilized dehydrogenase.

During the last decades, carbon nanotubes (single- or multiwalled) have emerged as attractive materials in electroanalysis [19, 20]. Indeed they display attractive chemical stability, strong absorptive properties and excellent biocompatibility [21, 22]. CNTs-based electrodes are known to decrease the overpotential for the oxidation of NADH, however, the extent of decrease is not sufficient for the selective detection and regeneration of cofactor [23]. Recently, Wooten, et al demonstrates that further decrease in the NADH overpotential can be achieved at CNTs that were activated by microwaving in concentrated nitric acid [24]. An alternative method of incorporation the mediators onto carbon nanotubes (CNTs) for NAD^+ regeneration have attracted considerable study. A number of mediators such as toluidin blue [25], nile blue [26, 27], meladola blue [28], methylene green (MG) [29] and an osmium polymer [30] have been immobilized by adsorption onto CNTs, resulting in a remarkable improvement of electocatalysis toward NADH oxidation. Another approach to form stable films of mediators on electrode surfaces, is to use electropolymerization which has many

advantages including selectivity, sensitivity and homogeneity in electrochemical deposition, strong adherence to electrode surface and chemical stability of the film [31, 32, 33].

CNTs/mediator composite as electrode materials has been already explored for the construction of dehydrogenase-based biosensors [34]. Of particular interest is the report by Yan et al which described the assembly of integrated, electrically contacted $NAD(P)^+$-dependent enzyme-SWCNT electrodes [27]. The SWCNTs were functionalized with Nile Blue, and the affinity complexes of dehydrogenase with cofactor were crosslinked with glutaric dialdehyde and the biomolecule-functionalized SWCNT materials were deposited on glassy carbon electrodes. This is the unique example of reagentless device based on the combination of dehydrogenase and carbon nanotubes.

The combination of sol-gel material and carbon nanotubes has also been considered for electroanalytical applications [35]. Recently, co-immobilization of lactate dehydrogenase and functionalized carbon nanotubes in sol-gel has been developed for biosensor [36]. The nanocomposite was prepared by the sol-gel process incorporating a redox mediator and carbon nanotubes, which was mixed with enzyme solution in a certain ratio for enzyme encapsulation. To date, and to our knowledge, no attempt was made to use sol-gel thin film to co-immobilized dehydrogenase and NAD^+ cofactor on the electrode surface of CNTs/mediator composite. Moreover, electrochemically-assisted deposition of sol-gel biocomposite on carbon nanotube assembly is also a new approach.

We have investigated here various strategies for the elaboration of a reagentless sensor based on NAD-dependant dehydrogenase using the electrochemically-assisted deposition of the sol-gel biocomposite on carbon nanotubes (CNTs). CNTs have been functionalized by three different protocols in order to provide them catalytic properties for NADH detection. These protocols are (1) micro-wave treatment (*MWCNTs-μW*), (2) electrochemical deposition of poly(methylene green) (*MWCNTs-PMG*), and (3) wrapping with a polyacrylate polymer holding osmium(III) complexes (*MWCNTs-Os*). The catalytic properties of the functionalized carbon nanotubes have been first checked by covering them with an additional drop-coated sol-gel layer before use as support for electrodeposited sol-gel films. The electrochemical response of the biocomposite containing the immobilized protein has been compared when NAD^+ was simply introduced in the solution or when it was chemically attached to the sol-gel matrix (*i.e.,* reagentless device). The study has been developed with the enzyme D-sorbitol dehydrogenase and D-sorbitol was used as a model analyte. Immobilization of Rh (III) complex on SWCNTs has also been studied.

2. Deposition sol-gel film at microwaved MWCNTs (*GCE/MWCNTs-μW*)

A recent report by Wooten et al. described that microwave treatment of MWCNTs resulted in a dramatic shift of the oxidative peak potential of NADH (E_{NADH}) to a lower value, from +0.4 V to about 0 V [24]. The efficient system could be interesting to be further used in combination with immobilized dehydrogenase and cofactor to develop the reagentless device.

2.1 Electrocatalytic oxidation of NADH at *GCE/MWCNTs-μW*

Figure VI-1A shows the cyclic voltammograms recorded at a glassy carbon electrode modified with the original (i.e., not treated) MWCNTs. Before addition of NADH, no electrochemical signal could be observed between -0.4 and +0.6 V. A well defined voltammetric signal with a peak potential located at ~ +0.4 V (versus Ag/AgCl reference electrode) appears when NADH was added to the solution. It corresponds to the electrochemical oxidation of the NADH cofactor on MWCNTs modified electrode. ***Figure VI-1B*** shows the cyclic voltammograms recorded at the glassy carbon electrode modified with acid-microwaved MWCNTs. A well defined voltammetric signal with a peak potential located at ~ 0 V appears when NADH was added to the solution and this signal increased with the NADH concentration. The microwaving of MWCNTs in acidic solution for 20 min resulted in a dramatic shift of the oxidative peak potential of NADH (E_{NADH}) to a lower value, from ~ +0.4 V to ~ 0 V (in agreement with previous observations [24]). The shift in E_{NADH} illustrated can be attributed to the redox mediation of NADH oxidation by surface quinones (Q) (formed during the microwave treatment).

$$Q + NADH + H^+ \rightarrow QH_2 + NAD^+ \quad (1)$$

which is followed by the recycling of quinone species on the surface of treated MWCNTs.

$$QH_2 \rightarrow Q + 2e^- + 2H^+ \quad (2)$$

Because reactions 1 and 2 are faster than the direct electrooxidation of NADH to NAD^+, the mediated process (1)-(2) allows conversion of the NADH to NAD^+ at less-positive potentials close to the formal potential of the Q/QH_2 redox couple (~ 0 V).

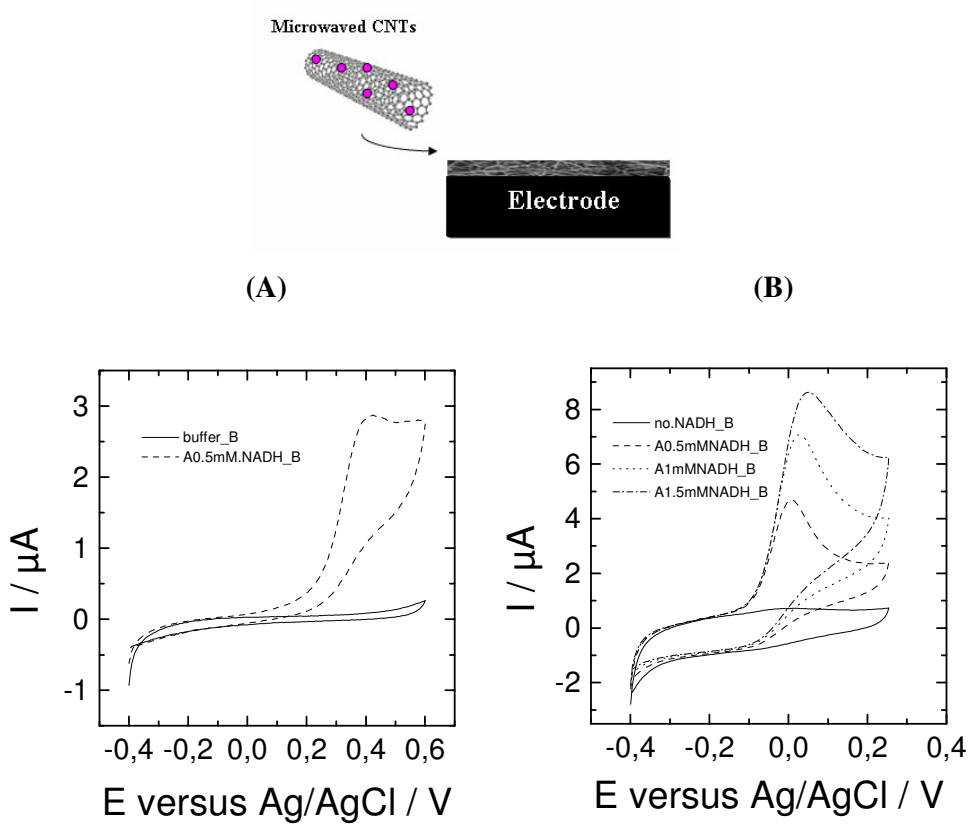

Figure VI-1. *Cyclic voltammograms recorded at (A) GCE/MWCNTs, (B) GCE/MWCNTs-µW in deoxygenated solutions with and without NADH. Measurements have been performed in 0.1 M Tris-HCl buffer (pH 9), Scan rate, 5 mV/ s.*

2.2 Importance of bilayers (drop-coated sol-gel film)

The efficient system was further used in combination with the sol-gel biocomposite. ***Figure VI-2A*** shows the electrochemical response of glassy carbon electrode modified by *chitosan/TEOS/MWCNTs-µW/PEI/DSDH* film. Here, the film was prepared in a rather simple way: simply mixing everything together and casting the solution on the GCE surface. It is shown that the addition of D-sorbitol into the solution led to noticeable modification of the current response around 0.8V. This signal is ascribed to the direct oxidation at GCE of NADH produced by the enzyme encapsulated into the film. This result indicates that MWCNTs in the sol-gel matrix display poor electrical properties and/or poor catalytic properties. The loss of electrocatalytic activity of MWCNTs-µW was possibly due to the deposition of insulating sol-gel material on the surface of the individual MWCNTs-µW during the film formation. A more

interesting result was obtained with *GCE/MWCNTs-µW* covered with an additional layer of sol-gel with encapsulated DSDH. It is shown in ***Figure VI-2B*** that the addition of D-sorbitol into the solution led to a significant current increase around 0.4V. So a dramatic shift of the oxidative peak potential of NADH (E_{NADH}) was obtained from +0.8 V (one layer) to +0.4 V (bilayer). More interesting thing is that the catalytic current increased 4 times with bilayer modified electrode in comparison with one layer modified electrode when in the presence of 2mM D-sorbitol, indicating that the bilayer assembly could display higher electroactive surface area. But despite the good electrochemical response, the microwaved MWCNTs did not display the expected electrocatalytic activity at 0V when covered by the sol-gel biocomposite layer.

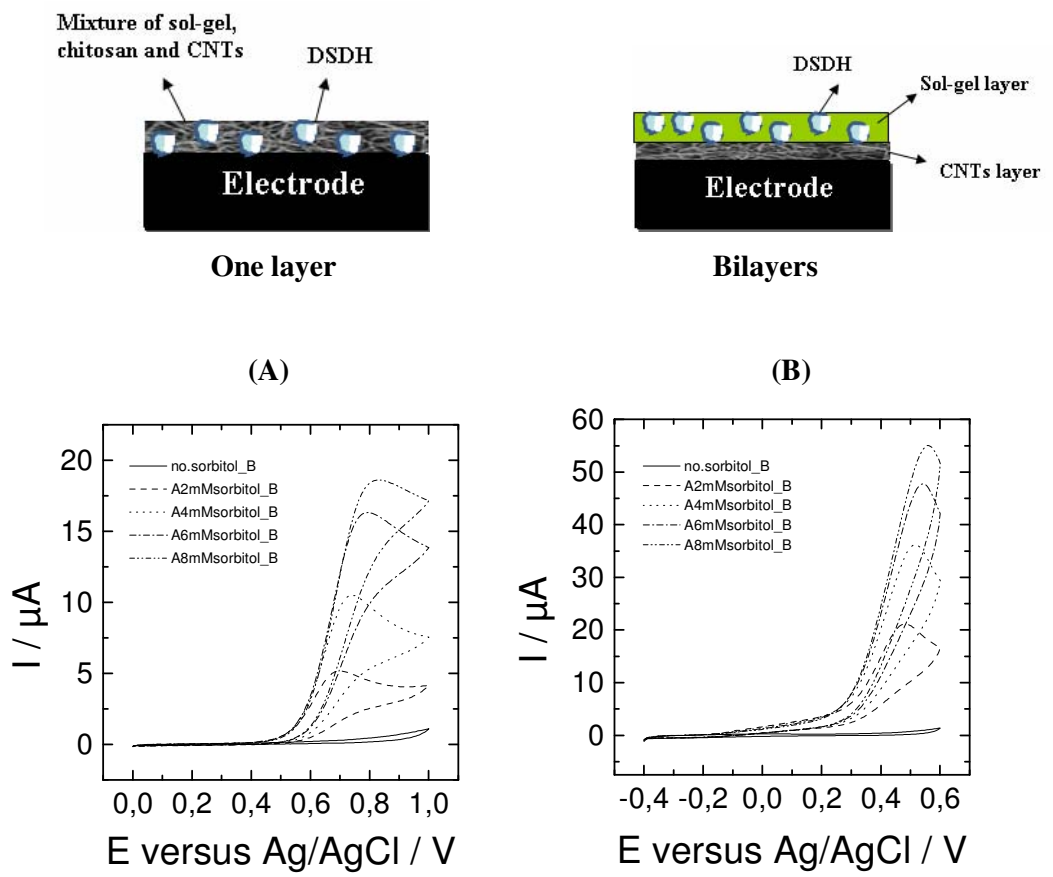

Figure VI-2. *Electrochemical response of (A) GCE/chitosan/TEOS/MWCNTs-µW/PEI/DSDH; (B) GCE/MWCNTs-µW&TEOS/PEI/DSDH in the absence and in the presence of D-sorbitol from 2 to 8 mM. Cyclic voltammograms have been performed at 5 mV/s in deoxygenated 0.1 M Tris-HCl buffer containing 1mM NAD^+.*

2.3 Electrodeposition of sol-gel thin films at *GCE/MWCNTs-µW*

2.3.1 Immobilization of DSDH in electrogenerated sol-gel thin film (cofactor in solution)

Electrochemically-assisted deposition of the sol-gel biocomposite has been applied here on a first layer of MWCNTs-µW. As a control experiment, ***Figure VI-3 A*** shows the electrochemical response obtained with a bare GCE directly modified by electrodeposited sol-gel layer with encapsulated DSDH (without the chitosan/MWCNTs-µW layer). A well-defined electrochemical response was observed at +0.8V in the presence of 6mM D-sorbitol. ***Figure VI-3 B*** shows its amperometric responses at different applied potential. No electrocatalytic response was obtained upon addition of D-sorbitol in stirred solution at +0.4 V (see curve a). Faintly visible electrocatalytic response started to be observed at +0.5V, and the optimal potential was found to be +0.8V. ***Figure VI-3 C*** shows the electrochemical response obtained with a GCE modified with a first MWCNTs-µW layer subsequently covered with an additional electrogenerated sol-gel layer with encapsulated DSDH (as deposited by electrolysis at -1.3 V for 60 s from a sol containing DSDH). A well-defined electrochemical response was observed increasing regularly by increasing the D-sorbitol concentration from 2 to 14 mM. The peak potential of this signal was located between +0.4 and +0.5 V, a potential higher than the one observed previously with GCE modified with acid-microwaved MWCNTs (***Figure VI-1B***). As observed with drop-coating film, the sol-gel electrodeposition disturbed significantly the electrocatalytic properties of the functionalized carbon nanotubes. But the potential for NADH oxidation is still lower than on GCE (~+0.7 V). The interesting were the peak current intensities, more than 10 times higher with microwaved MWCNTs modified GCE (35 µA for 6 mM, ***Figure VI-3 C***) than with bare GCE (3.2 µA for 6 mM, ***Figure VI-3 A***). The presence of MWCNTs on the glassy carbon electrode surface greatly improved the electrocatalytic efficiency of the sol-gel based bioelectrode by comparison with the bare GCE, but the benefit of the microwave treatment was lost. ***Figure VI-3 D*** shows the amperometric responses recorded at different applied potentials. The optimal applied potential was found to be in the range between +0.4 and +0.5 V whereas a loss in sensitivity by ca. 50 % was found when operating at +0.3 V. These experiments confirm the critical role of MWCNTs in both decreasing overpotential and increasing current response.

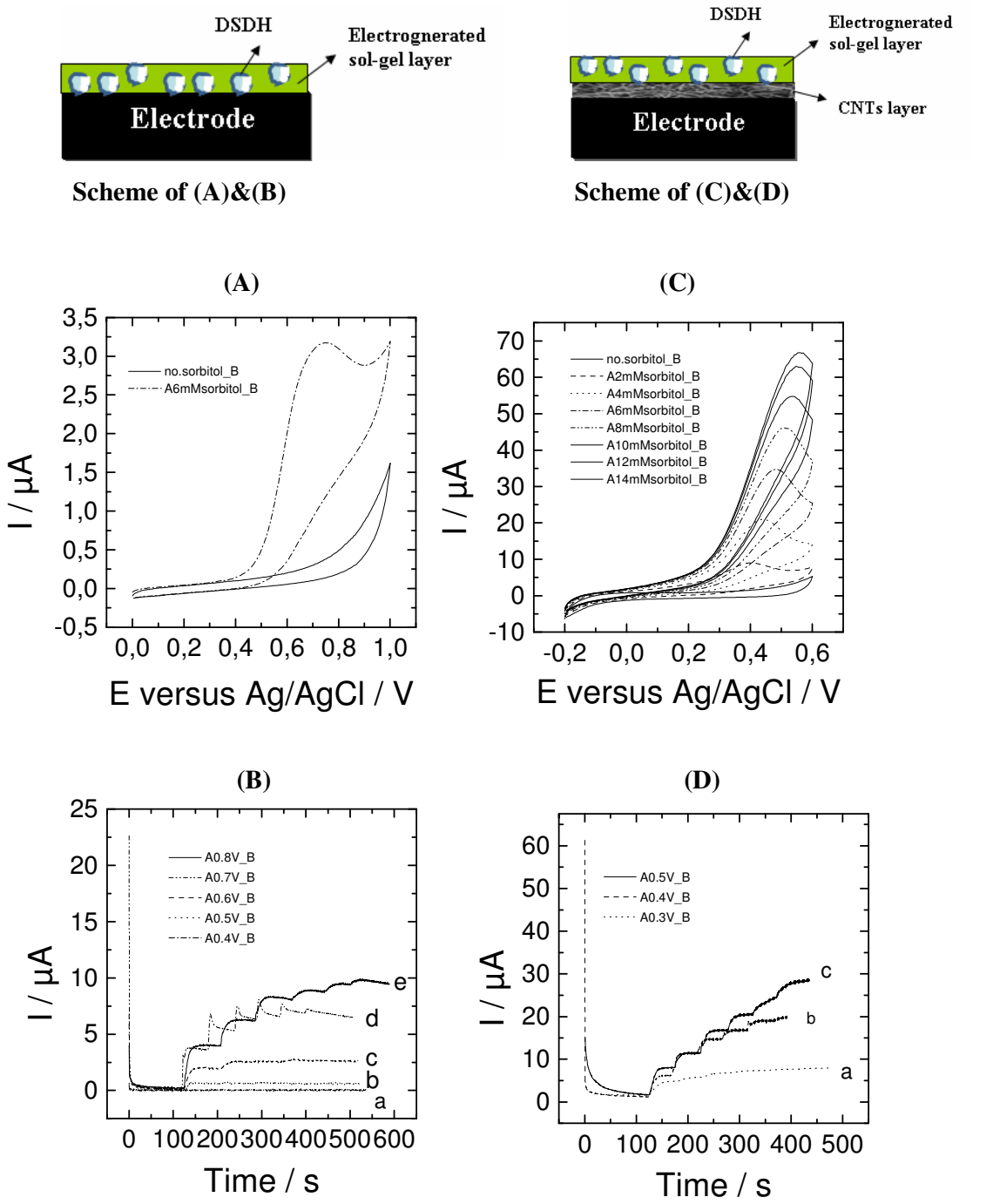

Figure VI-3. *(A) Electrochemical response of GCE/TEOS/PEI/DSDH in the absence and in the presence of 6mM D-sorbitol. (B) Amperometric responses recorded at an applied potential of (a) 0.4 V; (b) 0.5V; (c) 0.6V; (d) 0.7V; (e) 0.8V to successive additions of 1 mM sorbitol in the solution. (C) Electrochemical response of GCE/MWCNTs-µW &TEOS/PEI/DSDH in the absence and in the presence of D-sorbitol from 2 to 8 mM. (D) Amperometric responses recorded at an applied potential of (a) 0.3 V; (b) 0.4V; (c) 0.5V to successive additions of 1 mM sorbitol in the solution. All measurements have been performed in 0.1 M Tris-HCl buffer containing 1mM NAD^+. Cyclic voltammograms have been performed at 5 mV/s.*

2.3.2 Co-immobilization of DSDH and cofactor in electrogenerated sol-gel thin film

This efficient approach has been further used to develop a reagentless system (co-immobilization of DSDH and cofactor with MWCNTs-µW as mediator). ***Figure VI-4 A*** shows the cyclic voltammograms obtained with *GCE/MWCNTs-µW* covered with an additional electrodeposited sol-gel layer with encapsulated DSDH and NAD-GPS, which has been deposited by electrolysis at -1.3 V for 60 s with a sol containing both DSDH and NAD-GPS. It is shown that the addition of D-sorbitol into the solution did not lead to noticeable modification of the current response and no peak current could be observed at the potential of NADH oxidation (+0.4 V). To confirm the negative result, ***Figure VI-4 B*** shows the amperometric responses at an applied potential of +0.4 V. No electrocatalytic response was obtained upon addition of D-sorbitol in the stirred solution. The immobilized cofactor cannot communicate efficiently with the carbon nanotubes to allow effective regeneration of NADH back to NAD^+.

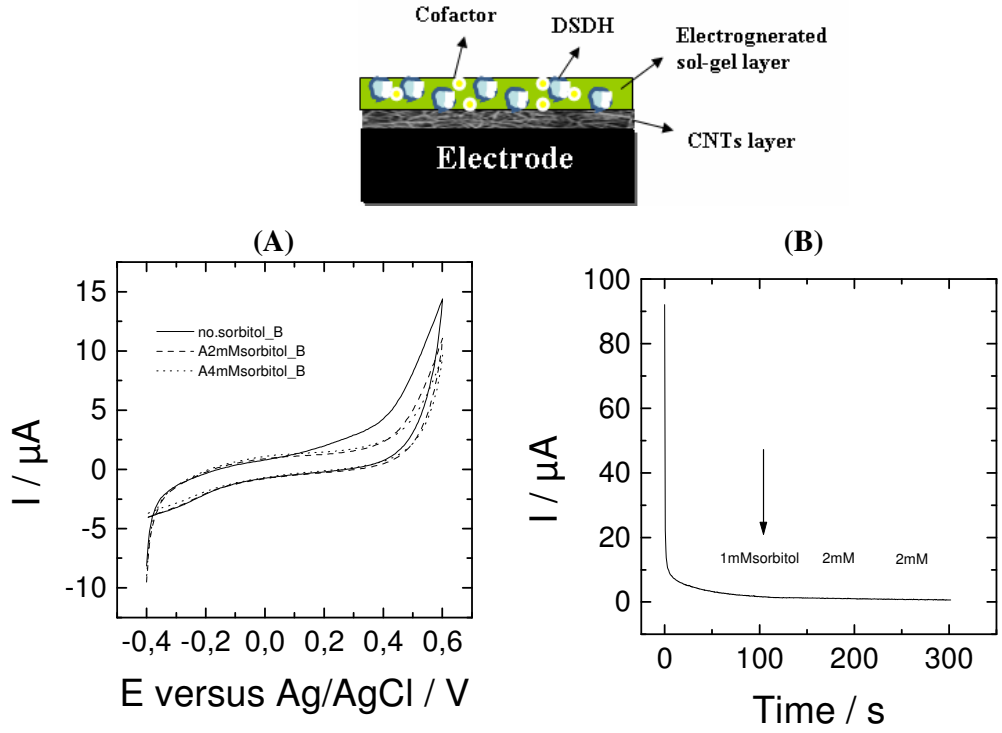

Figure VI-4. *Electrochemical response of GCE/MWCNTs-µW&TEOS/PEI/DSDH/NAD-GPS film. (A) Cyclic voltammograms in the absence and in the presence of D-sorbitol from 2 to 4mM. Potential scan rate: 5 mV/s. (B) Amperometric responses recorded at an applied potential of 0.4 V to successive additions of D-sorbitol in the solution.*

The presence of *MWCNTs-μW* on the GCE surface greatly improved the electrocatalytic efficiency of the bioelectrode and decreased to a certain extent the overpotential of NADH detection (from +0.8V to +0.4V). But the benefit of the microwave treatment was lost when *MWCNTs-μW* was covered with an additional sol-gel layer. Moreover, the system failed to regenerate the immobilized cofactor. One alternative modification of the multiwalled carbon nanotube is the electrodeposition of methylene green. We expected that this functionalization could be less sensitive than the surface quinones to the sol-gel deposition, and could be more suitable to regeneration of the immobilized cofactor.

3. Deposition of sol-gel film at MWCNTs modified by poly (methylene green) (*GCE/MWCNTs-PMG*)

3.1 Electrocatalytic oxidation of NADH at *GCE/MWCNTs-PMG*

The methylene green (MG) has shown to be a good NADH oxidation electrocatalysts [37, 38] and was employed in this study. The principle of this mediator can be schematized as follows:

$$NADH + MG_{(ox)} \longrightarrow NAD^+ + MG_{(red)} + H^+$$

$$MG_{(red)} \xrightarrow{\text{electrode}} MG_{(ox)} + e^-$$

Figure VI-5A shows the electropolymerization process of MG on the MWCNTs modified GC electrode. It is shown that the peak current increased with the number of cycles, which means more and more MG are deposited on the surface of the electrode. After a few cycles the deposition gradually reaches equilibrium. ***Figure VI-5B*** shows a comparative amperometic response of PMG modified GCE in the absence and presence of MWCNTs upon successive addition of 0.2 mM NADH to 0.1M pH 9.0 tri-HCl buffer at an applied potential of +0.2V. A catalytic response is obtained in the absence of MWCNTs, but current intensity were very low. A significant improvement in the current response was obtained when MG was electrodeposited on MWCNT modified GCE. An increasing electrocatalytic response was observed due to the addition of NADH. So with carbon nanotubes, PMG film induces a stable and significantly improved electrochemical response for the mediated oxidation of NADH.

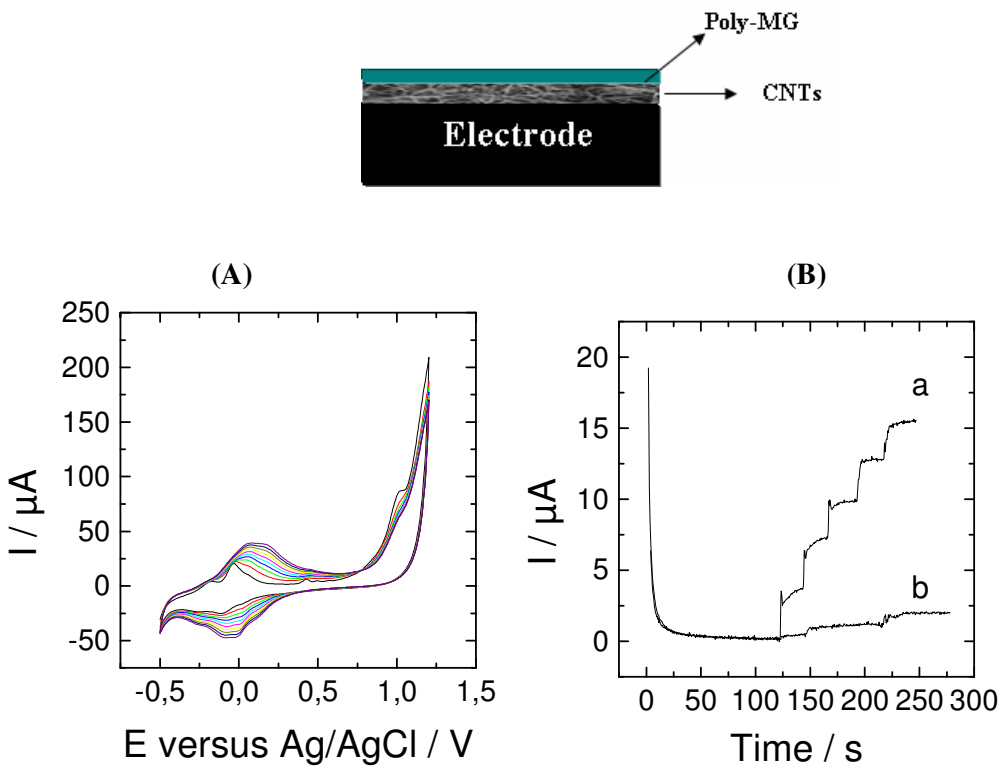

Figure VI-5. *(A) Cyclic voltammograms obtained using GCE/MWCNTs in 0.1 M pH 7.0 PBS containing 0.5 mM MG and 0.1 M KCl between -0.5 to 1.2V at a scan rate of 50 mV/s. Scan cycle, 10. (B) A comparative view of the amperometric response obtained at (a) GCE/MWCNTs-PMG and (b) GCE/PMG to successive additions of 0.2 mM NADH (Eappl = + 0.2 V vs. Ag/AgCl). Measurements have been performed in 0.1 M Tris-HCl buffer (pH 9).*

3.2 Drop-coating of sol-gel film at GCE/MWCNTs-PMG

3.2.1 Encapsulation of DSDH in sol-gel film drop-coated onto GCE/MWCNTs-PMG

The efficient system (GCE/MWCNTs-*PMG*) was first evaluated in combination with D-sorbitol dehydrogenase. ***Figure VI-6*** shows the amperometic response of different films to D-sorbitol in the Tris-HCl buffer containing 1mM NAD^+ at an applied potential of 0.2V. The background current was allowed to decay to a steady value before the addition of D-sorbitol. Obvious current responses were observed due to the addition of D-sorbitol on the GCE/MWCNTs-*PMG/&TEOS/PEI/DSDH*, and this signal increased with the D-sorbitol concentration (**curve a**). It corresponds to the electrochemical oxidation of the NADH

cofactor produced by the encapsulated DSDH while oxidizing D-sorbitol. **Curve b** and **c** shows the comparison of the response obtained with films prepared in the absence of MWCNTs and in the absence of PMG. In both cases, only small electrochemical signals were observed. So only the system including both MWCNTs and PMG display a good sensitivity to D-sorbitol. The effects can be ascribed to the increased electroactive surface area obtained with the introduction of MWCNTs for PMG deposition.

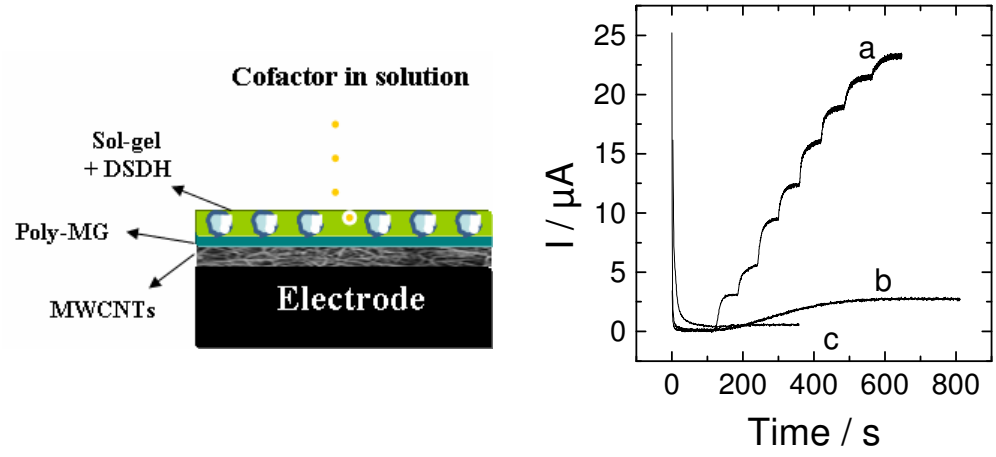

Figure VI-6. *A comparative view of the amperometric response obtained by using (a) GCE/MWCNTs-PMG&TEOS/PEI/DSDH; (b) GCE/PMG&TEOS/PEI/DSDH; (c) GCE/MWCNTs& TEOS/PEI/DSDH to successive additions of 0.5, 0.5, 1, 1, 2, 2, 3, 3mM D-sorbitol (Eappl = +0.2 V vs. Ag/AgCl). Measurements have been performed in 0.1 M Tris-HCl buffer (pH 9) containing 1mM NAD$^+$.*

D-sorbitol detection has also then been performed by cyclic voltammetry (***Figure VI-7A***) in 0.1 M Tris-HCl buffer (pH 9) containing 1 mM NAD$^+$ in the absence of D-sorbitol (dashed line) and in the presence of D-sorbitol from 2 to 6 mM (solid lines). In the absence of D-sorbitol, only the reversible electrochemical signal of MG was observed. The addition of 2 mM D-sorbitol induces the oxidation peak current increase at 0.2V, and this signal increased with D-sorbitol concentration. The applied potential in the amperometric experiment had a dramatic influence on the electrode response. The influence of the applied potential on the amperometric response to D-sorbitol under batch conditions was studied by using *GCE/MWCNTs-PMG/&TEOS/PEI/DSDH* in 0.1 M Tris-HCl buffer (pH 9) containing 1 mM NAD$^+$ at 0, +0.1 and +0.2V (***Figure VI-7B***). A detectable but comparatively small current response was observed with the addition of D-sorbitol at 0 and +0.1 V, and the current response started to level off after the fourth addition. In contrast, the modified electrode

responded rapidly to the changes of the concentration and displayed a higher sensitivity and wider detection range at +0.2 V. If a higher potential was applied, the direct uncatalysed oxidation of the enzymatically generated NADH may happen and lead to enzymatically inactive NAD-dimers and serious side reactions. In this experiment, +0.2 V was selected as the working potential which guarantees both good selectivity and sensitivity. This potential was very comparable with peak potential observed in cyclic voltammograms.

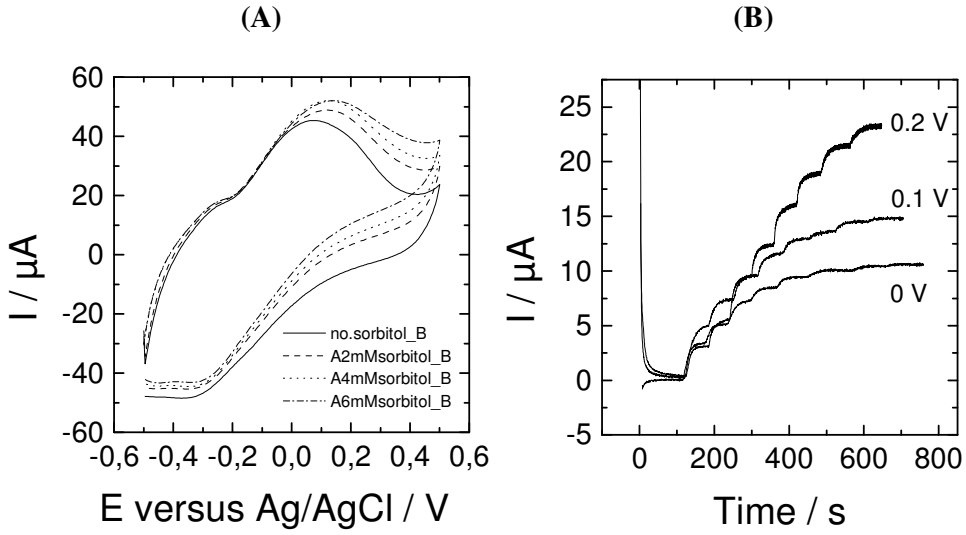

Figure VI-7. *(A) Cyclic voltammograms obtained by using GCE/MWCNTs-PMG/&TEOS/PEI/DSDH in the absence of D-sorbitol (solid line) and in the presence of D-sorbitol from 2 to 6mM(dashed lines), scan rate: 50mV/s. (B) A comparative view of the amperometric response at different applied potential to successive additions of 0.5, 0.5, 1, 1, 2, 2, 3, 3mM D-sorbitol. All measurements have been performed in 0.1 M Tris-HCl buffer (pH 9) containing 1 mM* NAD^+.

3.2.2 Encapsulation of DSDH and cofactor in sol-gel film drop-coated onto GCE/MWCNTs-PMG

As aforementioned, co-immobilizing all the necessary enzyme, cofactor and mediator onto the electrode surface without any additional reagents in solution is an advantage to reagentless device. ***Figure VI-8*** shows current response of *GCE/MWCNTs-PMG&TEOS/PEI/DSDH/*NAD^+ to D-sorbitol. The current increased regularly with D-sorbitol concentration during the first measurement. However, the second measurement made after

electrolyte medium exchange led to complete vanishing of the response. Possible reason is that NAD^+ is a small molecule, diffusing easily away from the electrode surface into solution.

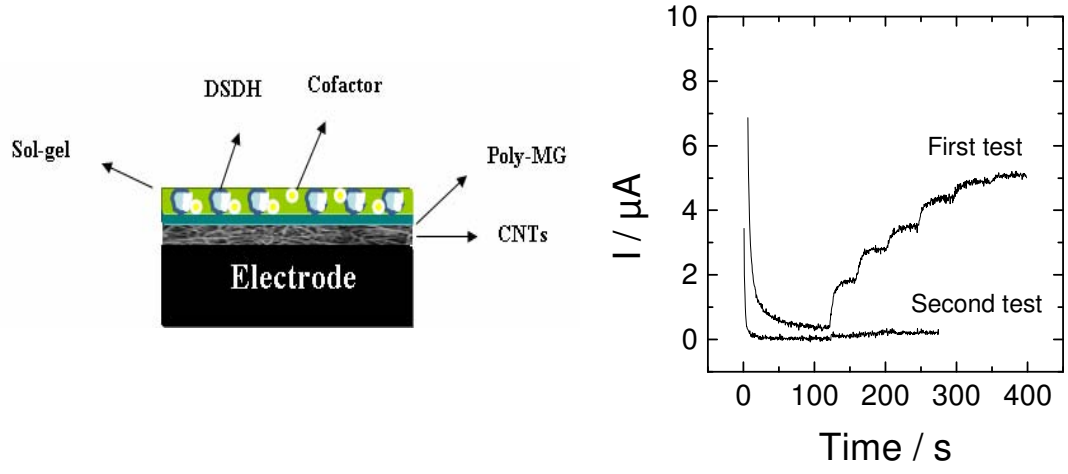

Figure VI-8. *Amperometric response recorded at +0.2 V with GCE/MWCNTs-PMG&TEOS/PEI/DSDH/NAD^+ in 0.1 M Tris-HCl buffer (pH 9), different concentration of D-sorbitol 0.5,0.5, 1, 1, 2, 2mM were added after 2 min of current recording.*

As disscussed in ***chapter IV***, Glycidoxypropyl- trimethoxysilan (GPS) [39, 40] provides a promising approach for NAD^+ immobilization. ***Figure VI-9*** compares the electrode response to 1 mM D-sorbitol of bioelectrodes obtained with (curve a) and without GPS (curve b) in the starting sol. Both electrodes showed comparable response around 3 µA at the beginning of the experiment. But the electrode prepared with GPS displayed a good operational stability, more than 75% current response was kept after continuous 14-h long experiments in a stirred solution (curve a). At the opposite, the bioelectrode prepared without GPS showed very low stability and the electrode response decreased dramatically during the first hours of experiments (curve b). Most of the catalytic activity was lost during the first 6 hours, as the electrode response almost reached null current. The immobilized cofactor in the sol-gel matrix can be regenerated by PMG deposited on MWCNTs. And as it was previously observed, this functionalization of NAD^+ with GPS can greatly enhance the stablilty of electrochemical response of the reagentless device.

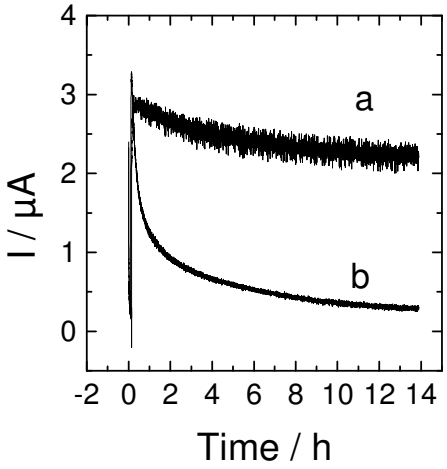

Figure VI-9. *Chronoamperograms recorded at 0.2 V with (a) GCE/MWCNTs-PMG&TEOS/PEI/DSDH/NAD-GPS; (b) GCE/MWCNTs-PMG&TEOS/PEI/DSDH/NAD$^+$. Measurements have been performed for 14 hours oxidation under convective conditions in 0.1 M Tris-HCl buffer (pH 9) containing 1 mM D-sorbitol.*

3.3 Electrodeposition of sol-gel thin film at GCE/MWCNTs-PMG

3.3.1 Electrodeposition of sol-gel thin film containing DSDH at GCE/MWCNTs-PMG (cofactor in solution)

The above approach has been extended to electrochemically-assisted deposition. First of all, the encapsulation of DSDH inside the electrodeposited silica gel has been investigated. ***Figure VI-10 A*** shows the electrochemical response obtained with *GCE/MWCNTs-PMG* covered with an additional electrodeposited sol-gel layer with encapsulated DSDH, which has been deposited by electrolysis at -1.3 V for 60 s with a sol containing DSDH (*GCE/MWCNTs-PMG/&TEOS/PEI/DSDH*), here the cofactor was not attached to the silica matrix. The addition of D-sorbitol induced the modification of oxidation peak current at 0.1-0.2 V, and this signal increased with the D-sorbitol concentration from 2 to 6 mM. ***Figure VI-10 B*** shows its amperometric responses at an applied potential of +0.2V. An increasing and stable electrocatalytic response was obtained upon addition of D-sorbitol in the stirred solution. The electrochemically-assisted deposition of silica thin films can be a good strategy to immobilize DSDH in an active form on *GCE/MWCNTs-PMG*.

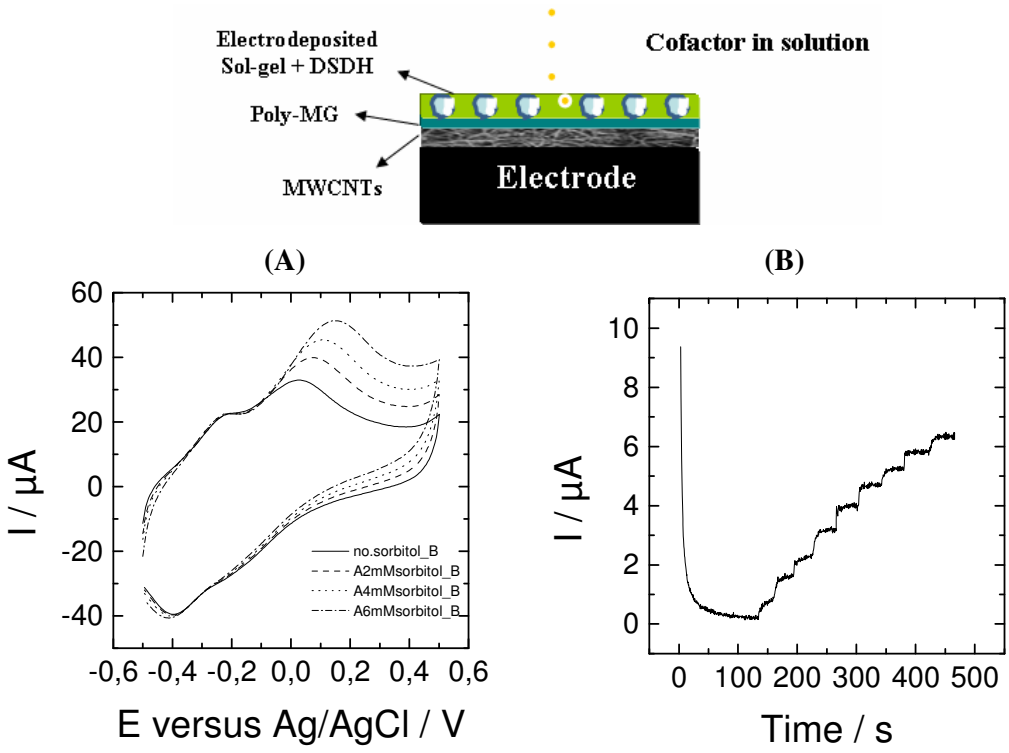

Figure VI-10. *Electrochemical response of GCE/MWCNTs-PMG/&TEOS/PEI/DSDH. (A) Cyclic voltammograms in the absence and in the presence of D-sorbitol from 2 to 6mM. Potential scan rate: 50 mV /s. (B) Amperometric response at an applied potential of 0.2 V to successive additions of 0.1, 0.2, 0.2, 0.5, 0.5, 0.5, 0.5, 1, 1mM D-sorbitol in the solution All measurements have been performed in 0.1 M Tris-HCl buffer (pH 9) containing 1 mM NAD^+.*

3.3.2 Electrodeposition of sol-gel thin film containing DSDH and cofactor at GCE/MWCNTs-PMG

Finally, the co-encapsulation of DSDH and cofactor inside the electrodeposited silica gel has been investigated. ***Figure VI-11 A*** shows the cyclic voltammograms obtained with a GCE modified by MG/CNTs and covered with an additional electrodeposited sol-gel layer with encapsulated DSDH and NAD-GPS, which has been deposited by electrolysis at -1.3 V for 60 s with a sol containing DSDH and NAD-GPS. It is shown here that the addition of D-sorbitol into the solution did not lead to noticeable current increase of the oxidation peak. ***Figure VI-11B*** shows its amperometric responses at an applied potential of 0.2 V. No electrocatalytic response was obtained upon addition of D-sorbitol in the stirred solution.

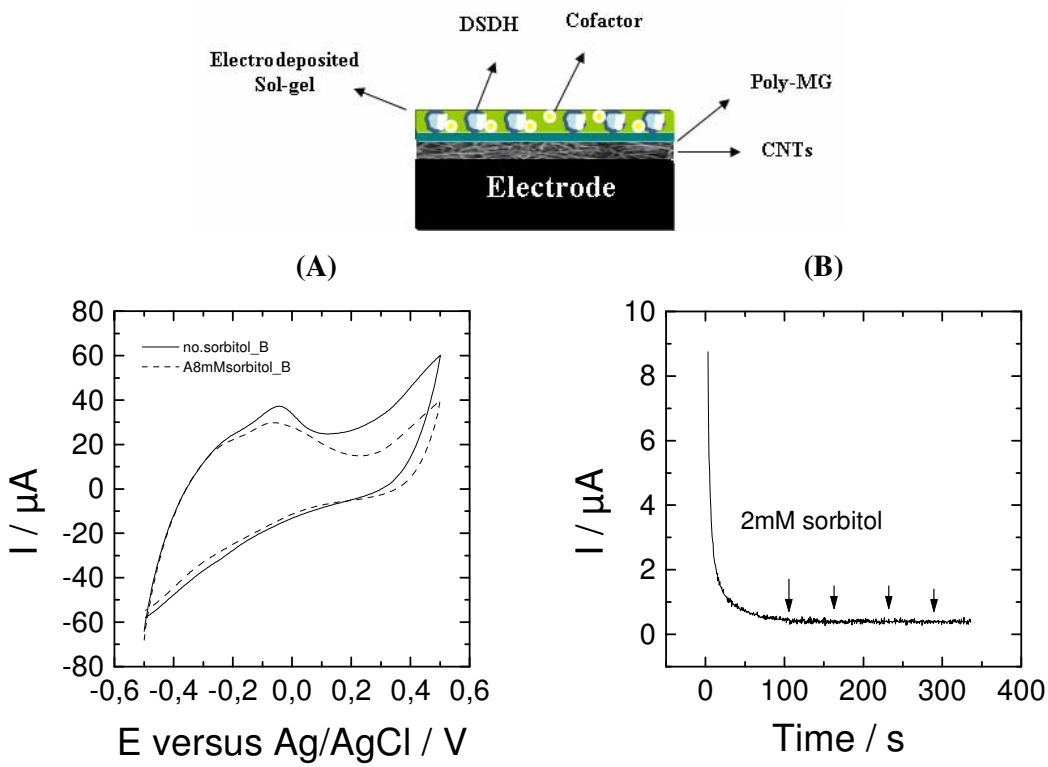

Figure VI-11. *Electrochemical response of GCE/MWCNTs-PMG/&TEOS/PEI/DSDH/NAD-GPS. (A) Cyclic voltammograms in the absence and in the presence of 8mM D-sorbitol. Potential scan rate: 50 mV /s. (B) Amperometric response at an applied potential of +0.2 V to successive additions of 2mM D-sorbitol in the solution. All measurements have been performed in 0.1 M Tris-HCl buffer (pH 9).*

In order to evaluate the reason of the negative results, additional measurements have been performed with this film (***Figure VI-12***). It confirms that the addition of D-sorbitol into the solution does not lead to current increase, however, an increasing and stable electrocatalytic response was obtained upon addition of NADH in stirred solution (***Figure VI-12A***). It proves that electrodeposition process did not interfere with the redox behavior of the electron transfer moiety of MG. ***Figure VI-12B*** shows a similar experiment. No modification of the amperometric response was observed when adding two times, successively, 1 mM D-sorbitol. Then 1 mM NAD^+ was added in the solution and a significant increase in the current response was observed, indicating a good enzymatic activity of the immobilized protein. DSDH encapsulated in the electrodeposited sol-gel film was active, but the immobilized cofactor did not interact with the carbon nanotubes modified with poly(methylene-green).

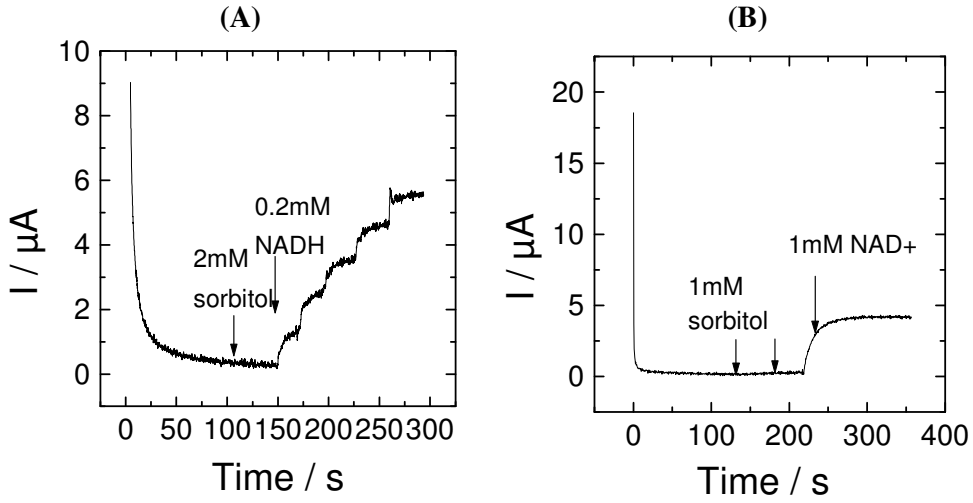

Figure VI-12. *Electrochemical response of GCE/MWCNTs-PMG/&TEOS/PEI/DSDH/NAD-GPS. (A) Amperometric response at an applied potential of 0.2 V to successive additions of 2mM D-sorbitol and 0.2 mM NADH in the solution (B) Amperometric response at an applied potential of 0.2 V to additions of 1mM D-sorbitol and 1mM NAD^+ in the solution. All measurements have been performed in 0.1 M Tris-HCl buffer (pH 9).*

The strategy based on *MWCNTs-PMG* can decrease the oxidation overpotential to be 0.2V for the smooth regeneration of cofactor and the mediator was now stable in the presence of sol-gel layer. Co-immobilization of DSDH and cofactor on *MWCNTs-PMG* could be obtained by drop-coating. However, this strategy did not allow the extension to electrochemically-assisted deposition. A bad communication was observed between the immobilized cofactor and the poly(methylene-green) deposited on MWCNTs. A system base MWCNT wrapped by Osmium(III) polymer has finally been tested. This functionalization is expected to give sufficient flexibility to mediator to interact with the sol-gel material electrochemically deposited on its surface.

4. Deposition of sol-gel film at MWCNT wrapped by Osmium(III) polymer (*GCE/MWCNTs-Os*)

4.1 Carbon nanotubes as Osmium immobilization support

The final system considered in this study was the carbon nanotubes modified with an osmium polymer. At first, the osmium polymer was simply mixed with the carbon nanotube in 0.2wt% chitosan. As display in ***Figure VI-13A***, this protocol led to a well-defined CV. But

this electrochemical signal was not stable with time and decreased when multiple potential scan were performed. So, simply mixing MWCNTs and Os-polymer solution in the presence of chitosan did not result in the stable immobilization of osmium polymer in the MWCNT layer. A second protocol for immobilization of this polymer with carbon nanotube was tested. MWCNTs have been first sonicated for 1h and then incubated in osmium-polymer solution for 12h. In these conditions, the positively-charged polymer can wrap on the sidewall surface of MWCNT (*MWCNT-Os*). ***Figure VI-13B*** shows cyclic voltammograms recorded with *GCE/MWCNT-Os*. The electrochemical response was characterized by an important capacitive current and well defined oxidation and reduction peaks at 0.25 V and 0.1 V, respectively. Moreover, the stability of the electrochemical response was maintained over tens of potential scans in this configuration.

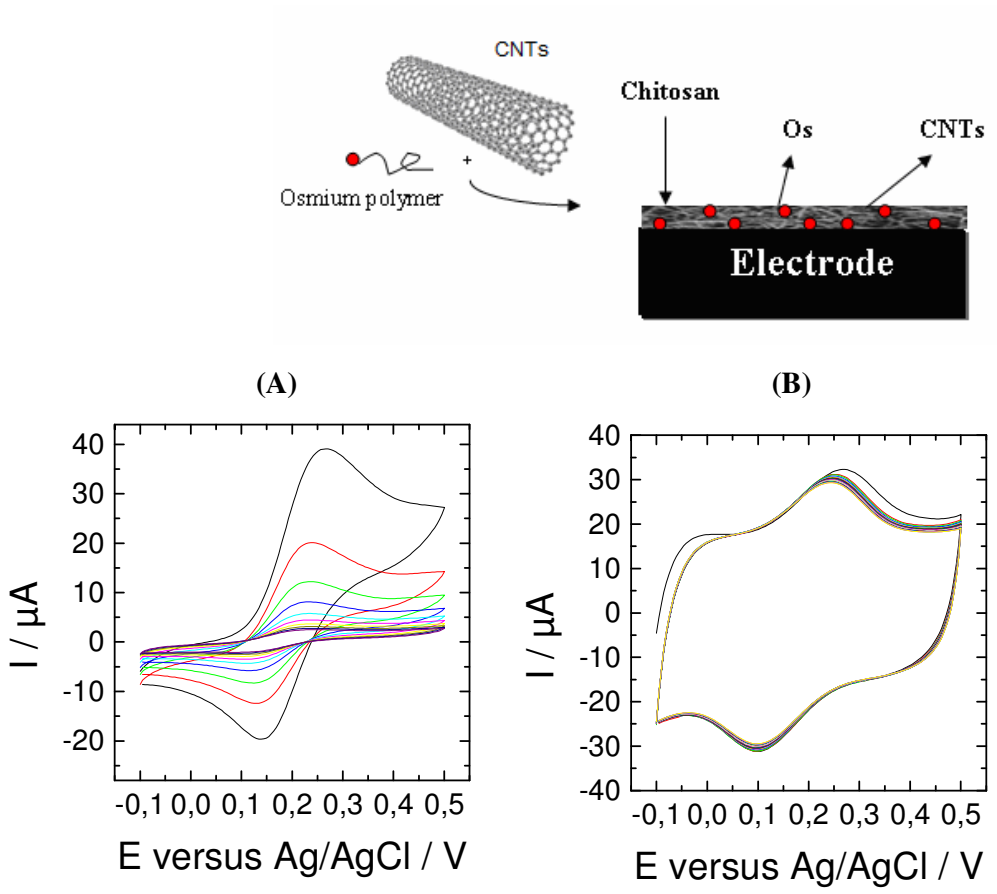

Figure VI-13. *Cyclic voltammograms recorded with (A) GCE/MWCNTs/Os (B) GCE/MWCNTs-Os. 10 successive scans in the 0.1 M Tris-HCl buffer (pH 9), potential scan rate: 50 mV/s.*

4.2 Drop-coating of sol-gel film at *GCE/MWCNTs-Os*

4.2.1 Electrocatalytic oxidation of NADH

GCE/MWCNT-Os was then modified by drop-coated sol-gel thin films. First of all, the encapsulation of DI inside the drop-coated silica gel has been investigated. *GCE/MWCNT-Os* was covered with an additional drop-coated sol-gel layer containing DI (*GCE/MWCNT-Os&TEOS/PEI/DI*). ***Figure VI-14*** shows the amperometric response to successive additions of 0.2 mM NADH at an applied potential at + 0.3 V. An increasing and stable electrocatalytic response was observed due to the addition of an aliquot of NADH. Diaphorase kept good catalytic characteristic toward NADH oxidation inside the drop-coated sol-gel film, and the immobilized osmium efficiently transfered the electron between the electrode and the diaphorase.

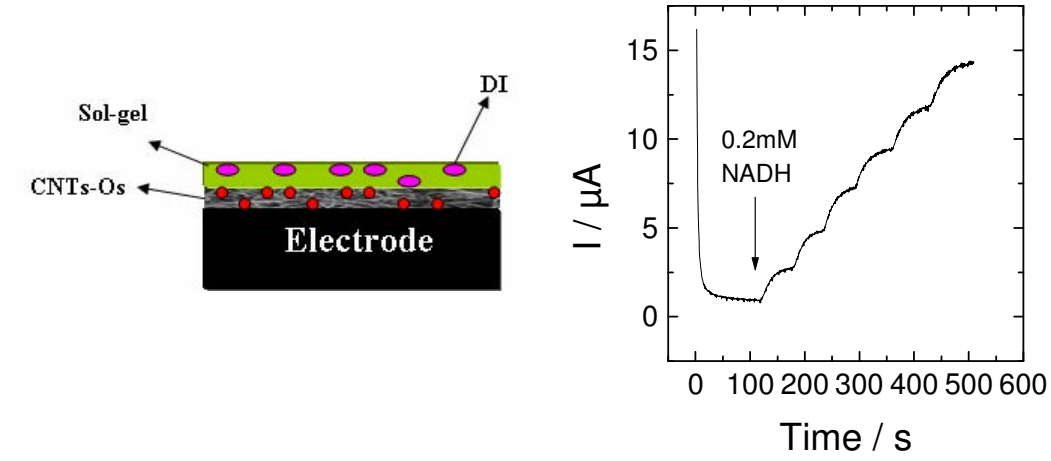

Figure VI-14. *Amperometric response obtained at GCE/MWCNT-Os&TEOS/PEI/DI to successive additions of 0.2 mM NADH (Eappl = + 0.3 V vs. Ag/AgCl). Measurements have been performed in 0.1 M Tris-HCl buffer (pH 9).*

4.2.2 Co-immobilization of DSDH, DI and cofactor at *GCE/MWCNTs-Os*

The co-encapsulation of GPS functionalized cofactor, DSDH and DI on *GCE/MWCNT-Os* was then evaluated. The protocol for the electrode preparation was rather simple; cofactor, DSDH and diaphorase are mixed together inside the sol and are casted on *GCE/MWCNT-Os*. It is shown in ***Figure VI-15A*** that the addition of D-sorbitol into the solution could lead to noticeable anodic current increase. ***Figure VI-15 B*** shows its amperometric responses at an applied potential of 0.3V. An increasing and stable electrocatalytic response was obtained

upon addition of D-sorbitol in stirred solution. The co-immobilization of DSDH, DI, osmium and NAD-GPS in bilayer did not prevent the efficient communication among them. NAD-GPS kept enough mobility to reach center of dehydrogenase, and the dehydrogenase catalysted the oxidation of D-sorbitol, and the DI/Osmium decreased the overpotential of NADH detection for the smooth regeneration of the cofactor.

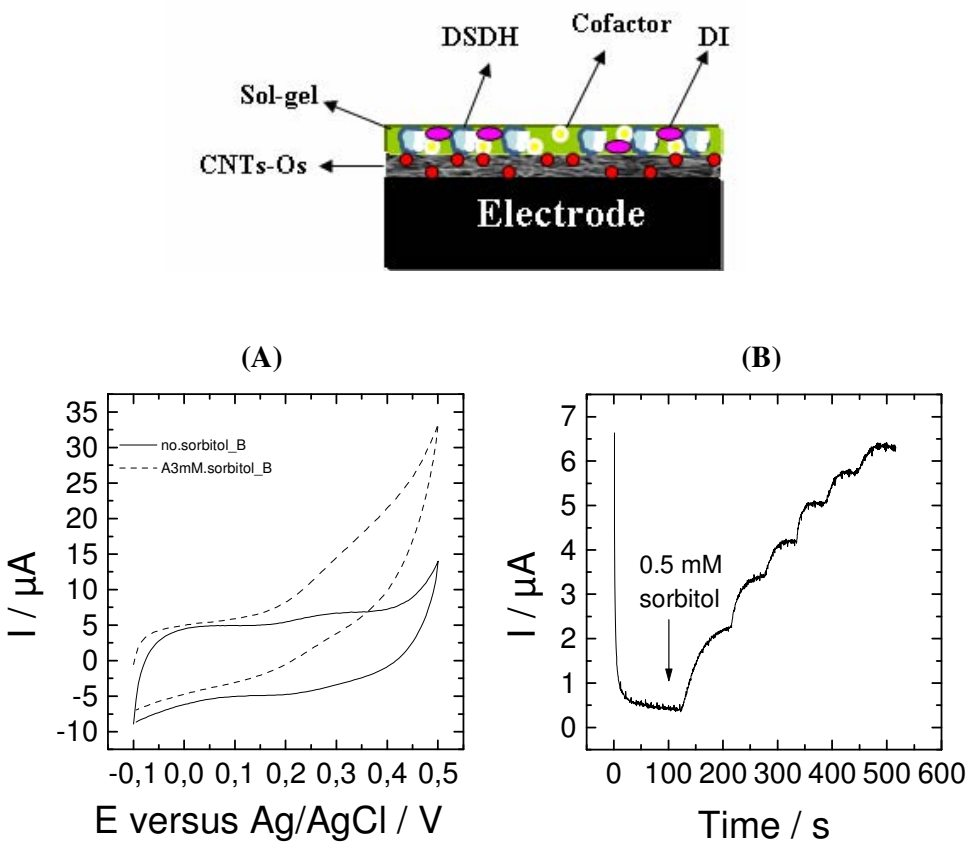

Figure V-15. *Cyclic voltammograms recorded with GCE/MWCNT-Os&TEOS/PEI/DI/NAD-GPS in the absence and in the presence of 3 mM D-sorbitol. Potential scan rate: 50 mV/s. (B) Amperometric responses recorded at an applied potential of 0.3 V to successive additions of 0.5 mM D-sorbitol in 0.1 M Tris-HCl buffer (pH 9).*

4.3 Electrodepostion of sol-gel film at *GCE/MWCNTs-Os*

4.3.1 Electrocatalytic oxidation of NADH

This approach has been extended to electrochemically-assisted deposition. First of all, the encapsulation of DI inside the electrodeposited silica gel has been investigated. ***Figure VI-16*** shows the amperometric responses at an applied potential of 0.3V. An increasing and stable electrocatalytic response was obtained upon addition of NADH in stirred solution. The cyclic

voltammograms recorded before addition of NADH (Inset of ***Figure VI-16***) shows that the electrochemical signal from the osmium complexes has been significantly decreased in the presence of the sol-gel material. Nethertheless, the addition of NADH leads to a significant increase in the current intensity. The shape of the catalytic signal was poorly resolved and could be a mix between the detection of NADH through osmium complex and diaphorase and the simultaneous detection of NADH at the carbon nanotube surface, as reported in ***Figure VI-1A***.

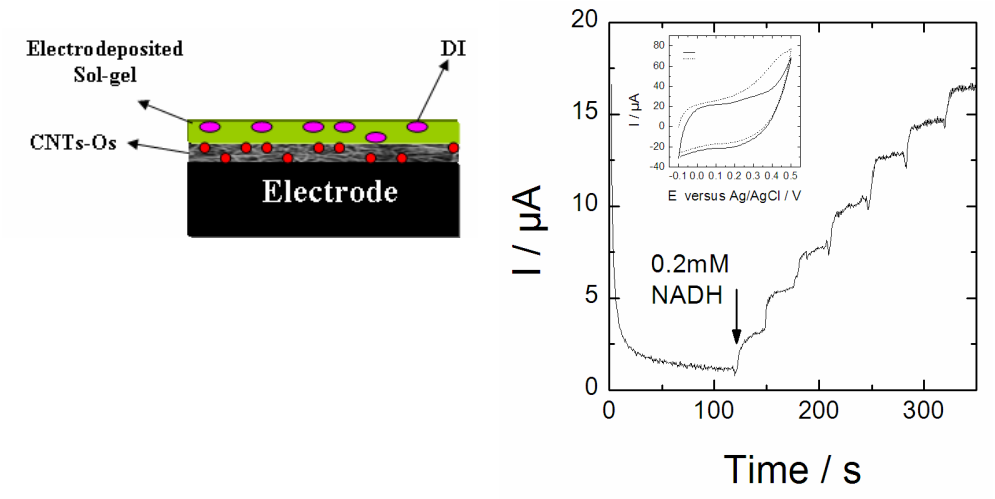

Figure VI-16. *Amperometric response obtained at GCE/MWCNT-Os&TEOS/PEI/DI to successive additions of 0.2 mM NADH (Eappl = + 0.3 V vs. Ag/AgCl). Inset plot shows cyclic voltammograms recorded before and after addition of 1.4mM NADH. Films have been deposited by electrolysis at -1.3 V for 60 s. Measurements have been performed in 0.1 M Tris-HCl buffer (pH 9).*

4.3.2 Co-immobilization of DSDH, DI and cofactor at *GCE/MWCNTs-Os*

The co-encapsulation of DSDH, DI and cofactor inside the electrodeposited silica gel has been finally investigated. ***Figure VI-17A*** shows the cyclic voltammograms obtained with *GCE/MWCNT-Os* covered with an additional electrodeposited sol-gel layer with encapsulated DSDH, DI and NAD-GPS, which has been deposited by electrolysis at -1.3 V for 60 s with a sol containing DSDH, DI and NAD-GPS. In the absence of D-sorbitol, only the reversible electrochemical signal of Os was observed. The addition of D-sorbitol induces an increase of the anodic current and a decrease of the cathodic current. It corresponds to the electrochemical oxidation of the NADH cofactor produced by the encapsulated DSDH while oxidizing D-sorbitol. ***Figure VI-17B*** shows amperometric responses of the modified electrode to D-sorbitol in a stirred solution. An increasing and stable electrocatalytic response was

obtained upon the addition of 0.4 mM D-sorbitol. Inset plot shows the corresponding calibration plot, the current intensity increases regularly with the D-sorbitol concentration up to 2.8 mM and starts to level off for higher concentrations. ***Figure VI-17C*** shows the response of *GCE/MWCNT-Os&TEOS/PEI/DI/NAD-GPS* to 2 mM D-sorbitol. The amperometric signal of the bioelectrode kept a rather stable (yet slightly decreasing) value for *ca.* 14 hours of continuous reaction.

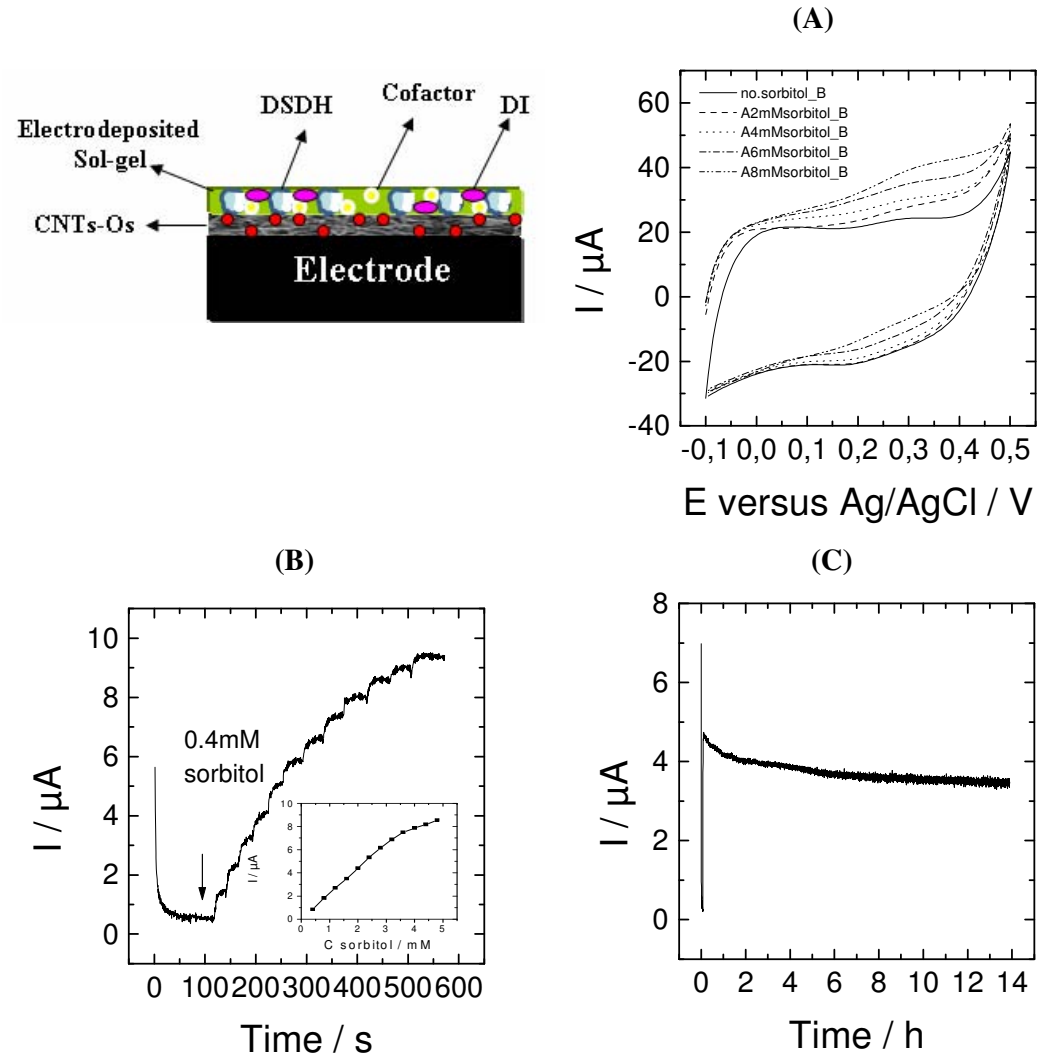

Figure VI-17*. (A) Cyclic voltammograms recorded with GCE/MWCNT-Os&TEOS/PEI/DI/NAD-GPS in the absence and in the presence of D-sorbitol from 2 to 8mM. Potential scan rate: 50 mV/s. (B) Amperometric responses recorded at an applied potential of 0.3 V to successive additions of 0.4mM D-sorbitol in stirred solution.* Inset plot shows the *corresponding calibration plot. (C) Amperometric response obtained in the same conditions. measurements have been performed for 14 hours under convective conditions in 0.1 M Tris-HCl buffer (pH 9) containing 2 mM D-sorbitol.*

Up to now, carbon nanotubes wrapped by osmium has been the only system that was successfully combined with sol-gel electrodeposition for bioencapsulation of dehydrogenase and cofactor. With *MWCNT-μW* and *MWCNT-PMG,* the functionalization was confined at the surface of the nanotube as part of the material (*MWCNT-μW)* or as a thin surface layer *(MWCNT-PMG).* The NADH cofactor had to come close the carbon nanotube surface in order to be regenerated in the enzymatically active NAD^+. When cofactor was free diffusing in the solution, the regeneration was always successful and carbon nanotubes provided higher surface area resulting in higher sensitivity of the bio-electrode to D-sorbitol with comparison to the bare GCE. However the immobilization of the cofactor in the electrochemically deposited sol-gel thin film did not provide a sufficient mobility to the cofactor and the molecule did not interact with the functionalized MWCNT (*MWCNT-μW* or *MWCNT-PMG).* Osmium polymer is composed by a polyacrylate backbone with the osmium complex attached by 5 atoms linkers. While the polymer is linked to the MWCNT by wrapping, the linker gives sufficient flexibility to the mediator to interact with the sol-gel material electrochemically deposited on its surface. The same polymer was first introduced in the sol-gel matrix. But the electrochemical properties of the polymer were lost during the electrodeposition process (see **Chapter V**). A first immobilization on the carbon nanotube surface before sol-gel electrodeposition gave the unique opportunity to conserve the electrochemical activity of the osmium complexes and to display good flexibility for effective interaction with the encapsulated diaphorase that catalyses the NADH oxidation.

5. The interest of SWCNTs for $[Cp^*Rh(bpy)Cl]^+$ immobilization: towards a device operating in reduction

5.1 $[Cp^*Rh(bpy)]^{2+}$ as suitable mediator for NADH regeneration

The direct electrochemical reduction of $NAD(P)^+$ requires high overpotentials and usually leads to enzymatically inactive NAD-dimers generated due to the one-electron transfer reaction [41, 42]. The mediators for the regeneration of NADH should react with NAD^+ and not transferring directly the electrons (or hydride ion) to the substrate, and the potential window for electrochemical activation of the catalysts is rather narrow (-0.59 ～ -0.9 V vs. SCE) [43]. (2,2'-bipyridyl) rhodium complexes are the best systems for the regeneration of

NAD^+. As illustrated on ***Figure VI-18***, their electrocatalytic behaviour is rather complicated, involving first a two-electron electrochemical reduction of Rh^{III} (M_{ox}) into transient Rh^I species (M_{red1}; this reaction occurring itself in several steps [44]) that can be transformed upon protonation into a rhodium hydride complex (M_{red2}), which is then likely to transfer the hydride to $NAD(P)^+$ under formation of only 1,4-NAD(P)H [45, 46].

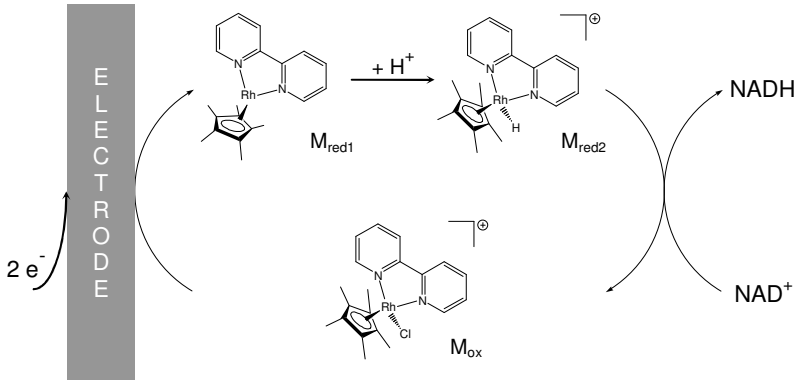

Figure VI-18. *The mechanism of $[Cp^*Rh(bpy)]^{2+}$ electrocatalytic process.*

5.2 Substituent effects and mediator immobilization attempts

Derivatives functionalized with thiol groups are attractive for immobilization of reagents in the form of self-assembled monolayers (SAMs) on gold electrodes [47, 48], and the amine-functionalized ones are good precursors to form organosilane reagents likely to be grafted onto metal oxides or incorporated within sol-gel matrices then deposited onto electrode surfaces [49, 50, 51]. We have examined the behaviour of several functionalized mediators of this family bearing various organic groups, which could be used as precursors to immobilize such compounds onto electrode surfaces. Here, we just give one example. Compounds **11** is a thiol-functionalized Rh complex. ***Figure VI-19*** shows cyclic voltammograms recorded with compounds **11** immobilized as a self-assembled monolayer on gold electrode. These derivatives can be indeed immobilized on gold electrodes as SAMs while keeping their electrochemical activity (with peak currents directly proportional to the scan rate as expected for adsorbed species, see ***Figure VI-19A*** for **11**), yet not stable upon continuous potential cycling (***Figure VI-19B***), and no electrocatalytic activity can be observed in the presence of NAD^+ (***Figure VI-19C***).

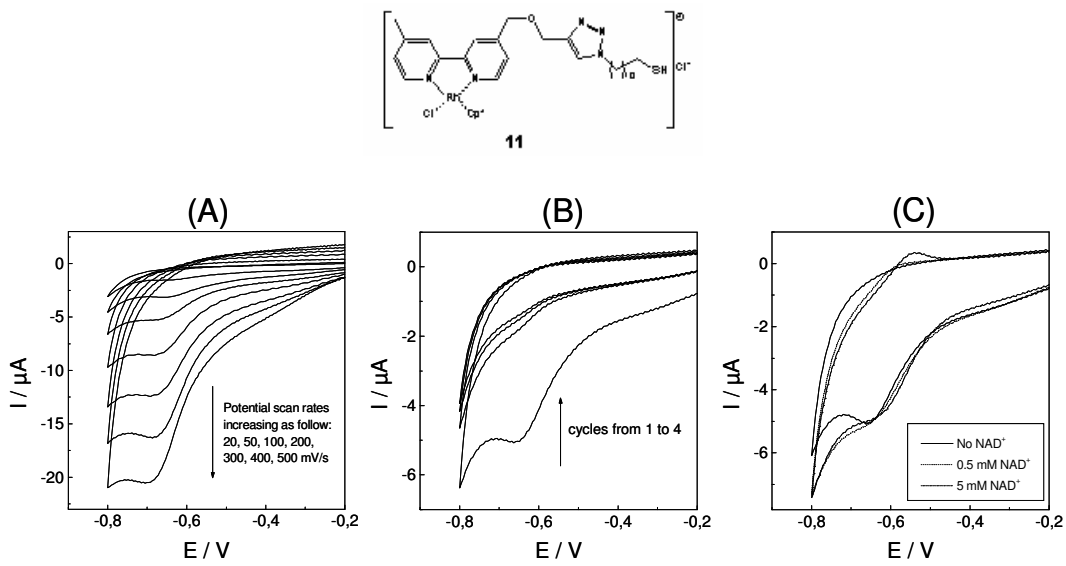

Figure VI-19. *Cyclic voltammograms recorded with compounds* ***11*** *immobilized as a self-assembled monolayer on gold electrode: (A) effect of potential scan rate; (B) effect multisweep; (C) electrode response in the absence and presence of increasing* NAD^+ *concentrations. Potential scan rate: 100 mV/ s.*

Another immobilization approache has been tested: the covalent binding to the sol-gel film on the basis of alkoxysilane-functionalized derivatives (***Figure VI-20)***. However, after immobilization within sol-gel films, the voltammetric response of this mediator decreased dramatically (or even vanished) and they lost their capacity to regenerate the NADH cofactor.

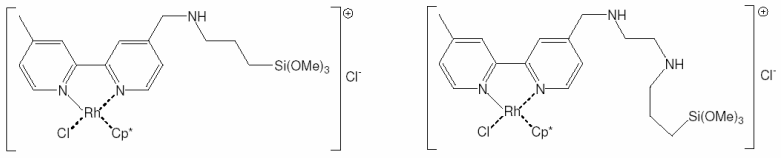

Figure VI-20. *[Cp*Rh(bpy)]*$^+$*- type mediators functionalized with siloxy-function.*

The $[Cp^*Rh(bpy)Cl]^+/[Cp^*Rh(bpy)H]^+$ system, in solution, is a good mediator to regenerate NADH. However, as discussed above after immobilization as SAM on gold or within sol-gel films, the voltammetric response of this mediator decreases dramatically (or even vanished) and they lose their capacity to regenerate the NADH cofactor. The main conclusion from our studies is that the presence of thiol or nitrogen-containing groups, either in solution or as part of the mediator derivative, totally prevents any electrocatalytic activity

of this mediator. This has been found on the basis of deep investigation of a number of functionalized $[Cp^*Rh(bpy)Cl]^+$ compound synthesised by the group of Prof. Demir (Turkish partner) and studied by Dr. Fengli Qu and Dr. Rihab Nasraoui. All these results highlight the difficulty to functionalize $[Cp^*Rh(bpy)Cl]^+$-based mediators while maintaining their catalytic properties toward NADH regeneration. We find some alternatives "soft" immobilization procedures not requiring the resort to functional groups harmful to the mediator functioning.

5.3 Interest of carbon nanotubes as immobilization support

The noncovalent functionalization of single-walled carbon nanotubes (SWCNTs) with molecular metal-containing compounds via π-π-stacking starts to become a versatile alternative to covalent bonding [52]. An approach has thus been tested here for the immobilization of the non functionalized $[Cp^*Rh(bpy)Cl]^+$ complex, with the aim to overcome the aforementioned deactivation of the electrocatalytic processes when using derivatized $[Cp^*Rh(bpy)Cl]^+$ derivatives. ***Figure VI-21A*** shows that it works quite nicely as a well-defined cathodic peak appeared at -0.7 V (curve a), which is found to increase in the presence of NAD^+ added in the medium (curve b), demonstrating that both the electrochemical and the electrocatalytic properties of the mediator are maintained after immobilization by π-π-stacking on CNTs.

Even more interesting is the stability of the electrochemical response upon multisweep (see ***Figure VI-21B***), which is maintained over tens of potential scans. ***Figure VI-21C*** shows that the response to NAD^+ is indeed due to the adsorbed $[Cp^*Rh(bpy)Cl]^+$ mediator and not to any intrinsic electrocatalytic properties of SWCNTs towards NAD^+ reduction, as no detectable signal can be observed when using non modified CNTs (see curve a). In the presence of mediator, an increasing and stable electrocatalytic response is obtained upon addition of NAD^+ in stirred solution (see curve b). The optimal applied potential is found to be in the range between -0.7 and -0.8 V whereas a loss in sensitivity by ca. 50 % is found when operating at -0.6 V (see ***Figure VI-21D***). These results demonstrate that adsorption of $[Cp^*Rh(bpy)Cl]^+$ by π-π-stacking on CNTs is an efficient procedure, yet simple, fast and direct, to irreversibly immobilize an electrocatalytically active mediator onto an electrode surface for effective NADH regeneration. However, this strategy does not show good operational behaviour when associated to a dehydrogenase enzyme with silica sol-gel for protein encapsulation.

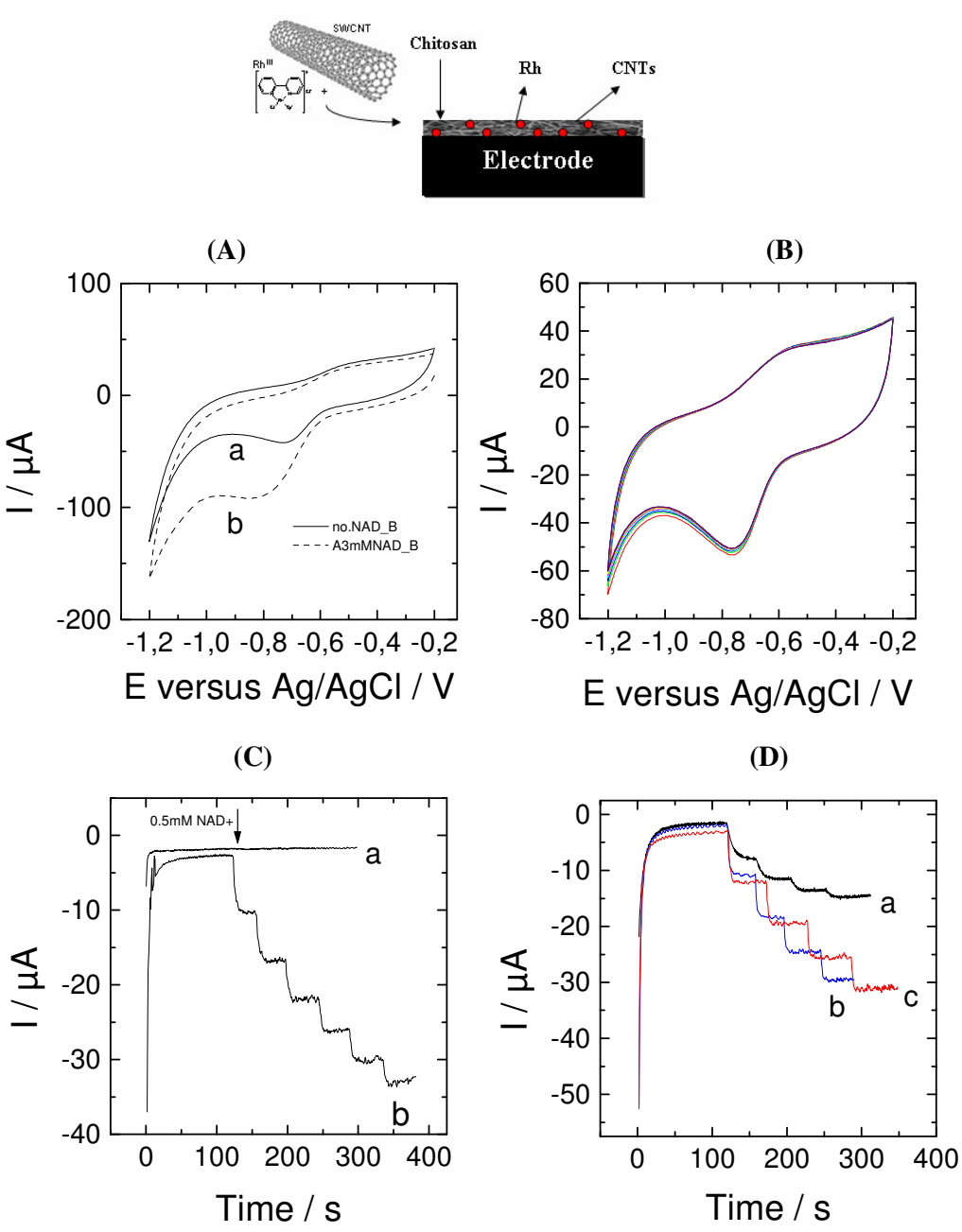

Figure VI-21. *Cyclic voltammograms recorded with a GCE modified by chitosan/SWCNTs with adsorbed $[Cp^*Rh(bpy)Cl]^+$ species (A) in the absence (a) and in the presence (b) of 3 mM NAD^+. Potential scan rate: 50 mV s^{-1}. (B) 10 successive scans in the electrolyte solution (0.05 M phosphate buffer, pH 6.5). (C) Amperometric responses recorded using GCE modified by a chitosan layer containing (a) bare CNTs or (b) CNTs with adsorbed $[Cp^*Rh(bpy)Cl]^+$ species at an applied potential of -0.8 V to successive additions of 0.5 mM NAD^+ in the solution. (D) Amperometric responses recorded with a GCE modified by chitosan/CNTs with adsorbed $[Cp^*Rh(bpy)Cl]^+$ species at an applied potential of (a) -0.6 V; (b) -0.7V; (c) -0.8V to successive additions of 0.5 mM NAD^+ in the solution (magnetically stirred at 300 rpm).*

6. Conclusion

The goal of the study was the implementation of a reagentless device displaying an efficient interaction between the immobilized dehydrogenase and cofactor in the electrogenerated sol-gel matrix and the functionalized multi-walled carbon nanotubes (MWCNTs). In this work, three different protocols have been developed to functionalize MWCNTs. They include (1) the simple microwave treatment of MWCNTs, (2) electrochemical deposition of poly(methylene green) on MWCNTs, and (3) wrapping of MWCNTs with an Osmium(III) polymer. All the developed strategies show significantly decreased overpotentials for NADH oxidation. A sol-gel thin film has been further deposited functionalized carbon nanotubes by drop-coating for encapsulation of D-sorbitol dehydrogenase (and diaphorase when necessary) and co-immobilization of the NAD^+ cofactor. The catalytic property of macrowaved MWCNTs was significantly disturbed by sol-gel material and failed to regenerate the cofactor at 0V. The modification of the MWCNTs with electrodeposited poly(methylene-green) and wrapped Osmium(III) polymer were not so sensitive to the sol-gel material, and allowed the smooth regeneration of the immobilized cofactor in drop-coated sol-gel film. However, when the reagentless devices obtained by drop-coating were extended to electrochemically-assisted deposition, a direct interaction between NAD^+ immobilized in the sol-gel matrix and the functionalized MWCNTs was not possible with *MWCNTs-μw* and *MWCNTs-PMG*. Sol-gel deposition by electrogenerated limited the interaction of NAD^+ with the mediator confined on MWCNTs. Only MWCNT wrapped with Osmium(III) polymer and in the presence of diaphorase allowed to observe the electrochemical detection of D-sorbitol in a reagentless configuration. This is probably due to high mobility of the osmium complexes immobilized on MWCNTs.

For the reduction reaction, we studied the immobilization of functionalized mediators of $[Cp^*Rh(bpy)Cl]^+$ family. The presence of substituents bearing nucleophilic moieties such as S- or N-containing groups, on the bipyridine ligand, was proven to be harmful to the electrocatalytic properties of the $[Cp^*Rh(bpy)Cl]^+$ mediator, limiting therefore most immobilization strategies based on covalent bonding onto electrode surfaces. A way to circumvent this problem is the soft immobilization of such $[Cp^*Rh(bpy)Cl]^+$ mediator by π-π-stacking onto CNTs. However, this strategy does not show good operational behaviour when associated to a dehydrogenase enzyme with silica sol-gel for protein encapsulation.

References

[1] Tse, D.C.S.; Kuwana, T., Electrocatalysis of dihydronicotinamide adenosine diphosphate with quinones and modified quinone electrodes. *Anal. Chem.* **1978**, *50(9)*, 1315-1318.

[2] Cenas, N. K.; Kanapoeniene, J. J.; Kulys, J. J., NADH oxidation by quinone electron acceptors. *Biochim. Biophys. Acta* **1984,** *767(1)*, 108-112.

[3] Essaadi, K.; Keita, B.; Nadjo, L.; Contant, R., Oxidation of NADH by oxometalates. *J. Electroanal. Chem.* **1994,** *367 (1-2)*, 275-278.

[4] Somasundrum, M.; Hall, J.; Bannister, J.V., Amperometric NADH determination via both direct and mediated electron transfer by NADH oxidase from Thermus aquaticus YT-1. *Anal. Chim. Acta* **1994**, *295 (1-2)*, 47-57.

[5] Torstensson, A.; Gorton, L., Catalytic oxidation of NADH by surface-modified graphite electrodes. *J. Electroanal. Chem.* **1981,** *130*, 199-207.

[6] Kulys, J.J., The development of new analytical systems based on biocatalysts. *Anal. Lett.* **1981,** *14 (B6)*, 377-397.

[7] Gorton, L.; Tortensson, A.; Jaegfeldt, J.; Johansson, G., Electrocatalytic oxidation of reduced nicotinamide coenzymes by graphite electrodes modified with an adsorbed phenoxazinium salt, Meldola Blue. *J. Electroanal. Chem.* **1984**, *161 (1)*, 103-120.

[8] Fan, N.; Feng, H.; Gorton, L.; Cotton, T. M., Electrochemical and SERS studies of chemically modified electrodes: Nile Blue A, a mediator for NADH oxidation. *Langmuir* **1990**, 6 (1), 66-73.

[9] Karyakin, A. A.; Karyakina, E. E.; Schuhmann, W.; Schmidt, H. L., Electropolymerized azines. Part 2. In a search of the best electrocatalyst of NADH oxidation. *Electroanalysis* **1999,** *11(8)*, 553-557.

[10] Gao, Q.; Wang, W.; Ma, Y.; Yang, X., Electrooxidative polymerization of phenothiazine derivatives on screen-printed carbon electrode and its application to determine NADH in flow injection analysis system. *Talanta* **2004**, *62(3),* 477-482.

[11] Malinauskas, A.; Ruzgas, T.; Gorton, L., Electrochemical study of the redox dyes Nile Blue and Toluidine Blue adsorbed on graphite and zirconium phosphate modified graphite. *J. Electroanal. Chem.* **2000**, *484(1)*, 55-63.

[12] Wienkamp, R.; Steckhan, E., Indriect electrochemical regeneration of NADH by a bipyridiner-hodium (I) complex as electron-transfer agent. *Angew. Chem. Int. Ed.* **1982**, *21*, 782-783.

[13] Franke, M.; Steckhan, E., Tris(2,2′-bipyridyl-5-sulfonic acid)rhodium(III), an Improved Redox Catalyst for the Light-Induced and the Electrochemically Initiated Enzymatic Reduction of Carbonyl Compounds. *Angew. Chem. Int. Ed.* **1988**, *27(2)*, 265-267.

[14] Grammenudi, S.; Franke, M.; Voegtle, F.; Steckhan, E., The rhodium complex of a tris(bipyridine) ligand - its electrochemical behavior and function as mediator for the regeneration of NADH from NAD^+. *J. Incl. Phenom.* **1987**, *5(6)*, 695-707.

[15] Steckhan, E.; Herrmann, S.; Ruppert, R.; Dietz, E.; Frede, M.; Spika, E.,Analytical study of a series of substituted (2,2'-bipyridyl) (pentamethylcyclopentadienyl) rhodium and -iridium complexes with regard to their effectiveness as redox catalysts for the indirect electrochemical and chemical reduction of $NAD(P)^+$. *Organometallics* **1991**, *10(5)*, 1568-1577.

[16] Canivet, J.; Süss-Fink, G.; Stepnicka, P., Water-soluble phenanthroline complexes of rhodium, iridium and ruthenium for the regeneration of NADH in the enzymatic reduction of ketones. *Eur. J. Inorg. Chem.* **2007**, *(30),* 4736-4742.

[17] Hollmann, F.; Witholt ,B.; Schmid, A., $[CpRh(bpy)(H_2O)]^{2+}$: a versatile tool for efficient and non-enzymatic regeneration of nicotinamide and flavin coenzymes. *J. Mol. Catal. B* **2003**, *19-20*, 167-176.

[18] Vuorilehto, K.; Lütz, S.; Wandrey, C., Indirect electrochemical reduction of nicotinamide coenzymes. *Bioelectrochem.* **2004**, *65(1)*, 1-7.

[19] Dumitrescu, I.; Unwin, P. R.; MacPherson, J. V., Electrochemistry at carbon nanotubes: perspective and issues. *Chem. Commun.* **2009**, *45*, 6886-6901.

[20] Fernandez-Abedul, M. T.; Costa-Garcia, A., Carbon nanotubes (CNTs)-based electroanalysis. *Anal. Bioanal. Chem.* **2008**, *390(1)*, 293-298.

[21] Baughman, R. H.; Zakhidov, A.; De Heer, W.A., Carbon nanotubes--the route toward applications. *Science* **2002**, *297 (5582)*, 787-792.

[22] Rao, C. N. R.; Satishkumar, B. C.; Govindaraj, A.; Nath, M., Nanotubes .*Chem. Phys. Chem.* **2001**, *2*, 78-105.

[23] Musameh, M.; Wang, J.; Merkoci, A.; Lin, Y., Low-potential stable NADH detection at carbon-nanotube-modified glassy carbon electrode. *Electrochem. Commun.* **2002**, *4(10)*, 743-746.

[24] Wooten, M.; Gorski, W., Facilitation of NADH Electro-oxidation at Treated Carbon Nanotubes. *Anal. Chem.* **2010**, *82(4)*, 1299–1304

[25] Lawrence, N. S.; Wang, J., Chemical adsorption of phenothiazine dyes onto carbon

nanotubes: Toward the low potential detection of NADH. *Electrochem. Commun.* **2006**, *8(1)*, 71-76.

[26] Zhu, L.; Yang, R.; Jiang, X.; Yang, D., Amperometric determination of NADH at a Nile blue/ordered mesoporous carbon composite electrode. *Electrochem. Commun.* **2009**, *11(3)*, 530-533.

[27] Yan, Y.; Yehezkeli, O.; Willner, I., Integrated , electrically contacted NAD (P)$^+$-dependent enzyme-carbon nanotube electrodes for biosensors and biofuel cell applications. *Chem.-Eur. J.* **2007**, *13(36)*, 10168-10175.

[28] Zhu, L; Zhai, J.; Yang, R.; Tian, C.; Guo, L., Electrocatalytic oxidation of NADH with Meldola's blue functionalized carbon nanotubes electrodes. *Biosens. Bioelectron.* **2007**, *22(11)*, 2768-2773.

[29] Lin, Y.; Zhu, N.; Yu, P.; Su, L. ; Mao, L., Physiologically Relevant Online Electrochemical Method for Continuous and Simultaneous Monitoring of Striatum Glucose and Lactate Following Global Cerebral Ischemia/Reperfusion. *Anal. Chem.* **2009**, *81(6)*, 2067–2074.

[30] Antiochia, R.; Gorton, L., Development of a carbon nanotube paste electrode osmium polymer-mediated biosensor for determination of glucose in alcoholic beverages. *Biosens. Bioelectron.* **2007**, *22(11)*, 2611-2617.

[31] Kumar, S. A.; Chen, S. M., Electrocatalytic reduction of oxygen and hydrogen peroxide at poly(p-aminobenzene sulfonic acid)-modified glassy carbon electrodes. *J. Mol. Catal. Chem. A: Chem.* **2007**, *278(1-2)*, 244-250.

[32] Kumar, S. A.; Tang, C. F.; Chen, S. M., Poly(4-amino-1-1'-azobenzene-3, 4'-disulfonic acid) coated electrode for selective detection of dopamine from its interferences. *Talanta* **2008**, *74(4)*, 860-866.

[33] Kumar, S. A.; Chen, S. M.; Electrochemical, microscopic, and EQCM studies of cathodic electrodeposition of ZnO/FAD and anodic polymerization of FAD films modified electrodes and their electrocatalytic properties, *J Solid State Electrochem.* 2007, 11(7), 993-1006

[34] Jacobs, C. B.; Peairs, M. J.; Venton, B. J., Carbon nanotube based electrochemical sensors for biomolecules. *Anal. Chim. Acta* **2010**, *662(2)*, 105-127.

[35] Gong, K.; Yan, Y.; Zhang, M.; Su, L.; Xiong, S.; Mao, L., Electrochemistry and electroanalytical applications of carbon nanotubes: A review. *Anal. Sci.* **2005**, *21(12)*, 1383-1393.

[36] Arvinte, A.; Sesay, A. M.; Virtanen, V.; Bala, C., Evaluation of meldola blue - carbon nanotube - sol - gel composite for electrochemical NADH sensors and their application for lactate dehydrogenase-based biosensors. *Electroanalysis* **2008**, *20(21)*, 2355-2362.

[37] Zhou, D.; Fang, H.; Chen, H.; Ju, H.; Wang, Y., The electrochemical polymerization of methylene green and its electrocatalysis for the oxidation of NADH. *Anal. Chim. Acta* **1996,** *329(1-2)*, 41–48.

[38] Dai, Z. H.; Liu, F. X.; Lu, G. F.; Bao, J. C., Electrocatalytic detection of NADH and ethanol at glassy carbon electrode modified with electropolymerized films from methylene green. *J Solid State Electrochem* **2008**, *12(2)*, 175-180.

[39] Oakey, L.; Mulcahy, P., Immobilized cofactor derivatives for kinetic-based enzyme capture strategies: direct coupling of $NAD(P)^+$. *Anal. Biochem.* **2004**, *335(2)*, 316-325.

[40] Liu, W.; Zhang, S.; Wang, P., Nanoparticle-supported multi-enzyme biocatalysis with in situ cofactor regeneration. *J. Biotechnol* **2009**, *139(1)*, 102-107.

[41] Gorton, L.; Domínguez, E., in *Encyclopedia of electrochemistry*, Vol. 9 (Eds: A. J. Bard, M. Stratmann, G. S. Wilson), Wiley-VCH, GmbH, Weinheim, Germany, **2002**, 67-143.

[42] Damian, A.; Maloo, Kh.; Omanovic, S. Direct electrochemical regeneration of NADH on Au, Cu and Pt-Au electrodes. *Chem. Biochem. Eng. Q.* **2007**, *21(1)*, 21-32.

[43] Karyakin, A. A.; Ivanova, Y. N.; Karvakina, E. E, Equilibrium (NAD^+/NADH) potential on poly(Neutral Red) modified electrode. *Electrochem. Commun.* **2003**, *5(8)*, 677-680.

[44] Steckhan, Eberhard. Electroenzymic synthesis. *Top. Curr. Chem.* **1994**, *170*, 83-111.

[45] Lo, H. C.; Buriez, O.; Kerr, J. B.; Fish, R. H., Bioorganometallic chemistry part 11. regioselective reduction of NAD^+ models with $[Cp^*Rh(bpy)H]^+$: structure-activity relationships and mechanistic aspects in the formation of the 1,4-NADH derivatives. *Angew. Chem. Int. Ed.* **1999**, *38(10)*, 1429-1432.

[46] Lo H C.; Leiva C.; Buriez O.; Kerr J. B.; Olmstead M. M.; Fish R. H., Bioorganometallic chemistry. 13. Regioselective reduction of NAD^+ models, 1-benzylnicotinamde triflate and beta-nicotinamide ribose-5'-methyl phosphate, with in situ generated $[CpRh(Bpy)H]^+$: structure-activity relationships, kinetics, and mechanistic aspects in the formation of the 1,4-NADH derivatives. *Inorg. Chem.* **2001**, *40(26)*, 6705-6716.

[47] Gooding, J. J.; Hibbert, D. B., The application of alkanethiol self-assembled monolayers to enzyme electrodes. *Trends Anal. Chem.* **1999,** *18(8)*, 525-533.

[48] Mirsky, V. M., New electroanalytical applications of self-assembled monolayers.

Trends Anal. Chem. 2002, *21(6+7)*, 439-450.

[49] Sayen, S.; Walcarius, A., Electro-assisted generation of functionalized silica films on gold. *Electrochem. Commun.* 2003, *5(4)*, 341-348.

[50] Sibottier, E.; Sayen, S.; Gaboriaud, F.; Walcarius, A., Factors Affecting the Preparation and Properties of Electrodeposited Silica Thin Films Functionalized with Amine or Thiol Groups. *Langmuir* **2006**, *22(20)*, 8366-8373.

[51] Sanchez, A.; Walcarius, A., Surfactant-templated sol-gel silica thin films bearing 5-mercapto-1-methyl-tetrazole on carbon electrode for Hg(II) detection. *Electrochim. Acta* **2010**, *55(13)*, 4201-4207.

[52] Rybak-Akimova, E. V.; Voronina, O. E.; Wikstrom, J., in Chemistry of Carbon Nanotubes, Vol. 2 (Eds: V. Basiuk, E. Basiuk), American Scientific Publishers, Los Angeles, CA, **2008**, Chap. 18, 82-108.

Conclusion et perspectives

Le but des travaux menés dans cette thèse était l'immobilisation sous une forme stable et active de protéines de type déshydrogénase, du cofacteur NAD^+/NADH et d'un médiateur électrochimique au sein d'une matrice sol-gel déposée sous forme de couche mince à la surface d'une électrode par évaporation du sol ou électrogénération. Cette électrode ainsi modifiée doit alors être utilisée en électrosynthèse enzymatique. Afin d'atteindre les objectifs posés au commencement du projet, ce travail a été divisé en trois grandes étapes : (1) immobilisation au sien du film sol-gel de protéines de type déshydrogénase sous une forme active, (2) immobilisation du cofacteur et (3) immobilisation du médiateur électrochimique et co-immobilisation avec la déshydrogénase et le cofacteur.

Les besoins identifiés pour l'électrosynthèse enzymatique sont l'immobilisation stable d'une quantité importante de déshydrogénase actives à la surface de l'électrode du réacteur. Les études de faisabilité sur l'encapsulation de déshydrogénase au sein de la matrice sol-gel ont été menés en utilisant la D-sorbitol déshydrogénase (DSDH) comme enzyme modèle et en déposant la couche mince par évaporation du sol. Il est rapidement apparu que la DSDH était très sensible à l'environnement sol-gel et que son encapsulation dans une matrice de silice pure conduisait à une absence d'activité électrocatalytique. L'intérêt d'additifs dans le sol initial a ainsi été évalué et il a été montré que l'ajout de polyélectrolytes positivement chargés permettait d'augmenter de façon importante l'activité catalytique de la protéine encapsulée. Les charges positive du polymère (par exemple, Poly(dimethyldiallylammonium chloride), PDDA) ont en effet une interaction favorable avec la protéine négativement chargée pendant le processus d'encapsulation. Ce protocole a ensuite été adapté et optimisé pour le dépôt électrochimiquement assisté de cette couche mince sol-gel. Il a également été montré que la diaphorase pouvait être co-encapsulée avec la DSDH et permettre la régénération du cofacteur NADH en présence du médiateur ferrocènedimethanol. Cette procédure de bioencapsulation sol-gel électrochimique a ensuite été appliquée à la modification d'électrodes macroporeuses et il a été montré que la plus grande surface électroactive apportée par cette macroporosité permettait d'augmenter de façon significative la réponse bioélectrocatalytique vis-à-vis de l'oxydation du D-sorbitol.

Un des plus gros défis de ce travail concernait l'immobilisation du cofacteur NAD^+/ NADH tout en permettant de conserver son activité pendant un temps le plus long possible. Une stratégie efficace pour répondre à cet objectif a ainsi été développée dans la seconde partie de ce travail. Elle met en œuvre la réaction chimique entre NAD^+ et le groupement epoxy du composé glycidoxypropylsilane (GPS) avant sa co-condensation avec le tetraethoxysilane (TEOS) en présence des protéines (déshydrogénase et diaphorase) et de poly(ethyleneimine) (PEI). Toutes ces opérations se font dans des conditions douces compatibles avec la bioencapsulation sol-gel. Par comparaison avec l'encapsulation simple de NAD^+ avec ou sans nanotubes de carbone ou l'encapsulation de NAD-dextran, la procédure utilisant GPS est moins couteuse, et plus simple à mettre en œuvre. Enfin, ce protocole conduit à une activité catalytique très stable, pendant plus de 12h en solution en présence de convection. Finalement cette méthode développée pour le dépôt du film par évaporation du sol a été adaptée pour l'électrogénération sur électrode d'or macroporeuse. Dans toutes ces études le médiateur électrochimique ferrocènediméthanol se trouvait dans la solution.

Finalement, la dernière partie de ce travail a été consacrée à l'immobilisation du médiateur électrochimique à la surface de l'électrode de façon à ce qu'il puisse communiquer efficacement avec l'électrode et avec la diaphorase ou directement avec le cofacteur et ainsi obtenir la régénération électrochimique du cofacteur. Différentes stratégies ont ainsi été étudiées pour obtenir le système final contenant l'ensemble des éléments de cette chaîne bioélectrocatalytique co-immobilisés dans la matrice sol-gel. Ces études ont d'abord été développées en déposant le film sol-gel par évaporation du sol. Comme pour les études précédentes la DSDH est utilisée comme protéine modèle, le cofacteur est immobilisé par couplage avec le GPS et le médiateur est introduit dans la matrice sol-gel à l'aide de polymère portant des espèces ferrocène ou osmium ou à l'aide d'un ferrocène fonctionnalisé par un groupement silane pouvant être co-condensé avec les autres silanes du sol (TEOS et GPS). Il a tout d'abord été montré que GPS permettait d'augmenter fortement la stabilité de l'immobilisation du médiateur en plus de son rôle dans l'immobilisation du cofacteur. Ceci est du à la plus grande stabilité mécanique des films préparés avec GPS. La co-immobilisation de ces médiateurs avec le cofacteur et les protéines (DSDH et diaphorase) a ainsi permis d'obtenir pour la première fois dans une matrice sol-gel une activité catalytique stable. Finalement, les tentatives pour transposer ce résultat obtenu par évaporation du sol à l'électrogénération ont échoués. La distribution du médiateur électrochimique dans les

matrices sol-gel obtenus par électrochimie semble ne pas être suffisamment homogène ou leur mobilité ne pas être suffisante pour permettre le transport électronique et une interaction avec l'électrode ou la diaphorase.

Afin de résoudre le problème posé par l'absence d'activité catalytique avec les films préparés par électrogénération, nous avons développé une stratégie différente, basée sur le dépôt de la couche mince sol-gel à la surface de nanotubes de carbone fonctionnalisés par différents médiateurs. Cette fonctionnalisation des nanotubes de carbone a été obtenue par la formation de fonctions quinones par traitement micro-ondes, par électropolymérisation du vert de méthylène et par recouvrement des nanotubes par un polymère de type acrylate portant des complexes d'osmium(III). Seul ce dernier système a alors permis d'observer, en présence de diaphorase, une régénération du cofacteur immobilisé dans la matrice sol-gel obtenue par électrogénération. La flexibilité du polymère d'osmium et l'intermédiaire de la diaphorase permettent alors la régénération douce du cofacteur enymatique. Tous les composants immobilisés communiquent efficacement à l'intérieur du gel de silice pour permettre l'oxydation électrocatalytique du D-sorbiltol. Les nanotubes de carbone fonctionnalisés par un médiateur preséntant une certaine faisabilité est un bon substrat d'électrode pour l'électrogénération sol-gel pour la co-immobilisation du cofacteur et des protéines.

La couche mince sol-gel qui a été développée au cours de cette thèse peut être appliquée à la préparation de composés chiraux par électrosynthèse enzymatique. Tous les éléments participant à cette synthèse étant immobilisés sur l'électrode, cette approche est intéressante autant d'un point de vue économique que environnemental, en évitant l'utilisation de solvant et en réduisant es étapes de purification au minimum. Un tel concept correspond aux standards de la chimie verte avec un procédé induisant très peu de déchets. Cependant, il est encore nécessaire d'améliorer l'efficacité du procédé avant application à une échelle industriel, ceci passe notamment par le dépôt de ces couches minces sol-gel sur des électrodes macroporeuses de grandes dimensions et leur intégration dans le réacteur.

Les découvertes faites dans cette thèse peuvent également être utilisées pour le développement de biocapteurs à base de déshydrogénase ne nécessitant l'ajout d'aucun réactif supplémentaire dans le milieu à analyser. Il existe en effet plus de 300 sortes de déshydrogénase catalysant l'oxydation d'une grande variété de substrats (éthanol, glucose,

lactate, etc) qui peuvent être d'un grand intérêt d'un point de vue analytique du fait de leur présence ou utilisation dans l'industrie alimentaire, l'environnement ou pour suivre certaines pathologies. Les résultats de cette étude sont également d'un grand intérêt pour le développement futur de systèmes électrochimiques à base de déshydrogénase, tel que les biopiles à combustible et biobatteries.

Conclusion and outlook

The focus of the research work carried out in this thesis is on the development of different strategies allowing the stable immobilization of a dehydrogenase, the cofactor NAD^+/NADH and an electron mediator in a sol-gel matrix deposited (either by evaporation or by electrogeneration) as a thin film on an electrode surface. This layer is intended to be applied in electro-enzymatic synthesis for the production of fine chemicals. To achieve the objective of the project, we have divided the work into three steps: (1) dehydrogenase immobilization, (3) cofactor immobilization and (3) mediator immobilization and co-immobilization with dehydrogenase and cofactor.

The first requirements for electrosynthesis involves a stable immobilization of a large amount of active dehydrogenase on the electrode surface of the reactor. Thus, the feasibility of dehydrogenase encapsulation in sol-gel film is first evaluated using D-sorbitol dehydrogenase (DSDH) as a model enzyme by drop-coating. However, DSDH is sensitive to the sol composition during the encapsulation in a silica gel. The direct encapsulation of DSDH in a pure silica gel leads to total deactivation of the protein. We have thus evaluated the interest of various polyelectrolytes in combination with sol-gel deposition of silica films with encapsulated DSDH. We have chosen positively-charged polyelectrolytes because of the expected favorable interactions with the negatively-charged enzyme surface. Then, electrochemically-assisted deposition of silica gel layer has been successfully adapted to the encapsulation of DSDH as well as the co-encapsulation of DSDH and diaphorase in the presence of Poly(dimethyldiallylammonium chloride) (PDDA). The process and the sol composition have been optimized on flat glassy carbon electrodes before being applied to gold macroporous electrodes. At the end, the electrochemically-assisted deposition of the sol-gel bio-composite has been extended to macroporous electrodes displaying a much bigger electroactive surface area. The macroporous texture of the gold electrode improves thus significantly the catalytic efficiency of the sol-gel biocomposite. The bioelectrocatalytic response looks promising for electro-enzymatic applications.

The durable attachment of NAD^+/NADH cofactors with long-term activity was the biggest challenge in the project. A successful strategy for cofactor immobilization in sol-gel thin films has been developed in the second part of our work. It involves the chemical bonding of NAD^+

to the epoxide group of glycidoxypropylsilane (GPS) before co-condensation of the organoalkoxisilane with tetraethoxysilane in the presence of the proteins (dehydrogenase and diaphorase) and a poly(etheleneimine) additive (PEI). All the operations were performed in smooth conditions compatible with the sol-gel bio-encapsulation process. By comparison with the simple encapsulation of NAD^+ or NAD-dextran or adsorption of NAD^+ on carbon nanotubes, the strategy with GPS is either cheaper or simpler to implement, and leads by far to more stable sol-gel films and durable bioelectrocatalytic responses. At the end, the efficient drop-coating method has been extended to the electrochemically-assisted deposition of sol-gel film with encapsulated enzymes and cofactor on macroporous electrodes.

Finally, the last part of this work has been devoted to the development of different strategies for mediator immobilization which could used for the elaboration of reagentless device with co-immobilized dehydrogenase and cofactor. First of all, a series of successful strategies for co-immobilization of all components (dehydrogenase, cofactor and electron mediator) in sol-gel films have been developed by using one step drop-coating. here DSDH was chosen as model enzyme, NAD^+ functionalized with GPS was used as mediator, and ferrocene species or osmium polymers were introduced inside the matrix as co-immobilized mediators. The importance of introducing GPS as an additive into the TEOS sol-gel-derived films has been pointed out with respect to the stable mediator immobilization. However, such co-immobilization applied to electrochemically-assisted deposition of sol-gel thin films was not successful due to some problems to keep mediators in an active form.

To overcome this problem, we have developed different strategies for the elaboration of a reagentless devices based on deposition of the sol-gel biocomposite on mediators functionalized multi-walled carbon nanotubes (MWCNT). Surface modification of the carbon nanotube with quinone moieties by microwave treatment or the electrodeposition of poly(methylene-green) on the MWCNT resulted in good electrocatalytic detections of the free diffusing NADH produced by the immobilized dehydrogenase. However these systems failed to regenerate the cofactor immobilized in electrogenerated sol-gel film as the mediators immobilized on carbon nanotubes did not display enough mobility to react with NAD^+ linked to the sol-gel matrix. Finally, the sol-gel thin film with co-immobilized dehydrogenase, diaphorase and cofactor was deposited on MWCNT wrapped by osmium polymer. The flexibility of the osmium complexes allowed the smooth regeneration of the immobilized

cofactor. All the components are able to communicate inside the silica gel layer for efficient electro-catalytic oxidation of D-sorbitol. The combination of the carbon nanotubes with the Osmium(III) polymer was a suitable electrode material for further electrogeneration of sol-gel materials with co-immobilized proteins and cofactor.

The layer developed in this study can be applied in electro-enzymatic synthesis for the manufacture of chiral fine chemicals. Because all reactive agents have been immobilized on the electrode surface, it represents an environmentally friendly process by avoiding organic solvents and reducing purification steps to a minimum. This concept meets the standards of green chemistry and leads to processes which come close to zero waste emissions. However, it will still take some time to improve the reaction productivity before electroenzymatic processes can be applied on an industrial scale. The finding of this work can also be applied in the development of dehydrogenase-based reagentless biosensors. It is reported there are more than 300 kinds of dehydrogenases. These enzymes catalyze the oxidation of a variety of substrates including alcohols, aldehydes, glucose and etc., which are of great interests from the analytical point of view because of the practical application on food industry, environment, and clinical chemistry. This study also offers a facile and versatile approach to the development of some other integrated dehydrogenase-based electrochemical devices, such as biofuel cells and biobattery.

Publications

[1] **Zhijie Wang**, Mathieu Etienne, Gert-Wieland Kohring, Alain Walcarius. Critical effect of polyelectrolytes on the electrochemical response of dehydrogenases entrapped in sol-gel thin films. **Electroanalysis,** 2010, *22(17-18)*, 2092-2100.

[2] **Zhijie Wang**, Mathieu Etienne, Gert-Wieland Kohring, Yémima Bon-Saint-Côme, Alexander Kuhn, Alain Walcarius. Electro-assisted deposition of sol-gel bio-composite with co-immobilized dehydrogenase and diaphorase. **Electrochimica Acta**. 2011, *56 (25)*, 9032-9040.

[3] Alain Walcarius, Rihab Nasraoui, **Zhijie Wang**, Fengli Qu, Veronika Urbanova, Mathieu Etienne, Mehmet Göllü, Ayhan S. Demir, Janine Gajdzik, Rolf Hempelmann. Factors affecting NADH regeneration by $[Cp^*Rh(bpy)]^{2+}$ derivatives: impact on their immobilization onto electrode surfaces. **Bioelectrochemistry,** 2011, *82*, 46-54.

[4] **Zhijie Wang**, Mathieu Etienne, Fabienne Quilès, Gert-Wieland Kohring, Alain Walcarius. Durable Cofactor Immobilization in Sol-Gel Bio-Composite Thin Films for Reagentless Biosensors and Bioreactors Using Dehydrogenases. submitted.

[5] Yémima Bon Saint Côme, Hélène Lalo, **Zhijie Wang**, Mathieu Etienne, Janine Gajdzik, Gert-Wieland Kohring, Alain Walcarius, Rolf Hempelmann, Alexander Kuhn. Multiscale-tailored bioelectrode surfaces for optimized catalytic conversion efficiency. **Langmuir**, 2011, *27* (20), 12737–12744.

[6] **Zhijie Wang**, Mathieu Etienne, Gert-Wieland Kohring, Alain Walcarius. Electrochimical deposition of sol-gel thin film on functionalized carbon nanotubes for the elaboration of dehydrogenase based reagentless biosensor. submitted.

[7] **Zhijie Wang**, Mathieu Etienne, Gert-Wieland Kohring, Alain Walcarius. A reagentless D-sorbitol biosensor based on dehydroganse immobilized in sol-gel/carbon nanotubes/poly(methylene green) composite. In preparation.

Conferences participations

International Conferences

1. **Wang, Z.**; Etienne, M.; Kohring, G.; Klein, T.; Walcarius, A., Effect of poly(dimethyldiallylammonium chloride) on enzyme encapsulation into a sol-gel matrix. **Poster**, "*Modern Electroanalytical Methods 2009*", 9-13 December, 2009, Prague.
2. **Wang, Z.**; Etienne, M.; Kohring, G.; Walcarius, A., Electro-assisted deposition of protein encapsulated sol-gel thin film for bio-electrocatalytic applications. **Poster**, "*61st Annual Meeting of the International Society of Electrochemistry*", September 26 - October 01, 2010, Nice, France.

Workshop

1. **Wang, Z.**; Etienne, M.; Kohring, G.; Walcarius, A., Electro-assisted deposition of protein encapsulated sol-gel thin film for bio-electrocatalytic applications. **Poster**, "*ISGS Summer School 2010*", 18-21 July, 2010, Clermont-Ferrand, France.

In this thesis, the research work was focused on designing functional layers based on silica sol-gel thin films to co-immobilize dehydrogenase, cofactor and electron mediator to get the most highly active systems and such modifications of electrode surfaces should be adaptable to the macroporous electrodes.

Immobilization of dehydrogenase in an active form in a sol-gel matrix was obtained with using a positively-charged polyelectrolyte as additive in the starting sol. This polymer provides a good environment for the protein in the sol-gel. The optimal sol can be deposited by evaporation or by electrodeposition and was successfully deposited in macroporous electrodes. Diaphorase was also successfully co-immobilized with dehydrogenase for the electroenzymatic regeneration of the NAD^+ cofactor.

The immobilization of the cofactor was investigated by simple entrapment, adsorption to carbon nanotube, encapsulation of NAD^+ chemically attached to dextran (NAD-dextran), and by in-situ coupling with glycidoxypropyltrimethoxysilane (GPS). The last approach allowed stable immobilization of the cofactor, and was extended to electrodeposition and applied to macroporous electrodes.

Several strategies for mediator immobilization have been developed and used for the elaboration of the reagentless device. Fc-PEI, Fc-Silane or Osmium polymer were successfully co-immobilized with dehydrogenase and cofactor in the sol-gel matrix deposited by drop-coating. However, the same strategies did not operate when the sol-gel films have been electrodeposited.

Some other strategies based on carbon nanotubes (CNTs) for mediator immobilization were finally developed in attempting to overcome the above problems. They include (1) micro-wave treatment (MWCNTs-μW), (2) electrochemical deposition of poly(methylene green) (MWCNTs-PMG), and (3) wrapping with a polyacrylate polymer holding osmium(III) complexes (MWCNTs-Os). The elaboration of a reagentless device by sol-gel electrodeposition was only achieved using a sol containing dehydrogenase, diaphorase and the cofactor (NAD-GPS) on carbon nanotube wrapped by an osmium polymer. Carbon nanotubes provided also a unique opportunity for the immobilization in an active form of rhodium complexes used for NADH regeneration (reduction reaction).

Keywords: Silica, sol-gel, dehydrogenase, NAD^+/NADH cofactor, electron mediator, polyelectrolyte, bioencapsulation, electrochemically-assisted deposition, thin films, reagentless device, porous electrodes, carbon nanotubes.

La recherché menée dans cette thèse concerne l'élaboration de couches minces sol-gel permettant la co-immobilisation de déshydrogénase, du cofacteur NAD^+/NADH et d'un médiateur électrochimique afin d'obtenir le système présentant une activité électrocatalytique optimale et pouvant être déposé au sein d'électrodes macroporeuses.

L'immobilisation de la D-sorbitol déshydrogénase (DSDH, l'enzyme modèle de cette étude) sous une forme active dans la matrice sol-gel a été obtenue en utilisant un polyélectrolyte positivement chargé comme additif dans le sol de départ. La présence de ce polymère dans le sol de silice procure un environnement favorable à l'activité enzymatique de la déshydrogénase. Le film peut être déposé par évaporation du sol optimal ou électrogénéré par électrolyse de ce même sol, ce dernier procédé ayant été appliqué à la fonctionnalisation d'électrodes d'or macroporeuses. La diaphorase a également pu être co-encapsule avec la DSDH pour la régénération électroenzymatique du cofacteur NAD^+.

L'immobilisation du cofacteur dans cette matrice sol-gel a ensuite été étudiée. Le cofacteur a tout d'abord été simplement encapsulé dans la matrice sol-gel en présence ou non de nanotubes de carbone. L'encapsulation d'une forme macromoléculaire du NAD^+ (NAD-dextran) a également été étudiée et finalement une voie alternative a été étudiée, utilisant le couplage chimique du NAD^+ avec le groupement époxy du glycidoxypropylsilane (NAD-GPS). Cette dernière approche s'est montrée être la plus intéressante, notamment en ce qui concerne la stabilité du signal électrocatalytique. Les études de faisabilité ont été menées en utilisant le dépôt sol-gel par évaporation du sol sur électrode plane et la méthode a ensuite été transposée aux électrodes macroporeuses pour dépôt par électrogénération.

Plusieurs stratégies d'immobilisation du médiateur électrochimique ont alors été étudiées. Les espèces de type ferrocène ou des complexes d'osmium(III) peuvent être incorporées dans la matrice sol-gel par encapsulation de polymères portant ces médiateurs (Fc-PEI et polymère d'osmium) ou par co-condensation avec un ferrocène fonctionnalisé par un groupement silane. Ces trois systèmes se sont montrés opérationnels lorsque la couche mince sol-gel était déposées par évaporation du sol contenant l'ensemble des éléments de la co-immobilisation (DSDH, diaphorase, NAD-GPS et médiateur). Par contre le dépôt par électrogénération ne permet aux médiateurs de transférer les électrons entre la diaphorase et l'électrode, empêchant toute activité catalytique.

Finalement d'autres stratégies basées sur la fonctionnalisation de nanotubes de carbone par différents médiateurs électrochimiques ont alors été étudiées pour dépasser le problème rencontré avec les films déposés par électrogénération (perte de la fonction de médiateur). Les nanotubes de carbones ont été fonctionnalisés par des fonctions quinone grâce à un traitement micro-onde, par électropolymérisation du vert de méthylène, ou par recouvrement par un polymère de type acrylate portant des complexes d'osmium(III). Il alors été possible de co-immobiliser l'ensemble des éléments de ce processus électrocatalytique en utilisant l'électrogénération d'une couche mince sol-gel servant à immobiliser les protéines (DSDH et diaphorase) et le cofacteur (NAD-GPS) à la surface des nanotubes fonctionnalisés par le polymère d'osmium(III). Enfin, les nanotubes de carbone ont permis l'immobilisation sous une forme active de complexes de Rh(III) permettant la régénération du cofacteur NADH.

Keywords: Silice, sol-gel, déshydrogénase, cofacteur NAD^+/NADH, médiateur, polyélectrolyte, bioencapsulation, électrogénération, film, électrodes macroporeuses, nanotubes de carbone.